RESEARCH

2009-32

Hydraulic and Mechanical Properties of Recycled Materials

Technical Report Documentation Page

1. Report No. 2009-32	2.	3. Recipients Accession No.	
4. Title and Subtitle Hydraulic and Mechanical Properties of Recycled Materials		5. Report Date October 2009	
		6.	
7. Author(s) Satish Gupta, Dong Hee Kang, and Andry Ranaivoson		8. Performing Organization Report No.	
9. Performing Organization Name and Address University of Minnesota Department of Soil, Water, & Climate 1991 Upper Buford Circle St. Paul, MN 55108		10. Project/Task/Work Unit No. 11. Contract (C) or Grant (G) No. (c) 89261 (wo) 4	
12. Sponsoring Organization Name and Address Minnesota department of Transportation 395 John Ireland Boulevard, Mail Stop 330 St. Paul, MN 55155		13. Type of Report and Period Covered Final Report 14. Sponsoring Agency Code	
15. Supplementary Notes http://www.lrrb.org/pdf/200932.pdf			

16. Abstract (Limit: 250 words)

Construction and maintenance of roads requires large volume of aggregates for use as base and subbase materials. Because of the cost of virgin aggregates, federal and state agencies are encouraging the recycling of waste materials including materials in old pavements. This study assessed the suitability of four recycled materials relative to virgin aggregates for use as base and subbase materials. The four recycled materials were the reclaimed asphalt pavement (RAP), fly ash (FA), reclaimed concrete material (RCM), and foundry sand (FS). Assessment of these materials was done in terms of their hydraulic, mechanical, and leaching properties when mixed in with various proportions of virgin aggregates. Except for slightly higher fine content in some RAP-aggregate mixtures, particle size distribution of all mixtures was within the Mn/DOT specification band for Class 5 materials. Water retention (pore size distribution), hydraulic conductivity, resilient modulus, and shear strength measurements were generally similar to that of 100% aggregates. Exception was the mixtures of FS. Heavy metal concentrations in the leachate were also generally less than the EPA drinking water standards. We concluded that FA, RAP, and RCM mixtures will be good substitutes of virgin aggregates as base and subbase materials.

17. Document Analysis/Descriptors Modulus of resilience, Shear strength, Pore size distribution, water retention, Permeability coefficient, hydraulic conductivity, Breakthrough curves, Fly ash, Recycled asphalt pavement, Recycled concrete material, Recycled materials, Foundry sand, Virgin aggregates		18. Availability Statement No restrictions. Document available from: National Technical Information Services, Springfield, Virginia 22161	
19. Security Class (this report) Unclassified	20. Security Class (this page) Unclassified	21. No. of Pages 219	22. Price

HYDRAULIC AND MECHANICAL PROPERTIES OF RECYCLED MATERIALS

Final report

Satish C. Gupta
Dong Hee Kang
Andry Ranaivosoon
Department of Soil, Water, & Climate
University of Minnesota

October 2009

Published by
Minnesota Department of Transportation
Research Services Section
395 John Ireland Boulevard, MS 330
St. Paul, MN 55155

ACKNOWLEDGMENTS

The authors gratefully acknowledge the help and support of Ruth Roberson of the Minnesota Pollution Control Agency (previously with the Minnesota Department of Transportation), Nancy Whiting of Purdue University (previously with the Minnesota Department of Transportation), and John Siekmeier of the Minnesota Department of Transportation (Mn/DOT) as Technical Liaisons at various stages of the project. We also thank Professor Joesph Labuz and his student Jason Lim of the Civil Engineering Department at the University of Minnesota for allowing us to use their equipment for resilient modulus measurements as well as for their help with the set-up. The authors also thank Dr. Mihai Marasteanu of the Civil Engineering Department at the University of Minnesota and Mr. Todd Wille of SPE Engineering & Testing, Hugo, MN for allowing the use of their gyratory compactors for specimen preparation. We are also thankful to Dr. Robert Edstrom and John Siekmeier of Mn/DOT for their reviews and comments on the draft of the final report. Finally, this project would not have been possible without funding from the Minnesota Local Road Research Board.

TABLE OF CONTENTS

LIST OF TABLES

LIST OF FIGURES

EXECUTIVE SUMMARY

Construction and maintenance of roads requires large volume of aggregates for use as base and subbase materials. Because of the cost of virgin aggregates, federal and state agencies are encouraging the recycling of waste materials including materials in old pavements. However, there is limited information on mechanical, hydraulic, and leaching characteristics of various recycled materials. The goal of this study was to assess the suitability of four recycled materials relative to virgin aggregates for use as base and subbase material in road construction. The four recycled materials were the reclaimed asphalt pavement (RAP), fly ash (FA), reclaimed concrete material (RCM), and foundry sand (FS). Assessment of these materials was done in terms of their hydraulic, mechanical, and leaching characteristics when mixed in with various proportions of virgin aggregates. In total 17 mixtures of recycled materials and one sample of 100% virgin aggregate were tested. Table 1 lists mixing proportions of various recycled materials as well as the corresponding maximum dry density (MDD) and the optimal water contents (OWC) at which the specimens were packed before testing. Maximum dry density was achieved through packing in a gyratory compactor. Specific tests were: water retention/pore size distribution curves, saturated and unsaturated hydraulic conductivities, resilient modulus (M_R) at optimal water content and water content corresponding to 300 kPa suction, shear strength at optimal water content and water content corresponding to 300 kPa suction, and leaching characteristics under both saturated and unsaturated conditions.

Table 1. Maximum dry densities and the corresponding optimum water contents for various mixtures of recycled materials with aggregates.

Materials	**MDD (Mg/m^3)**	**OWC (%)**
RAP25%+ Aggregate 75%	2.07	7.8
RAP50%+ Aggregate 50%	2.07	6.6
RAP75%+ Aggregate 25%	2.08	5.4
RAP100%	2.12	4.0
Fly Ash 5% +RAP25%+Aggregate 70%	2.05	8.2
Fly Ash 15% +RAP25%+Aggregate 60%	1.95	10.2
Fly Ash 5% +RAP50%+Aggregate 45%	2.07	7.4
Fly Ash 15% +RAP50%+Aggregate 35%	1.97	8.6
Fly Ash 5% +RAP75%+Aggregate 20%	2.06	6.6
Fly Ash 15% +RAP75%+Aggregate 10%	2.00	7.4
RCM 25%+ Aggregate 75%	2.00	9.8
RCM 50%+ Aggregate 50%	1.98	9.4
RCM 75%+ Aggregate 25%	1.95	9.4
RCM 100%	1.94	9.4
Foundry Sand 5%+ Aggregate 95%	2.07	9.4
Foundry Sand 10%+ Aggregate 90%	2.07	9.4
Foundry Sand 15%+ Aggregate 85%	2.07	9.4
Aggregate 100%	2.07	9.2

Except for slightly higher fine content in some RAP-aggregate mixtures, particle size distribution of all mixtures fell within the Minnesota Department of Transportation (Mn/DOT) specification band for Class 5 materials. MDD varied from 1.94 to 2.12 Mg/m^3 whereas the OWC varied from 4.0 % for 100% RAP to 10.2% for 15% FA+25% RAP+60% aggregate mixture. Water retention (pore size distribution) curves of recycled mixtures were nearly similar to that of 100% aggregates. Subsequent measurements on saturated (0.2 kPa hydraulic head) and unsaturated (-2.0 kPa suction) hydraulic conductivities showed that except for FS, the corresponding conductivities of the mixtures (ranges: 12-302 cm/day, 1-185 cm/day) were higher than that of virgin aggregates (88 cm/day, 1 cm/day) thus suggesting that drainage characteristics of recycled materials will be somewhat better or similar to that of 100% virgin aggregates. M_R values of all recycled material mixtures increased with an increase in confining pressure but there was little effect of the deviator stress. Except for FS, M_R values of aggregates generally increased with the addition of recycled materials thus suggesting that performance of the recycled material (FA, RAP, and RCM) mixtures with aggregates will be better than that of the virgin aggregates. For FS-Aggregate mixtures, M_R values of the mixture decreased with an increase in the amount of FS thus suggesting that FS may be less desirable for use in road construction. However, other types of FS materials will need to be tested to confirm this finding. There was a slight increase in M_R values with a decrease in degree of saturation for all mixtures thus validating the observations from previous Mn/DOT funded studies that lower degree of saturation helps to increase the stiffness of the base and subbase materials and in turn increases the longevity of the roads. Using our data base, we further extracted the coefficients of two models describing M_R based on either bulk and octahedral shear stresses or confining and deviator stresses. These coefficients can be used to predict M_R of recycled material-aggregate mixtures at other stress values. These values are also needed in new national pavement design guide being finalized in National Cooperative Highway Research Program (NCHRP) Project 1-37A to operate design guide software.

In general, addition of RAP and RCM increased the shear strength (cohesion values) of the mixtures. Except for three mixtures, friction angles were nearly similar (38º to 49º) for all mixtures. Increasing the FA content also improved the cohesion and thus shear strength of the mixture. Since 100% virgin aggregate and FS mixtures failed before reaching sequence #30 in M_R measurement, shear strength measurements of these materials could not be determined. Because of the lack of shear strength data for 100% virgin aggregate, recycled mixtures could not be compared in terms of shear strength to 100% virgin aggregate.

Leaching tests were run in both batch and flow-thru modes. Concentration of heavy metals in a batch test was generally higher than that from the flow thru test and in several cases did not meet the EPA drinking water standard. This is expected considering that reaction time of water with particles is limited in a flow through set-up than in a batch mode. In batch mode, recycled material and aggregate particles are thoroughly in contact with water and thus provide maximum potential for solubility and desorption. Heavy metal concentrations from breakthrough studies are more reflective of the field conditions.

In general, heavy metal concentrations in the leachate from RAP mixtures were less than the EPA drinking water standard. The concentration of some heavy metals (Pb) in the leachate from some RCM mixtures was higher than the drinking water standards. For all fly ash mixtures under both saturated and unsaturated conditions, concentration of some heavy metals (Cr, Al) in the leachate was generally higher than the drinking water standards. There was no presence of arsenic in the leachate during any of the flow thru experiments. Since the leaching experiments

were done in batch (continuous shaking) and in small column studies (30.5 cm length), there is minimal risk that these chemicals will enter the ground water system because of the presence of additional soil below the base and subbase layers. Therefore, we concluded that limited addition of FA, RAP, and RCM to virgin aggregates will results in minimal impact in terms of chemical leaching to ground or surface waters.

Based on the above tests, we conclude that FA, RAP, and RCM mixtures will be good substitutes for virgin aggregates as base and subbase materials in road construction. However, further in-situ testing of these materials needs to be undertaken before field implementation of our findings.

CHAPTER 1-BACKGROUND AND RESEARCH OBJECTIVES

PROJECT BACKGROUND

Generation of waste in household, industry, and highway reconstruction has spurred recycling nationwide. One of the venues for use of recycled materials is in pavement construction. Recycled materials used in pavement construction include asphalt shingle, fly ash, municipal solid waste (MSW) bottom ash, shredded tires, reclaimed concrete and recycled asphalt. However, there is limited information on how addition of recycled material in the base aggregates affects hydraulic (water retention, hydraulic conductivity), mechanical (resilient modulus, shear strength), and leaching properties. There is some information in the literature on the mechanical properties of recycled materials but most of this characterization is at saturation. Since materials below the pavement are mainly unsaturated, we also need these characterizations at various degrees of unsaturated conditions. Change in hydraulic properties (water flow) due to addition of recycled materials can occur because of non-wettability, cementation, movement of cementing agent with depth and its subsequent deposition, and the presence of small pathways.

Chesner et al. (1998) showed that MSW has good bearing capacity and low susceptibility to freeze-thaw but poor durability (Los Angeles Abrasion test: 40-60%). In a road section experiment comparing bottom ash with conventional aggregate in asphalt mixtures, it was found that 50 percent mixture of ash performed as well as the control section after 5 years of service (Zhang et al., 1999). Fly ash has also been used as a component of base or sub-base materials (fly ash 8-20% with coarse aggregates and 15-30% with sandy aggregates) in pavement construction. Fly ash also imparts pozzolanic effect; which is an ability to combine with calcium to form cementitious compounds. As a result of this, mixture of fly ash and aggregates tend to have very low permeability (10^{-5} and 10^{-6} cm/sec), which further decreases with time due to pozzolanic reaction. Strength measurements on a series reclaimed asphalt shingles (RAS) mixed with different soils showed that addition of RAS material (< 25.4 mm) improves the strength of weak material like clay but decreases the strength of strong materials like silty sand, clean sand, and crushed stone gravel (Hooper and Mar, 2004). Mixing reclaimed concrete materials (RCM) with natural aggregates, Chini et al. (2001) showed that the compressive strength of the mixture decreased as percentage of RCM in the mix increased. Barksdale et al. (1992) showed that aggregate base materials mixed with recycled concrete material and dolomite performed better with respect to rutting and resilient modulus than sand and crushed gravel blend. Reclaimed asphalt pavement (RAP) aggregates have been shown to have adequate bearing capacity, good drainage, and very good durability (Hanks and Magni, 1989). However, the bearing capacity in this study decreased with increasing RAP content. A laboratory study by Papp et al. (1998) showed that RAP and RCM yielded higher resilient modulus compared to dense graded aggregate (DGA). However, with the use of recycled material in road construction, there is some concern on the release of contaminants through the pavement. Apul et al. (2001) showed that release of contaminants through pavement layers into the environment depends upon the hydraulic regime, the extent of cracking, transverse and longitudinal joint lengths, shoulder infiltration rates, and subgrade capillary rise into the pavement. Townsend and Brantley (1998) found that leaching of heavy metals (Ba, Cd, Cr, Cu, Pb, Ni, Zn) from RAP was below the detection limits except for lead. Lead leaching was higher under saturated than unsaturated conditions.

Some studies have been reported on the use of fly ash in road construction. Bloom et al. (2006) characterized the chemical contents of fly ashes from various power plants in Minnesota

and then using a computer model evaluated the suitability of these materials in terms of meeting Minnesota Pollution Control Agency's Soil Leaching Values (SLV). Benson et al. (2009) characterized the in-situ leaching of contaminant from two test sites in Minnesota where class C fly ash had been mixed with aggregates in base material. From 2004-2008, concentration of most contaminants in the leachate from Waseca site were below the EPA maximum contaminant levels (MCLs) and the Health Risk levels (HRLs) established by the Minnesota Department of Health. Concentrations exceeding MCL or HCL at least one time were: As, Pb, Sb, and Ti. The data from the second site at Chicago County, MN was considered unreliable due to periodic flooding of the lysimeter from perched water table during snowmelt.

The goal of this project is to assess the suitability of recycled materials in pavement construction by characterizing their hydraulic, mechanical, and leaching characteristics. The assessment of suitability is relative to virgin aggregates. The tested materials are the reclaimed asphalt pavement (RAP), fly ash (FA), reclaimed concrete material (RCM), and foundry sand (FS). In total seventeen recycled material mixtures produced by mixing four recycled materials with virgin aggregate and one sample of 100% virgin aggregates were characterized for water retention, resilient modulus, shear strength, leaching characteristics and hydraulic conductivity both under saturated and unsaturated conditions. Following text summarizes the general characteristics of various recycled materials used in this study.

Reclaimed Asphalt Pavement (RAP)

Recycled asphalt pavement (RAP) is produced through milling of the existing pavement containing asphalt and aggregates. RAP contains hardened asphalt cement such as aliphatic hydrocarbon compounds (Chesner et al., 1997). Removed pavement can be land filled but is commonly used again. To reduce the cost of road construction, most departments of transportation undertake some mixing of RAP with virgin aggregates. Page (1987) reported a cost savings of 15-30% compared to if all virgin materials are used in road construction. Studies (Garg and Thompson, 1996; Taha et al., 1999) have shown that RAP mixed with virgin aggregates could replace virgin aggregates as subbase and base material. RAP generally has higher dry density, CRB (California Bearing Ratio), M_R (resilient modulus), and field elastic modulus than the virgin aggregate. However, the optimum water content and the maximum bulk density of RAP are lower than that of the conventional granular materials (Sayed et al., 1993; Maher and Popp, 1997). The RAP gradation is also generally finer and denser than that of the virgin aggregate.

Since asphalt is made up of natural aggregates and oil products and also asphalt comes in contact with many chemicals generated from road traffic, there are environmental considerations on the use of RAP as a base or subbase material. However, Townsend and Brantley (1998) did not find any large quantities of EPA regulated chemicals in the leachate from reclaimed asphalt pavements, both in batch and flow through modes.

Fly Ash (FA)

Fly ash consists of fine, powdery particles that are predominantly spherical in shape, either solid or hollow, and mostly glassy in nature. The carbonaceous material in fly ash is composed of angular particles. The particle size distribution of most bituminous coal fly ashes is generally similar to that of silt.

ASTM C 618-03 classifies fly ash as pozzolanic or cementious materials (ASTM 2003). There are three classes of pozzolans; Class C, Class F, and Class N. The chief difference

between Class F and Class C fly ash is in the amount of calcium, silica, alumina, and iron contents. Class F produced from burning of anthracite or bituminous coal is typically low in calcium (in the range of 1 to 12 percent) and mostly in the form of calcium hydroxide and calcium sulfate. It also contains some glassy component in combination with silica and alumina. On the other hand, Class C Fly ash produced from burning of lignite or subbituminous coal contains 30-40 % calcium oxide. Besides having pozzolanic properties, Class C fly ash also has some self-cementing properties. Another difference between Class F and Class C is the amount of alkalis and sulfates (SO_4); they are generally higher in Class C than Class F fly ashes. The specific gravity of fly ash usually ranges from 2.1 to 2.8, while its specific surface area may range from 170 to 1000 m^2/kg (Chesner et al., 1997). Class N is raw or calcined natural pozzolan such as some diatomaceous earths, opaline cherts, and shales; tuffs, volcanic ashes, and pumicites; and calcined clays and shales (ASTM 2003). Class C and Class F fly ashes are of most importance for engineering uses.

Reclaimed Concrete Material (RCM)

Reclaimed concrete material (RCM) consists of sand and various sizes and shapes of gravel. Historically, disposal in landfills has been the most common method of managing concrete materials. However, recycling of RCM as a substitute for virgin aggregates has become an attractive option in pavement foundation construction. Because of the greater demand for aggregates, there is a growing interest in using alternative materials such as RCM as a substitute for aggregates in road construction. Jason (2005) estimated that the need for virgin aggregate will reach 2.5 billion tons in the US by 2020. Mn/DOT specification 3/38 describes how recycled concrete aggregates can be used in road foundation construction.

RCM has rougher surface texture, lower specific gravity, higher water absorption, and lower specific gravity than the natural aggregates. As size of the RCM particle decreases, specific gravity decreases but water absorption increases mainly due to higher proportion of mortar. Specific gravity of RCM has been reported to vary from 2.0 to 2.5 (ACPA, 1993). RCM is generally more permeable than natural aggregate and coarse RCM has favorable mechanical properties for aggregate use. These properties include good abrasion resistance, good soundness characteristics, and bearing strength.

Contaminant leaching and pH changes in the surrounding soil and water are environmental considerations for RCM use in road construction. The cementitious materials can result in heavy metals leaching. For example, leaching of Portland cement concrete with acetic acid (Toxicity Characteristic Leaching Procedure, TCLP) showed presence of arsenic, beryllium, cadmium, chromium, mercury, lead, and selenium in the leachate (Kanare and West, 1993). Long-term potential of leachable toxic metals from the Portland cement concrete were: arsenic=19.9 mg/kg, beryllium=1.4 mg/kg, chromium=72.7 mg/kg, lead=75.3 mg/kg, Nickel=72.0 mg/kg, and vanadium=44.1 mg/kg (Sangha et al., 1999). Because of the presence of calcium hydroxide, the pH of RCM-water mixtures can exceed 11 which could have an adverse effect on the surrounding environment (Mulligan, 2002).

Foundry Sand (FS)

Annually, the foundry waste in the United States is in the range of 9 to 13.6 million metric tons from different kind of castings (Collins and Ciesielski, 1994). Foundry sand consists primarily of clean, uniformly sized, high-quality silica sand. The grain size distribution of spent foundry sand is very uniform, with approximately 85 to 95 percent of the material falling between 0.15 to

0.6 mm sieve sizes. Five to 12 percent of the foundry sand can be expected to be smaller than 0.075 mm diameter. Spent foundry sand has good durability characteristics.

The oldest molding process and also the most popular technique used in foundry industry is green sand mold which consists of approximately 85 percent of high-quality silica sand, about 4~10 percent clay, 2 to 5 percent water, and about 5 percent carbonaceous materials. Virtually all sand cast molds for ferrous castings are of the green sand type (http://www.tfhrc.gov/hnr20/recycle/waste/fs1.htm). The other molding process is the chemically bonded sand cast systems where one or more organic binders in conjunction with catalysts and different hardening/setting procedures are used. Foundry sand makes up about 97 percent of this mixture (http://www.tfhrc.gov/hnr20/recycle/waste/fs1.htm). Chemically bonded systems are most often used to produce cavities that are not practical to produce by normal molding operations and also for molds for nonferrous castings (http://www.tfhrc.gov/hnr20/recycle/waste/fs1.htm). Spent foundry sand contains some leachable contaminants such as heavy metals and phenols that are absorbed by the sand during the molding and casting operations. Phenols are formed from high-temperature thermal decomposition and rearrangement of organic binders during the metal pouring process. The presence of heavy metals is of significant concerns in non-ferrous foundry sands (Chesner et al., 1997). Therefore, only sands used by iron and steel foundries are recommended for use during highway construction.

RESEARCH OBJECTIVES

1. Characterize the gradation of recycled materials mixed in with virgin aggregates.

2. Develop methodology for packing samples including estimates of optimum water content corresponding to maximum density.

3. Characterize water retention characteristics of mixtures of recycled materials with virgin aggregates.

4. Characterize the resilient modulus and shear strength of recycled material-virgin aggregate mixtures at optimal water content and at a water content corresponding to 300 kPa suction.

5. Characterize heavy metal leaching from recycled material-virgin aggregate mixtures at two degrees of saturation corresponding to 0.2 kPa and -2.0 kPa hydraulic head.

6. Characterize hydraulic conductivity of recycled material-virgin aggregate mixtures at two degrees of saturation corresponding to 0.2 kPa and -2.0 kPa hydraulic head.

7. Summarize results of hydraulic, mechanical and leaching characteristics of recycled materials mixtures with virgin aggregates in terms of their suitability as pavement base materials.

CHAPTER 2-RECYCLED MATERIAL PROPERTIES

SAMPLING LOCATIONS

Four recycled materials and virgin aggregates were supplied by Mn/DOT. The recycled materials were: recycled asphalt pavement (RAP), recycled concrete material (RCM), fly ash (FA), and foundry sand (FS). RAP was collected from trunk highway 61 (Fig. 2.1) whereas RCM was supplied by the city of Minneapolis (Fig. 2.2). Fly ash was taken from the Excel Energy coal burning power plant Riverside 8 and the foundry sand (from ferrous casting) was supplied by Dotson Iron Casting Company in Mankato, MN. Fly ash from Riverside 8 did not meet ASTM requirements for either class C or F (Li et al., 2009). Virgin aggregates were taken from a pit south of Jordan, MN.

Figure 2.1 Recycled asphalt collected from TH 61.

Figure 2.2 Recycled concrete material samples collected from a stockpile in the city of Minneapolis.

RECYCLED MATERIAL MIXTURE PREPARATION

Each recycled material (RAP, RCM, FA, and FS) was mixed with virgin aggregate at various proportions specified by Mn/DOT (Table 2.1). Each mixture was prepared separately a day or two before each test. Mixing process involved weighing out a known amount of a given recycled material and aggregates in the proportion desired and then mixing them in a plastic bag until the

mixtures appeared to be well-bended. The mixing was done by shaking the bag back and forth. Mixing proportions were mass based. A total of seventeen different recycled material mixtures were prepared for various tests. The eighteenth sample was 100% virgin aggregates.

Table 2.1 Proportion of recycled materials and aggregates in various mixtures. All proportions are mass based.

Sample #	Fly Ash	Aggregate	RAP	RCM	Foundry Sand
1	0	75	25	0	0
2	0	50	50	0	0
3	0	25	75	0	0
4	0	0	100	0	0
5	5	70	25	0	0
6	15	60	25	0	0
7	5	45	50	0	0
8	15	35	50	0	0
9	5	20	75	0	0
10	15	10	75	0	0
11	0	75	0	25	0
12	0	50	0	50	0
13	0	25	0	75	0
14	0	0	0	100	0
15	0	95	0	0	5
16	0	90	0	0	10
17	0	85	0	0	15
18	0	100	0	0	0

MATERIAL PROPERTIES

Particle Size Distribution

Particle size distribution of the 17 mixtures and virgin aggregates were obtained through sieve test analysis (ASTM, 2001). The process involved taking a representative sample of each mixture and sieving it through a 19 mm sieve. This sieved material was air dried for 2 days and then about 600 grams of the air dried material was sieved again through a nest of sieves. The material retained on each sieve in a nest sieves was weighed after shaking. The proportion of each grade was calculated as the ratio of the material remaining on the sieve to the total material added to the nest of sieves. The material remaining on the top of 19 mm sieve was discarded. Discarded material (>19 mm diameter) represented less than 10% by volume of the total material received for all four recycled materials and virgin aggregates. This procedure is same as that of Kim and Labuz (2007) and was followed because of the limitation of the mold diameter (152 mm) in which specimens were compacted. Each gradation test was run in duplicate. The gradation curve was plotted by cumulating the proportion of each subsequent higher grade vs. particle diameter. The gradation curves were compared with Mn/DOT specification band for Class 5 granular material (Mn/DOT, 2000) to evaluate the suitability of recycled material mixtures as substitutes of aggregates for base and subbase materials.

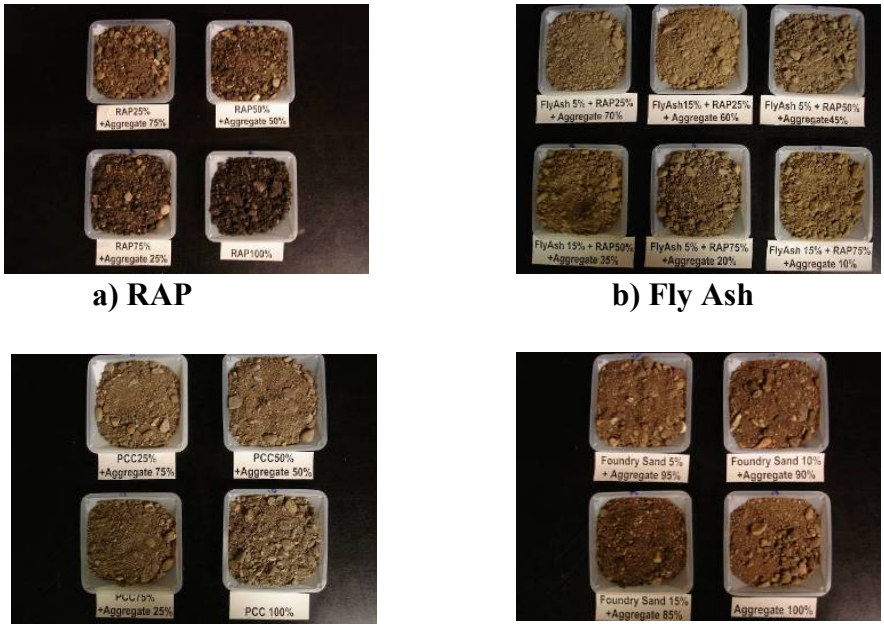

a) RAP **b) Fly Ash**

c) RCM **d) Foundry Sand**

Figure 2.3 Photographs of recycled material mixtures used in laboratory testing.

Compaction Test for Estimating Optimal Water Content and Maximum Dry Density

Compaction affects both the hydraulic and the mechanical properties (hydraulic conductivity, water retention, shear strength, and resilient modulus) of a given porous material. This affect is manifested by a reduction in the volume of large pores and an increase in the volume of medium and small pores. In road construction, all base and subbase materials are compacted to a near maximum density. Proctor test has been used as a standard for evaluating optimum water content needed for achieving maximum density in base and subbase materials. For many years, the use of Proctor compaction test has been called into question for simulating field compaction of granular materials. This is partially because maximum densities are not reached with this drop hammer test as compared to tests that use other compactors such as the vibratory or gyratory compactors. An additional problem with the Proctor test is that excess moisture can escape from the Proctor mold during compaction.

McRae (1962) showed that the gyratory compactor introduced by the Army Corps of Engineers is better able to simulate field compaction than the impact compaction procedure in a standard Proctor test. Based on the work by McRae (1962), ASTM has standardized the gyratory compaction method (ASTM D-3387). This method, however, has not been widely implemented in road research because there are no standards for gyratory variables (e.g. gyration angle, number of gyrations, normal stress, and rate of gyrations) that can be used for compacting subgrade and subbase materials. White et al. (2007) studied various (impact, static, vibratory, and gyratory) compaction techniques to mold specimens in the laboratory and how these techniques affected the strength (σ_{max}) and stiffness (M_R) of the molded specimens. Two soils used in their study were mixed glacial till "sandy lean clay" from MnROAD project in Albertsville, MN, and well graded sand with silt material from TH 64 south of Ackley, MN. The

authors concluded that the moisture-density curves were distinctly different between impact, static, vibratory, and gyratory compaction methods. There was no statistical difference in M_R values between impact and vibratory methods. However, vibratory compacted samples had similar or slightly higher σ_{max} than the impact compacted samples for the granular soil. Density growth curves from the gyratory compaction technique were generally similar to that with the static compaction technique. The maximum dry density achieved after 50 gyrations was greater than the standard static and the modified Proctor dry densities at three moisture contents. Kim and Labuz (2007) compared the compaction efficiency of standard Proctor and gyratory compaction methods relative to the field results that were obtained using the sand cone test. The results showed that gyratory compaction was better than the Proctor compaction in simulating field condition. Recent works by Browne (2006) also arrived at similar conclusions. It was for these reasons that a gyratory compactor was used in the present study to determine the optimum moisture content for achieving the maximum dry density of recycled material mixtures.

The gyratory compaction specifications were same as that of Kim and Labuz (2007) i.e. a 152 mm diameter specimen mold with the base rotation at constant 30 revolutions per minute, the mold positioned at a compaction angle of 1.25 degrees, the compaction pressure of 600 kPa, and a maximum application of 50 gyrations (Fig. 2.4). The compaction procedure involved pouring 5.0 kg sample of recycled material mixtures with virgin aggregate (passed through 19 mm sieve) at a given moisture content in the specimen mold and compacting the specimen until the compaction pressure of 600 kPa or 50 gyrations were reached. This process was repeated for different water contents until the maximum dry density and the optimum moisture content for each mixture were identified (Table 2.3). Moisture content of the sample was determined by weighing about 200 g of materials (triplicate) from the mold and drying it in an oven at 105^{o}C for 48 hours.

Figure 2.4 A gyratory compactor set-up.

RESULTS AND DISCUSSION

Particle Size Distribution of Recycled Materials

In Table 2.2 are listed the particle amount (average and standard deviation) passing a given size sieve for four recycled materials. The results show that RAP and FA contained coarser fractions than RCM and FS. The following text describes the particle size distribution of various mixtures of recycled materials with virgin aggregates and how their distribution fit within Mn/DOT Class 5 specifications.

Table 2.2 Gradation of recycled material mixtures.

Sieve Size (mm)	Percent Passing			
	RAP	**Fly Ash**	**RCM**	**Foundry Sand**
19.05	100±0.00	100.00±0.00	100.00±0.00	100.00±0.00
9.25	83.91±4.07	85.99±2.73	83.11±2.77	86.31±1.18
5.66	66.61±8.29	69.95±4.69	70.06±4.26	75.99±0.99
2.00	40.02±13.24	43.76±6.84	51.72±3.30	58.96±0.52
1.00	25.01±11.53	28.40±6.37	38.72±2.23	44.09±1.49
0.85	21.08±10.10	24.54±5.77	34.75±2.71	38.64±1.87
0.50	8.90±4.14	12.57±3.23	20.58±3.94	20.98±3.22
0.43	6.64±3.10	10.45±2.86	17.93±4.54	17.79±3.49
0.30	3.26±1.72	6.86±2.47	11.43±3.62	10.02±1.91
0.25	2.30±1.33	5.73±2.36	8.24±2.16	6.78±1.29
0.21	1.74±1.09	5.03±2.287	6.67±1.79	4.68±0.97
0.11	0.48±0.38	3.17±1.90	2.37±0.66	0.71±0.06

RAP – Aggregate Mixtures

The four RAP-aggregate mixtures were: 100% RAP, 75% RAP + 25% Aggregates, 50% RAP + 50% Aggregates, 25% RAP + 75% Aggregates. Figure 2.5 shows the gradation curve for the RAP mixtures as well as 100% RAP and virgin aggregates. From this it is apparent that the addition of RAP increases the amount of granular material and decreases the fine content of the mixture. Conversely, addition of virgin aggregates increases the fines and lessens the coarse particles in a RAP-aggregate mixture. Except for the presence of higher fine content, all RAP-aggregate mixtures fall within the Mn/DOT specification bands for Class 5 materials.

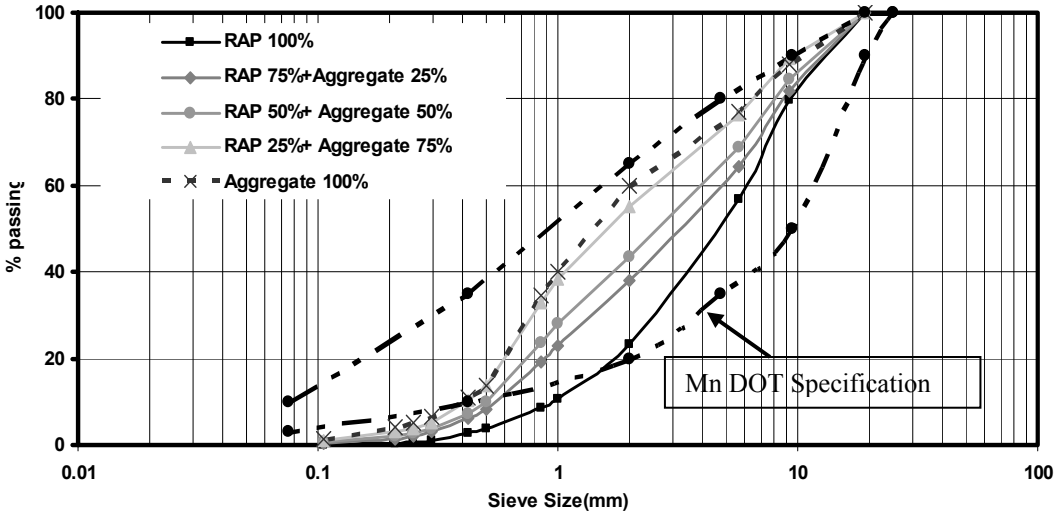

Figure 2.5 Gradation curves for mixtures of RAP and aggregate materials.

Fly Ash-RAP – Aggregate Mixtures

The six FA-RAP-aggregate mixtures were: 5% FA + 25% RAP+ 70% aggregate, 15% FA + 25% RAP+ 60% aggregate, 5% FA + 50% RAP+ 45% aggregate, 15% FA + 50% RAP+ 35% aggregate, 5% FA + 75% RAP+ 20% aggregate, and 15% FA + 75% RAP+ 10% aggregate. The particle size distribution of FA-RAP-aggregate mixtures is shown in Fig. 2.6. Except for fine contents, gradation curves of all FA-RAP-aggregate mixtures were within a narrow band and mostly met the Mn/DOT specification for Class 5. The fine contents of some FA-RAP-aggregate mixtures were slightly higher than the Class 5 specifications.

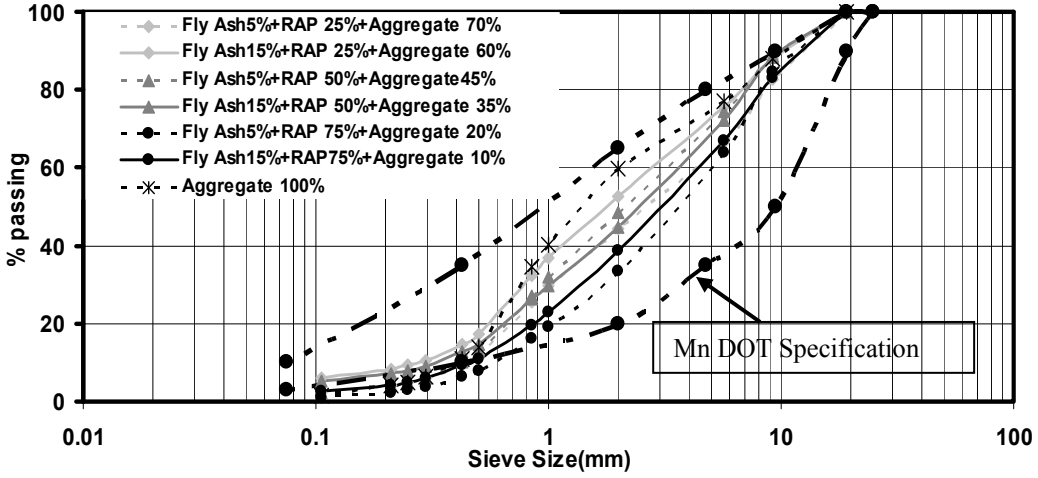

Figure 2.6 Gradation curves for mixtures of fly Ash, RAP, and aggregate mixtures.

Reclaimed Concrete Material (RCM) – Aggregate Mixture

The four RCM-aggregate mixtures were: 25% RCM + 75% Aggregates, 50% RCM + 50% Aggregates, 75% RCM + 25% Aggregates, and 100% RCM. The gradation curves from the sieve analysis (Figure 2.7) show that all mixtures of RCM and aggregate were within a very narrow band i.e. addition of 25 to 75% of aggregates in RCM did not change the gradation curves relative to 100% RCM material. Gradation curves of all RCM mixtures also fell within the Mn/DOT specification band for Class 5 materials. Relative to 100 % virgin aggregates, RCM mixtures generally had slightly higher coarser and finer fractions.

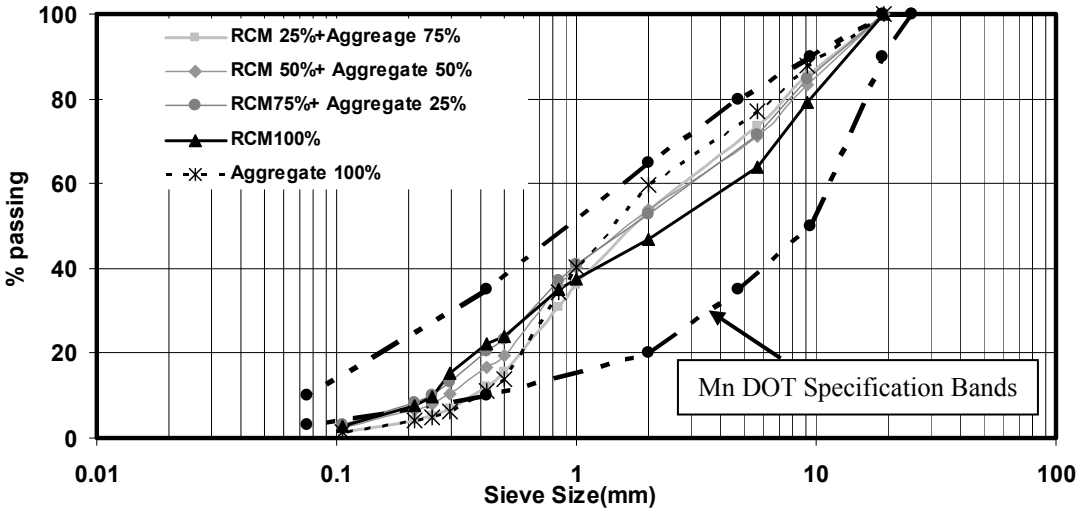

Figure 2.7 Gradation curves for mixtures of RCM and aggregate materials.

Foundry Sand – Aggregate Mixture

The three foundry sand-aggregate mixtures were: 5% FS + 95% aggregates, 10% FS + 90% aggregates, and 15% FS + 85% aggregates. The gradation curves of the mixtures were nearly same as that of the 100% virgin aggregates. The gradation curves also show (Fig. 2.8) that in the range of 5 to 15% addition (by mass) of foundry sand does not change the gradation curve of the mixtures. The above three gradation curves for foundry sand-aggregate mixtures fell within the specification band for Class 5 materials.

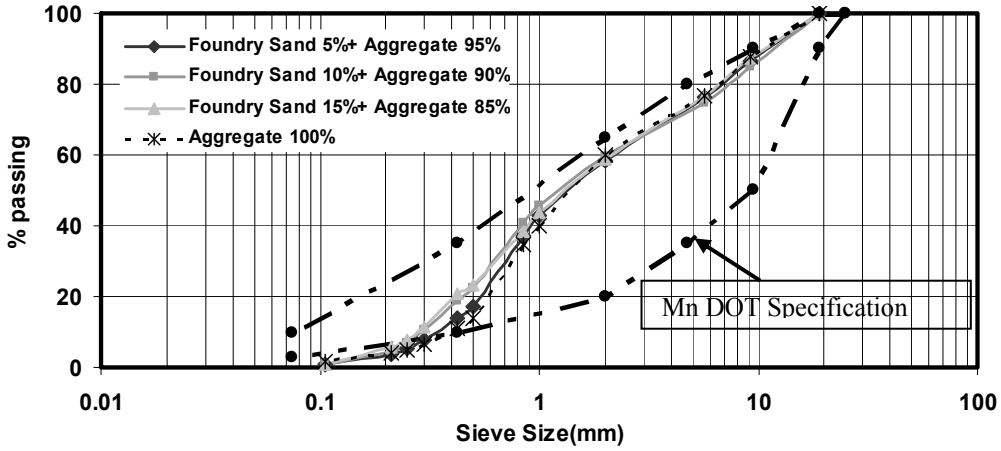

Figure 2.8 Gradation curves for mixtures of foundry sand and aggregate materials.

Optimal Water Contents and Maximum Densities

Maximum dry densities (MDD) and optimum moisture contents (OMC) for seventeen mixtures and 100% virgin aggregates are summarized in Table 2.3. Test results on the gyratory compaction curves for various mixtures are given in Figs. 2.9 to 2.12. The lowest optimum water content (4%) and the highest maximum dry density (2.12 g/cm^3) were for 100% RAP. The highest OMC was 10.2% for 15% FA-25% RAP- 60% aggregate mixture whereas the lowest MDD was 1.94 Mg/m^3 for RCM 100%. A mixture containing 15% FA had higher OMC but lower MDD than a mixture containing 5% FA 5%. Addition of RCM appeared to decrease the MDD value whereas foundry sand addition showed no affect on MDD and OMC. A comparison of OMC and MDD values for RAP mixtures (25% RAP- 75% aggregate, 50% RAP- 50% aggregate, 75% RAP-25% aggregate) between our study and that of Kim and Labuz (2007) showed that their values of MDD were slightly lower (2.032 g/cm^3) than our results (2.065~2.12 g/cm^3). However, their values of OMC (7.2~8.7%) were slightly higher than that of our results (4.0~7.8 %). Kim and Labuz (2007) value of OMC for 100% aggregate was 8.8%, a slightly lower than our results (9.2%).

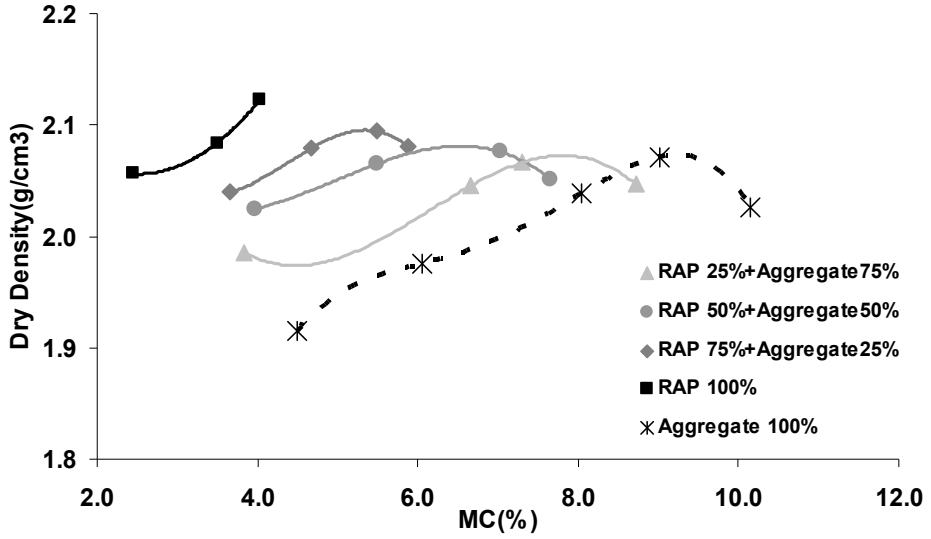

Figure 2.9 Gyratory compacted dry densities of RAP-aggregate mixtures as a function of water contents.

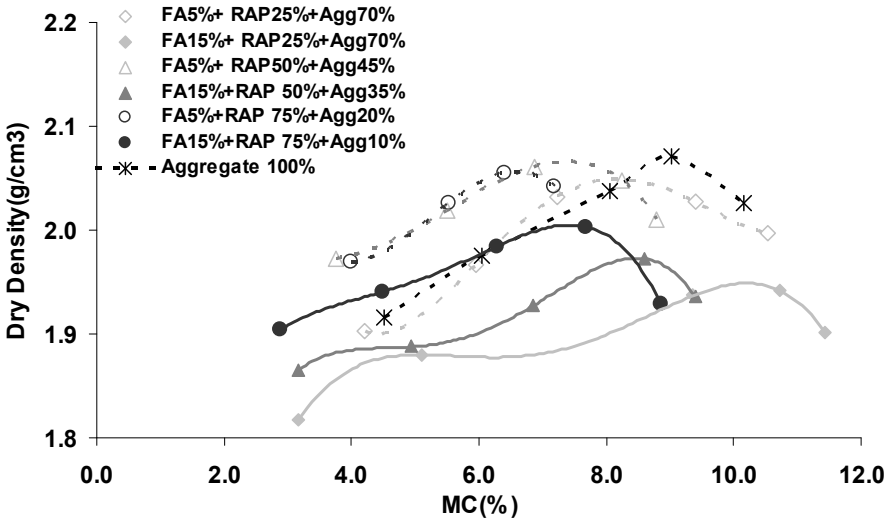

Figure 2.10 Gyratory compacted dry densities of FA-RAP-aggregate mixtures as a function of water contents.

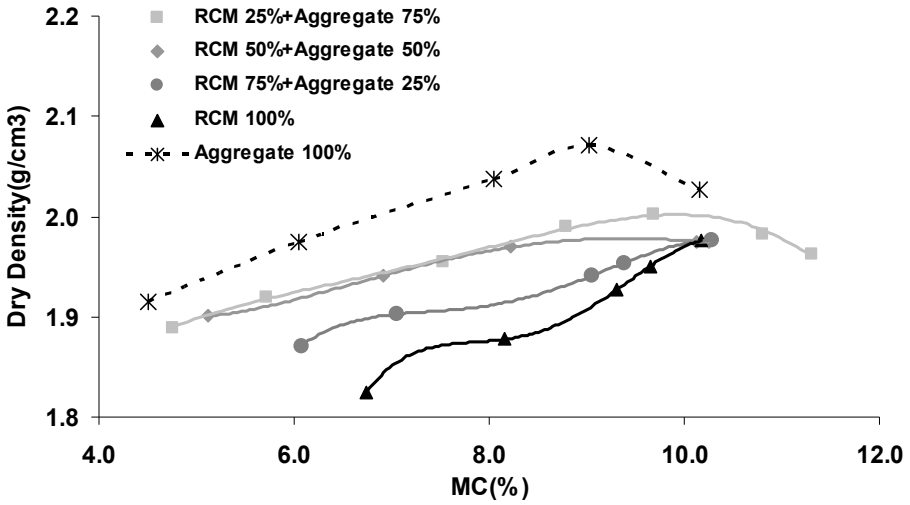

Figure 2.11 Gyratory compacted dry densities of RCM-aggregate mixtures as a function of water contents.

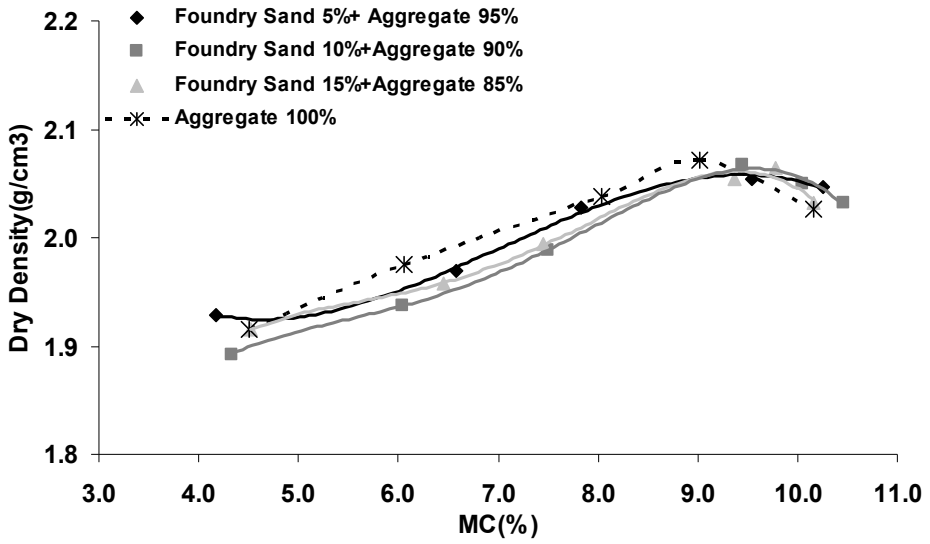

Figure 2.12Gyratory compacted dry densities of FS-aggregate mixtures as a function of water contents.

Table 2.3 Maximum dry densities and the corresponding optimum water contents for various mixtures of recycled materials with aggregates estimated using a gyratory compactor.

Materials	Maximum Dry Density (g/cm^3)	Optimum Moisture Content (%)
RAP25%+ Aggregate 75%	2.07	7.8
RAP50%+ Aggregate 50%	2.07	6.6
RAP75%+ Aggregate 25%	2.08	5.4
RAP100%	2.12	4.0
Fly Ash 5% +RAP25%+Aggregate 70%	2.05	8.2
Fly Ash 15% +RAP25%+Aggregate 60%	1.95	10.2
Fly Ash 5% +RAP50%+Aggregate 45%	2.07	7.4
Fly Ash 15% +RAP50%+Aggregate 35%	1.97	8.6
Fly Ash 5% +RAP75%+Aggregate 20%	2.06	6.6
Fly Ash 15% +RAP75%+Aggregate 10%	2.00	7.4
RCM 25%+ Aggregate 75%	2.00	9.8
RCM 50%+ Aggregate 50%	1.98	9.4
RCM 75%+ Aggregate 25%	1.95	9.4
RCM 100%	1.94	9.4
Foundry Sand 5%+ Aggregate 95%	2.07	9.4
Foundry Sand 10%+ Aggregate 90%	2.07	9.4
Foundry Sand 15%+ Aggregate 85%	2.07	9.4
Aggregate 100%	2.07	9.2

CONCLUSIONS

Mixtures of four recycled materials (FA, RAP, RCM, and FS) with virgin aggregates fell within the specification band for Class 5 materials. Maximum dry densities varied between 1.94 and 2.12 g/cm^3. Optimum water contents varied from 4.2% for 100% RAP to 10.2% for 15% Fly Ash +25% RAP25%+60% Aggregate mixtures. These water contents corresponded to suction <300 kPa.

CHAPTER 3-WATER RETENTION CHARACTERIZATION

INTRODUCTION

Soil water retention refers to the mechanism with which water is held in soil pores. The relationship between the amount of water and the force with which that water is held is called soil water retention characteristic curve (SWRCC) (Gupta and Wang, 2002). This relationship is unique for each soil or porous media. The soil water content can be expressed as gravimetric water content, volumetric water content, or degree of saturation. The force is generally expressed as soil matric potential or soil matric suction (Zapata, 1999).

Several mathematical models have been proposed to estimate the SWRCC. Gupta and Larson (1979) were among the first who developed Pedo-transfer functions to predict water retention characteristics of soils using easily measureable soil properties such as soil texture, organic matter, and bulk density. Since mid 1960's there have been many efforts in better mathematical representation (Brook and Corey, 1964; Campbell, 1974; van Genuchten, 1980) as well as prediction (Mualem, 1976; Arya and Paris, 1981) of hydraulic properties based on material characterization. The most popular representations of SWRCC are the analytical formulations developed by van Genuchten (1980) and Fredlund and Xing (1994).

Van Genuchten Function:

$$\Theta(h) = \left[\frac{1}{1 + (\alpha h)^n} \right]^m \qquad [3.1]$$

$$\Theta = \frac{\theta - \theta_r}{\theta_s - \theta_r} \qquad [3.2]$$

where Θ is the normalized water content, θ_s and θ_r are saturated and residual water contents respectively, α is inverse of the air-entry value, h is matric potential, and m and n are constants that describe the shape of the water retention curve and are related to each other as; m=1-1/n.

Fredlund and Xing Function:

$$\theta = \theta_s \left[1 - \frac{\ln\left(1 + \frac{h}{h_r}\right)}{\ln\left(1 + \frac{10^6}{h_r}\right)} \right] \left[\frac{1}{\ln\left[\exp(1) + \left(\frac{h}{a_f} \right)^{n_f} \right]} \right]^{mf} \qquad [3.3]$$

where h_r is the suction at which residual water content occurs, a_f is a soil parameter (kPa) which is a function of air entry value, n_f is slope of the line and describes the rate of water extraction once the air entry value has been exceeded, and m_f is a soil parameter which is a function of the residual water content. Fredlund and Xing (1994) function assume that soil water content is zero at a matric suction of 10^6 kPa. Our past work shows that the Fredlund and Xing function may estimate lower moisture contents than are reasonable for high clay soils as the function approaches 10^6 kPa suction. Work continues to clarify this issue, however this does not present a

large problem for the soil types and moisture content ranges common in most pavement foundation construction sites (Kang et al., 2010). Fredlund and Xing (1994) function is more often used in soil mechanics literature whereas Van Genuchten is more popular in soil science literature.

Although there is a large amount of data available on soil water retention characteristics for loose agricultural soil, water retention data for low clay and highly compacted materials such as aggregate base or granular subgrade are limited. Recently, Minnesota Department of Transportation (Mn/DOT) has been using small database in SoilVision® to estimate water retention of compacted aggregate base, granular, subbase and subgrade soils used in pavement construction (Gupta et al., 2004). In this chapter, we discuss the water retention characterization of 17 mixtures of 4 recycled materials with aggregates and a sample of 100% virgin aggregate (Table 2.1).

MATERIALS AND METHODS

The procedure for measuring water retention curves involved preparing a sample of a given mixture at optimum water content and then packing the specimen to a maximum density listed in Table 2.3. The specimen dimensions after compaction were 152.4 mm in diameter and 76.2 mm in height. Specimen preparation was done using a gyratory compactor. After compaction, the specimen was coated with molten Paraffin wax to prevent its collapse during saturation (Figure 3.1). The temperature of molten paraffin was around 60 ºC. This temperature has been identified as the best temperature that quickly solidifies paraffin wax without letting it penetrate into the soil pores (Blake, 1965; Abrol and Palta, 1968; Cresswell and Hamilton, 2002). After paraffin coating, the specimen was placed on a ceramic plate containing a small amount of fine clay soil. The clay soil on the ceramic plate helped improve the contact between the specimen and the ceramic plate. The specimen was then saturated from bottom up under a small head of water in a dish container. After saturation, the ceramic plate with specimen was taken out of the plastic container and placed in a pressure chamber (500 kPa or 1500 kPa). The lid of the pressure chamber was then closed and a known air pressure was applied. At any given pressure, the specimen was allowed to desorb until no more water came out of the specimen. At each pressure step, the desorbed water was collected in a burette and a record was made of the water volume.

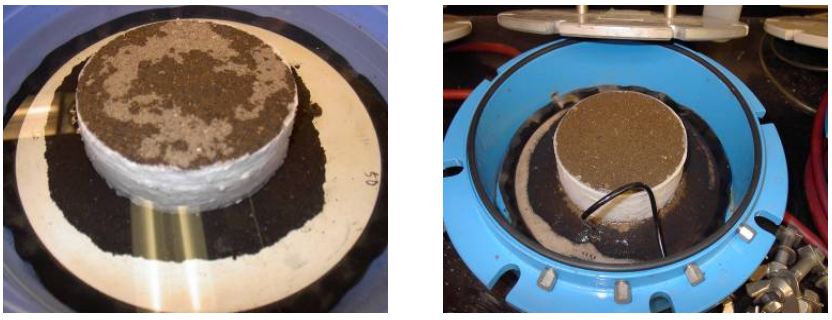

Figure 3.1 Paraffin coated specimen being saturated from bottom up under a small head of water and the placement of the specimen in the pressure chamber before the lid being bolted and air pressure being applied.

Once equilibrium was reached at a given pressure, the specimen was then subjected to the next air pressure and outflow was again measured. This process was repeated until the air pressure equivalent to the air entry value (500 kPa or 1500 kPa) of the ceramic plate was reached. At that point, the specimen was taken out of the pressure chamber, weighed, and then oven dried at 105 ^{o}C. Water content at a given pressure was then back calculated from the final water content of the specimen and the volume of outflow between pressure steps. Water retention curves for the recycled material covered a matric head in the range of -3 to -1000 kPa. Two sets of pressure plate apparatus, 500 kPa pressure chamber (3 to 306 kPa suction) and 1500 kPa (102 to 1020 kPa suction), comprise the setup for air pressure application. The pressure ranges overlapped and thus helped verify the accuracy of the results obtained from two different specimens in two different pressure apparatuses. Water retention test for small specimens (38.5 mm x 76mm) was also conducted to access the effect of specimen size. The results are listed in Appendix Figure A1 to A4 for Fredlund and Xing Equation, and Figures A6, A8, A10, and A12 for van Genuchten Equation.

RESULTS AND DISCUSSION

Figures 3.2 to 3.5 show the water retention characteristics of 17 mixtures of 4 recycled materials with aggregates and 100% virgin aggregate. The lines in the figures are the best fit of the Fredlund and Xing equation. The best fit lines for the van Genuchten's equation are given in Appendix A. The value of the coefficients for both Fredlund and Xing and van Genuchten's equations are given in Tables 3.1 and 3.2, respectively.

RAP – Aggregate Mixtures

Figure 3.2 shows the change in water retention of aggregates with addition of RAP. Relative to 100% aggregates, there is a slight decrease in the water retention of various mixtures at mid suctions from 100 to 10,000 kPa. In contrast, there is a large change in water retention of mixtures relative to 100% RAP. At any given suction, degree of saturation slightly decreased with addition of RAP to aggregates. Air entry of all RAP mixtures, 100% RAP, and 100% aggregates were about same.

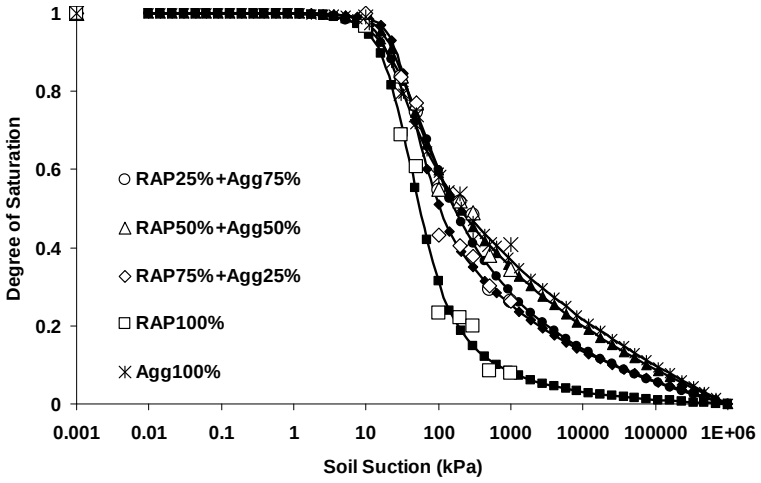

Figure 3.2 Water retention characteristic of RAP-Aggregate mixtures. Solid line is the best fit line representing Fredlund and Xing function. Empty symbols are measured values using large specimens (diameter: 152.4 mm and height: 76.2 mm).

FA-RAP – Aggregate Mixtures

At a given suction, water retention of FA-RAP-aggregate mixtures was slightly higher than that of the pure aggregates. However for a given RAP content, there was very little difference in water retention of the mixtures containing 5% or 15% fly ash. For mixtures containing 75% RAP, water retention was less than that of the 100% aggregates.

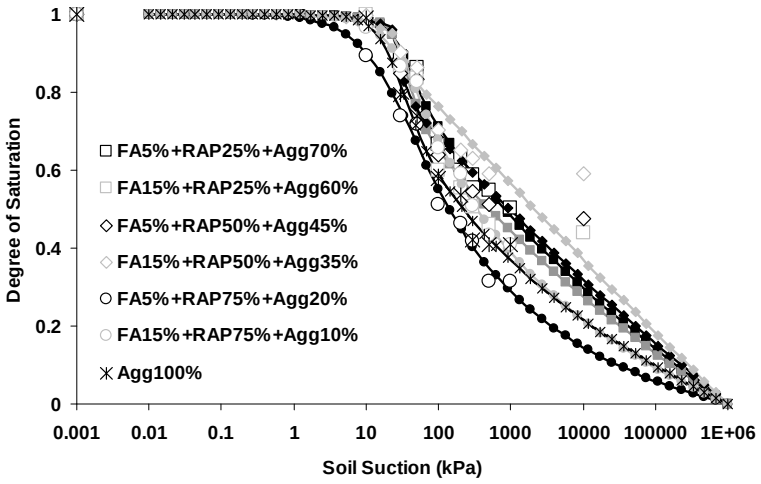

Figure 3.3 Water retention characteristic of FA-RAP-Aggregate mixtures. Solid line is the best fit line representing Fredlund and Xing function. Empty symbols are measured values obtained using large specimens (diameter: 152.4 mm and height: 76.2 mm).

Reclaimed Concrete Material – Aggregate Mixtures

Practically, there was no difference in water retention of various mixtures of RCM with aggregates. In general, water retention of RCM mixtures was higher than that of the 100% aggregates. There was a slight difference in the air-entry value of 100% RCM compared to other RCM mixtures and 100% aggregates. This difference may be due to one measurement near the air-entry value. Air-entry of all other RCM mixtures was nearly same among themselves as well as relative to 100% aggregates.

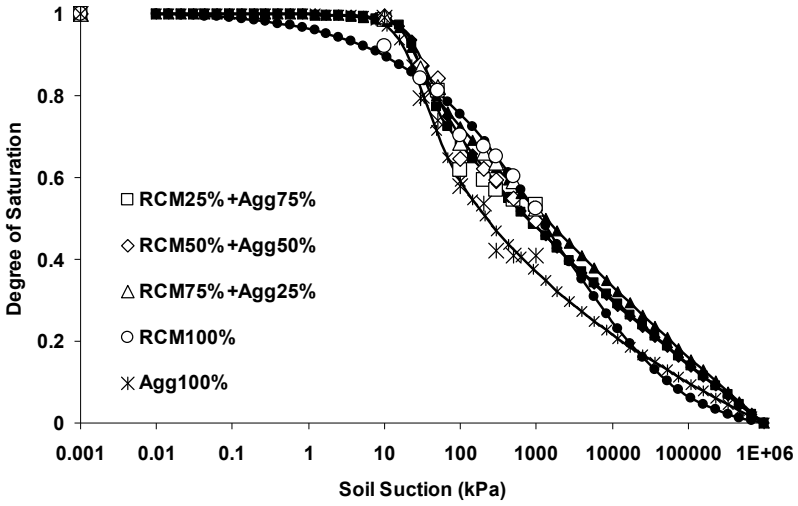

Figure 3.4 Water Retention characteristic of RCM-Aggregate mixtures. Solid line is the best fit line representing Fredlund and Xing function. Empty symbols are measured values obtained using larger specimens (diameter: 152.4 mm and height: 76.2 mm).

Foundry Sand – Aggregate Mixtures

There were small differences in the water retention of FS mixtures with aggregates. Water retention of 5% to 10% foundry sand mixture was nearly same as that of 100% aggregates. This is expected considering that foundry sand are coarse material and does not have much retention capacity of its own. At about 1,000 kPa, water retention of 15% foundry sand was slightly higher than that of 5 and 10% foundry sand mixtures and 100% aggregates. This suggests that addition of additional foundry sand over and above 15% may alter the water retention of foundry sand mixtures with aggregates. Air entry of all foundry sand mixtures with aggregates was about same.

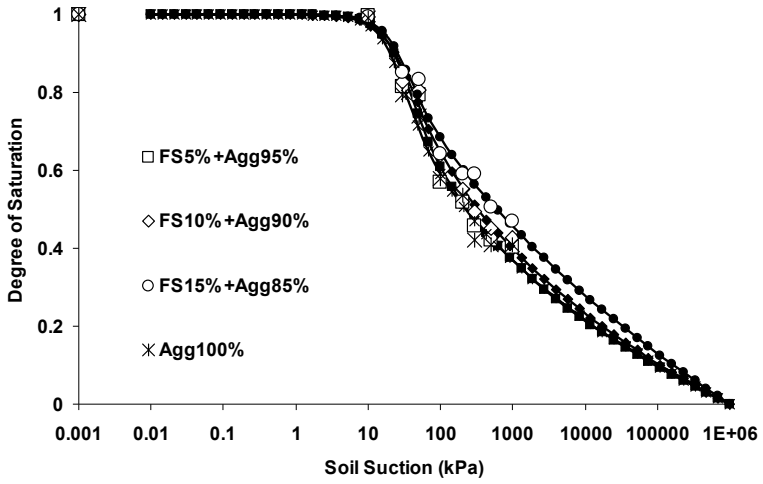

Figure 3.5 Water Retention characteristic of FS-Aggregate mixtures. Solid line is the best fit line representing Fredlund and Xing function. Empty symbols are measured values obtained using large specimens (diameter: 152.4 mm and height: 76.2 mm).

Table 3.1 Fredlund and Xing function parameters for recycled materials - aggregate mixtures.

	θ_s	a_f	n_f	m_f	h_r	R^2
100% Agg	0.26	19.26	2.71	0.31	135.66	0.98
25% RAP+75%Agg	0.23	33.35	1.48	1.68	455.17	0.98
50% RAP+50%Agg	0.20	25.06	2.58	0.36	172.31	0.99
75% RAP+25%Agg	0.18	31.45	3.20	0.46	142.29	0.98
100% RAP	0.16	31.34	2.05	1.15	149.66	0.98
5% FA+25% RAP+70% Agg	0.26	26.06	3.35	0.18	122.71	0.98
15% FA+25% RAP+60% Agg	0.32	24.88	20.00	0.08	57.06	0.89
5% FA+50% RAP+45% Agg	0.23	26.05	20.00	0.04	35.69	0.75
15% FA+50% RAP+35% Agg	0.29	19.38	1.17	0.69	392.23	0.99
5% FA+75% RAP+20% Agg	0.20	19.38	1.17	0.69	392.23	0.99
15% FA+75% RAP+10% Agg	0.24	30.75	1.60	0.45	408.07	0.99
25% RCM+75% Agg	0.28	21.44	6.01	0.13	71.52	0.97
50% RCM+50% Agg	0.28	22.89	3.66	0.17	104.24	0.98
75% RCM+25% Agg	0.27	18.97	5.48	0.10	67.84	0.99
100 % RCM	0.26	10.49	1.11	0.28	422.39	0.99
5% FS + 95% Agg	0.28	22.82	2.55	0.33	156.06	0.98
10% FS + 90% Agg	0.28	22.79	2.10	0.33	210.94	0.99
15% FS + 85% Agg	0.28	21.22	2.75	0.22	137.83	0.98

Table 3.2 van Genuchten function parameters for recycled materials - aggregate mixtures.

	θ_s	θ_r	α	n	m	R^2
100% Agg	0.26	0.11	0.08	3.00	0.10	0.98
25% RAP+75%Agg	0.23	0.06	0.04	2.13	0.20	0.98
50% RAP+50%Agg	0.20	0.07	0.06	3.00	0.11	0.99
75% RAP+25%Agg	0.18	0.05	0.04	3.00	0.17	0.98
100% RAP	0.16	0.01	0.03	1.88	0.79	0.98
5% FA+25% RAP+70% Agg	0.26	0.13	0.06	3.00	0.07	0.98
15% FA+25% RAP+60% Agg	0.32	0.14	0.11	3.00	0.06	0.93
5% FA+50% RAP+45% Agg	0.23	0.11	0.13	3.00	0.04	0.88
15% FA+50% RAP+35% Agg	0.29	0.17	0.05	1.20	0.33	0.99
5% FA+75% RAP+20% Agg	0.20	0.06	0.05	1.20	0.33	0.99
15% FA+75% RAP+10% Agg	0.24	0.10	0.04	1.76	0.18	0.99
25% RCM+75% Agg	0.28	0.15	0.09	3.00	0.06	0.96
50% RCM+50% Agg	0.28	0.14	0.07	3.00	0.07	0.98
75% RCM+25% Agg	0.27	0.14	0.09	3.00	0.06	0.99
100 % RCM	0.26	0.13	0.00	0.51	0.77	0.98
5% FS + 95% Agg	0.28	0.11	0.06	3.00	0.10	0.98
10% FS + 90% Agg	0.28	0.12	0.06	3.00	0.09	0.99
15% FS + 85% Agg	0.28	0.13	0.07	3.00	0.07	0.98

CONCLUSIONS

Water retention characteristics reflect the pore size distribution of a porous media which in turn affects the hydraulic conductivity, and stiffness and strength of the material. Above comparisons of the water retention characteristic with 100% virgin aggregates show that the shape of the pore size distribution curves of recycled mixtures used in this study are nearly similar to that of 100% aggregates. This suggests that for most part drainage, stiffness, and strength characteristics of recycled materials mixtures with virgin aggregates will also be somewhat similar to that of 100% virgin aggregates.

CHAPTER 4-RESILIENT MODULUS AND SHEAR STRENGTH CHARACTERIZATION

INTRODUCTION

Pavements are constructed on foundation layers called the base, subbase, and subgrade and thus pavement performance is highly affected by the stiffness of these layers. One commonly used parameter that defines soil stiffness is the resilient modulus (M_R), defined as the ratio of the peak axial repeated deviator stress to the peak recoverable axial strain of the specimen. The concept of the resilient modulus was developed by the Strategic Highway Research Program (SHRP) in 1987 and it has become one of the principal parameters in pavement design procedures. In 1996, the Federal Highway Administration (FHWA) proposed a standard protocol for M_R testing known as Long Term Pavement Performance Protocol (LTPP P46). A revised version of this protocol is described in National Cooperative Highway Research Program (NCHRP, 2004) and is currently followed by Mn/DOT. The major difference between both protocols for granular soils is the number of loading sequences; LTPP P46 had 15 sequences while NCHRP 1-28A has 30 sequences.

In the NCHRP 1-28A repeated test protocol, cycles of axial stress are applied to cylindrical specimens (305 mm in height and 152 mm in diameter) at a given confining pressure in a triaxial cell. Each test cycle consists of a haversine loading pulse for 0.1 or 0.2 s and the material recovery for a period of 0.8 s or 0.9 s. NCHRP 1-28A protocol also has a conditioning step before M_R data collection. The conditioning sequence is the application of a confining pressure of 103.5 kPa and 1000 cycles of 207 kPa deviator stress. In the measurement mode, the loading and relaxation cycles are repeated 100 times for each applied load and deviator stress combination. In total, the specimen goes through a total of 30 combinations of confining pressure and deviator stress (Table 4.1). M_R values are calculated from the recoverable axial strain and the corresponding cyclic axial stress for the last five cycles in each sequence (NCHRP, 2004).

In Table 4.1, contact stress is the axial stress applied to a specimen that maintains a positive contact between the specimen cap and the specimen. On the other hand, the cyclic stress is repetitive haversine axial stress applied to a test specimen. Maximum axial stress is the sum of contact stress and cyclic stress. Since the resilient modulus test is usually thought of as a non-destructive test, the same sample is used for all sequences under different loading and confinement. However in the NCHRP 1-28A loading protocol, larger stresses are applied to the specimen compared to the LTTP P46 protocol. This means, some specimens may fail at higher load sequences (Kim and Labuz, 2007). In our study there were some instances when the sample failed in the last few sequences of the M_R test.

In this study, we characterized the resilient modulus of 17 mixtures of 4 recycled materials (RAP, RCM, FA, FS) with virgin aggregates and one sample of 100% virgin aggregates. All resilient modulus measurements were performed at two water contents; the optimum water content (<300 kPa suction) and water content corresponding to 300 kPa suction. Figure 4.1 shows an example of the relationship between load and displacement for last 5 cycles of specimen representing a mixture of 5% FA + 20% RAP + 75% Aggregate.

Table 4.1 Testing sequences recommended by NCHRP 1-28A Protocol for M_R measurements of base/Sub-base materials.

Sequence	Confining Pressure	Contact Stress	Cyclic Stress	Maximum Stress	Nrep†
	kPa	kPa	kPa	kPa	
0	103.5	20.7	207.0	227.7	1000
1	20.7	4.1	10.4	14.5	100
2	41.4	8.3	20.7	29.0	100
3	69.0	13.8	34.5	48.3	100
4	103.5	20.7	51.8	72.5	100
5	138.0	27.6	69.0	96.6	100
6	20.7	4.1	20.7	24.8	100
7	41.4	8.3	41.4	49.7	100
8	69.0	13.8	69.0	82.8	100
9	103.5	20.7	103.5	124.2	100
10	138.0	27.6	138.0	165.6	100
11	20.7	4.1	41.4	45.5	100
12	41.4	8.3	82.8	91.1	100
13	69.0	13.8	138.0	151.8	100
14	103.5	20.7	207.0	227.7	100
15	138.0	27.6	276.0	303.6	100
16	20.7	4.1	62.1	66.2	100
17	41.4	8.3	124.2	132.5	100
18	69.0	13.8	207.0	220.8	100
19	103.5	20.7	310.5	331.2	100
20	138.0	27.6	414.0	441.6	100
21	20.7	4.1	103.5	107.6	100
22	41.4	8.3	207.0	215.3	100
23	69.0	13.8	345.0	358.8	100
24	103.5	20.7	517.5	538.2	100
25	138.0	27.6	690.0	717.6	100
26	20.7	4.1	144.9	149.0	100
27	41.4	8.3	289.8	298.1	100
28	69.0	13.8	483.0	496.8	100
29	103.5	20.7	724.5	745.2	100
30	138.0	27.6	966.0	993.6	100

†Nrep: Number of replications

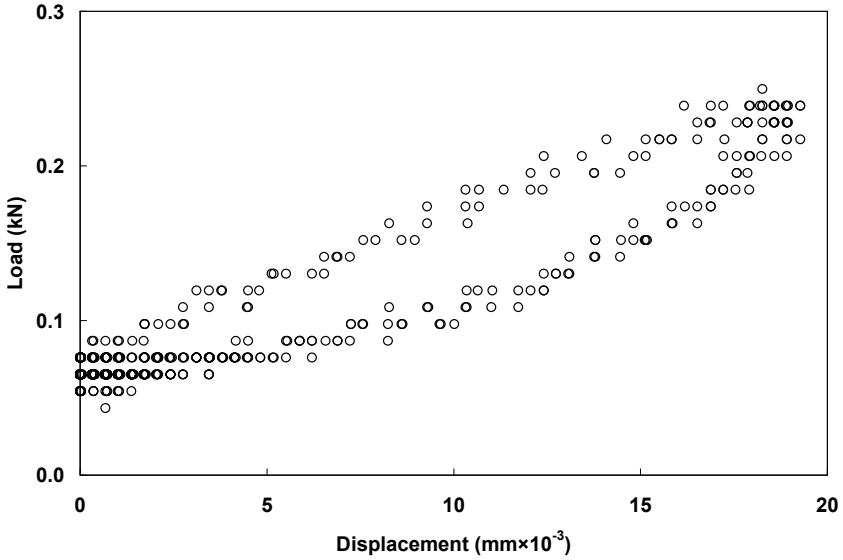

Figure 4.1 Variation in load vs. displacement in last five cycles of sequence 1 of a mixture containing 5% FA + 20% RAP + 75% Aggregate.

MATERIALS AND METHODS

Resilient Modulus Measurements

The procedure for testing resilient modulus of recycled material mixtures in this study was similar to that Kim and Labuz (2007). Briefly it involved preparation of two specimens of a given mixture at optimum water content, packing them to a target density using the gyratory compactor, stacking the two specimen one above the other, and subjecting the stacked specimens to 30 sequences of various applied loads at different confining pressures listed in Table 1. As we stated in earlier chapters, target water content was achieved by spraying a known amount of water to a given amount of a recycled mixture in a plastic bag and then thoroughly mixing the contents by shaking the bag back and forth. Spraying of the water was done in small increments. After mixing, the moist samples were allowed to equilibrate for 24 to 48 hours before packing the moist material in a 152 mm diameter mold using a gyratory compactor. The gyratory compactor was set at a maximum of 100 gyrations with compaction pressure of 600 kPa, base rotation of 30 revolution per minute, compaction angle of 1.25 degree and final specimen height of 140 mm.

Three resilient modulus tests were carried out for each recycled mixture. Two tests were run at optimum water content whereas the third test was run at lower than optimum water content. Specimens at lower than optimum water content were packed at optimal water content. However after packing, the specimens were coated with paraffin wax, saturated with deionized water, and then brought to equilibrium at an air pressure of 300 kPa in a pressure plate apparatus. Like in water retention tests, the specimens were coated with paraffin wax to prevent their collapse during saturation. Other steps in bringing the specimens to 300 kPa suction were same as in water retention measurements.

Resilient modulus test was done in the same triaxial cell (Research Engineering, Grass Valley, CA) as used by Kim and Labuz (2007). The cell had a capacity to hold a cylindrical

specimen 305 mm in height and 152 mm in diameter. The cell chamber was made of 13 mm thick Plexiglas that could withstand an air pressure of at least 170 kPa (Figure 4.2).

Figure 4.2 Loading frame and triaxial cell used for resilient modulus tests.

Two specimens stacked one over the other in the resilient modulus test had an initial total height of approximately 300 mm. Before stacking, the top surface of the bottom specimen was scratched to insure good contact between the specimens. Both specimens were placed on the lower platen. The top of the specimens was then covered with an upper platen and a rubber membrane was slid over the specimens and the platens. Four O-rings were placed in the appropriate grooves on both platens to prevent air leak from applied confining pressure. Membrane covered specimens were then placed inside the triaxial cell. A short stub rising from the base of the triaxial cell fit into a hole in the bottom side of the lower platen and thus help center the specimens. After the specimens were in place, two LVDT containing aluminum collars were then slid around the specimens. Each collar had three LVDTs mounted on it and were equally spaced. Each LVDT had spring-loaded tips and 12.7 mm stroke. First collar was positioned 105 mm above the base whereas the second collar was position at about 152 mm above the first collar. While the collars were being mounted around the specimens, spacers held the collars 152 mm apart. Once the collars were mounted securely, spacers were taken out. The two collars moved independently of each other during testing. This arrangement of the axially-mounted LVDTs on the two collars helped monitor the deformation of the specimen over the 152 mm gage length (Kim and Labuz, 2007).

With the LVDTs in place, the cords from the LVDTs and load cell were attached to the electrical feed throughs. Next the Plexiglas chamber was slid in place over the specimens and the fluid tubing was attached to the exterior of the cell. After assembling, the entire triaxial cell was then lifted and slid into the loading frame and the cords from the signal conditioners were then attached to the electrical feed through. Next, the triaxial cell's load shaft and the triaxial cell's top cap were bolted.

The servo-hydraulic load frame (MTS Systems, Eden Prairie, MN) used in the resilient modulus test had a maximum capacity of 22.2 kN and a maximum stroke of 102 mm (Kim and Labuz, 2007). The frame's actuator was mounted in a crossbeam which could be raised or

lowered to accommodate cells of different sizes. The triaxial cell rested on a steel plate at the base of the load frame and the sequences of load were applied using a digital controller named MTS Test Star on a personal computer.

The resilient modulus test protocol in this study followed the confining pressure and deviator stress sequence suggested in NCHRP 1-28 A. The only modification in this protocol was the complete removal of the axial load before and after changing the cell's confining pressure as suggested by Kim and Labuz (2007). The first step in the test protocol was the pressurization of the cell for the conditioning load sequence. The confining pressure was manually adjusted with a pressure controller and a gauge. Once the pressure within the chamber came to equilibrium, the load shaft was lowered until the load cell came into contact with the ball bearing on the upper platen and a small contact pressure was applied to the specimens. A data collection program named "M_R Data Acquisition" was opened on the personal computer connected to the instruments' signal conditioners. This program was created using LabVIEW (National Instruments, Austin, TX) and the program recorded data from the load cell and the LVDT strokes at a rate of 200 points per second.

The conditioning loading sequence was repeated 1000 times whereas the subsequent loading sequences were repeated 100 times. Each of the subsequent loading sequences were initiated in the same manner as the conditioning sequence but the deviator stress and the confinement pressures corresponded to levels listed in Table 4.1. After the completion of 30 sequences for the M_R test, the final load path programmed was a shear strength test. M_R test at optimal water content were run on two sets of specimens whereas M_R test at water content corresponding to 300 kPa suction was run only on one set of specimens.

Resilient Modulus Calculations

Resilient modulus and shear strength calculations were done using the procedures suggested by Kim and Labuz (2007). The load and displacement data recorded during M_R testing was stored in 30 separate data files corresponding to 30 sequences in Table 1. Each file consisted of the load, stroke, and three LVDT displacement values. The M_R value was calculated by dividing the cyclic axial stress ($\Delta\sigma_a$) with the recoverable axial strain ($\Delta\varepsilon_a$):

$$M_R = \frac{\Delta\sigma_a}{\Delta\varepsilon_a} \qquad [4.1]$$

The recoverable axial strain was calculated by averaging the three recoverable displacement values (d_1, d_2, d_3) divided by the gage length (l_o):

$$\Delta\varepsilon_a = \frac{\frac{1}{3}(d_1 + d_2 + d_3)}{l_o} \qquad [4.2]$$

The cyclic axial stress induced in the specimen was the peak load (P_{max}) minus the load during the recovery period (P_o) divided by the cross-sectional area of the specimen:

$$\Delta\sigma_a = \frac{\left(P_{\max} - P_o\right)}{\pi * r^2} \quad [4.3]$$

where r is the radius of the specimen. This calculation was repeated for each of the final five cycles in each loading sequence. The M_R Calculator also calculated the mean stress (θ) for each loading sequence as:

$$\theta = \frac{\sigma_1 + 2\sigma_3}{3} \quad [4.4]$$

where σ_1 - σ_3 is the deviator stress and σ_3 is the confining pressure. M_R calculator exported calculated values to a data file for each of the 30 cycles.

Quality Control of Resilient Modulus Measurements

Three criteria were used to insure quality control in resilient modulus measurements. These are deformation homogeneity and rotation angle for the specimen and signal to noise ratio for LVDTs. Details on these criteria are given in Kim and Labuz (2007).

Deformation Homogeneity: One of the basic assumptions in testing specimens for resilient modulus or shear strength measurements is that there is uniform deformation. Davich et al. (2004) showed that occasionally there occur some discrepancies between three LVDT readings during resilient modulus measurements. There are several reasons for these discrepancies including specimen ends may not be parallel, the specimen may have tilted during testing, or there is some slippage of the collar. Davich et al. (2004) suggested the use of homogeneous deformation coefficient (α) to quantify deformation homogeneity of the specimen:

$$\alpha = 3\frac{\sqrt{\delta_1^2 + \delta_2^2 + \delta_3^2}}{d_1 + d_2 + d_3} \quad [4.5]$$

where δ_i is the difference between the average LVDT displacement and the displacement from LVDT 'i', and d_i is the LVDT displacement. An α-value of 0 would suggest a perfect agreement among all three LVDTs whereas a large values of α would suggest large discrepancies between the displacement values.

We calculated the α-values for each loading sequence of each specimen in M_R test. Figure 4.3 shows an example of the variation of α-values for a specimen at different confining pressures. An α- value of 0.1 refers to about 10% difference from the mean value. The α-values for 75% RAP + 25% Aggregate mixture varies from 0.05 to 0.2, which means that individual LVDT reading varied from 5 to 20% of the mean displacement. The α-values for other recyclable mixtures are listed in Table A11 through A46 of the Appendix A.

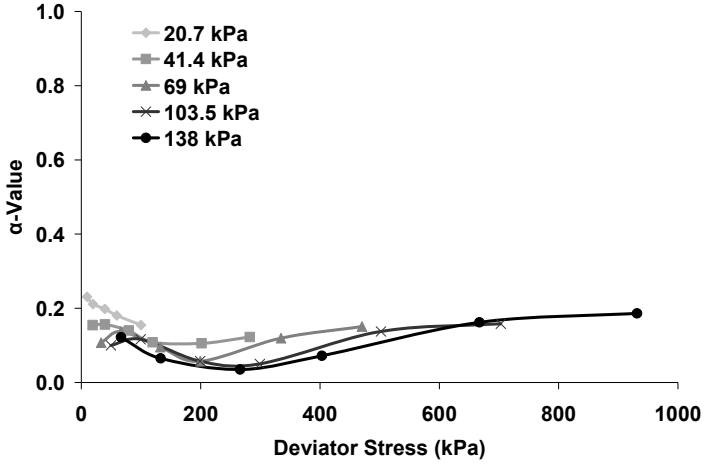

Figure 4.3 α-values vs. deviator stress of RAP 75% + Aggregate 25% mixture.

Angle of Rotation: One of the reasons for non-uniform specimen deformation in resilient modulus measurements may be the rotation of the specimen. Based on Chadbourn's (2005) procedure, Kim and Labuz (2007) suggested a procedure for calculating the angle of rotation using the LVDT measurements. During load application, some rotation may occur and the displacement values from the three LVDT can vary due to specimen alignment. From Chadbourn (2005), angle of rotation, θ, is calculated by using

$$\cos\theta = \frac{\frac{3}{4}D}{\sqrt{\delta_1^2 + \delta_2^2 + \delta_3^2 - \delta_1\delta_2 - \delta_1\delta_3 - \delta_2\delta_3 + \frac{9}{16}D^2}} \qquad [4.6]$$

where θ is angle of rotation, δ_i is axial displacement ($LVDT_i$), and D is diameter of specimen. Angles of rotation of all specimens for the last 5 cycles in 30 sequences were analyzed. The maximum limit of angle of rotation is 0.1°.

The angle of rotation for RAP 75% is shown in Fig. 4.4. At any given deviator stress, the angle of rotation at 20.7 kPa confining pressure was higher than other confining pressure. For most all confining pressure for this specimen, the angle of rotation was less than 0.04 degrees. In the Appendix A11 to A46, we have listed the angle of rotation for all specimens at all confining pressure. The angle of rotation was higher in nearly all foundry sand-aggregate mixtures at higher sequences. Except for 5% foundry sand-95% aggregate, all foundry sand mixture failed before the #30 sequence. We speculate that these higher angles were because of the failure of the samples and thus some rotation.

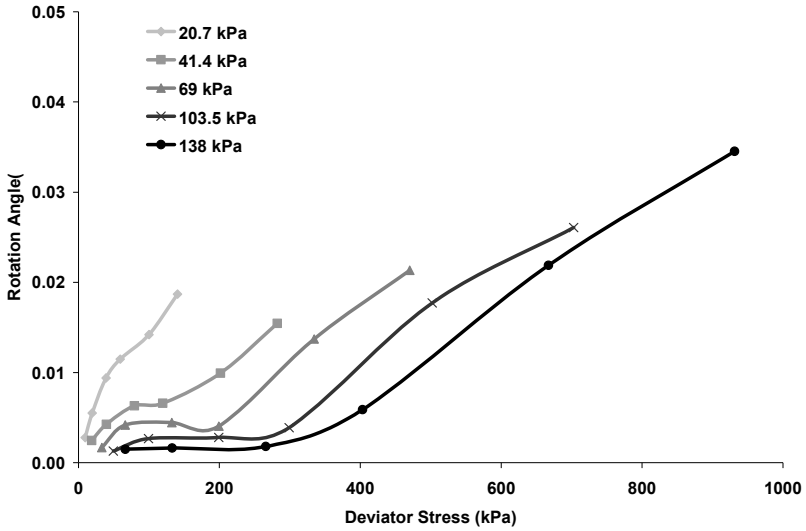

Figure 4.4 Rotation angle vs. deviator stress of 75% RAP + 25% Aggregate mixture.

Signal to Noise Ratio: Since very small displacements are measured using LVDT, there is some concern that signal to noise ratio (SNR) may be excessive thus affecting the resilient modulus results. SNR is defined as the ratio of peak displacement to standard deviation of the noise. Kim and Labuz (2007) compared the SNR of his measurements to Mn/DOT minimum limit equal to 3 for each cycle. These authors discarded the data for those cycles which had more than 1 LVDT or loading cycles that failed to pass the limit. Figure 4.5 is an example of the displacement for one LVDT that met the signal to noise ratio of 3 in our resilient modulus tests. Kim and Labuz (2007) also used the SNR value of 10 as the minimum limit for each loading cycle. Figure 4.6 shows an example of the SNR values for a loading cycle in our measurements.

$$SNR = \frac{Peak}{3 \times SDev(Baseline)} \qquad [4.7]$$

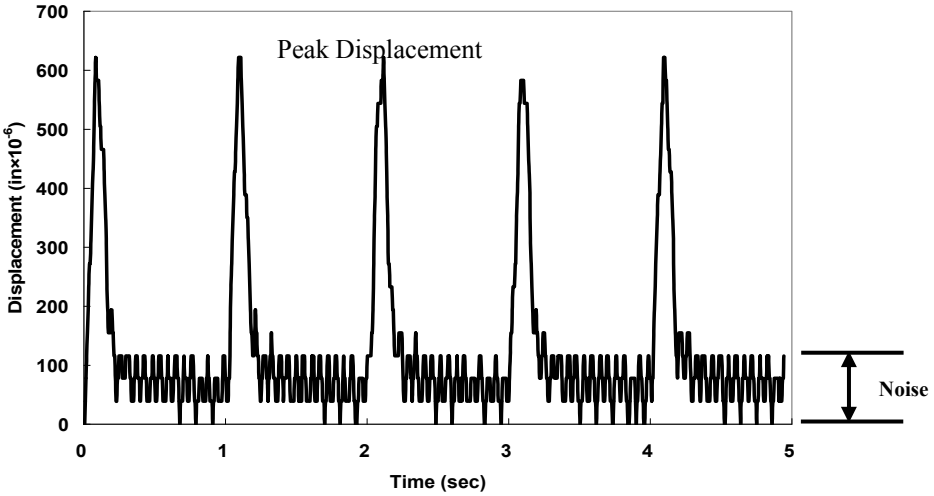

Figure 4.5 Example displacement history of a specimen for a mixture of 75% RCM+25% Aggregate that met the Mn/DOT specification for SNR (signal to noise ratio) = 3.

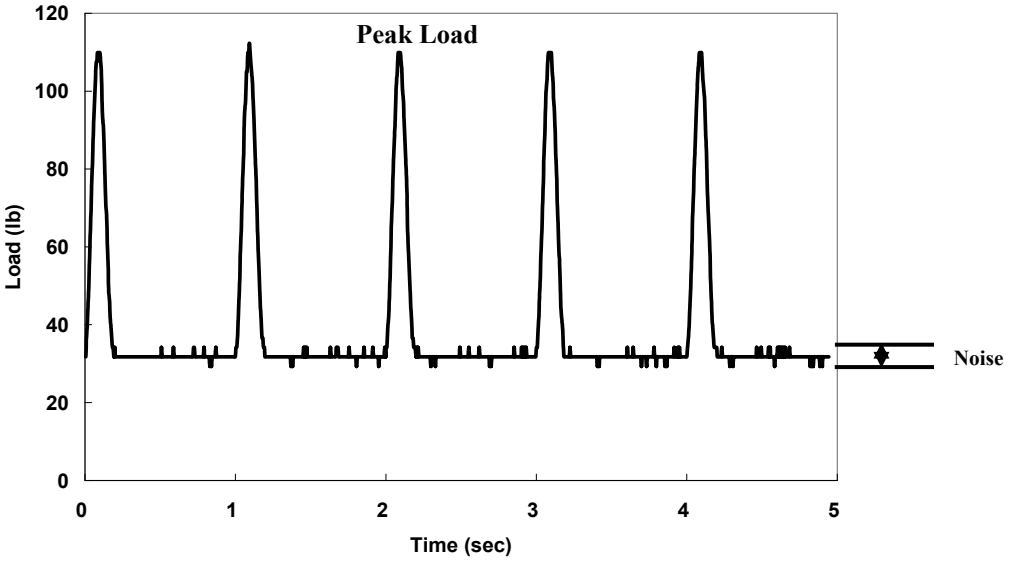

Figure 4.6 Example load history of a specimen for a mixture of 75% RCM+25% Aggregate that met the Mn/DOT specification for SNR(signal to noise ratio) =10.

Table 4.2 Target and tested specimen preparation parameters.

Material	Target		Test 1. Optimal Condition		Test 2. Unsaturated Condition†	
	Optimum Moisture Content (%)	Maximum Dry Density (g/cm^3)	Moisture Content (%)	Dry Density (g/cm^3)	Moisture Content (%)	Dry Density (g/cm^3)
Agg100%	9.2	2.070	8.8	2.065	7.2	2.087
RAP25%+ Agg75%	7.8	2.065	6.4	2.069	5.3	2.087
RAP50%+ Agg50%	6.6	2.070	6.2	2.083	4.2	2.110
RAP75%+ Agg25%	5.4	2.078	5.6	2.084	3.2	2.109
RAP100%	4.0	2.120	4.5	2.126	3.2	2.119
FA5% +RAP25%+Agg70%	8.2	2.050	8.6	2.032	5.6	2.037
FA15% +RAP25%+Agg60%	10.2	1.950	10.3	1.867	8.7	1.860
FA5% +RAP50%+Agg45%	7.4	2.065	7.8	2.042	5.2	2.012
FA15% +RAP50%+Agg35%	8.6	1.970	8.2	1.890	6.9	1.836
FA5% +RAP75%+Agg20%	6.6	2.060	6.4	2.050	3.8	1.978
FA15% +RAP75%+Agg10%	7.4	2.000	7.4	1.892	7.1	1.883
RCM 25%+ Agg75%	9.8	2.000	9.2	1.996	7.8	2.014
RCM 50%+ Agg50%	9.4	1.980	9.7	1.951	7.8	1.903
RCM 75%+ Agg25%	9.4	1.950	9.3	1.925	8.2	1.906
RCM 100%	9.4	1.940	9.4	1.907	8.5	1.900
FS 5%+ Agg95%	9.4	2.070	9.2	2.070	7.2	2.093
FS 5%+ Agg95%	9.4	2.070	9.3	2.067	7.3	2.083
FS 5%+ Agg95%	9.4	2.070	9.4	2.075	7.2	2.079

†Soil water suction=300 kPa.

Shear Strength

After the M_R test the specimens were also tested for shear strength. For shear strength test, a small contact load was applied to the specimen following the completion of the NCHRP 1-28 A load sequences. The specimen was loaded at a constant rate of 0.76 mm/s, a rate used by Mn/DOT for shear strength tests. The loading continued until the specimen failed and the observed axial load began to fall. At this point the actuator was halted and load was slowly removed from the specimen. In all cases, the specimen failed within few seconds. Since there were two specimens at optimal water content, the first specimen was sheared at a confining pressure of 34.5 kPa whereas the second specimen was sheared at a confining pressure of 68.9 kPa. Since there was only one specimen at drier moisture content corresponding to 300 kPa suction, the shearing test was run at a confining pressure of 68.9 kPa only. Figure 4.7 shows the load vs. displacement relationship for a specimen during shearing. Most specimens followed a similar relationship. Since during M_R testing some specimen failed before the completion of 30th sequence, shear strength testing could not be done on those specimens. These specimens included the specimens containing foundry sand, 25% RAP+75 aggregate mixtures, and 100 % virgin aggregate.

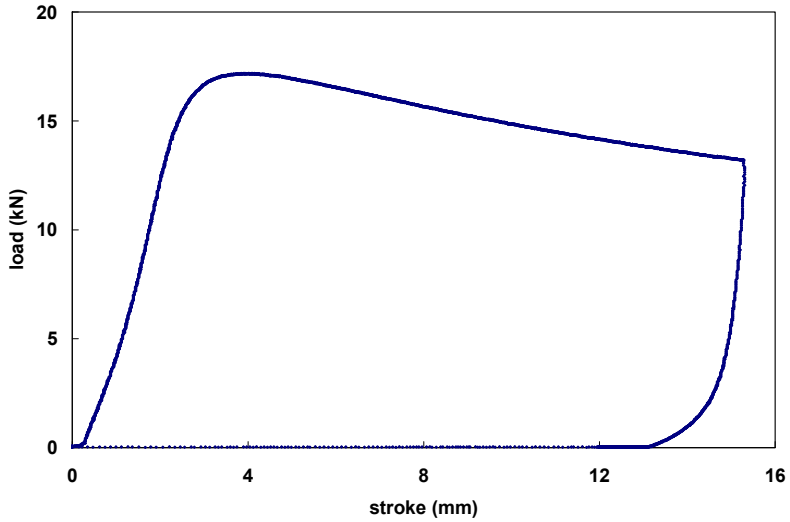

Figure 4.7 Examples load vs. displacement during shearing.

Shear strength at the optimal water content was calculated using the procedures described in ASTM standard test method for unconsolidated-undrained triaxial compression on cohesive soil (D 2850-95). The relationships used to calculate cohesion (c) values and the friction angle (ϕ) are as follows:

$$c = \left(\frac{\sigma_{11} - \sigma_{31}\left(\frac{\sigma_{12} - \sigma_{11}}{\sigma_{32} - \sigma_{31}}\right)}{2 * \left(\frac{\sigma_{12} - \sigma_{11}}{\sigma_{32} - \sigma_{31}}\right)^{0.5}} \right) \qquad [4.8]$$

$$\phi = 2 * \left(a\tan\left(\frac{\sigma_{12} - \sigma_{11}}{\sigma_{32} - \sigma_{31}} \right)^{0.5} - 45 \right) \quad [4.9]$$

where σ_{11} and σ_{12} are the vertical stresses at failure on the first and second specimen, respectively; and σ_{31} and σ_{32} are the confining stresses on the first (34.5 kPa) and the second (68.9 kPa) specimen, respectively. We also used the above formulas with corresponding stresses at 1% strain to calculate cohesion and friction angle of various specimens.

Since only one specimen was sheared at a drier water content corresponding to 300 kPa suction, shear strength was calculated using the vertical stress at failure, the confining stress, and one additional measurement on shear angle (θ) on the specimen. Figure A.34 is an example of shear angle measurement on the specimen. The relationship used to estimate c and ϕ for drier specimens were as follows:

$$\theta = 45 + \frac{\phi}{2} \quad [4.10]$$

$$\sigma_1 = 2c\sqrt{K_p} + K_p\sigma_3 \quad [4.11]$$

$$K_p = \frac{1 + \sin\phi}{1 - \sin\phi} \quad [4.12]$$

where σ_1 is vertical stress at failure and σ_3 is confining pressure.

RESULTS AND DISCUSSION

Resilient Modulus

100% Aggregates: Figures 4.8 and 4.9 show the variation in M_R value of 100% virgin aggregates as a function of deviator stress and confining pressure at optimal and drier water contents (corresponding to 300 kPa suction). These values are also plotted in a 3-D graphs in the Appendix Figures A21 through A33. At a given deviator stress, M_R values increased with an increase in confining pressure. However, there was little to no effect of the deviator stress at a given confining pressure. M_R values of 100% virgin aggregates were less than 400 MPa. The specimens for 100% aggregate also failed before reaching #30 sequences.

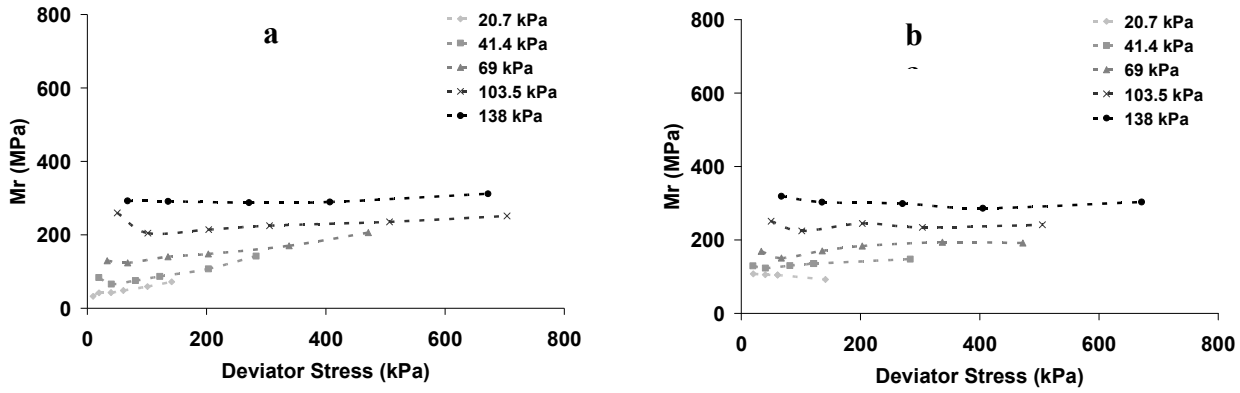

Figure 4.8 Variation in resilient modulus of a mixture of 100% Aggregates as a function of deviator stress for various confining pressures. Figure 4.8.a is for specimens at optimum moisture content (MC=8.8%) whereas figure 4.8.b is for specimens at a drier water content corresponding to 300 kPa suction (MC=7.2%). The deviator stress varied from 4.1 kPa to 27.6 kPa.

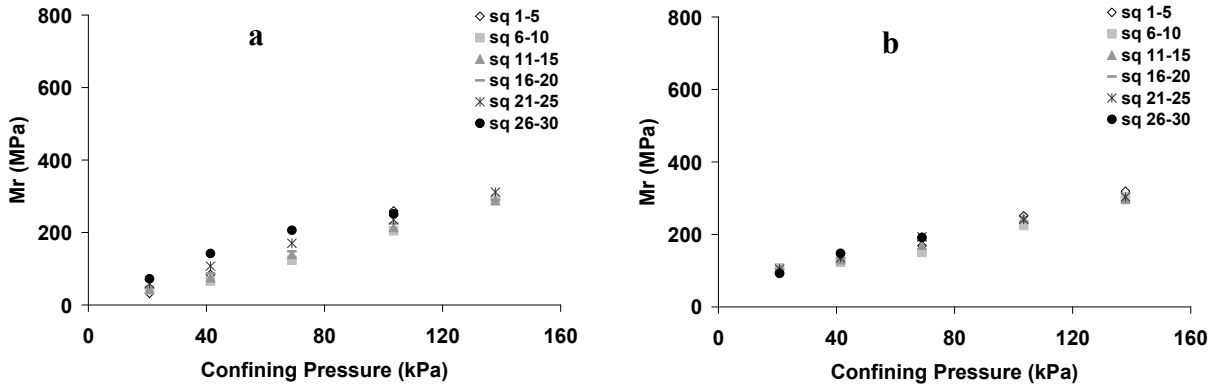

Figure 4.9 Variation in resilient modulus of a mixture of 100% Aggregates as a function of confining pressure for various sequences in Table 4.1. Figure 4.9.a is for specimens at optimum moisture content (MC=8.8%) whereas figure 4.9.b is for specimens at a drier water content corresponding to 300 kPa suction (MC=7.2%). The deviator stress varied from 4.1 kPa to 27.6 kPa.

RAP-Aggregate Mixtures: Figures 4.10 to 4.13 show the variation in M_R values as a function of deviator stress and confining pressures for three RAP-aggregate mixtures and 100% RAP material at two different water contents (optimal water content and drier conditions corresponding to 300 kPa suction). For all three RAP-Aggregate mixtures, M_R values at drier (3.2%) than optimum water content (4.5%) were 1.1 to 1.3 times higher than the M_R values of the optimal water content. However there was no effect of water content on M_R value of 100% RAP at any given deviator stress and a confining pressure. For any given RAP material, the effect of the deviator stress was rather small at any given confining pressure (Figures 4.14 to 4.17). At a given confining pressure, M_R value of a given RAP- aggregate mixture decreased

with an increase in water content. This effect was much more pronounced at lower proportion of RAP in the mixture than at higher RAP content. For 100% RAP materials, the effect of water content on M_R value was minimal at a given confining pressure. At given water content and a confining pressure, the effect of RAP addition to aggregates on M_R values was small. With addition of RAP, M_R values slightly increased with an increase in RAP content of the mixture. For 100% RAP, M_R values were maximum for a given water content and a confining pressure. At any given confining pressure, all RAP mixtures met or exceeded the M_R values of the 100% virgin aggregates.

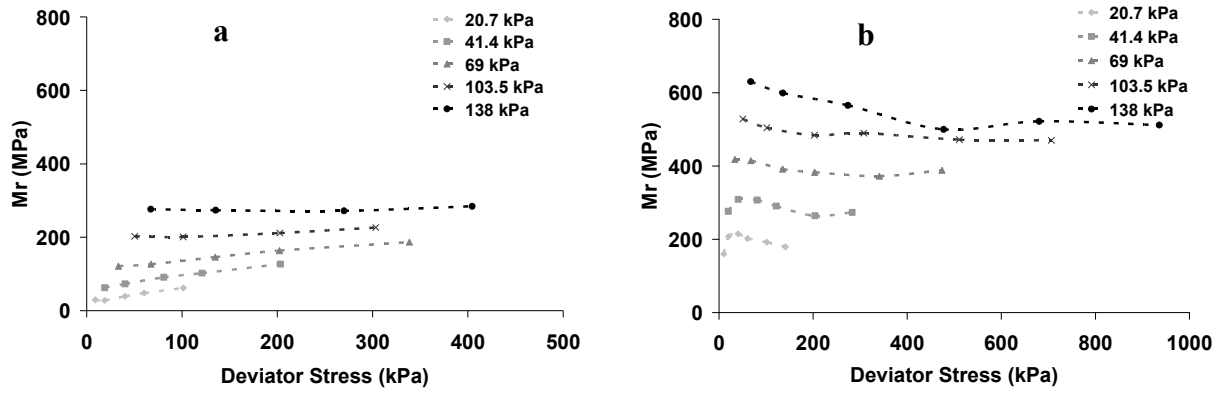

Figure 4.10 Variation in resilient modulus of a mixture of 25% RAP + 75% Aggregates as a function of deviator stress for various confining pressures. Figure 4.10.a is for specimens at optimum moisture content (MC=6.4%) whereas figure 4.10.b is for specimens at a drier water content corresponding to 300 kPa suction (MC=5.3%). The confining pressure varied from 20.7 kPa to 138 kPa.

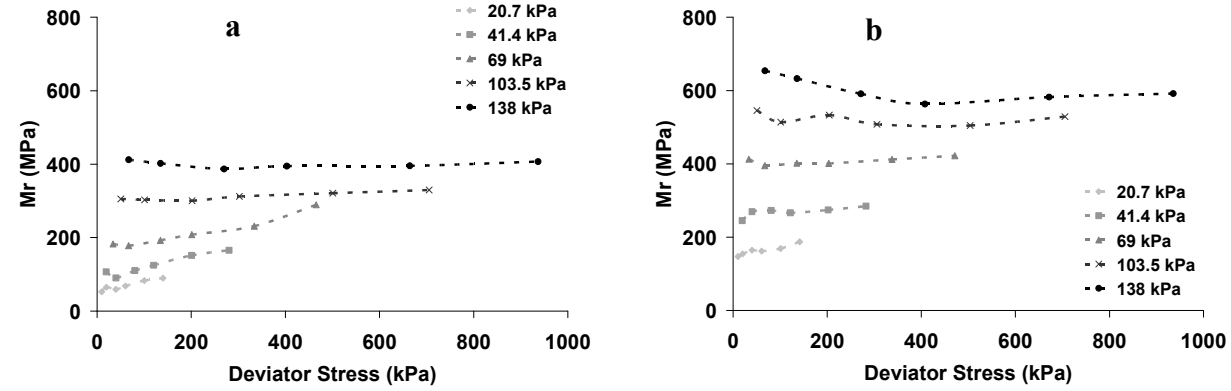

Figure 4.11 Variation in resilient modulus of a mixture of 50% RAP + 50% Aggregates as a function of deviator stress for various confining pressures. Figure 4.11.a is for specimens at optimum moisture content (MC=6.2%) whereas figure 4.11.b is for specimens at a drier water content corresponding to 300 kPa suction (MC=4.2%). The confining pressure varied from 20.7 kPa to 138 kPa.

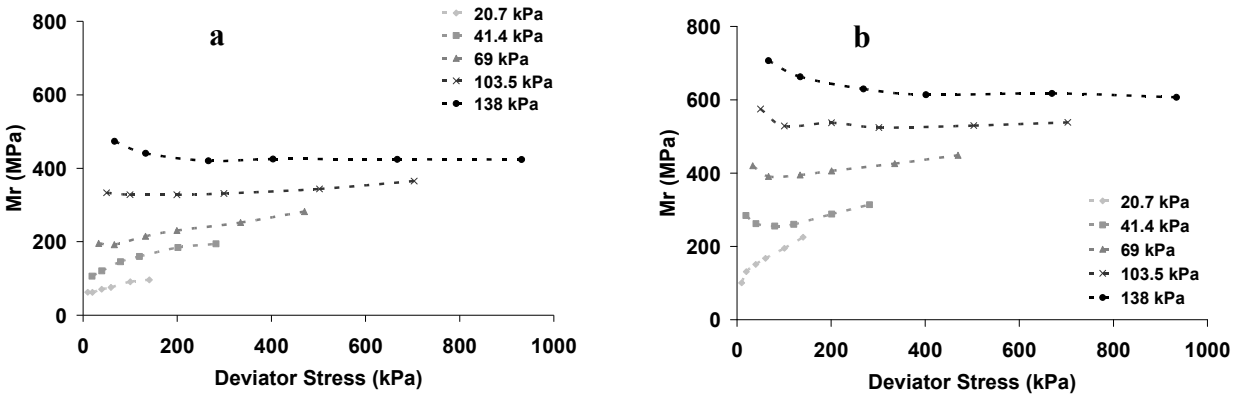

Figure 4.12 Variation in resilient modulus of a mixture of 75% RAP + 25% Aggregates as a function of deviator stress for various confining pressures. Figure 4.12.a is for specimens at optimum moisture content (MC=5.6%) whereas figure 4.12.b is for specimens at a drier water content corresponding to 300 kPa suction (MC=3.2%). The confining pressure varied from 20.7 kPa to 138 kPa.

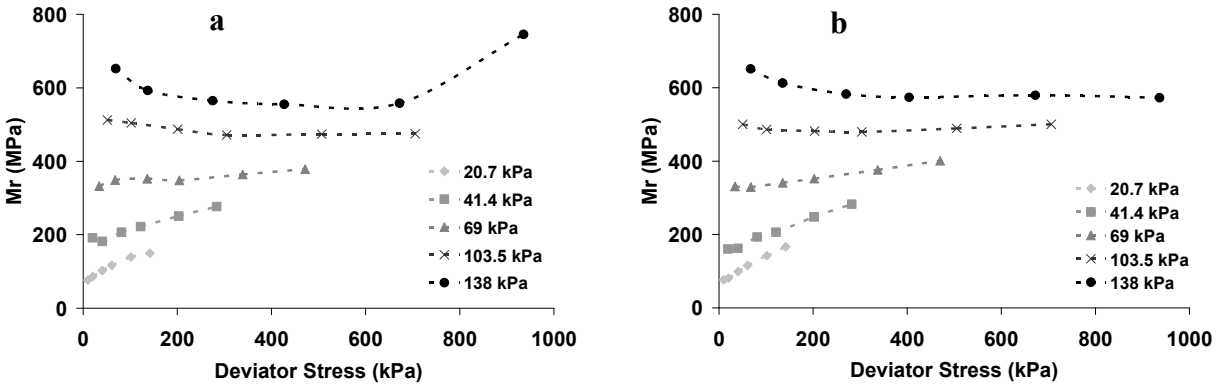

Figure 4.13 Variation in resilient modulus of a mixture of 100% RAP as a function of deviator stress for various confining pressures. Figure 4.13.a is for specimens at optimum moisture content (MC=4.5%) whereas figure 4.13.b is for specimens at a drier water content corresponding to 300 kPa suction (MC=3.2%). The confining pressure varied from 20.7 kPa to 138 kPa.

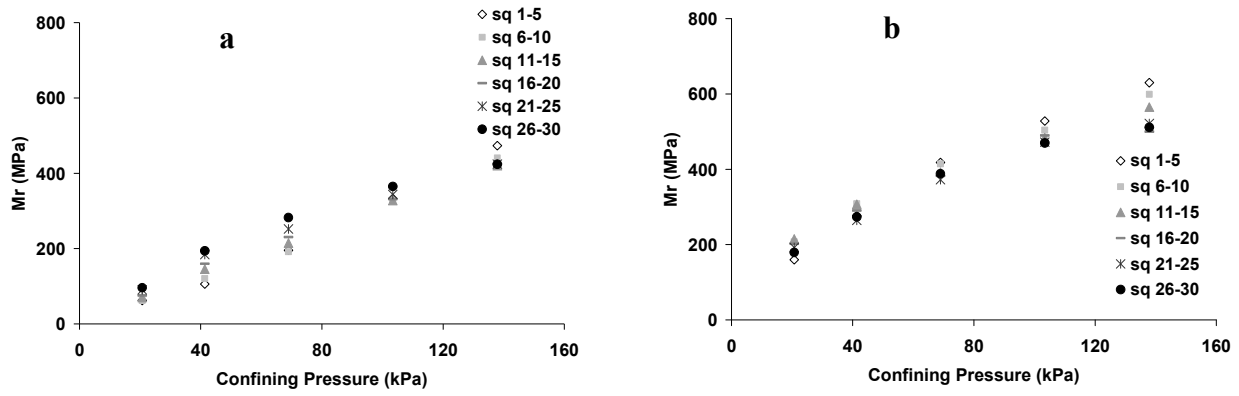

Figure 4.14 Variation in resilient modulus of a mixture of 25% RAP + 75% Aggregates as a function of confining pressure for various sequences in Table 4.1. Figure 4.14.a is for specimens at optimum moisture content (MC=6.4%) whereas figure 4.14.b is for specimens at a drier water content corresponding to 300 kPa suction (MC=5.3%). The deviator stress varied from 4.1 kPa to 27.6 kPa.

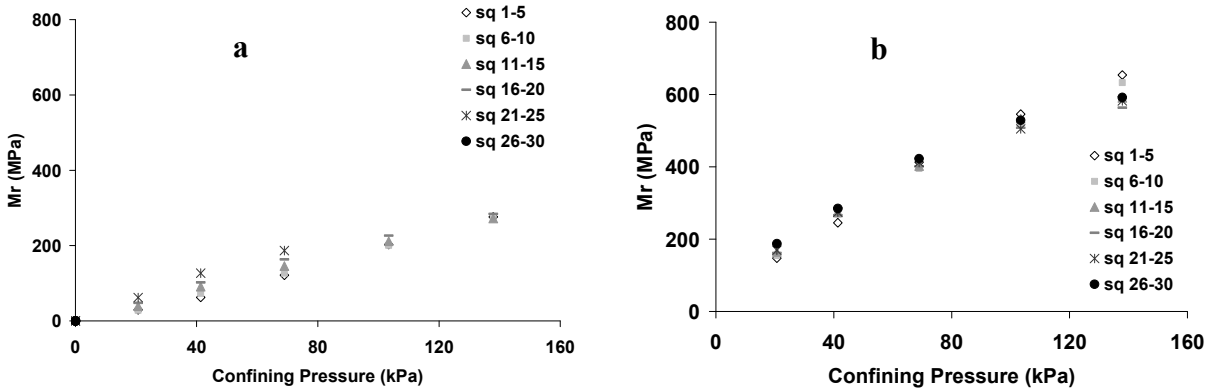

Figure 4.15 Variation in resilient modulus of a mixture of 50% RAP + 50% Aggregates as a function of confining pressure for various sequences in Table 4.1. Figure 4.15.a is for specimens at optimum moisture content (MC=6.2%) whereas figure 4.15.b is for specimens at a drier water content corresponding to 300 kPa suction (MC=4.2%). The deviator stress varied from 4.1 kPa to 27.6 kPa.

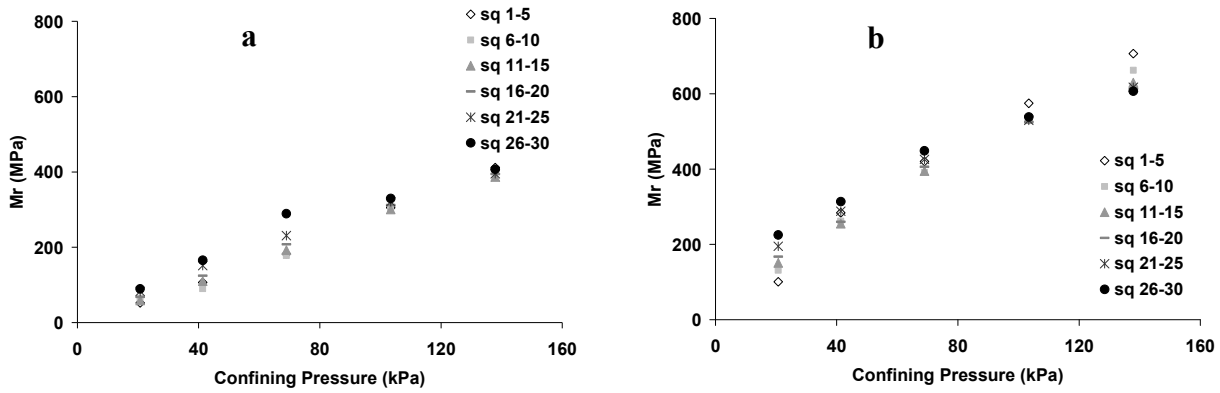

Figure 4.16 Variation in resilient modulus of a mixture of 75% RAP + 25% Aggregates as a function of confining pressure for various sequences in Table 4.1. Figure 4.16.a is for specimens at optimum moisture content (MC=5.6%) whereas figure 4.16.b is for specimens at a drier water content corresponding to 300 kPa suction (MC=3.2%). The deviator stress varied from 4.1 kPa to 27.6 kPa.

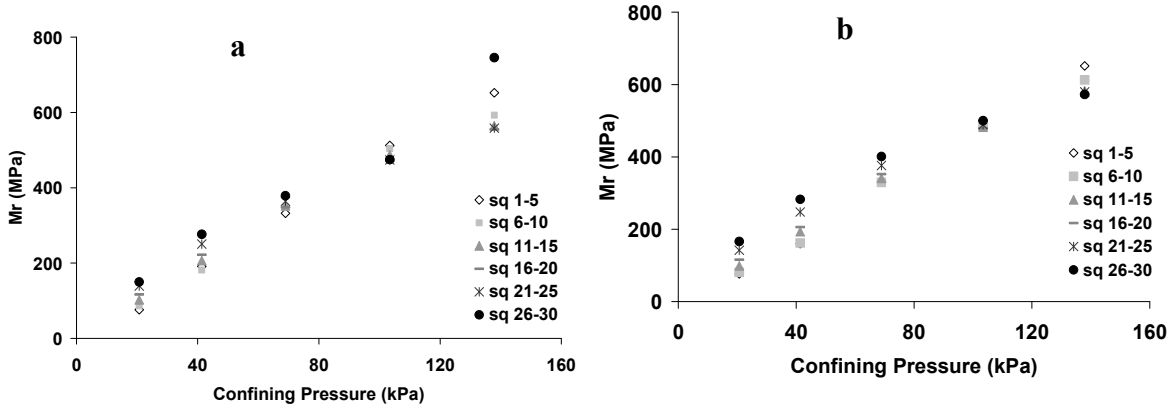

Figure 4.17 Variations in resilient modulus of a mixture of 100% RAP as a function of confining pressure for various sequences in Table 4.1. Figure 4.17.a is for specimens at optimum moisture content (MC=4.5%) whereas figure 4.17.b is for specimens at a drier water content corresponding to 300 kPa suction (MC=3.2%). The deviator stress varied from 4.1 kPa to 27.6 kPa.

Fly Ash-RAP-Aggregate Mixtures: Figures 4.18 to 4.29 show the variation in M_R values as a function of deviator stress and confining pressures as 5 and 15% of fly ash was added to various RAP-aggregate mixtures at two different water contents (optimal water content and drier conditions corresponding to 300 kPa suction). In terms of deviator stress and confining pressure effects, the trends in M_R values of the Fly ash-RAP-Aggregate mixtures were nearly similar to that of RAP-aggregate mixtures i.e. an increase in M_R values with an increase in confining stress but minimal change with an increase in deviator stress. The effect of water content on M_R values was more noticeable at lower fly ash content than higher fly ash content.

At 5% fly ash in the mixtures, M_R values increased with a decrease in water content. At 15% fly ash content, there were minimal differences in M_R values between the optimal water content and the water corresponding to 300 kPa suction. For a given wetness condition, it appears that addition of fly ash and the reduction in the proportion of aggregates in the RAP-aggregate mixtures also reduces M_R value at a given confining pressure. This decrease is most likely due to an increase in water content of the mixture when fly ash is added to RAP-aggregate mixture. Fly ash being fine particles have tendency to retain more moisture at a given suction. Since wet fly ash-aggregates mixtures were allowed to equilibrate for 24-48 hrs before compaction, it appears that fly ash lost some of its effectiveness as a binding agent. M_R values of all fly ash mixtures with RAP and aggregates were nearly same as that of the 100% virgin aggregates.

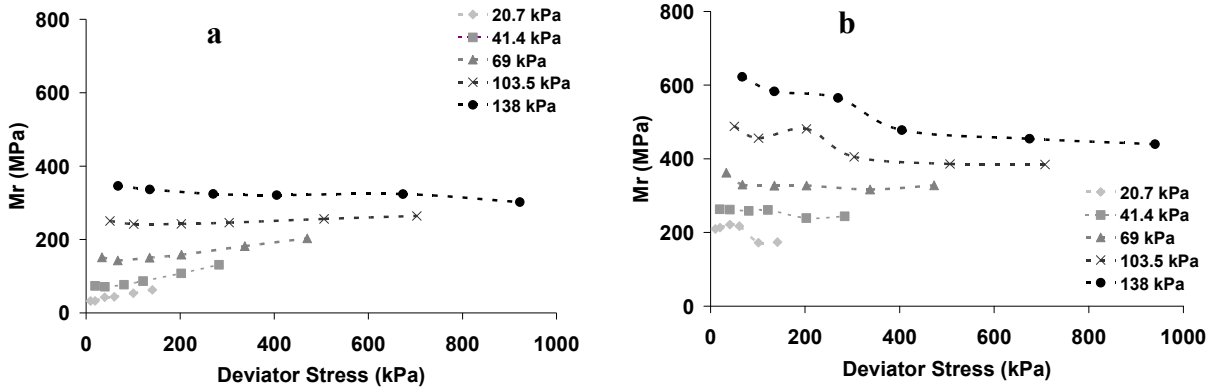

Figure 4.18 Variation in resilient modulus of a mixture of 5% Fly Ash+ 25% RAP + 70% Aggregates as a function of deviator stress for various confining pressures. Figure 4.18.a is for specimens at optimum moisture content (MC=9.2%) whereas figure 4.18.b is for specimens at a drier water content corresponding to 300 kPa suction (MC=5.6%). The confining pressure varied from 20.7 kPa to 138 kPa.

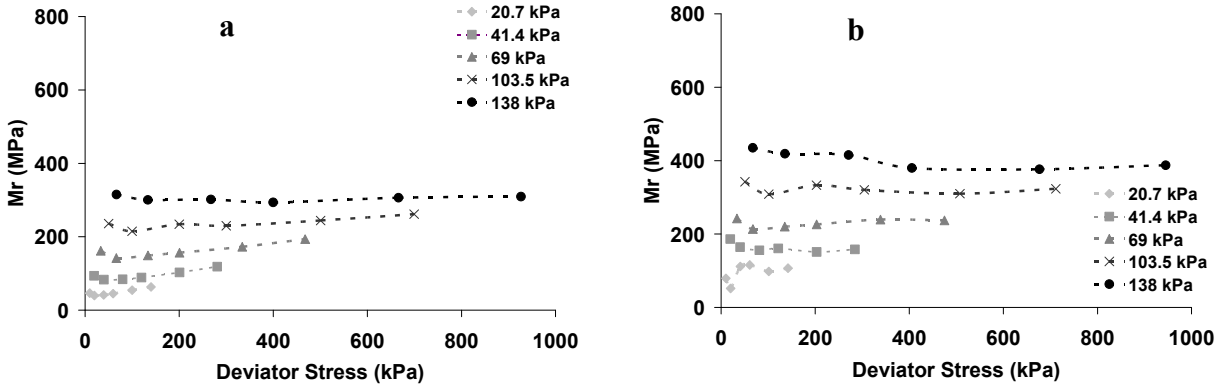

Figure 4.19 Variation in resilient modulus of a mixture of 15% Fly-Ash +25% RAP + 60% Aggregates as a function of deviator stress for various confining pressures. Figure 4.19.a is for specimens at optimum moisture content (MC=9.7%) whereas figure 4.19.b is for specimens at a drier water content corresponding to 300 kPa suction (MC=8.7%). The confining pressure varied from 20.7 kPa to 138 kPa.

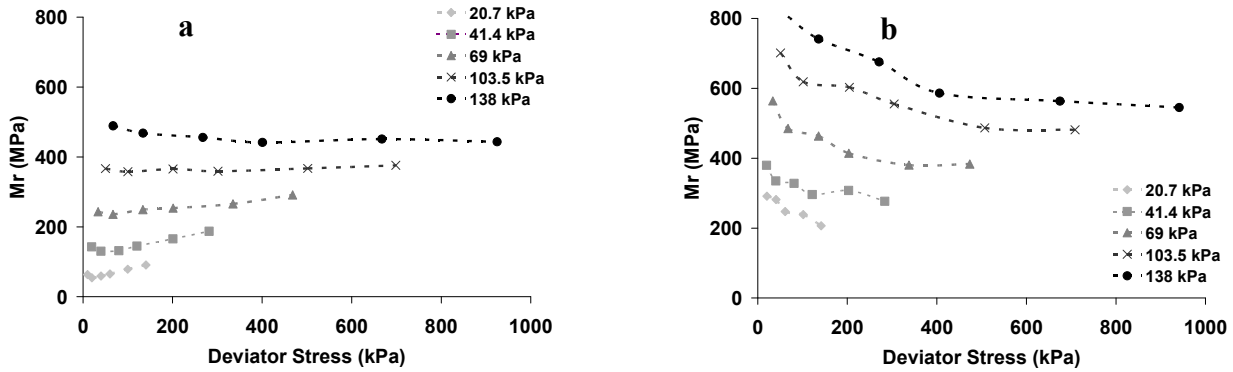

Figure 4.20 Variation in resilient modulus of a mixture of 5% Fly Ash+ 50% RAP + 45% Aggregates as a function of deviator stress for various confining pressures. Figure 4.20.a is for specimens at optimum moisture content (MC=9.3%) whereas figure 4.20.b is for specimens at a drier water content corresponding to 300 kPa suction (MC=5.2%). The confining pressure varied from 20.7 kPa to 138 kPa.

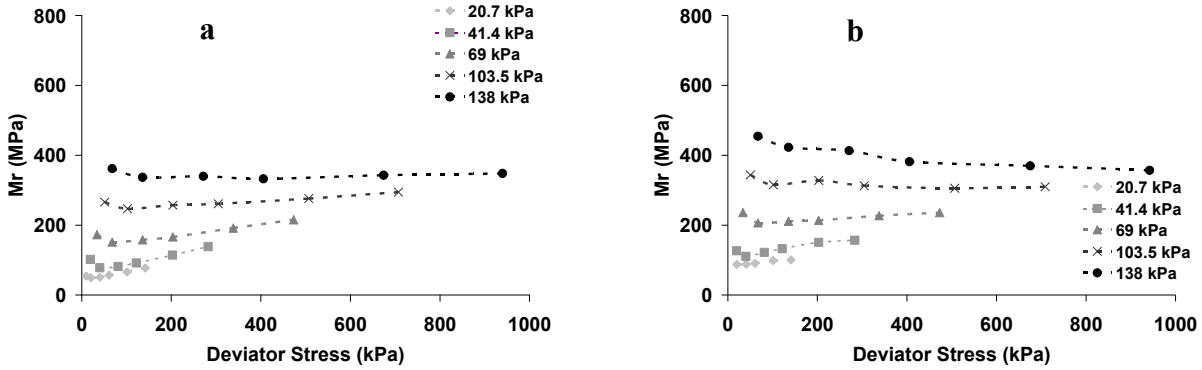

Figure 4.21 Variation in resilient modulus of a mixture of 15% Fly Ash+ 50% RAP + 35% Aggregates as a function of deviator stress for various confining pressures. Figure 4.21.a is for specimens at optimum moisture content (MC=9.3%) whereas figure 4.21.b is for specimens at a drier water content corresponding to 300 kPa suction (MC=5.2%). The confining pressure varied from 20.7 kPa to 138 kPa.

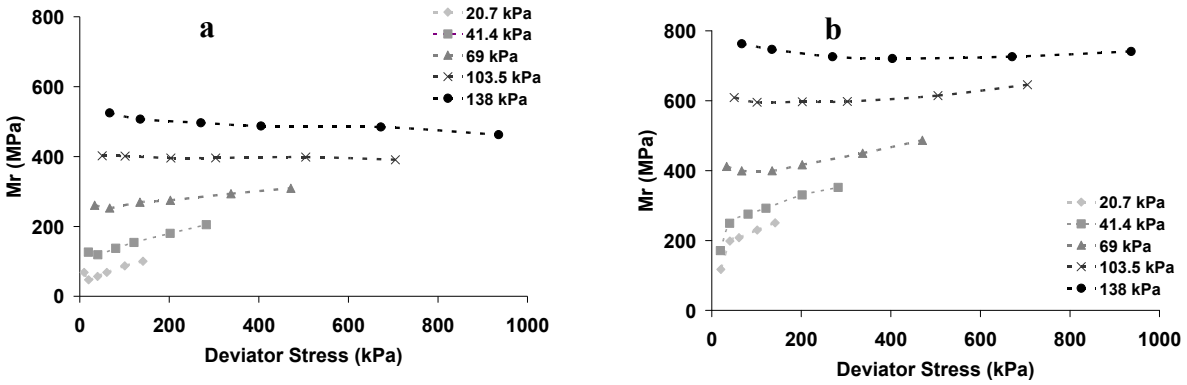

Figure 4.22 Variation in resilient modulus of a mixture of 5% Fly Ash+ 75% RAP + 20% as a function of deviator stress for various confining pressures. Figure 4.22.a is for specimens at optimum moisture content (MC=6.4%) whereas figure 4.22.b is for specimens at a drier water content corresponding to 300 kPa suction (MC=3.8%). The confining pressure varied from 20.7 kPa to 138 kPa.

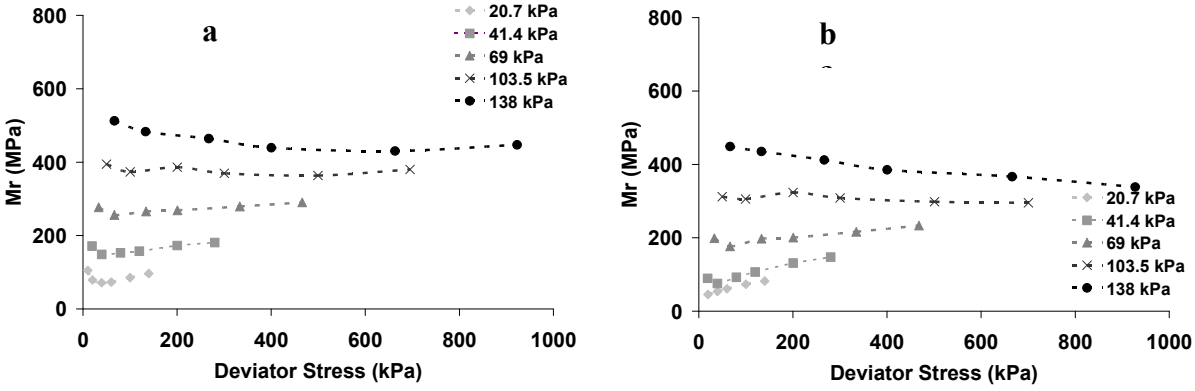

Figure 4.23 Variation in resilient modulus of a mixture of 15% Fly Ash+75% RAP + 10% Aggregates as a function of deviator stress for various confining pressures. Figure 4.23.a is for specimens at optimum moisture content (MC=7.4%) whereas figure 4.23.b is for specimens at a drier water content corresponding to 300 kPa suction (MC=7.1%). The confining pressure varied from 20.7 kPa to 138 kPa.

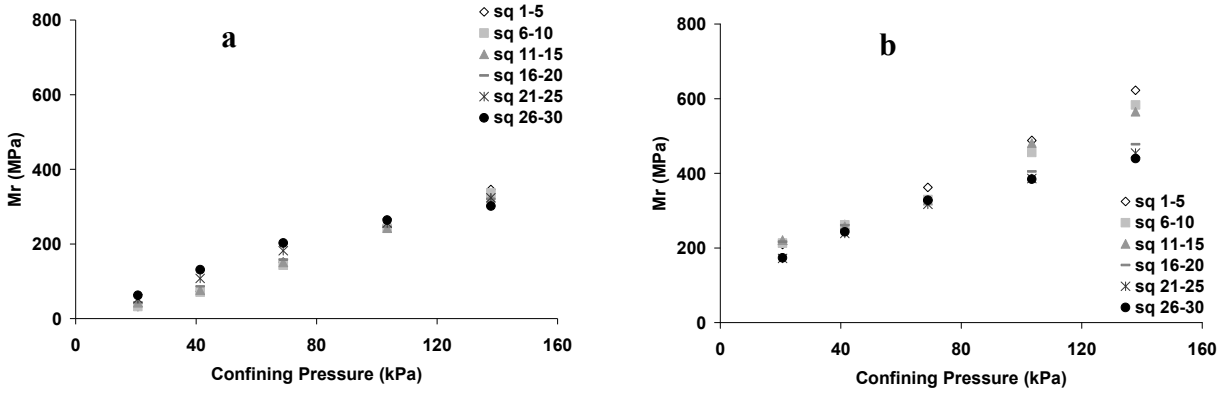

Figure 4.24 Variation in resilient modulus of a mixture of 5% Fly Ash+ 25% RAP + 70% Aggregates as a function of confining pressure for various sequences in Table 4.1. Figure 4.24.a is for specimens at optimum moisture content (MC=9.2%) whereas figure 4.24.b is for specimens at a drier water content corresponding to 300 kPa suction (MC=5.6%). The deviator stress varied from 4.1 kPa to 27.6 kPa.

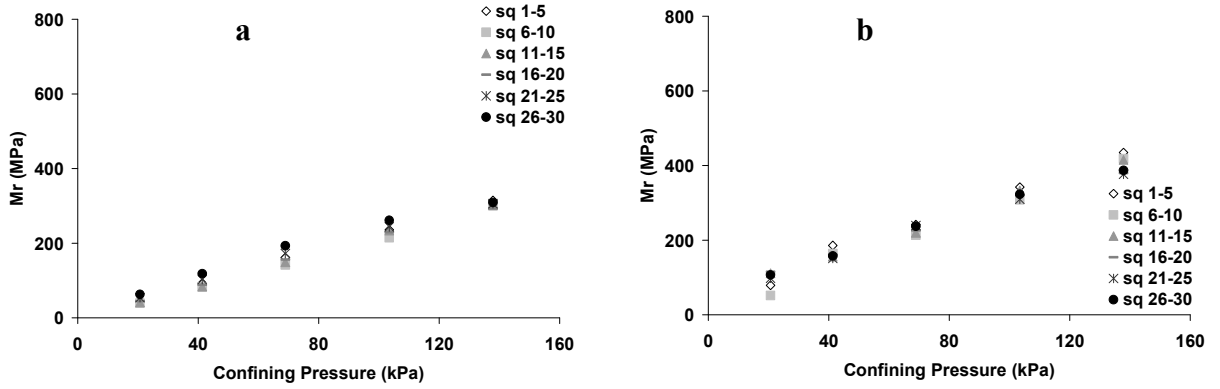

Figure 4.25 Variation in resilient modulus of a mixture of 15% Fly Ash+ 25% RAP + 60% Aggregates as a function of confining pressure for various sequences in Table 4.1. Figure 4.25.a is for specimens at optimum moisture content (MC=9.7%) whereas figure 4.25.b is for specimens at a drier water content corresponding to 300 kPa suction (MC=8.7%). The deviator stress varied from 4.1 kPa to 27.6 kPa.

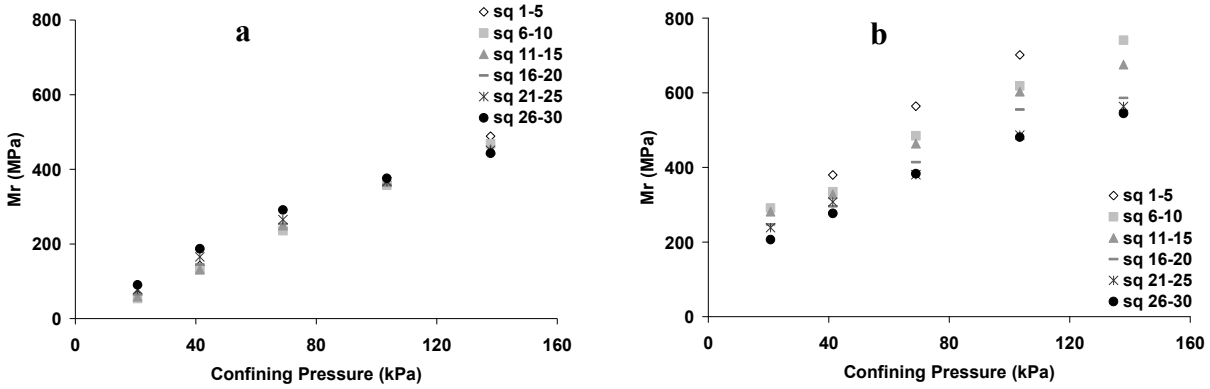

Figure 4.26 Variation in resilient modulus of a mixture of 5% Fly Ash+ 50% RAP + 45% Aggregates as a function of confining pressure for various sequences in Table 4.1. Figure 4.26.a is for specimens at optimum moisture content (MC=9.3%) whereas figure 4.26.b is for specimens at a drier water content corresponding to 300 kPa suction (MC=5.2%). The deviator stress varied from 4.1 kPa to 27.6 kPa.

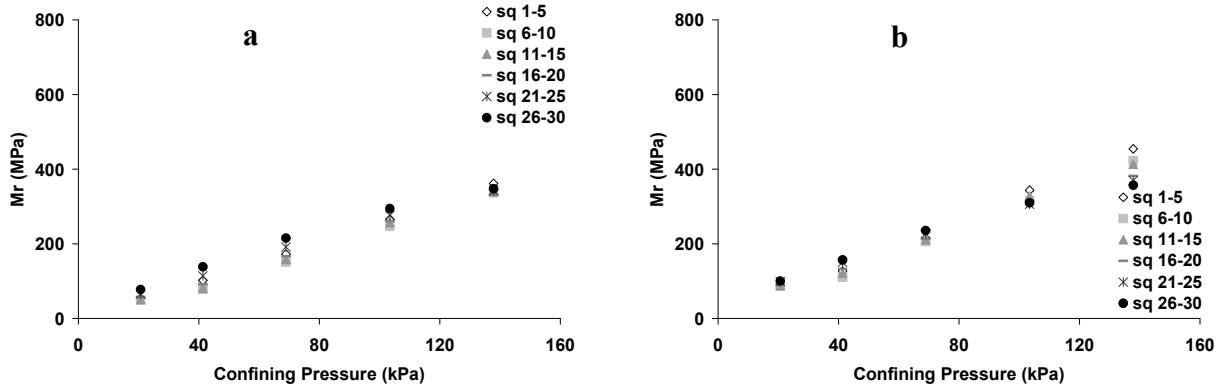

Figure 4.27 Variation in resilient modulus of a mixture of 15% Fly Ash+ 50% RAP + 35% Aggregates as a function of confining pressure for various sequences in Table 4.1. Figure 4.27.a is for specimens at optimum moisture content (MC=8.2%) whereas figure 4.27.b is for specimens at a drier water content corresponding to 300 kPa suction (MC=6.9%). The deviator stress varied from 4.1 kPa to 27.6 kPa.

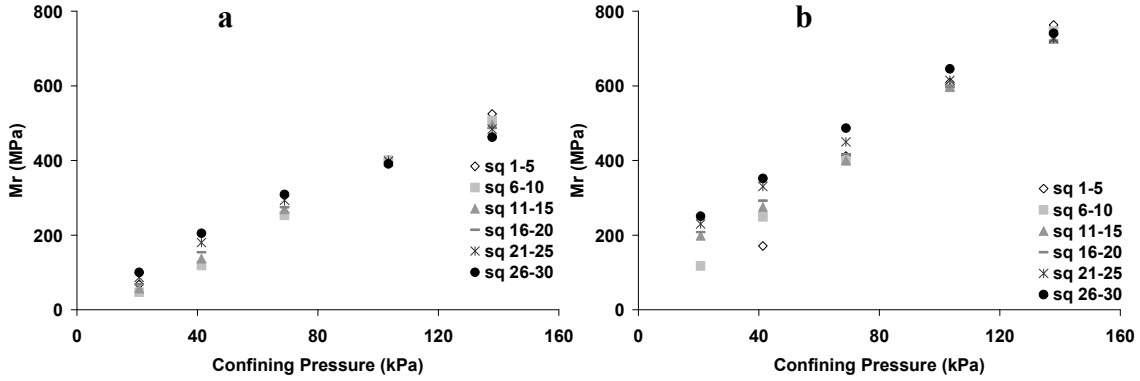

Figure 4.28 Variation in resilient modulus of a mixture of 5% Fly Ash+ 75% RAP + 20% Aggregates as a function of confining pressure for various sequences in Table 4.1. Figure 4.28.a is for specimens at optimum moisture content (MC=6.4%) whereas figure 4.28.b is for specimens at a drier water content corresponding to 300 kPa suction (MC=3.8%). The deviator stress varied from 4.1 kPa to 27.6 kPa.

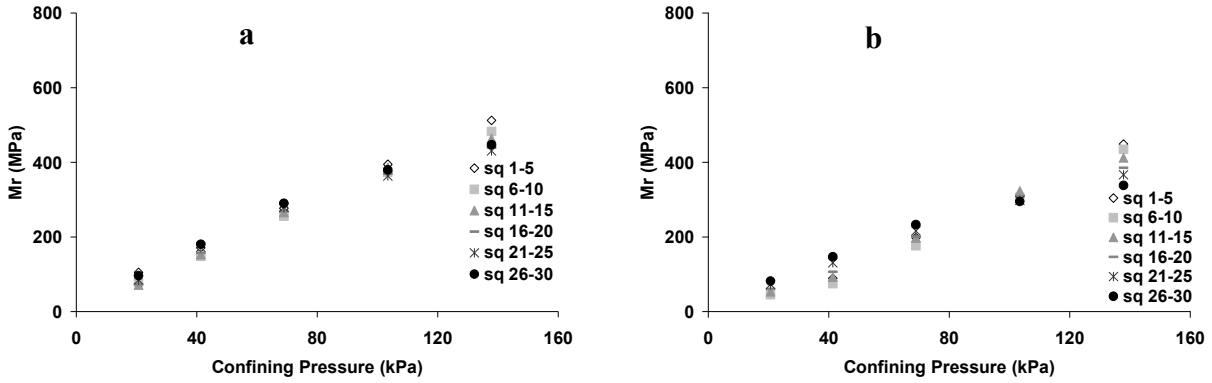

Figure 4.29 Variation in resilient modulus of a mixture of 15% Fly Ash+ 75% RAP + 10% Aggregates as a function of confining pressure for various sequences in Table 4.1. Figure 4.29.a is for specimens at optimum moisture content (MC=7.4%) whereas figure 4.29.b is for specimens at a drier water content corresponding to 300 kPa suction (MC=7.1%). The deviator stress varied from 4.1 kPa to 27.6 kPa.

RCM-Aggregate Mixtures: Figures 4.30 to 4.37 show the variation in M_R values as a function of deviator stress and confining pressures for three RCM-Aggregate mixtures at two different water contents (optimal water content and drier conditions corresponding to 300 kPa suction). In terms of deviator stress and confining pressure effects, the trends in M_R values of the RCM-Aggregate mixtures were nearly similar to that of RAP-aggregate mixtures i.e. an increase in M_R values with an increase in confining stress but minimal change with an increase in deviator stress. However, the differences in M_R values between the optimal water content and the water content corresponding to 300 kPa suction were small. This is mainly because there was very little

difference in water contents of the RCM mixtures at these two wetness conditions. The wetness effects were mostly apparent at higher proportions of RCM (75%) in the mixtures. For 75% RCM + 25% Aggregate mixture, M_R values were higher in specimens at 300 kPa than in specimens at optimal water content. For 100% RCM, M_R values were nearly same at two wetness conditions studied in this project. M_R values of all RCM mixtures were nearly same as that of the 100% virgin aggregates.

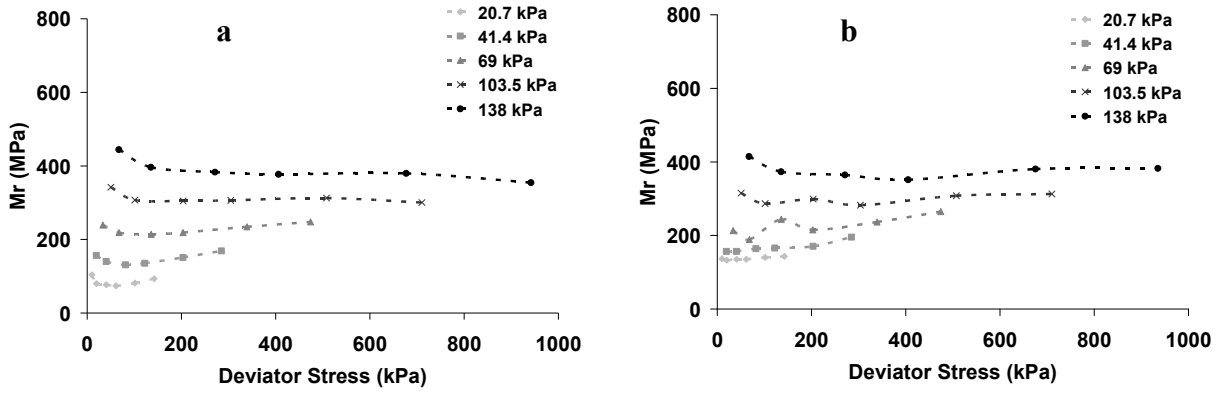

Figure 4.30 Variation in resilient modulus of a mixture of 25% RCM + 75% Aggregates as a function of deviator stress for various confining pressures. Figure 4.30.a is for specimens at optimum moisture content (MC=9.2%) whereas figure 4.30.b is for specimens at a drier water content corresponding to 300 kPa suction (MC=7.8%). The confining pressure varied from 20.7 kPa to 138 kPa.

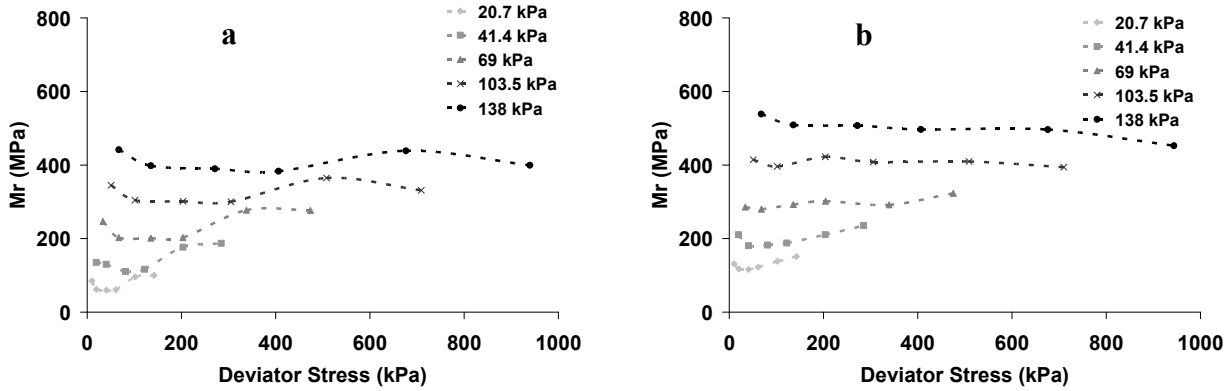

Figure 4.31 Variation in resilient modulus of a mixture of 50% RCM + 50% Aggregates as a function of deviator stress for various confining pressures. Figure 4.31.a is for specimens at optimum moisture content (MC=9.7%) whereas figure 4.31.b is for specimens at a drier water content corresponding to 300 kPa suction (MC=7.8%). The confining pressure varied from 20.7 kPa to 138 kPa.

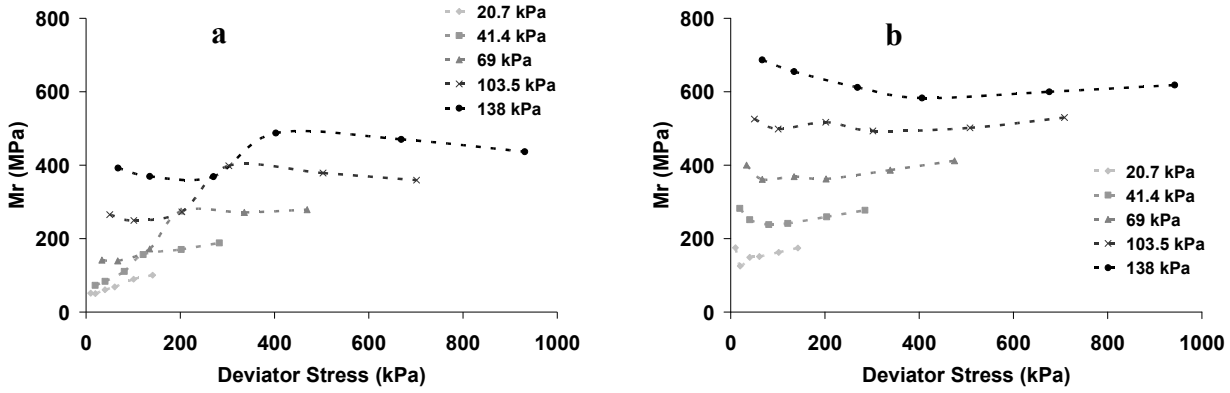

Figure 4.32 Variation in resilient modulus of a mixture of 75% RCM + 25% Aggregates as a function of deviator stress for various confining pressures. Figure 4.32.a is for specimens at optimum moisture content (MC=9.3%) whereas figure 4.32.b is for specimens at a drier water content corresponding to 300 kPa suction (MC=8.2%). The confining pressure varied from 20.7 kPa to 138 kPa.

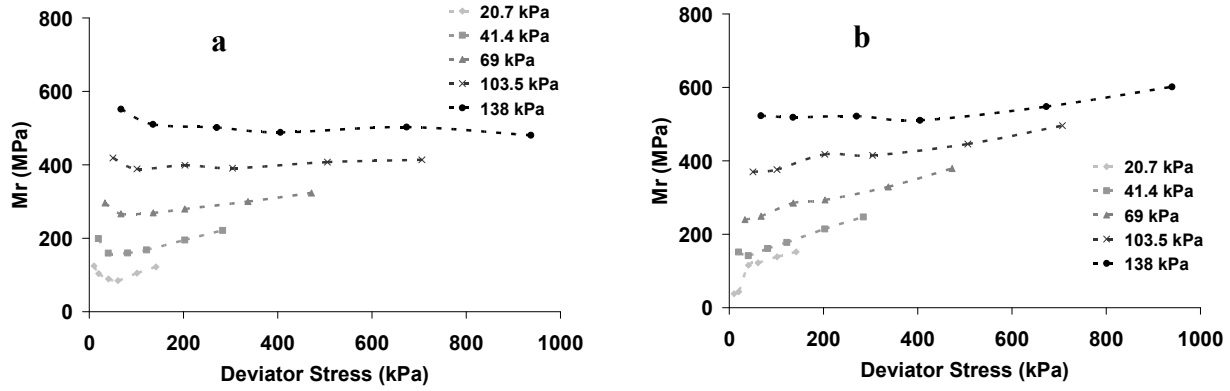

Figure 4.33 Variation in resilient modulus of a mixture of 100% RCM as a function of deviator stress for various confining pressures. Figure 4.33.a is for specimens at optimum moisture content (MC=9.4%) whereas figure 4.33.b is for specimens at a drier water content corresponding to 300 kPa suction (MC=8.5%). The confining pressure varied from 20.7 kPa to 138 kPa.

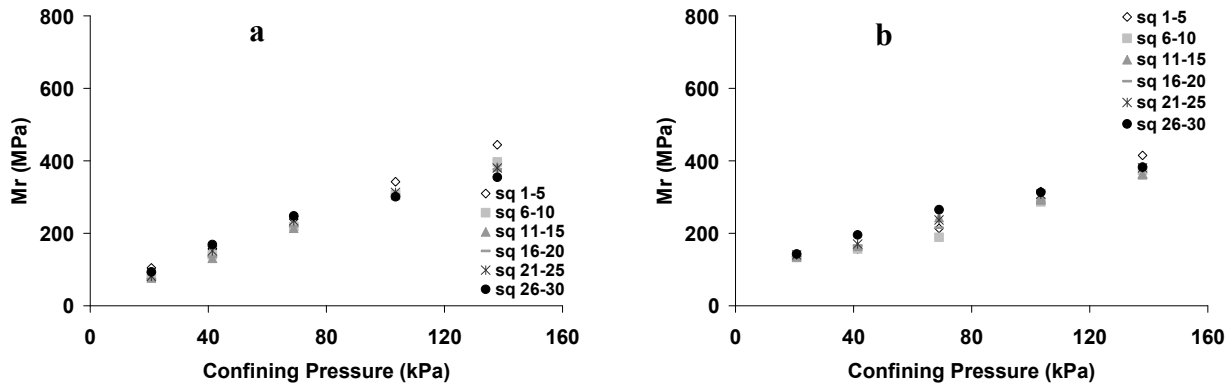

Figure 4.34 Variation in resilient modulus of a mixture of 25% RCM + 75% Aggregates as a function of deviator stress for various confining pressures. Figure 4.34.a is for specimens at optimum moisture content (MC=9.2%) whereas figure 4.34.b is for specimens at a drier water content corresponding to 300 kPa suction (MC=7.8%). The deviator stress varied from 4.1 kPa to 27.6 kPa.

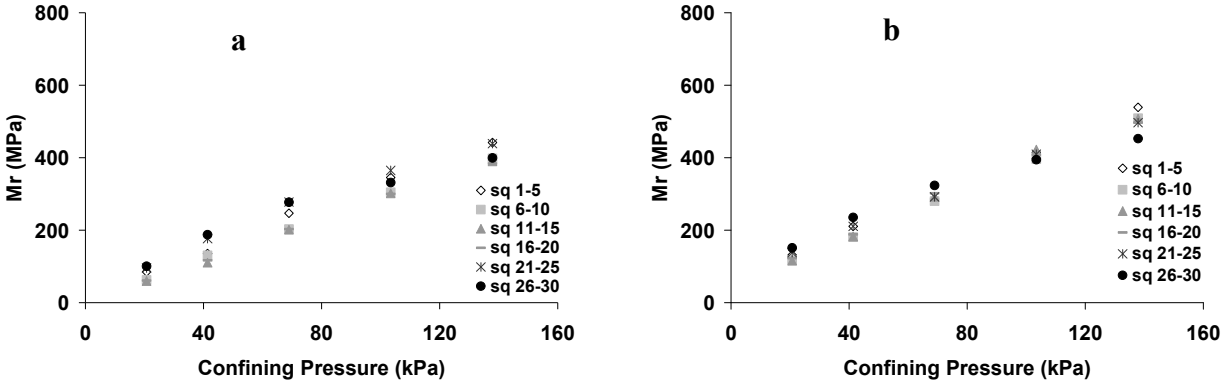

Figure 4.35 Variation in resilient modulus of a mixture of 50% RCM + 50% Aggregates as a function of confining pressure for various sequences in Table 4.1. Figure 4.35.a is for specimens at optimum moisture content (MC=9.7%) whereas figure 4.35.b is for specimens at a drier water content corresponding to 300 kPa suction (MC=7.8%). The deviator stress varied from 4.1 kPa to 27.6 kPa.

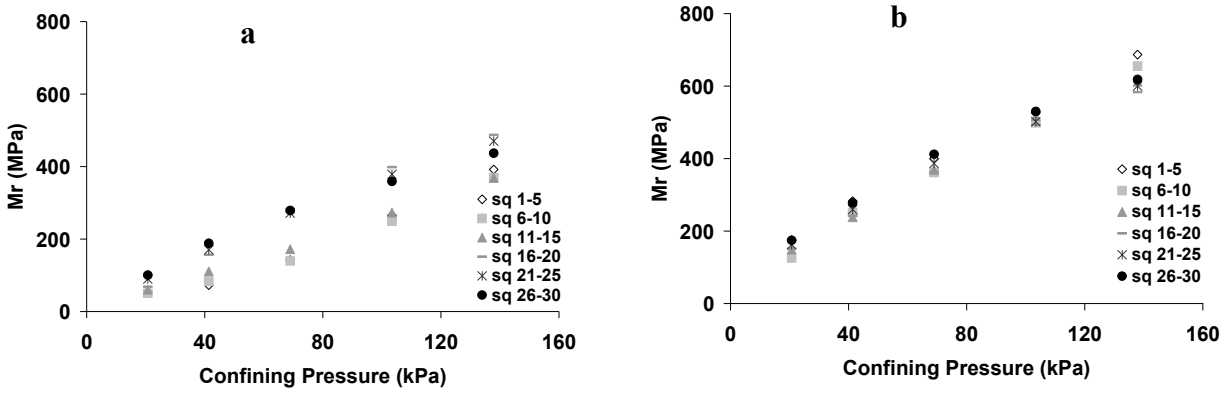

Figure 4.36 Variation in resilient modulus of a mixture of 75% RCM + 25% Aggregates as a function of confining pressure for various sequences in Table 4.1. Figure 4.36.a is for specimens at optimum moisture content (MC=9.3%) whereas Figure 4.36.b is for specimens at a drier water content corresponding to 300 kPa suction (MC=8.2%). The deviator stress varied from 4.1 kPa to 27.6 kPa.

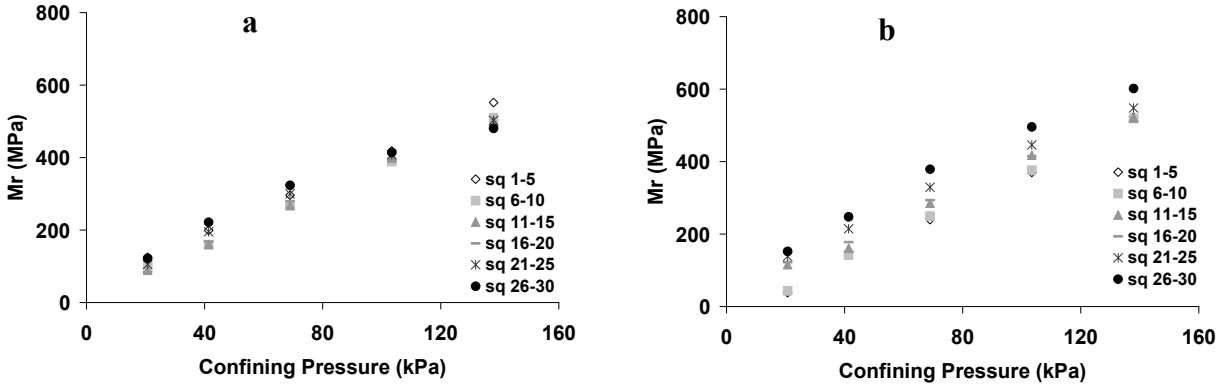

Figure 4.37 Variation in resilient modulus of a mixture of 100% RCM as a function of confining pressure for various sequences in Table 4.1. Figure 4.37.a is for specimens at optimum moisture content (MC=9.4%) whereas figure 4.37.b is for specimens at a drier water content corresponding to 300 kPa suction (MC=8.5%). The deviator stress varied from 4.1 kPa to 27.6 kPa.

Foundry Sand-Aggregate Mixtures: Figures 4.38 to 4.43 show the variation in M_R values as a function of deviator stress and confining pressures for three FS-Aggregate mixtures at two different water contents (optimal water content and drier conditions corresponding to 300 kPa suction). Because of the lack of strength, the specimens containing FS failed before reaching sequence #30. For the sequences tested, the trends in M_R values of the FS-Aggregate mixtures in terms of deviator stress and confining pressure effects were nearly similar to that of RAP-aggregate mixtures i.e. an increase in M_R values with an increase in confining stress but minimal change with an increase in deviator stress. However, the differences in M_R values between the optimal water content and the water content corresponding to 300 kPa suction were only apparent at small proportion of foundry sand in the mixtures. At higher proportion of foundry sand, the differences in M_R values between two wetness conditions were minimal. This is mainly because there was very little difference in water contents of the mixtures at these two wetness conditions. At a given water content, M_R values of the FS-Aggregate mixtures decreased with an increase in presence of foundry sand. For a given sequence, M_R values of 5% foundry sand aggregate mixtures met or exceeded the values of 100% virgin aggregates whereas at 10% foundry sand, M_R values of the mixtures were slightly lower or same as that of 100% aggregates.

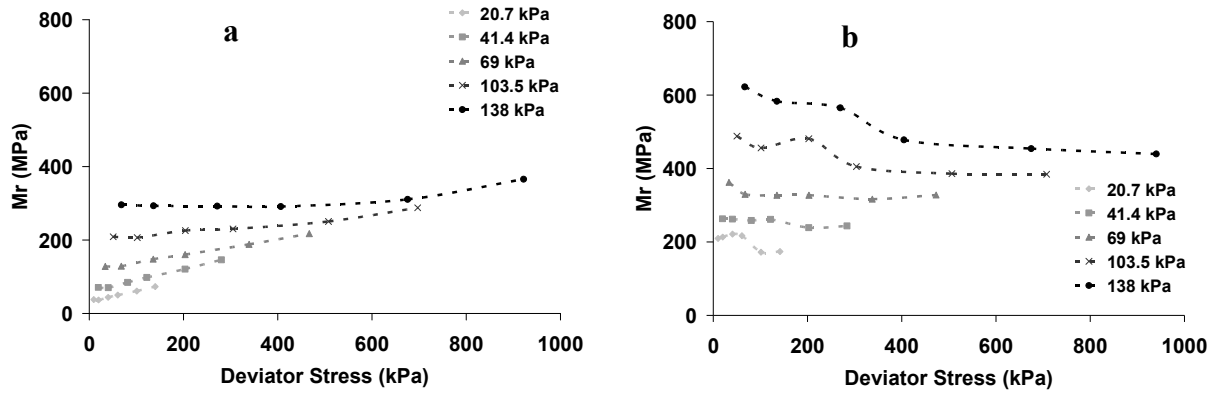

Figure 4.38 Variation in resilient modulus of a mixture of 5% Foundry Sand + 95% Aggregates as a function of deviator stress for various confining pressures. Figure 4.38.a is for specimens at optimum moisture content (MC=9.2%) whereas figure 4.38.b is for specimens at a drier water content corresponding to 300 kPa suction (MC=7.2%). The deviator stress varied from 4.1 kPa to 27.6 kPa.

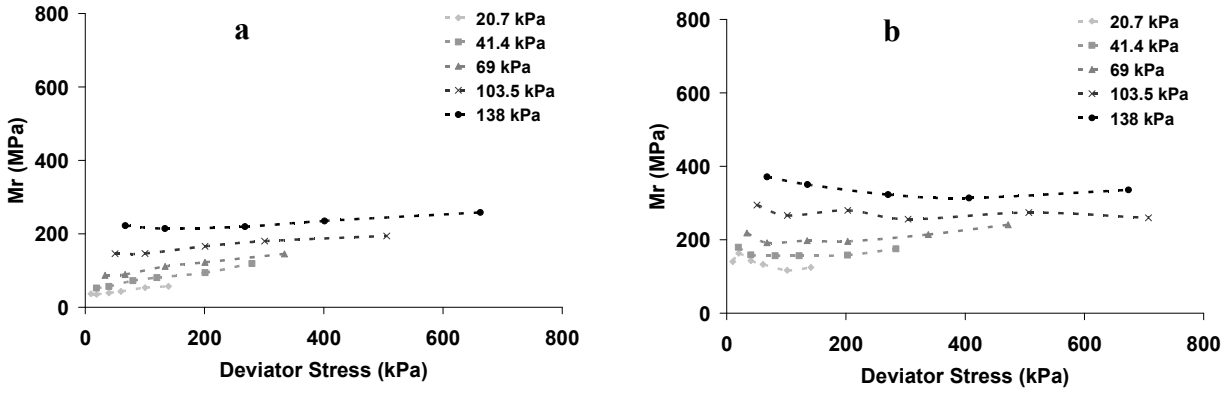

Figure 4.39 Variation in resilient modulus of a Mixture of 10% Foundry sand + 90% Aggregates as a function of deviator stress for various confining pressures. Figure 4.39.a is for specimens at optimum moisture content (MC=9.3%) whereas figure 4.39.b is for specimens at a drier water content corresponding to 300 kPa suction (MC=7.3%). The deviator stress varied from 4.1 kPa to 27.6 kPa.

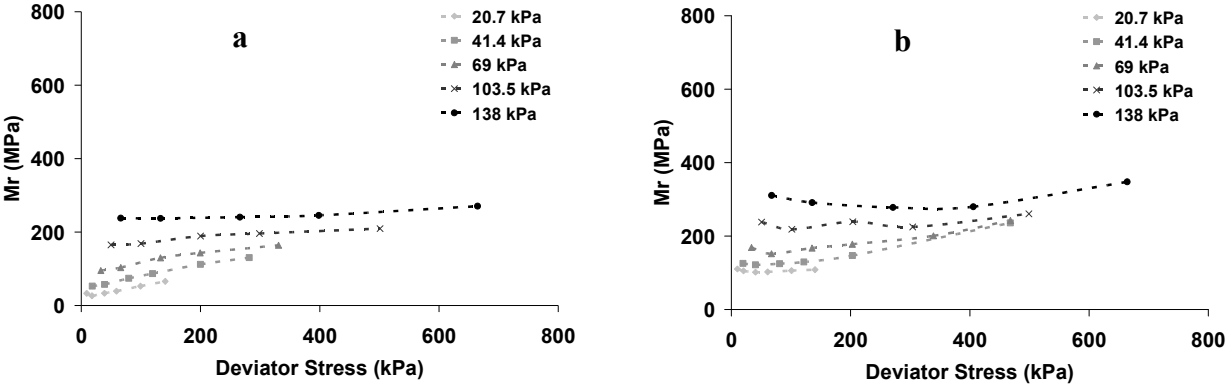

Figure 4.40 Variation in resilient modulus of a mixture of 15% Foundry Sand + 85% Aggregates as a function of deviator stress for various confining pressures. Figure 4.40.a is for specimens at optimum moisture content (MC=9.4%) whereas figure 4.40.b is for specimens at a drier water content corresponding to 300 kPa suction (MC=7.2%). The deviator stress varied from 4.1 kPa to 27.6 kPa.

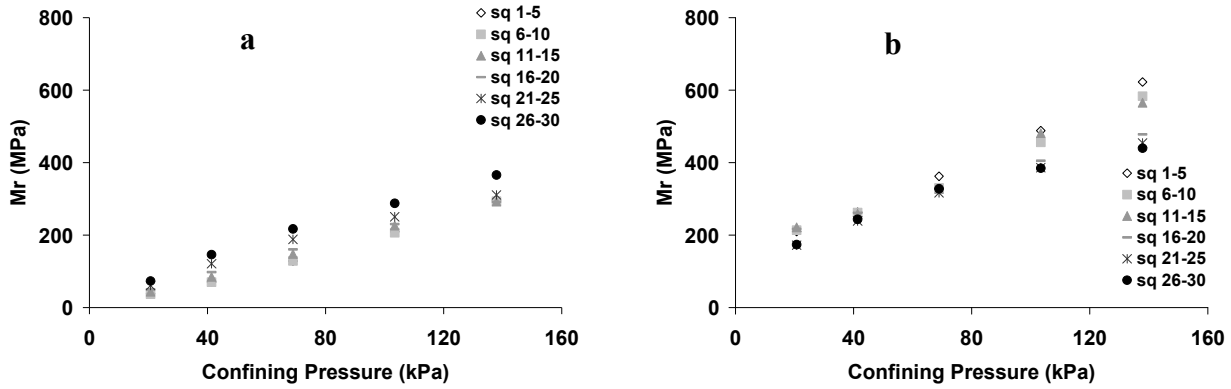

Figure 4.41 Variation in resilient modulus of a mixture of 5% Foundry Sand + 95% Aggregates as a function of confining pressures for various sequences in Table 4.1. Figure 4.41.a is for specimens at optimum moisture content (MC=9.2%) whereas figure 4.41.b is for specimens at a drier water content corresponding to 300 kPa suction (MC=7.2%). The deviator stress varied from 4.1 kPa to 27.6 kPa.

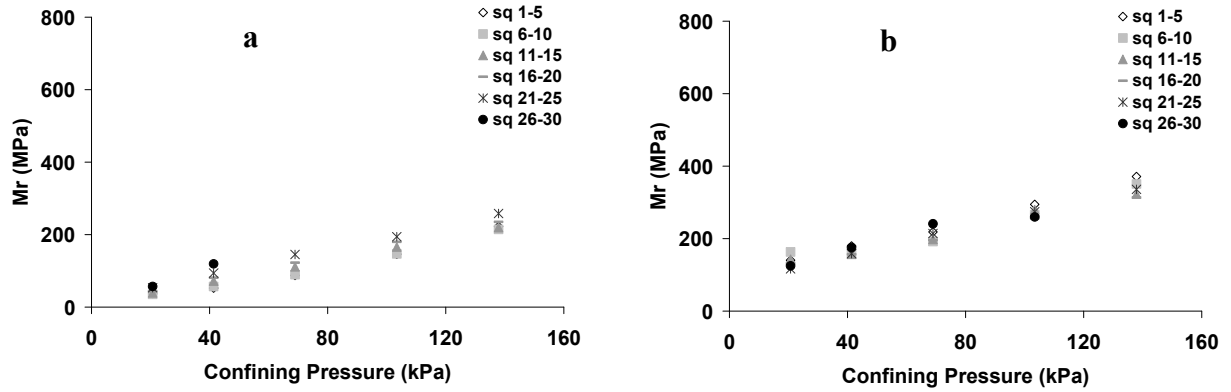

Figure 4.42 Variation in resilient modulus of a mixture of 10% Foundry Sand + 90% Aggregates as a function of confining pressures for various sequences in Table 4.1. Figure 4.42.a is for specimens at optimum moisture content (MC=9.3%) whereas figure 4.38.b is for specimens at a drier water content corresponding to 300 kPa suction (MC=7.3%). The deviator stress varied from 4.1 kPa to 27.6 kPa.

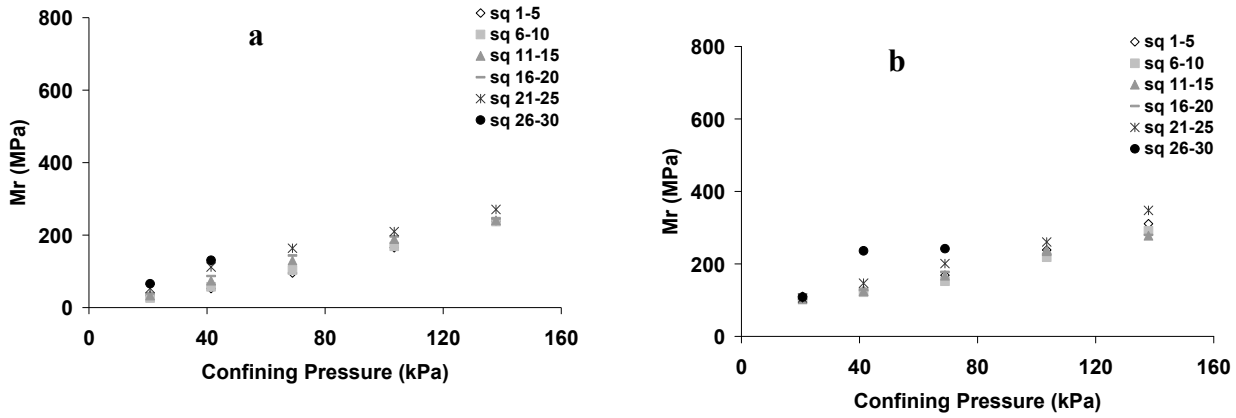

Figure 4.43 Variation in resilient modulus of a mixture of 15% Foundry Sand + 85% Aggregates as a function of confining pressures for various sequences in Table 4.1. Figure 4.43.a is for specimens at optimum moisture content (MC=9.4%) whereas figure 4.43.b is for specimens at a drier water content corresponding to 300 kPa suction (MC=7.2%). The deviator stress varied from 4.1 kPa to 27.6 kPa.

Tables of M_R values for each sequence from all 36 specimens are listed in Appendix Table A 11~ A46.

Model Fitting

Several different models have been proposed in the literature to describe the M_R data. Some models are based on its dependency on bulk and octahedral stresses (Uzan, 1985; Witczak and Uzan, 1988; Witczak et al. 2004) whereas others are based on confining and deviator stresses (Pezo, 1993). These models are as follows:

Bulk & Octahedral Shear Stress Model

$$Mr = k_1 P_a \left(\frac{\theta}{P_a} \right)^{k_2} \left(\frac{\tau_{oct}}{P_a} + 1 \right)^{k_3} \quad [4.13]`$$

where
M_r = resilient modulus (units are 1000 x the units for stress inputs)
P_a = atmospheric pressure (same units as stress inputs)
θ = bulk stress
τ_{oct} = octahedral shear stress, and
k_1, k_2, k_3 are empirical coefficients.

$$\theta = \sigma_1 + 2\sigma_3 = \sigma_d + 3\sigma_3 \quad [4.14]$$

$$\tau_{oct} = \frac{1}{3}\sqrt{(\sigma_1 - \sigma_2)^2 + (\sigma_1 - \sigma_3)^2 + (\sigma_2 - \sigma_3)^2} \quad [4.15]$$

$$if \sigma_2 = \sigma_3, \quad [4.16]$$

$$\tau_{oct} = \frac{\sqrt{2}}{3}\sigma_d \quad [4.17]$$

Confining & Deviator Stress Model

$$Mr = k_4 P_a \left(\frac{\sigma_3}{P_a} \right)^{k_5} \left(\frac{\sigma_d}{P_a} \right)^{k_6} \quad [4.18]$$

where
σ_3= confining stress
σ_d= deviator stress, and
k_4, k_5, and k_6 are empirical coefficients

We fitted both types of models to our data and extracted the coefficients (k_1 thru k_6) that can potentially be used to calculate M_R values for other stress conditions. The above models have also been modified to simulate unsaturated conditions (Gupta et al., 2007). The above coefficients can potentially be used in the modified models to predict M_R values at other stresses and under unsaturated conditions. Furthermore, the new national pavement design guide being

finalized in NCHRP Project 1-37A also requires these coefficients to operate design guide software. These values are given in Tables 4.3 through Table 4.6. Except for three materials, the fit of these model to our data was excellent with R^2 >0.9. The three materials that had R^2 <0.9 were 5% FA + 50% RAP + 45% Agg, 10% FS + 90% Agg, and 5% FA +50% RAP + 45% Agg. All three materials were at water contents corresponding to 300 kPa suction. Except for k_1, there was no specific trend in k values with addition of recycled materials. k_1 increased with addition of recycled materials for RAP, FA, and RCM. However, k_1 value decreased with addition of FS. Overall, k values of the recycled materials are similar to the corresponding values for 100% aggregates thus indicating that recycled mixtures tested in this study are similar to that of 100% virgin aggregates in terms of their stiffness.

Table 4.3 Coefficients k_1, k_2, k_3 of the model describing M_R based on bulk and octahedral stresses. These coefficients are for tests conducted at optimum water content.

	k_1	**k_2**	**k_3**	**R^2**
Agg 100%	0.442	1.191	-0.636	0.97
RAP 25%+Agg 75%	0.487	1.092	-0.466	0.98
RAP 50%+Agg 50%	0.799	1.270	-0.986	0.98
RAP 75%+Agg 25%	0.993	1.189	-0.958	0.95
RAP 100%	1.153	1.226	-0.972	0.98
Fly Ash 5% +RAP 25%+Agg 70%	0.445	1.381	-0.934	0.97
Fly Ash 15%+RAP 25%+Agg 60%	0.466	1.233	-0.867	0.94
Fly Ash 5% +RAP 50%+Agg 45%	0.674	1.414	-1.111	0.97
Fly Ash 15% +RAP 50%+Agg 35%	0.611	1.216	-0.903	0.94
Fly Ash 5% +RAP 75%+Agg 20%	0.786	1.311	-0.903	0.95
Fly Ash 15% +RAP 75%+Agg 10%	0.968	1.256	-1.117	0.92
RCM 25%+Agg 75%	0.677	1.044	-0.590	0.92
RCM 50%+Agg 50%	0.737	1.161	-0.818	0.93
RCM 75%+Agg 25%	0.715	1.120	-0.647	0.91
RCM 100%	0.983	1.211	-0.937	0.95
Foundry Sand 5%+Agg 95%	0.402	1.115	-0.480	0.99
Foundry Sand 10%+Agg 90%	0.397	0.997	-0.376	0.98
Foundry Sand 15%+Agg 85%	0.397	1.146	-0.481	0.99

Table 4.4 Coefficients k_4, k_5, k_6 of the model describing M_R based on confining and deviator stresses. These coefficients are for tests conducted at optimum water content.

	k_4	k_5	k_6	R^2
Agg 100%	1.785	0.743	0.218	0.95
RAP 25%+Agg 75%	1.841	0.684	0.257	0.97
RAP 50%+Agg 50%	3.051	0.824	0.100	0.97
RAP 75%+Agg 25%	3.422	0.787	0.068	0.94
RAP100%	4.119	0.771	0.102	0.96
Fly Ash 5% +RAP 25%+Agg 70%	2.032	0.872	0.172	0.95
Fly Ash 15%+RAP 25%+Agg 60%	1.842	0.828	0.115	0.96
Fly Ash 5% +RAP 50%+Agg 45%	2.994	0.923	0.100	0.96
Fly Ash 15% +RAP 50%+Agg 35%	2.343	0.846	0.074	0.96
Fly Ash 5% +RAP 75%+Agg 20%	3.221	0.788	0.187	0.95
Fly Ash 15% +RAP 75%+Agg10%	3.600	0.903	-0.008	0.98
RCM 25%+Agg 75%	2.306	0.736	0.118	0.95
RCM 50%+Agg 50%	2.670	0.770	0.109	0.94
RCM 75%+Agg 25%	2.617	0.733	0.165	0.91
RCM 100%	3.622	0.827	0.069	0.97
Foundry Sand 5%+Agg 95%	1.584	0.728	0.216	0.98
Foundry Sand 10%+Agg 90%	1.397	0.667	0.207	0.98
Foundry Sand 15%+Agg 85%	1.619	0.744	0.232	0.97

Table 4.5 Coefficients k_1, k_2, k_3 of the model describing M_R based on bulk and octahedral stresses. These coefficients are for tests conducted at water content corresponding to 300 kPa suction.

	k_1	k_2	k_3	R^2
Agg 100%	0.985	0.787	-0.653	0.89
RAP 25%+Agg 75%	2.107	0.857	-0.869	0.91
RAP 50%+Agg 50%	1.778	1.006	-0.904	0.96
RAP 75%+Agg 25%	1.686	1.101	-0.976	0.98
RAP100%	1.129	1.159	-0.878	0.99
Fly Ash 5% +RAP 25%+Agg 70%	2.108	0.778	-0.858	0.83
Fly Ash 15%+RAP 25%+Agg 60%	0.989	1.133	-1.035	0.92
Fly Ash 5% +RAP 50%+Agg 45%	3.495	0.575	-0.781	0.23
Fly Ash 15% +RAP 50%+Agg 35%	0.934	1.125	-1.001	0.92
Fly Ash 5% +RAP 75%+Agg 20%	1.736	1.056	-0.794	0.97
Fly Ash 15% +RAP 75%+Agg 10%	0.601	1.478	-1.256	0.97
RCM 25%+Agg 75%	1.304	0.700	-0.524	0.88
RCM 50%+Agg 50%	1.337	1.013	-0.875	0.94
RCM 75%+Agg 25%	1.677	1.037	-0.918	0.93
RCM 100%	0.874	1.297	-0.877	0.96
Foundry Sand 5%+Agg 95%	1.248	0.684	-0.636	0.83
Foundry Sand 10%+Agg 90%	1.366	0.648	-0.615	0.78
Foundry Sand 15%+Agg 85%	1.001	0.657	-0.364	0.88

Table 4.6 Coefficients k_4, k_5, k_6 of the model describing M_R based on confining and deviator stresses. These coefficients are for tests conducted at water content corresponding to 300 kPa suction.

	k_4	k_5	k_6	R^2
Agg 100%	2.294	0.553	0.019	0.95
RAP 25%+Agg 75%	4.839	0.602	-0.034	0.97
RAP 50%+Agg 50%	4.947	0.686	0.014	0.99
RAP 75%+Agg 25%	5.004	0.692	0.054	0.94
RAP 100%	3.816	0.720	0.117	0.96
Fly Ash 5% +RAP 25%+Agg 70%	4.434	0.583	-0.077	0.95
Fly Ash 15%+RAP 25%+Agg 60%	3.088	0.765	0.014	0.94
Fly Ash 5% +RAP 50%+Agg 45%	6.325	0.611	-0.226	0.61
Fly Ash 15% +RAP 50%+Agg 35%	2.991	0.789	0.005	0.96
Fly Ash 5% +RAP 75%+Agg 20%	5.219	0.639	0.122	0.93
Fly Ash 15% +RAP 75%+Agg 10%	2.710	0.956	0.080	0.96
RCM 25%+Agg 75%	2.864	0.506	0.031	0.93
RCM 50%+Agg 50%	3.859	0.706	0.017	0.98
RCM 75%+Agg 25%	4.962	0.740	-0.003	0.98
RCM 100%	3.438	0.732	0.216	0.91
Foundry Sand 5%+Agg 95%	2.569	0.517	-0.019	0.95
Foundry Sand 10%+Agg 90%	2.714	0.505	-0.034	0.92
Foundry Sand 15%+Agg 85%	2.228	0.465	0.083	0.89

Shear Strength

Table 4.7 lists the estimated cohesion and friction angles for specimen compacted at optimal water contents. These values are calculated both at failure and at 1% strain. In general, friction angles calculated from measurement at failure were nearly same (38º to 49º) for most mixtures of RAP + Aggregate, Fly ash + RAP + Aggregate, and RCM + Aggregate. The exceptions were the highest value of 58 º for 5% Fly Ash + 50% RAP + 45% Aggregate. The lowest two values were 19º and 30º for 75% RCM + 25%Aggreagte and 15% Fly ash + 25% RAP + 60% Aggregates, respectively. Cohesion values calculated from measurement at failure of all RAP-Aggregate mixtures were also nearly similar. However, addition of 5% Fly ash decreased the cohesion whereas addition of 15% Fly ash increased the cohesion of the specimens. There was no clear trend in the cohesion values of RCM-Aggregate mixtures. It appears that fly ash reacted with water prior to compaction thus loosing some of its effectiveness.

Table 4.7 Shear strength parameters of recycled material mixtures with aggregates at optimal water contents. Shear strength parameters are calculated both at 1% strain and at failure.

Materials	Confining Pressure (kPa)	Deviator Stress (kPa) at 1% Strain	Deviator stress (kPa) at failure	Strain at Failure (ε (%))	At 1% Strain		At Failure	
					Cohesion (c), kPa	Friction Angle (ϕ)	Cohesion (c), kPa	Friction Angle (ϕ)
RAP 50%+Agg 50%	35	674	692	1.26	176	30	1421	385
	69	742	802	1.42				
RAP 75%+Agg 25%	35	701	733	1.32	126	426	143	40
	69	838	856	1.29				
RAP100%	35	753	806	1.42	304	11	1212	47
	69	769	994	1.53				
Fly Ash 5% +RAP 25%+Agg 70%	357	453	585	1.57	104	32	76	48
	69	531	778	1.52				
Fly Ash 15%+RAP 25%+Agg 60%	35	399	738	1.38	8	57	179	30
	69	747	747	1.00				
Fly Ash 5% +RAP 50%+Agg 45%	35	550	559	0.53	34	56	29	57
	69	877	921	1.26				
Fly Ash 15% +RAP 50%+Agg 35%	35	431	858	0.91	32	52	123	49
	69	681	1065	1.48				
Fly Ash 5% +RAP 75%+Agg 20%	35	631	764	1.61	60	53	118	46
	69	903	942	1.42				
Fly Ash 15% +RAP 75%+Agg10%	35	956	978	0.89	256	30	199	40
	69	1025	1103	0.52				
RCM 25%+Agg 75%	35	N.A	N.A	N.A	N.A	N.A	N.A	N.A
	69	613	619	0.86				
RCM 50%+Agg 50%	35	635	654	0.78	119	40	1315	38
	69	759	767	1.11				
RCM 75%+Agg 25%	35	N.A	770	0.94	N.A	N.A	265	19
	69	762	802	1.36				
RCM 100%	35	930	940	1.11	8	49	1913	40
	69	919	1063	1.27				

† One specimen failed during M_R testing and thus shear strength could not be calculated using this method.

Table 4.8 Shear strength parameters of recycled material mixtures with aggregates at optimal water content. Since only one specimen was sheared, shear strength parameters are estimated from shearing angle on the specimen.

Materials	Moisture Content (%)	σ_3 (kPa)	σ_1-σ_3 (kPa)	Cohesion (c), kPa	Friction Angle (ϕ)
RAP 50%+Agg 50%	6.2	34	2837	290	9
		69	3289	211	27
Fly Ash 5% +RAP 25%+Agg 70%	8.6	34	2397	183	37
		69	3188	139	34
Fly Ash 15%+RAP 25%+Agg 60%	10.3	34	2791	255	27
		69	3064	201	27
Fly Ash 5% +RAP 50%+Agg 45%	7.8	34	2292	403	13
		69	3777	229	8
Fly Ash 15% +RAP 50%+Agg 35%	8.2	34	3518	197	33
		69	4365	226	16
Fly Ash 15% +RAP 75%+Agg10%	7.4	34	4011	206	30
		69	4521	110	30
RCM 50%+Agg 50%	9.7	34	2681	218	36
		69	3145	309	13
RCM 75%+Agg 25%	9.3	34	3157	309	28
		69	3289	320	6
RCM 100%	9.4	34	3853	302	24
		69	4358	270	25

Cohesion and friction values of each individual specimen at optimal water contents were also calculated using the shearing angle measurements on these specimens after failure (Table 4.8). Friction angles using this procedure were generally lower whereas cohesion values were generally higher than the values listed in Table 4.7.

Cohesion values calculated at 1% strain did not quite correspond to the values at failure (Table 4.7). However, friction angle were nearly same but again the trend in cohesion and friction angle with addition of recycled materials at 1% strain did not match with trends in corresponding values at failure.

Table 4.9 lists the corresponding cohesion and friction angle values for the drier specimens (water contents corresponding to 300 kPa suction). These values estimated from shearing angle on the specimen were comparable to corresponding values for optimal water contents. There was no clear trend on the effects of mixing recyclable material on either of the shearing strength parameters.

Table 4.9 Shear strength parameters of recycled material mixtures with aggregates at water contents corresponding to 300 kPa suction. Since only one specimen was sheared, shear strength parameters are estimated from shearing angle on the specimen.

Sample Name	**Moisture Content %**	**σ_3 (kPa)**	**σ_1-σ_3 (kPa)**	**Cohesion (c), kPa**	**Friction Angle (ϕ)**
50% RAP+50%Agg	7.8	69	954	335	18
75% RAP+25%Agg	6.6	69	983	195	35
100% RAP	5.4	69	933	182	43
5% FA+25% RAP+70% Agg	4.0	69	990	321	29
15% FA+25% RAP+60% Agg	8.2	69	1135	321	21
5% FA+50% RAP+45% Agg	10.2	69	1219	88	54
15% FA+50% RAP+35% Agg	7.4	69	1001	203	39
5% FA+75% RAP+20% Agg	8.6	69	1140	185	39
15% FA+75% RAP+10% Agg	6.6	69	1219	122	47
25% RCM+75% Agg	7.4	69	1074	102	48
50% RCM+50% Agg	9.8	69	1004	564	4
75% RCM+25% Agg	9.4	69	989	335	18
100 % RCM	9.4	69	922	195	35
50% RAP+50%Agg	9.4	69	1219	182	43

CONCLUSIONS

The M_R and shear strength measurements in this study show that FA, RAP, and RCM will be good substitutes for virgin aggregates as base and subbase materials in road construction. However, these materials should be further tested in-situ before full implementation of these findings.

CHAPTER 5-LEACHING CHARACTERIZATION

INTRODUCTION

Construction and maintenance of roads requires large volume of aggregates for use as base or subbase materials. At the same time, a large volume of waste materials is also produced that can be potentially recycled in road construction. Both the Federal Highway Administration (FHWA) and the Environmental Protection Agency (EPA) encourage beneficial use of recycled materials including the recycling of pavement materials. However, some of the recycled materials may contain toxic substances such as heavy metals that could leach with water and end up in aquifer or streams thus impacting the human and environmental health. Therefore, an assessment of leaching characteristics of the recycled materials is needed before implementing their use in road construction.

The fate and transport of contaminants depend on the solubility, desorption/adsorption, diffusion and advection processes. In case of granular materials used for base and subbase, solubility and desorption plays an important role in determining the extent to which a chemical is released. In terms of their transport, the next important factor is the hydraulic conductivity of the granular material under both saturated and unsaturated conditions. However, there is lack of information on the fate and transport of chemicals in recycled materials as their hydraulic behavior when mixed with virgin aggregates. In this study, we evaluated the potential leachability of chemicals from 17 mixtures of four recycled materials with virgin aggregates and 100% virgin aggregates. The leachability tests were run in both batch and flow through modes under saturated and unsaturated conditions. In the flow through mode, we also measured the hydraulic conductivities of these mixtures under both saturated and unsaturated conditions.

MATERIALS AND METHODS

Batch Test

Batch test was run on 17 recycled mixtures, 100% virgin aggregate, 100% fly ash and 100% foundry sand. The procedure involved mixing 10 g of air dry material (<9 mm) with 200 mL of Mili-Q water (Solid/Liquid ratio = 1:20) in a 250 mL Polytetrafluoroethylene (PTFE) bottles. Mixing was done in end-over-end rotary mixer (speed=20±2rpm) to insure good contact between the sample and the leachate. Mixing was done for two different periods: 18 hours and 7 days. After mixing, the suspension was filtered using borosilicate glass fiber filter (0.6 μm) and the filtrate was collected in 50 mL centrifuge tubes. The filtrates were acidified (pH<2) with 0.2 mL of nitric acid and then stored at 4 ^{o}C until chemical analysis by the Soil Testing Laboratory at the University of Minnesota. The laboratory follows a strict QA/QC protocol. Heavy metal concentrations in the leachate were measured using the Inductively Coupled Plasma (ICP).

Figure 5.1 A rotary end-over-end mixer used for mixing recycled-aggregate mixtures with Mili-Q water in a batch test.

Flow thru Leaching Test

Flow thru leaching tests were run on specimens (152 mm diameter and 152 mm length) that have been compacted at optimal water content in a gyratory compactor. The compaction parameters were the same as in water retention and resilient modulus measurements i.e. compaction pressure of 600 kPa, 100 gyrations, base rotation of 30 revolutions per minute, and mold position at a compaction angle of 1.25 degrees. Target densities were the maximum densities. A total of 4 flow thru tests were run per mixture; two under saturated conditions and two under unsaturated conditions.

Figure 5.2 Assembly of specimens into leaching columns.

After compaction, the specimens were assembled into a leaching column made up of 152.4 mm diameter and 300 mm long clear PVC tubes. Since the diameter of the specimen was

slightly smaller than that of the PVC tube, molten (~60 ºC) paraffin wax was poured in the space between the specimen and the tube to prevent side wall or preferential flow during leaching. Paraffin wax around 60 ºC solidifies rapidly without penetrating into the specimen. The PVC tube column assembly containing specimen was then slid into a PVC cap (with a bottom outlet) that contained a piece of foam and about 3 cm of acid washed grade 12 sand (Sigma-Aldrich, Milwaukee, WI). The specification of the sand were particle size varying from 0.075 to 0.65 mm, pore volume of 0.43 cm^3/g, and surface area of 300 cm^2/g. The foam at the bottom of the PVC cap prevented leaching of specimen particles during flow thru test whereas sand helped in providing good contact between the specimen and the foam. The columns were vertically placed on a stand and the surface of each column then covered with about 3 cm of acid washed grade 12 sand. Although the PVC tube snuggly fitted into the PVC cap, the seam between the pipe and the cap was further sealed with silicon rubber from a hardware store. The silicon was allowed to dry at least overnight. Assembled columns were then allowed to saturate from bottom up using the deionized water (Huang et al., 1998) until the sand at the surface of the specimen appeared saturated. At that point, the top of the PVC column was covered with a plastic sheet (to prevent evaporation) and the bottom outlet in the PVC cap was closed so as to allow the specimen to equilibrate for 2 days (Buczko et al., 2004). After two days, the column was leached with 0.01M LiBr solution. Bromide in the solution acted as a conservative tracer during the breakthrough leaching process.

Breakthrough curves were run at two hydraulic heads (0.2 and -2.0 kPa) on all 17 recycled mixtures and 100% virgin aggregates. The distribution of bromide solution at the soil surface was done with a Plexiglas disk (Fig. 5.2). The diameter of disk was about the same as the diameter of the specimen but slightly smaller than the diameter of the PVC pipe. The Plexiglas disk was designed to simulate the bottom of the tension infiltrometer (Munyankusi et al., 1994). The top of the disk was connected to a Marriotte bottle system. The bottom of the disk had a stainless steel screen that was covered with a pad made from a humidifier belt and a nylon membrane with a 37 μm diameter openings (Model D-CMN-37Sm, All Parts Equipment, Miami, FL). An O-ring was slipped around the groove of the Plexiglas plate to keep the membrane in place and provide a tight seal to prevent the back entry of air when the disk was transferred from the solution reservoir to the top of the specimen.

Before the start of the breakthrough experiment, the outlet at the bottom of the column was opened and the excess solution at the surface of the specimen was allowed to drain. After the excess solution at the surface disappeared, the Plexiglas plate was connected to the Marriotte bottle and the LiBr solution in the bottle was allowed to infiltrate into the specimen. Two sets of breakthrough curves were run. The first two curves were run at 0.2 kPa head (saturated) whereas the last two curves were run at -2.0 kPa head (unsaturated). The hydraulic head at the specimen surface was maintained by adjusting the tubes in the Marrotte bottle. The head at the bottom of the column was adjusted by either leaving it open to the atmosphere (saturated flow) or by applying 2.0 kPa vacuum at the base of the column (unsaturated flow). An on line air pressure regulator (Soil Measurement Systems, Tucson, AZ.) was used to control this small hydraulic head at the bottom of the column under unsaturated conditions. A water manometer hooked on line with the pressure regulator monitored the suction at the bottom of the column.

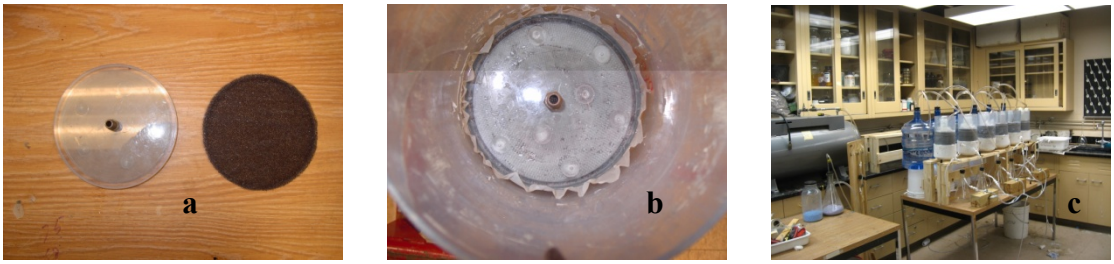

Figure 5.3 A flow thru assembly for running breakthrough curves under unsaturated conditions. Fig. 5.3a is the Plexiglas disk with foam, Fig. 5.3b is the assembled Plexiglas disk on the surface of the recycled material-aggregate mixture column, and Fig. 5.3c is the unsaturated flow thru assembly with Mariotte bottle set-up.

Breakthrough set-ups were also used to measure the hydraulic conductivity of the specimens. This was done by measuring the outflow rate as the discrete outflow samples were taken for tracer analysis at various times during the breakthrough experiment. At each sampling time about 150 mL of the leachate was collected for pH, bromide, and heavy metal analysis. Collected leachate was then sub sampled for pH and bromide measurements and the remaining leachate was acidified with nitric acid (<2 pH) and stored at 4 ^{o}C until heavy metal analysis. pH of the leachate was measured with Orion pH electrode (9107BN, Orion Research, Boston, MA). For bromide measurements, each 100 mL sub sample of the leachate was mixed with two milliliters of ionic strength adjustor (ISA: 5M $NaNO_3$, Orion research Incorporated, Boston, MA) and then bromide concentration analyzed using a specific ion electrode (Orion 9435 Bromide Electrode and 90-02 Double Junction Reference Electrode, Orion research Incorporated, Boston, MA). Heavy metals in the acidified leachate were analyzed using Inductively Coupled Plasma Atomic Emission Spectrophotometry (ICP-AES) (Perkin Elmer Model 3000 DV). The heavy metals analyzed were aluminum, arsenic, barium, beryllium, cadmium, chromium, copper, iron, lead and zinc. All metal analysis was done by the Soil Testing laboratory at the University of Minnesota using ICP. Concentration data given in this report refers to water dissolved concentrations. Batch concentrations refer to equilibrium conditions between mixtures and water whereas flow thru concentrations refers to non-equilibrium conditions as they might exists under field scenarios.

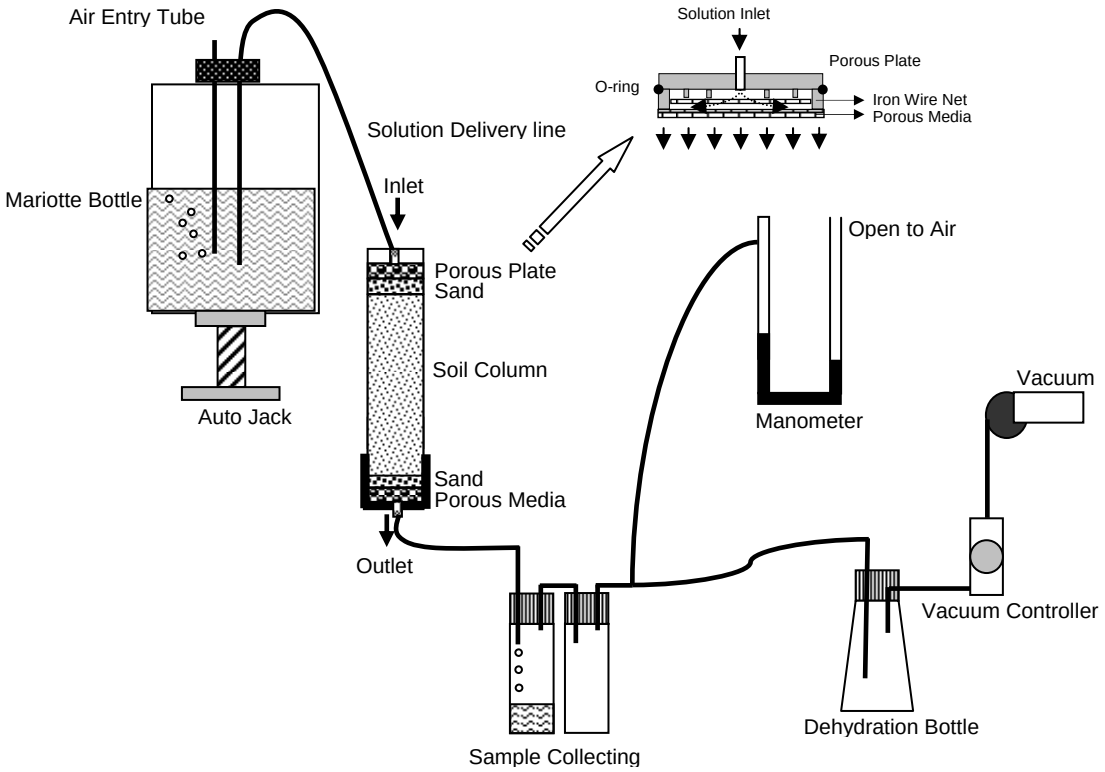

Figure 5.4 Schematic of column experiment.

RESULTS AND DISCUSSION

pH

pH of the leachate from the recycled material mixtures varied with the recycled material as well as whether the leachate was obtained in a batch mode or in a flow thru set-up (Table 5.1). In general, fly ash and reclaimed concrete mixtures with aggregates had higher pH values than the mixtures of RAP or foundry sand. Highest pH value of 11.6 (batch), 12.4 (Saturated Flow thru) and 12.1 (unsaturated flow thru) corresponded to 100% RCM. The differences between these values are relatively minor and mainly reflect the variability among the samples. For saturated flow, we only made the pH measurements for the RCM mixtures. For these mixtures, leachate pH generally followed the trends: saturated flow > unsaturated flow > batch mode. For other mixtures, leachate pH was higher from batch than flow thru set-up under unsaturated conditions. This is most likely due to limited contact between particles and water as it is moving through the mixtures under unsaturated conditions.

Generally, pH of the leachate increased with an increase in the FA content of the mixture. Highest pH value for FA mixtures was 11.19 for 100% FA in batch mode and 10.13 for 15% FA+75% RAP+10% Aggregates in flow thru mode under unsaturated conditions.

Table 5.1 pH of the leachate collected in batch and flow thru modes for various mixtures of recycled materials with aggregates.

Materials	Batch Test	Leaching Test	
		Saturated	Unsaturated
RAP25%+Agg75%	9.37		7.60
RAP50%+Agg50%	9.43		7.65
RAP75%+Agg 25%	9.49		7.62
RAP100%	9.67		7.57
Fly Ash 5% +RAP25% Aggregate 70%	10.58		9.19
Fly Ash 15% +RAP25%+Aggregate 60%	10.87		9.58
Fly Ash 5% +RAP50%+Aggregate 45%	10.68		9.07
Fly Ash 15% +RAP50%+Aggregate 35%	10.92		9.93
Fly Ash 5% +RAP75%+Aggregate 20%	10.77		8.27
Fly Ash 15% +RAP75%+Aggregate 10%	10.99		10.13
RCM 25% +Agg 75%	10.41	10.86	10.42
RCM 50%+Agg 50%	11.15	11.41	11.07
RCM 75%+Agg 25%	11.39	12.03	11.83
RCM 100%	11.57	12.37	12.12
Foundry Sand 5%+Agg95%	9.45		7.80
Foundry Sand 10%+Agg90%	9.41		7.70
Foundry Sand 15%+Agg85%	9.38		7.80
Aggregate 100%	9.19		7.71
Fly Ash 100%	11.19		
Foundry Sand 100%	9.97		

Heavy Metal Analysis

Batch Test: The concentration of heavy metals in the filtrate after 18 hrs (1 day) and 7 days of shaking the suspension of 17 mixtures of recycled materials and 100% virgin aggregates in water are shown in Table 5.2. In general, beryllium and cadmium concentrations in batch filtrate were less than the detection limit of the instrument for all 17 mixtures, one sample of virgin aggregate, 100% FA, and 100% FS. There was no systematic difference in concentration of heavy metals between 18 hrs and 7 day batch tests. In comparison to the EPA drinking water standard, concentration of most heavy metals in the 1:20 filtrate was higher. This is expected because recycled material and aggregate particles were thoroughly in contact with water and thus provided maximum potential for solubility and desorption.

Flow thru Set-up: Figures 5.5 to 5.8 shows the bromide breakthrough curve for various mixtures and three recycled materials (RAP, FA, FS) under both saturated (0.2 kPa hydraulic head) and unsaturated (2.0 kPa suction) flow conditions. For all materials, the centre of mass of the conservative tracer (Br^-) appeared around 1 pore volume for both saturated and unsaturated flow conditions thus suggesting there was no preferential or wall flow. Relatively, there were only slight differences in bromide BTC between replications thus suggesting that material packing with the gyratory compactor was consistent between replications.

Concentrations of heavy metals in the leachate from various mixtures of recycled materials during flow thru set-up under both saturated and unsaturated conditions are shown in Figures 5.9 to 5.24. In general, heavy metals concentrations in the leachate were less than the EPA drinking water standards. Heavy metal concentrations were also generally higher in the initial rather than the later aliquots of the leachate. This is mainly because the specimens were saturated for 48 hours before running the breakthrough test which means there was greater opportunity for increased solubility or desorption of heavy metals from the specimen in the first flushing of the percolate solution. For all fly ash mixtures under both saturated and unsaturated conditions, concentration of heavy metals in the leachate was generally higher than the drinking water standards. The concentration of some heavy metals in the leachate from RCM mixtures was also higher than the drinking water standards. There was no presence of arsenic in the leachate during any of the flow thru experiments.

Aluminum concentrations in the leachate from FA-RAP-Aggregate mixtures and RCM-aggregate mixtures were higher than the EPA drinking water standard (Figs. 5.9 and 5.10). However, aluminum concentration in the leachate were small from RAP and FS mixtures with aggregates under both saturated and unsaturated conditions. Except for RAP-Aggregate mixtures, cadmium concentrations in the leachate did not exceed the EPA drinking water standard for any of the mixtures of the recycled materials. Cadmium was not detected in the leachate from FA, RCM, and FS mixtures with aggregates under both saturated and unsaturated conditions (Figs. 5.11 and 5.12). Lead was not detected in the leachate from RAP-Aggregate mixtures under saturated condition or from FA, RAP mixtures with aggregates under both saturated and unsaturated conditions. Except for initial leachate sample from 75% RAP-Aggregate mixture under unsaturated conditions (Figs. 5.13 and 5.143), zinc concentration in the leachate was also lower than the EPA drinking water standard (Figs. 5.15 and 5.16).

In general, chromium concentrations in the leachate decreased with an increase in pore volumes of water passing thru the column (Figs. 5.17 and 5.18). Chromium was not detected in the leachate from RAP and FS mixtures with aggregates under both saturated and unsaturated conditions. However, chromium concentrations in the leachate from FA-RCM-Aggregate mixtures initially exceeded the limit of EPA drinking water standard but after around 3 pore volumes, the chromium concentrations were below the drinking water standard. Chromium concentration in the leachate for fly ash mixtures also increased with an increase in the proportion of fly ash in the mixtures. Maximum chromium concentration was around 1.3 mg/L under saturated flow thru condition and around 1.0 mg/L under unsaturated condition. Chromium was also detected in the leachate from RCM mixtures with aggregates but it was always less than the EPA drinking water standard under both saturated and unsaturated flow thru conditions.
Barium (Figs. 5.19 and 5.20), copper (Figs. 5.21 and 5.22), and iron (Figs. 5.23 and 5.24) concentrations of all eighteen materials were lower than the EPA drinking water standards. Highest barium and copper concentrations were detected for 100% RCM.

Concentration of heavy metals in a batch test (Figs. A.21 to A.40) was generally higher than that from the flow thru tests (Figs. 5.8 to 5.16 and A.41 to A.67). This is expected considering that reaction time of water with particles is limited in a flow through set-up than in a batch mode. In batch mode, particle and water molecules are near equilibrium conditions whereas in flow thru mode water molecules are in non-equilibrium conditions with recycled material particles. Heavy metal concentrations from breakthrough studies are closer to the concentrations that one would expect under field conditions.

Table 5.2 Dissolved metal concentrations (mg/L) in water filtrate from batch tests and the EPA drinking water standard.

Name	Al		As		Ba		Be		Cd		Cr		Cu		Fe		Pb		Zn	
Time (day)	1	7	1	7	1	7	1	7	1	7	1	7	1	7	1	7	1	7	1	7
EPA Drinking Water STD (mg/L)	0.05~0.2		0.01		2		0.004		0.005		0.1		1.3		0.3		0.015		5	
RAP25%+ Agg75%	0.40	0.32	0.01	<	0.16	0.12	<	<	<	<	<	<	<	<	7.10	0.77	0.89	<	<	0.01
RAP50%+ Agg 50%	0.36	0.57	0.01	<	0.14	0.12	<	<	<	<	<	<	<	0.00	6.58	1.14	2.32	<	<	0.01
RAP75%+ Agg 25%	0.26	0.69	0.01	<	0.13	0.11	<	<	<	<	<	<	<	0.00	3.65	1.47	2.12	<	<	0.01
RAP100%%	0.37	1.27	0.00	<	0.07	0.09	<	<	<	<	<	<	<	0.01	2.04	1.42	<	2.80	<	0.01
FA5% +RAP25%+Agg70%	8.91	2.58	<	<	0.22	0.28	<	<	<	<	<	<	<	<	<	<	<	<	<	0.00
FA15% +RAP25%+Agg60%	13.33	7.69	0.01	<	0.09	0.39	<	<	<	<	<	0.02	<	<	<	<	<	<	<	0.00
FA5% +RAP50%+Agg45%	10.30	5.07	<	<	0.23	0.28	<	<	<	<	<	<	<	<	<	<	<	<	<	0.01
FA15% +RAP50%+Agg35%	14.54	8.49	<	<	0.10	0.40	<	<	<	<	0.02	0.02	<	<	<	<	<	<	<	<
FA5% +RAP75%+Agg20%	15.40	10.12	<	<	0.23	0.33	<	<	<	<	<	<	<	<	<	<	<	<	<	0.01
FA15% +RAP75%+Agg10%	12.91	8.53	<	<	0.09	0.47	<	<	<	<	0.02	0.02	<	<	<	<	<	<	<	<
RCM 25%+Agg75%	0.08	0.09	<	<	0.02	0.03	<	<	<	<	<	<	<	0.00	<	<	<	<	<	<
RCM 50%+Agg50%	1.10	0.77	0.00	<	0.03	0.04	<	<	<	<	<	<	<	0.01	<	<	<	<	<	0.00
RCM 75%+Agg25%	2.29	1.84	0.01	<	0.04	0.07	<	<	<	<	<	0.01	<	0.01	<	<	<	<	<	0.01
RCM 100%	3.14	3.31	<	<	0.06	0.09	<	<	<	<	0.00	0.01	0.01	0.02	<	0.00	<	<	0.00	0.01
FS5%+ Agg95%	0.57	0.58	0.00	<	0.12	0.16	<	<	<	<	<	<	<	0.00	10.79	1.32	<	3.96	<	0.01
FS10%+Agg90%	0.86	1.64	0.00	<	0.18	0.23	<	<	<	<	<	<	<	0.01	8.34	3.34	1.91	5.46	<	0.03
FS15%+ Agg85%	0.60	1.80	0.00	0.00	0.14	0.28	<	<	<	<	<	<	<	0.01	17.77	2.88	1.98	4.17	<	0.03
Agg100%	0.66	0.65	<	<	0.16	0.15	<	<	<	<	<	<	<	0.01	19.06	1.77	<	7.44	<	0.02
Fly Ash 100%	<	3.54	0.01	<	<	0.19	<	<	<	<	<	0.15	<	<	<	<	<	<	<	<
Foundry Sand 100%	<	4.31	0.00	0.00	<	0.22	<	<	<	<	<	0.15	<	<	<	<	8.60	14.61	<	0.00

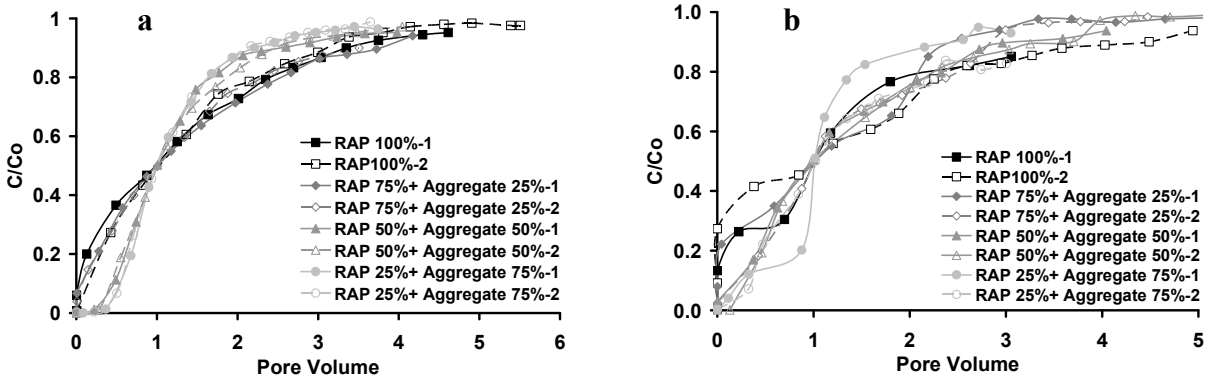

Figure 5.5 Bromide breakthrough curves for various mixtures of RAP with virgin aggregates under a) saturated and b) unsaturated conditions.

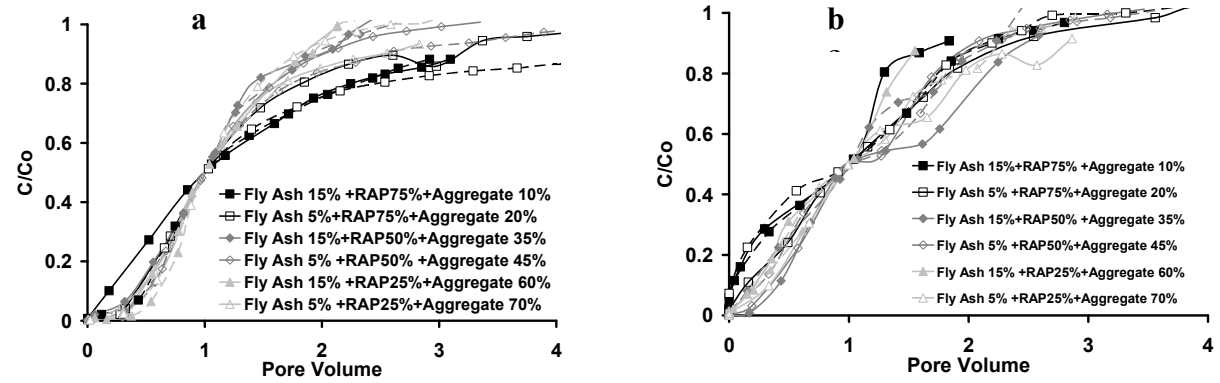

Figure 5.6 Bromide breakthrough curves for various mixtures of FA, RAP and Aggregates under a) saturated and b) unsaturated conditions.

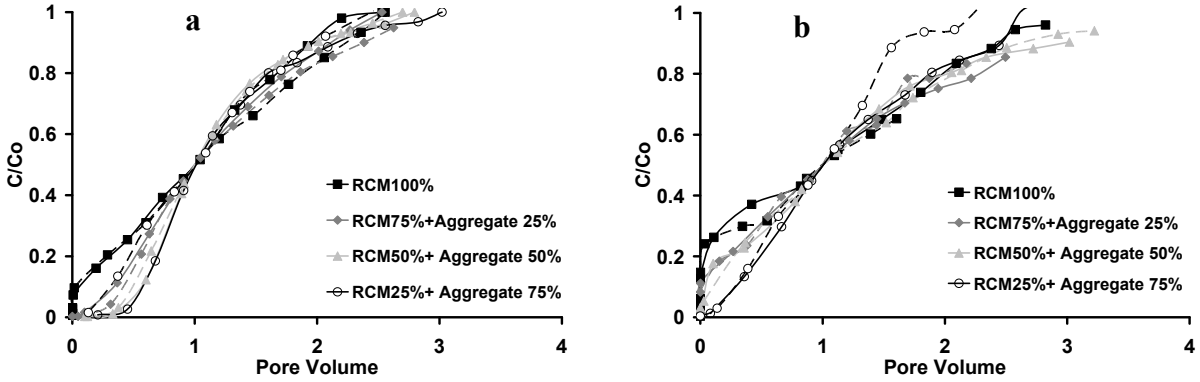

Figure 5.7 Bromide breakthrough curves for various mixtures of RCM and virgin aggregates under a) saturated and b) unsaturated conditions.

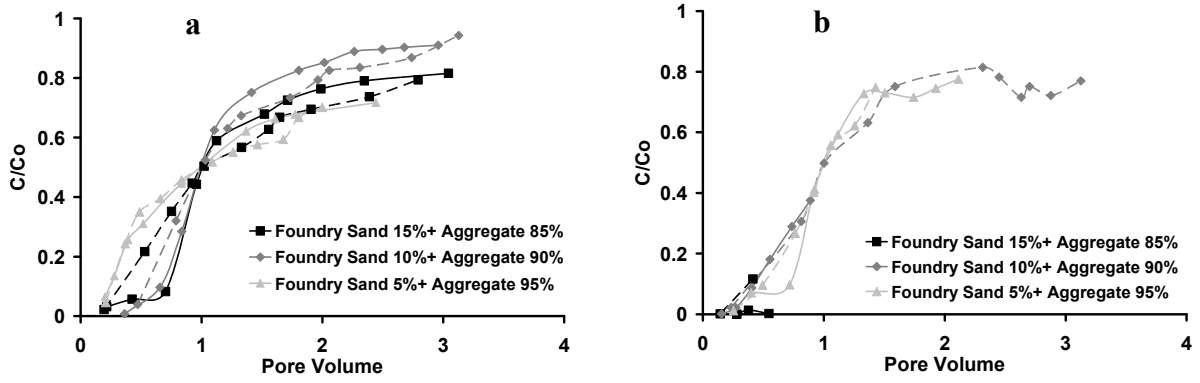

Figure 5.8 Bromide breakthrough curves for various mixtures of FS and virgin aggregates under a) saturated and b) unsaturated conditions.

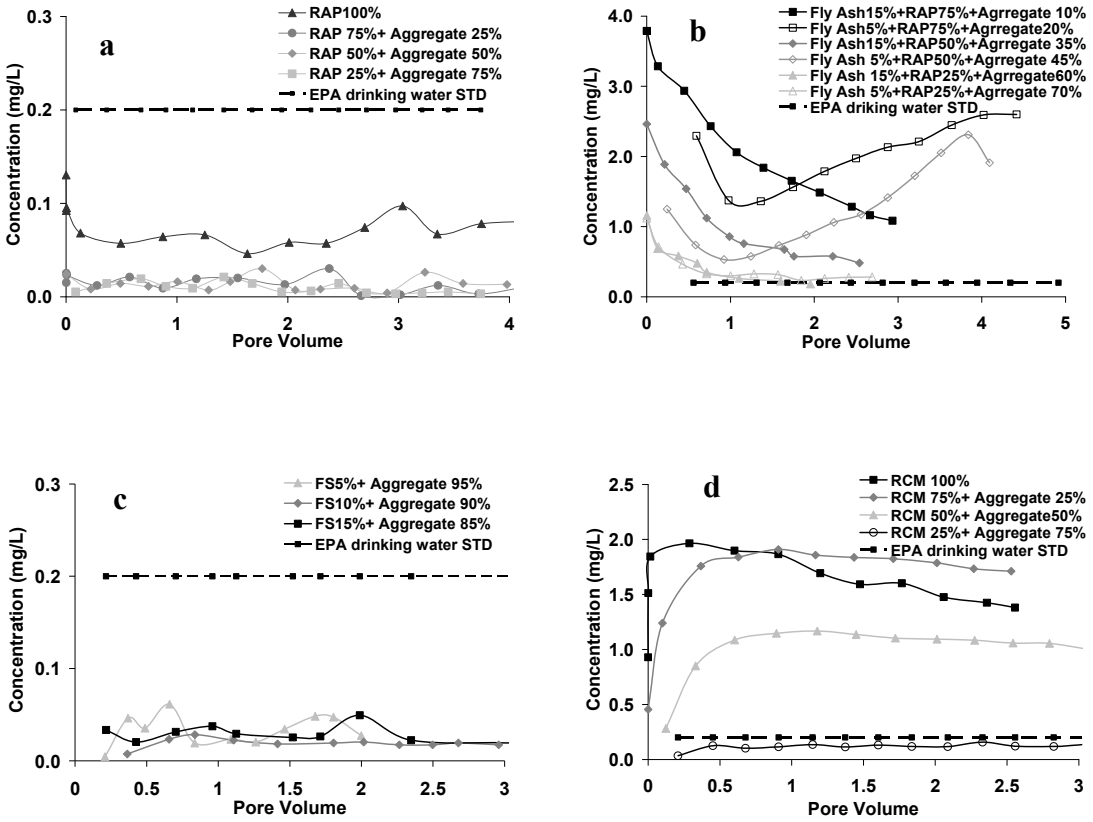

Figure 5.9 Aluminum concentrations in the leachate as a function of pore volume for 15 mixtures of recycled materials with virgin aggregates, 100% RCM, and 100% RAP under saturated conditions. EPA aluminum drinking water standard is 0.2 mg/L. Figure a) RAP, b) FA, c) RCM, and d) FS.

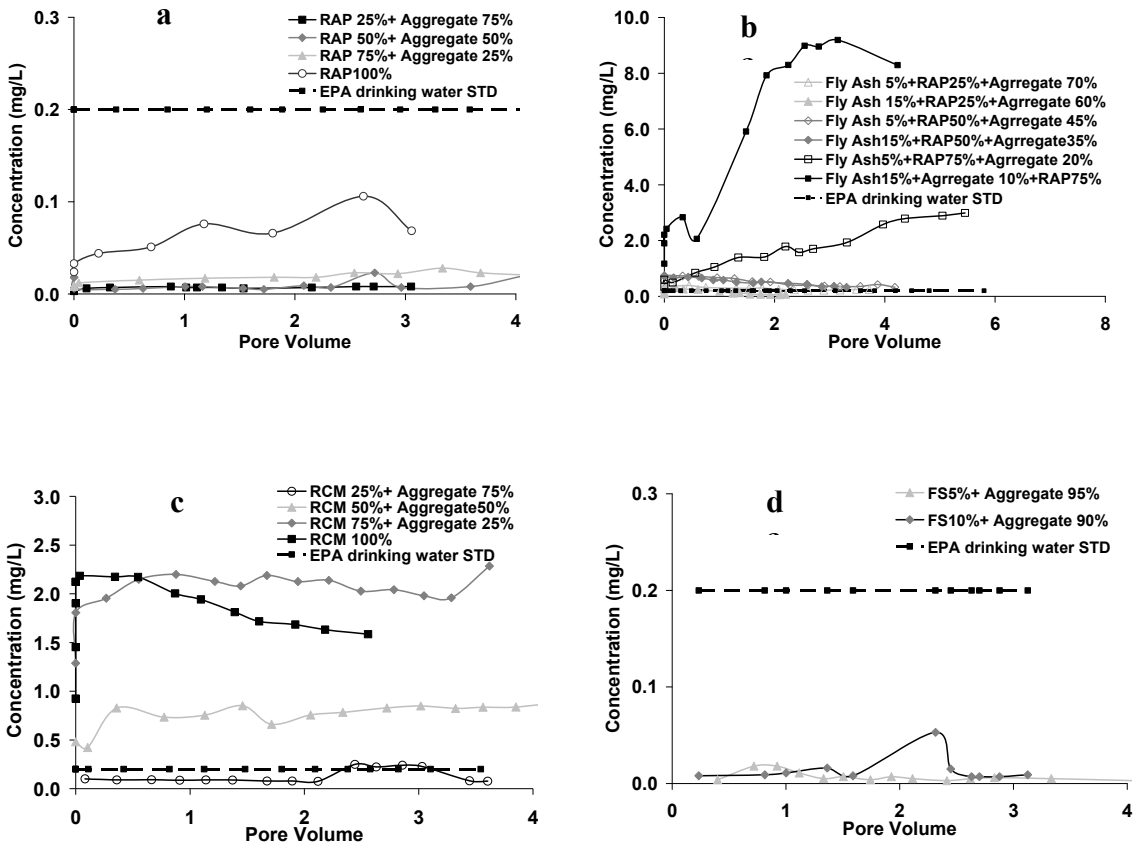

Figure 5.10 Aluminum concentrations in the leachate as a function of pore volume for 14 mixtures of recycled materials with virgin aggregates, 100% RAP, and 100% RCM under unsaturated conditions. EPA aluminum drinking water standard is 0.2 mg/L. Figure a) RAP, b) FA, c) RCM, and d) FS.

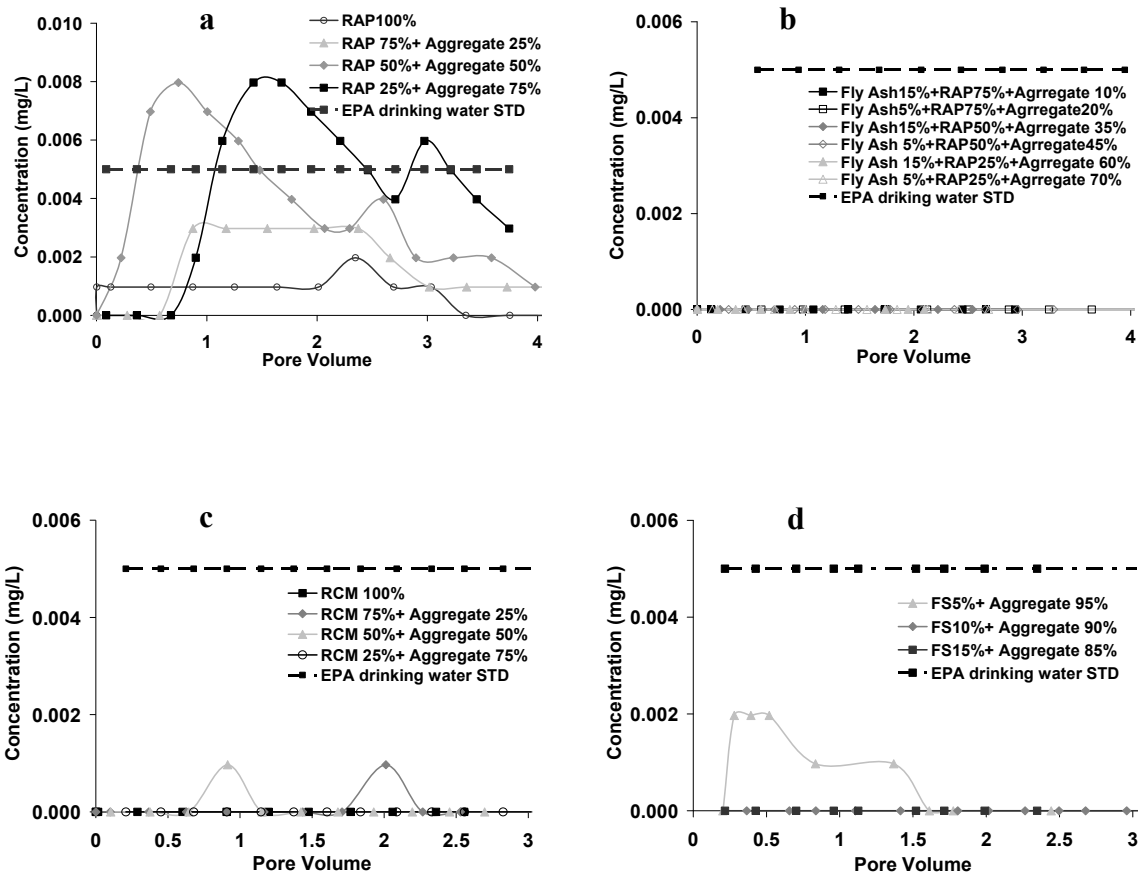

Figure 5.11 Cadmium concentrations in the leachate as a function of pore volume for 15 mixtures of recycled materials with virgin aggregates, 100% RAP, and 100% RCM under saturated conditions. EPA cadmium drinking water standard is 0.005 mg/L. Figure a) RAP, b) FA c) RCM, and d) FS.

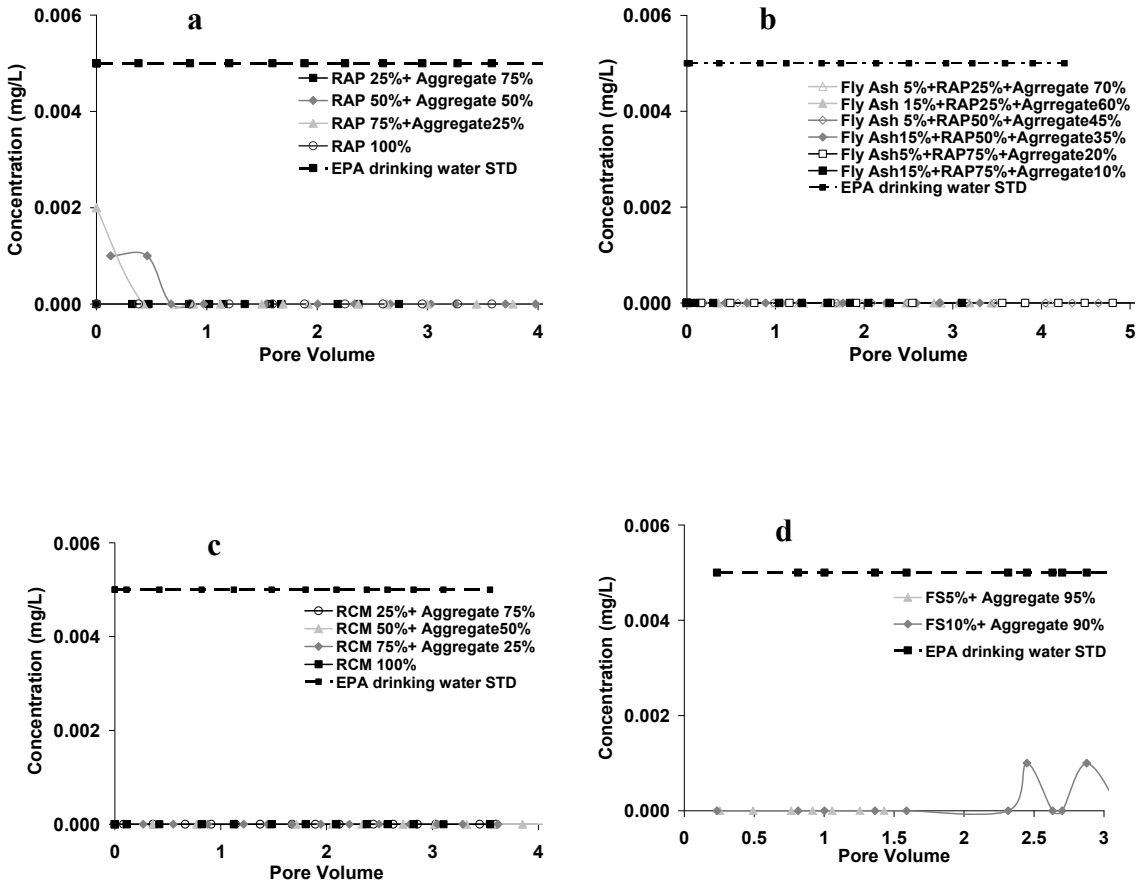

Figure 5.12 Cadmium concentrations in the leachate as a function of pore volume for 14 mixtures of recycled materials with virgin aggregates, 100% RAP, and 100% RCM under unsaturated conditions. EPA cadmium drinking water standard is 0.005 mg/L. Figure a) RAP, b) FA, c) RCM, and d) FS.

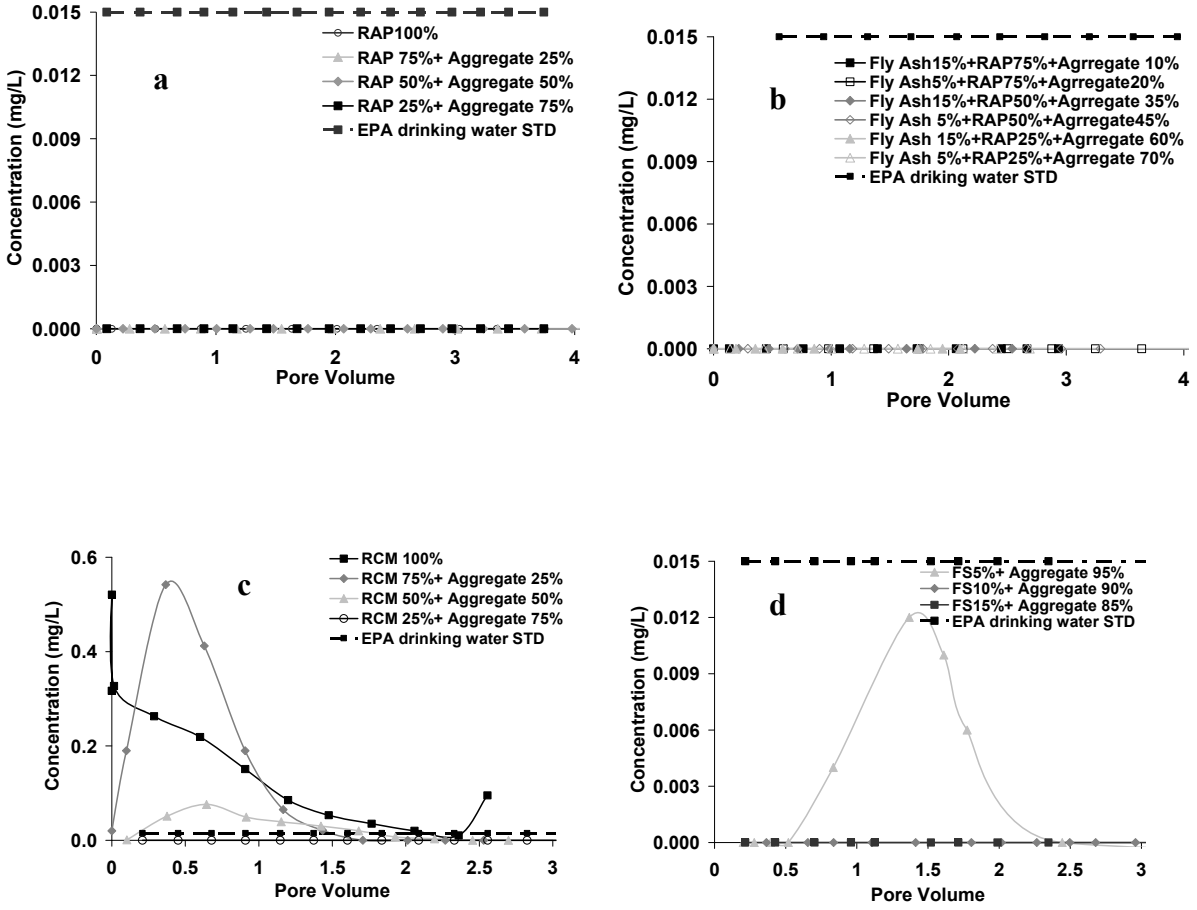

Figure 5.13 Lead concentrations in the leachate as a function of pore volume for 15 mixtures of recycled materials with virgin aggregates, 100% RAP, and 100% RCM under unsaturated conditions. EPA lead drinking water standard is 0.015 mg/L. Figure a) RAP, b) FA, c) RCM, and d) FS.

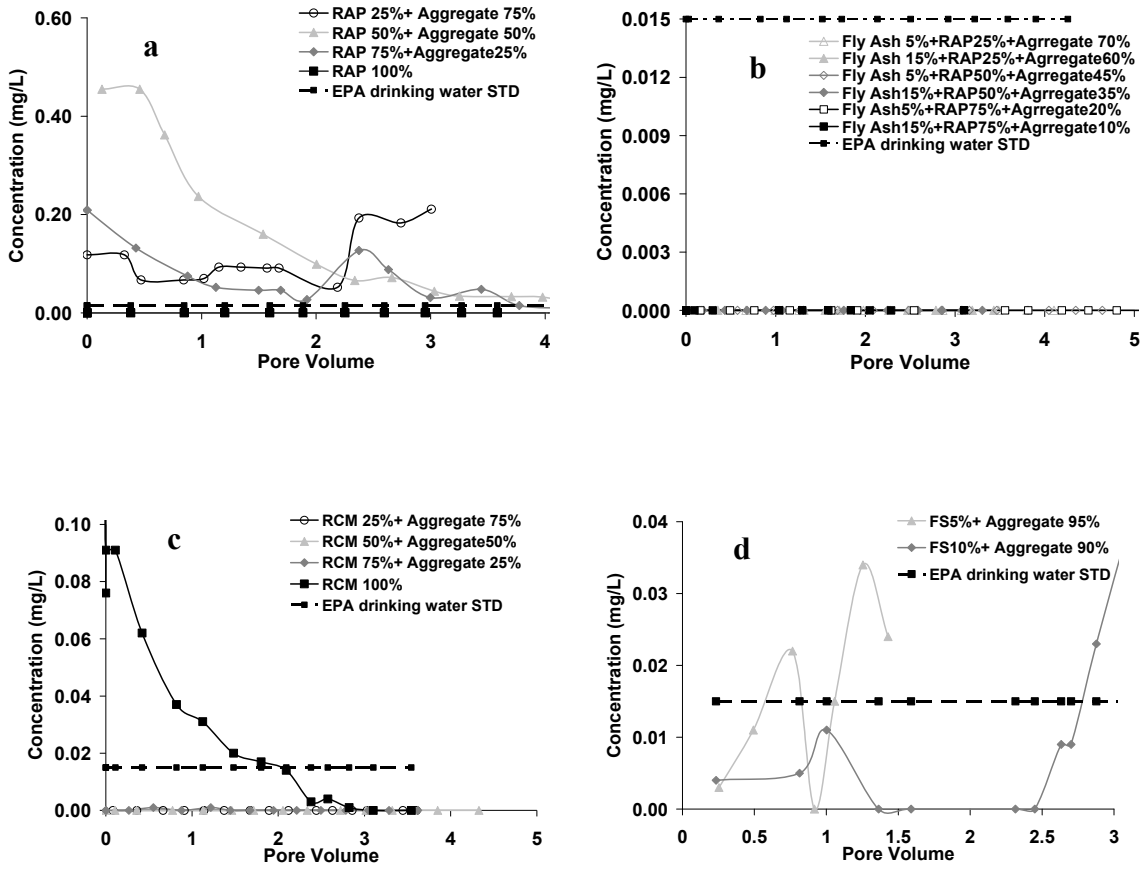

Figure 5.14 Lead concentrations in the leachate as a function of pore volume for 14 mixtures of recycled materials with virgin aggregates, 100% RAP, and 100% RCM under unsaturated conditions. EPA lead drinking water standard is 0.015 mg/L. Figure a) RAP, b) FA, c) RCM, and d) FS.

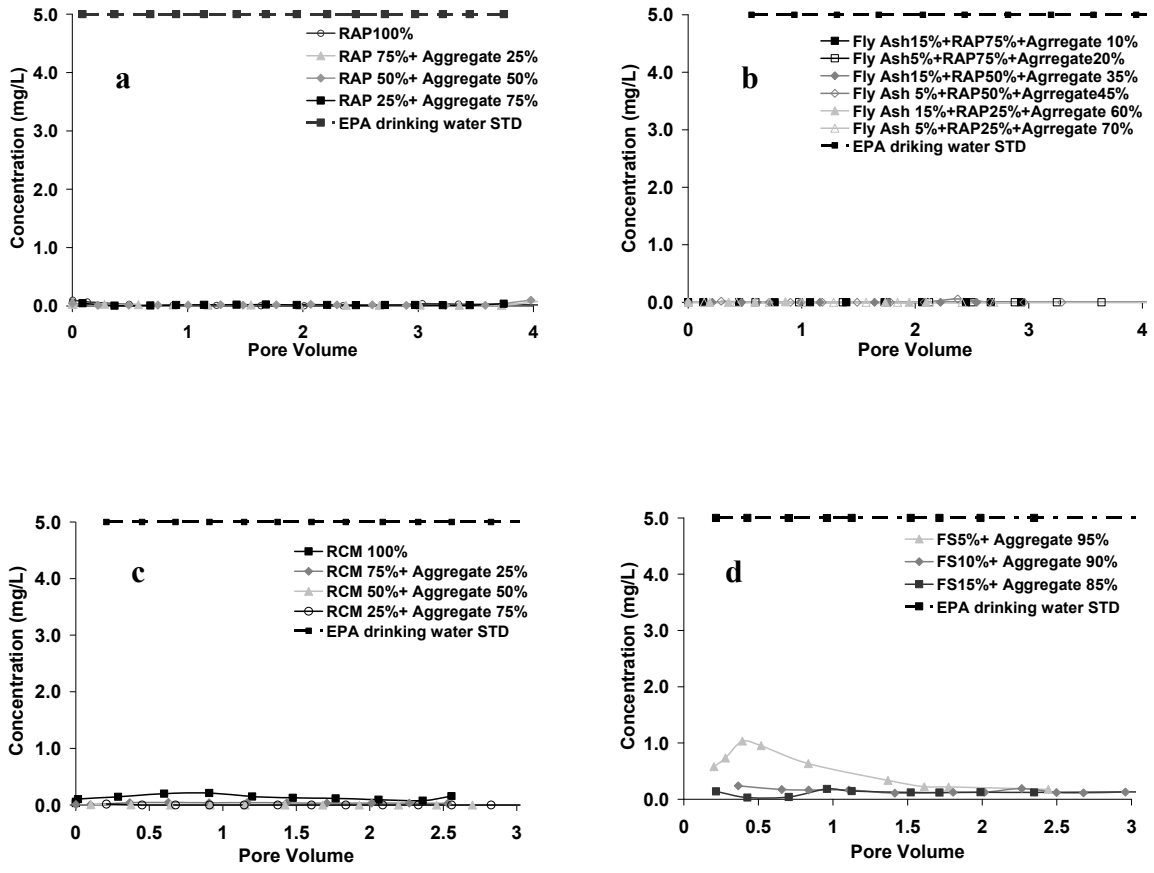

Figure 5.15 Zinc concentrations in the leachate as a function of pore volume for 14 mixtures of recycled materials with virgin aggregates, 100% RAP, and 100% RCM under saturated conditions. EPA zinc drinking water standard is 5 mg/L. Figure a) RAP, b) FA, c) RCM, and d) FS.

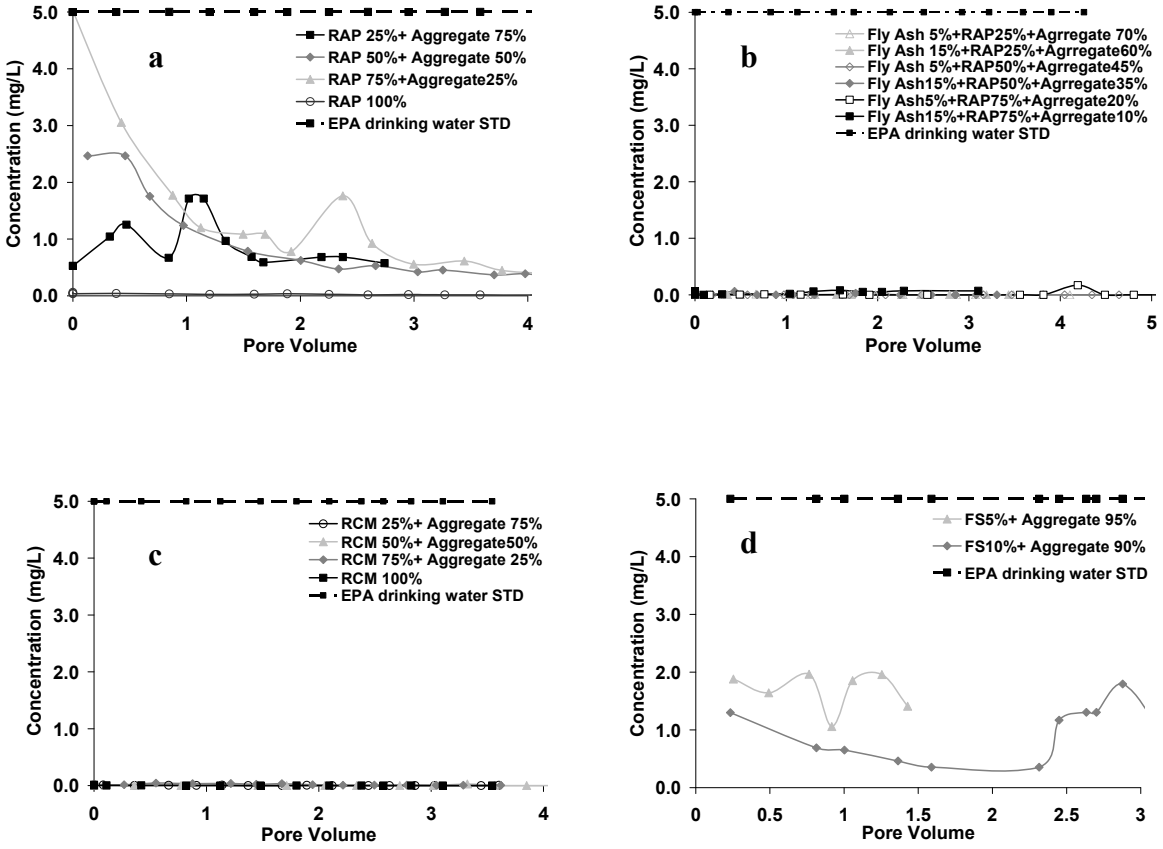

Figure 5.16 Zinc concentrations in the leachate as a function of pore volume for 14 mixtures of recycled materials with virgin aggregate, 100% RAP, and 100% RCM under unsaturated conditions. EPA zinc drinking water standard is 5 mg/L. Figure a) RAP, b) FA, c) RCM, and d) FS.

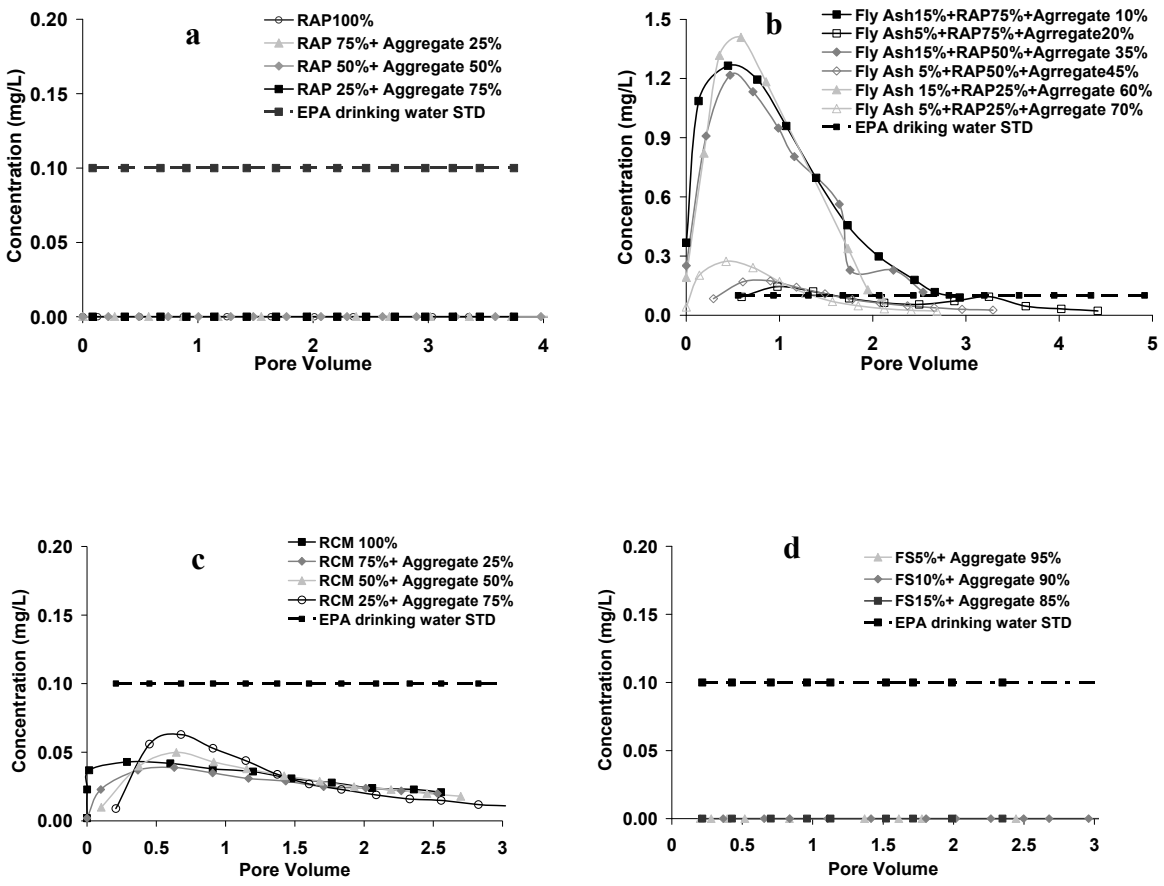

Figure 5.17 Chromium concentrations in the leachate as a function of pore volume for 15 mixtures of recycled materials with virgin aggregates, 100% RAP, and 100% RCM under saturated conditions. EPA chromium drinking water standard is 0.1 mg/L. Figure a) RAP, b) FA, c) RCM, and d) FS.

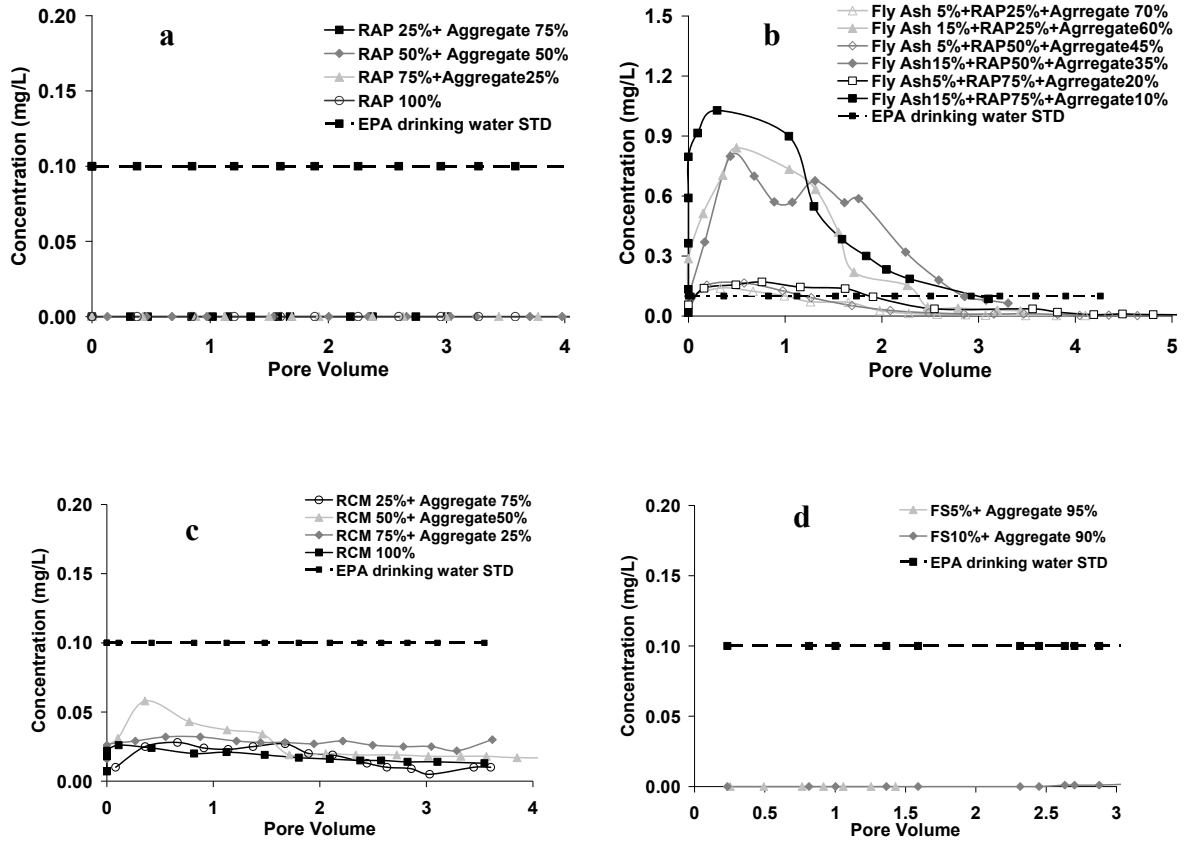

Figure 5.18 Chromium concentrations in the leachate as a function of pore volume for 14 mixtures of recycled materials with virgin aggregates, 100% RAP, and 100% RCM under unsaturated conditions. EPA chromium drinking water standard is 0.1 mg/L. Figure a) RAP, b) FA, c) RCM, and d) FS.

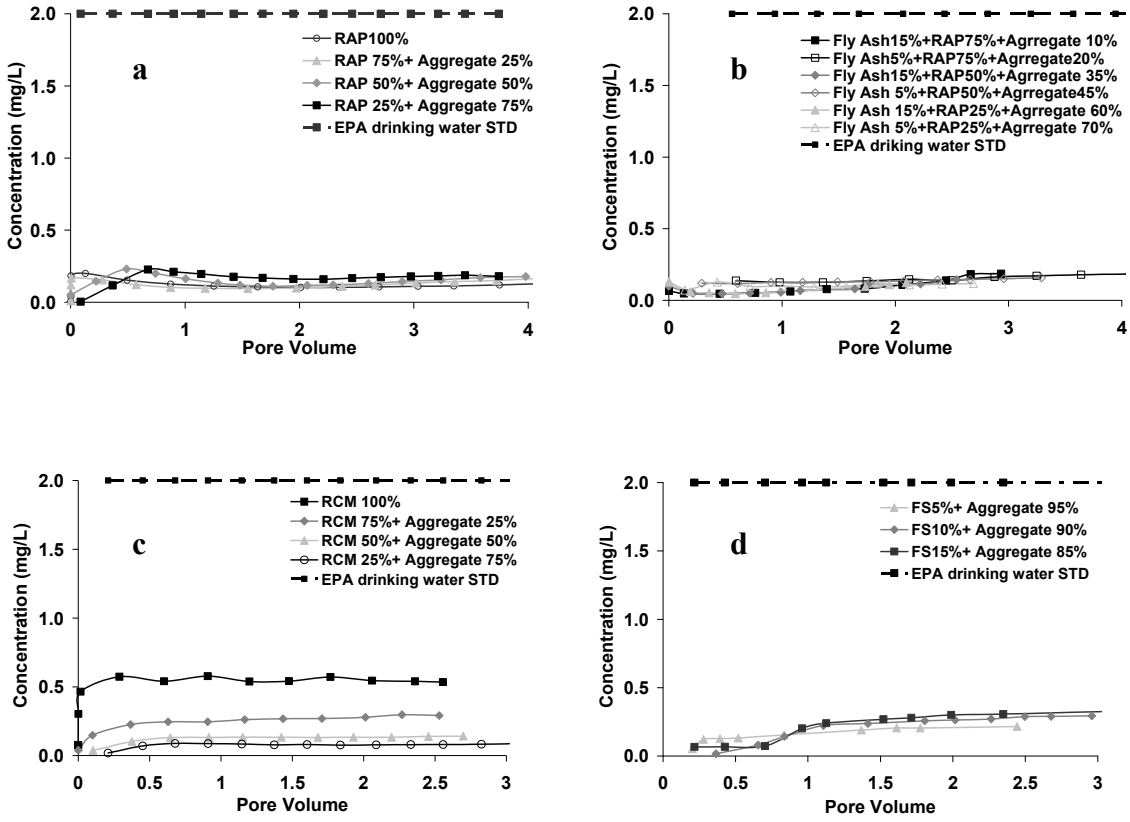

Figure 5.19 Barium concentrations in the leachate as a function of pore volume for 15 mixtures of recycled materials with virgin aggregates, 100% RAP, and 100% RCM under unsaturated conditions. EPA barium drinking water standard is 2 mg/L. Figure a) RAP, b) FA, c) RCM, and d) FS.

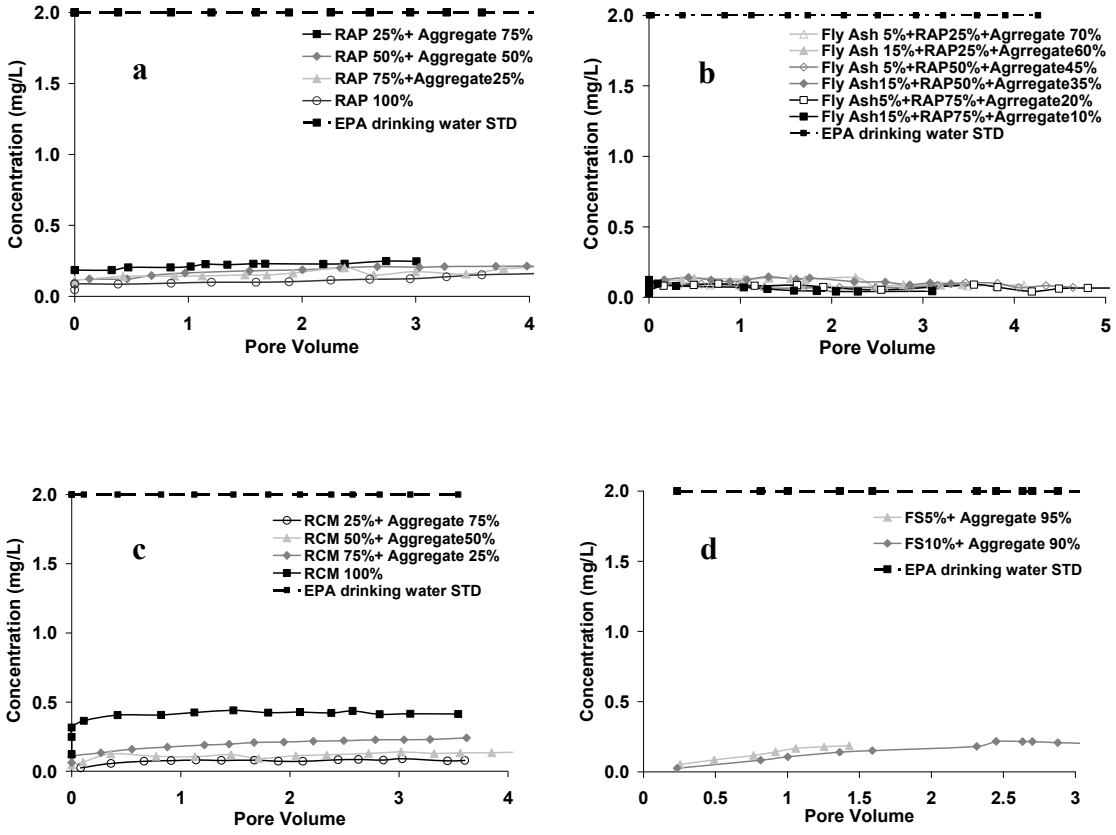

Figure 5.20 Barium concentrations in the leachate as a function of pore volume for 14 mixtures of recycled materials with virgin aggregates, 100% RAP, and 100% RCM under unsaturated conditions. EPA barium drinking water standard is 2 mg/L. Figure a) RAP, b) FA, c) RCM, and d) FS.

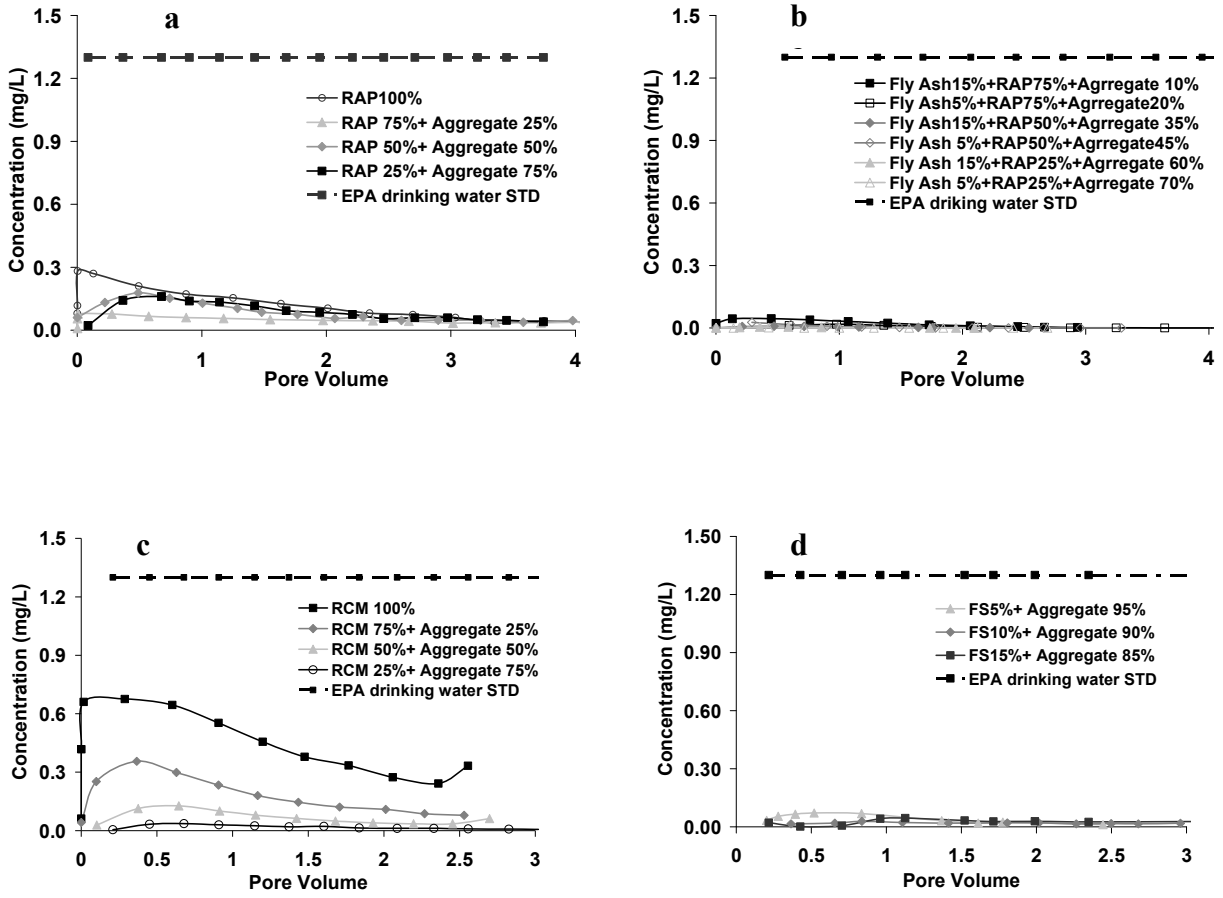

Figure 5.21 Copper concentrations in the leachate as a function of pore volume for 15 mixtures of recycled materials with virgin aggregates, 100% RAP, and 100% RCM under saturated conditions. EPA copper drinking water standard is 1.3 mg/L. Figure a) RAP, b) FA, c) RCM, and d) FS.

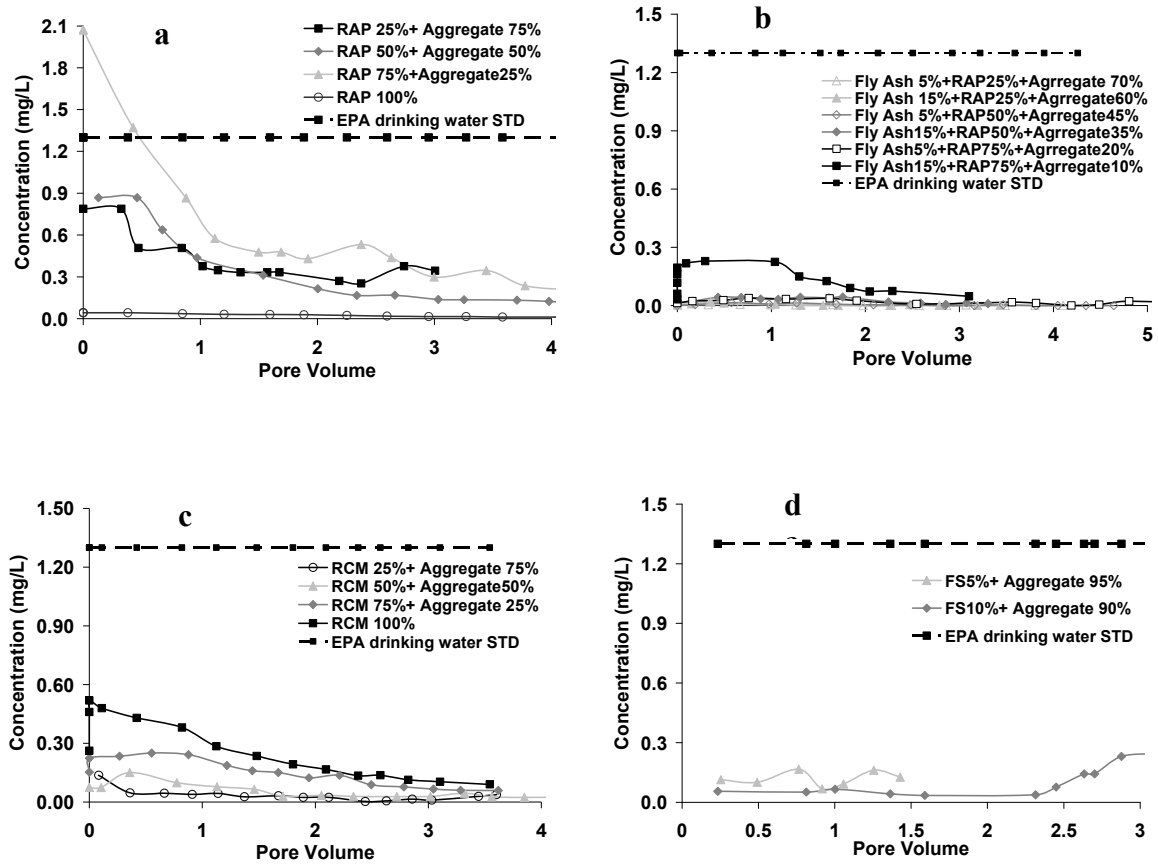

Figure 5.22 Copper concentrations in the leachate as a function of pore volume for 14 mixtures of recycled materials with virgin aggregates, 100% RAP, and 100% RCM under unsaturated conditions. EPA copper drinking water standard is 1.3 mg/L. Figure a) RAP, b) FA, c) RCM, and d) FS.

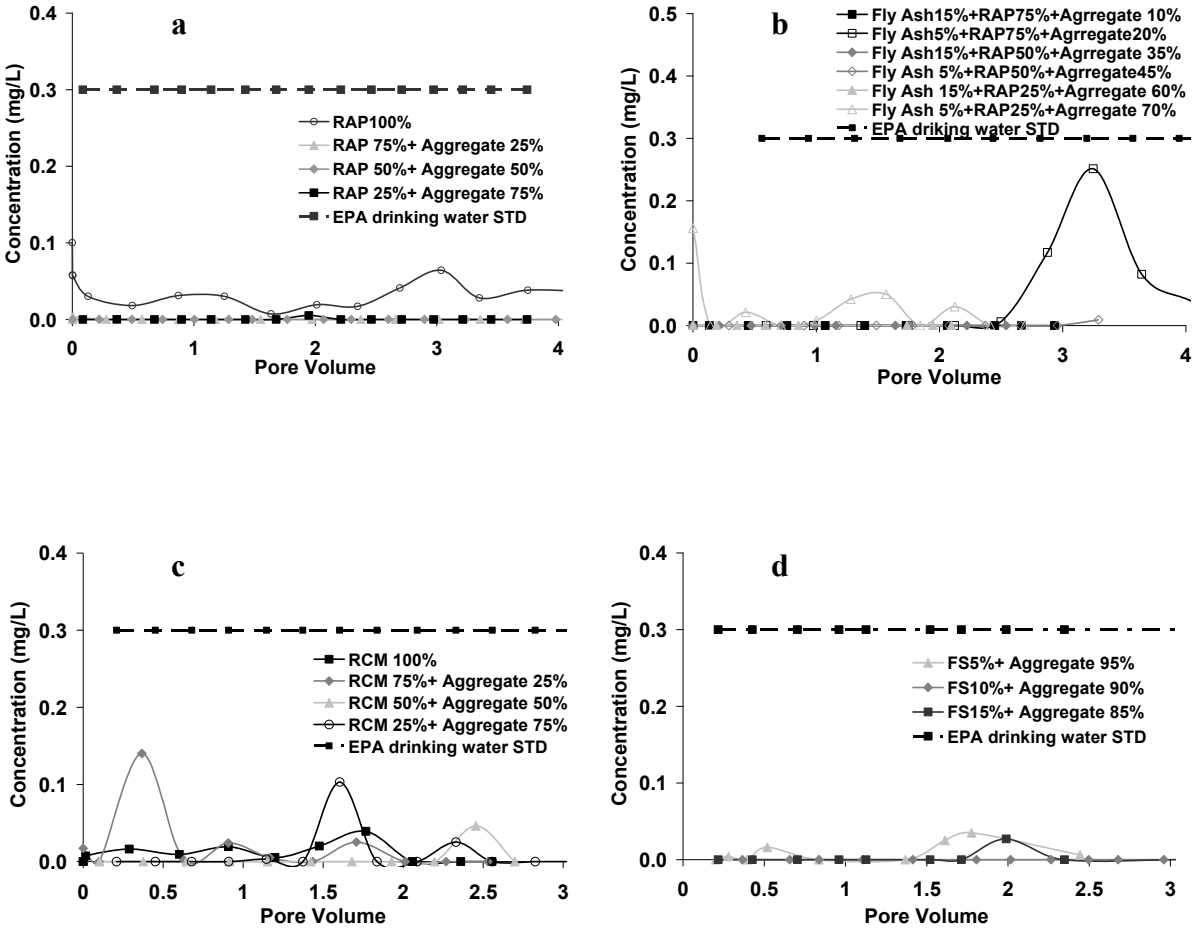

Figure 5.23 Iron concentrations in the leachate as a function of pore volume for 15 mixtures of recycled materials with virgin aggregates, 100% RAP, and 100% RCM under saturated conditions. EPA iron drinking water standard is 0.3 mg/L. Figure a) RAP, b) FA, c) RCM, and d) FS.

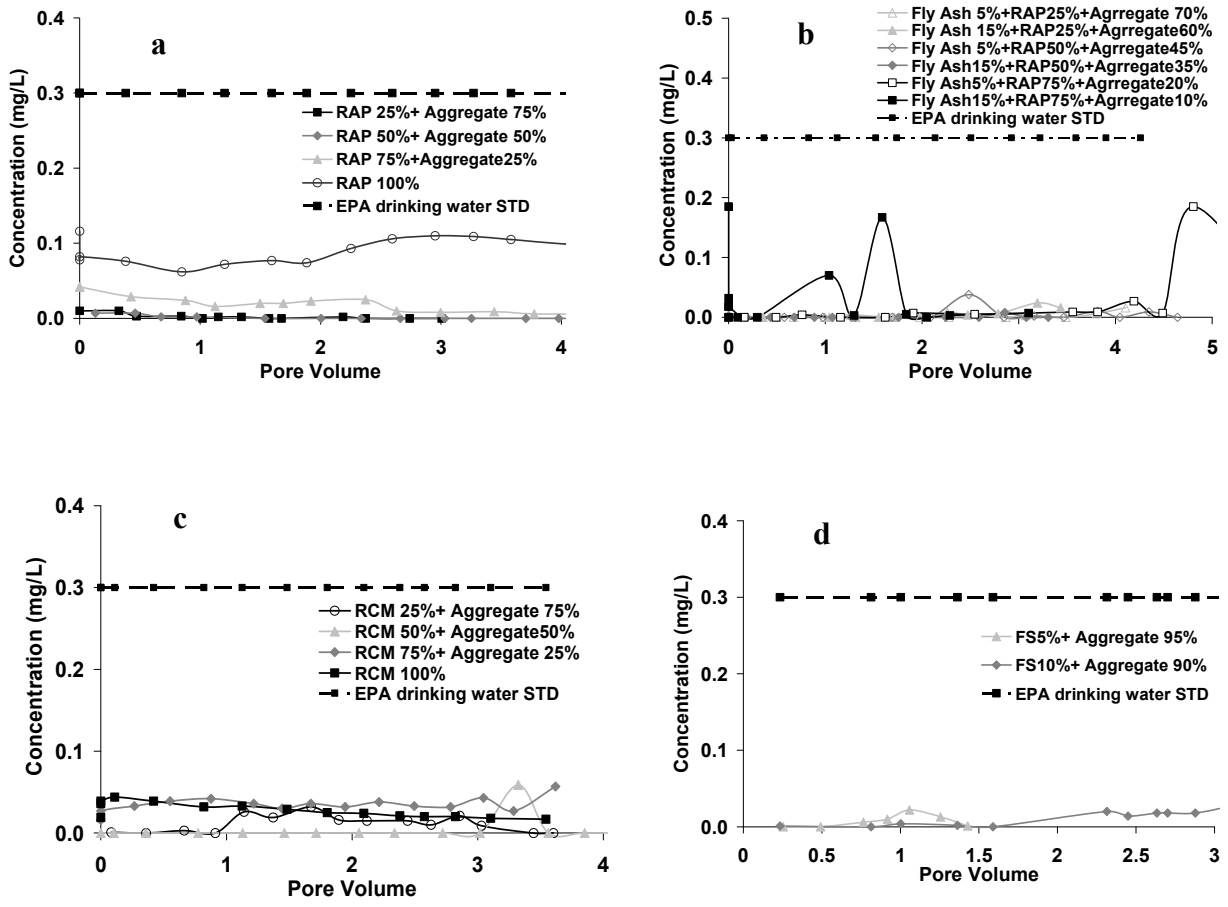

Figue 5.24 Iron concentrations in the leachate as a function of pore volume for 14 mixtures of recycled materials with virgin aggregates, 100% RAP, and 100% RCM under unsaturated conditions. EPA iron drinking water standard is 0.3 mg/L. Figure a) RAP, b) FA, c) RCM, and d) FS.

Hydraulic Conductivity

Saturated (0.2 kPa hydraulic head) and unsaturated (2 kPa suction) hydraulic conductivities of all 17 mixtures and 100% aggregate is given in Table 5.3. Assuming 100% aggregates represent the standard against which to compare other materials, saturated hydraulic conductivities of various RAP, FA-RAP, and RCM mixtures with aggregates were higher than that of the 100% aggregates under saturated (7.8 cm/day) and unsaturated (1.3 cm/day) conditions. Both saturated and unsaturated hydraulic conductivities of foundry sand mixtures with aggregate was less than that of the 100% aggregates. This is expected considering that the fine sand particles of the foundry sand fill up the spaces in between the aggregates during packing. Assuming 100% virgin aggregates provide adequate drainage characteristic for pavement design, this data shows that except for foundry sand mixtures with aggregates, other recycled materials (RAP, FA, RCM) mixtures with aggregates would provide adequate drainage.

Table 5. 3 Saturated (0.2 kPA hydraulic head) and unsaturated (2 kPa suction) hydraulic conductivities of various mixtures of recycled materials with aggregates and 100% virgin aggregates

Materials	**Hydraulic Conductivity (cm/day)**	
	Saturated condition	**Unsaturated condition**
100% Aggregate	**7.76**	**1.32**
25% RAP25% + 75% Aggregate	**143.56**	**1.44**
50% RAP50% + 50% Aggregate	**75.69**	**2.94**
75% RAP75% + 25% Aggregate	**34.33**	**35.41**
100% RAP	**184.59**	**38.25**
5% Fly Ash + 25% RAP + 70% Aggregate	**58.40**	**102.45**
15% Fly Ash% + 25% RAP + 60% Aggregate	**12.38**	**7.58**
5% Fly Ash + 50% RAP+ 45% Aggregate	**83.86**	**92.90**
15% Fly Ash + 50% RAP + 35% Aggregate	**20.51**	**26.00**
5% Fly Ash + 75% RAP + 20% Aggregate	**109.15**	**62.55**
15% Fly Ash + 75% RAP + 10% Aggregate	**52.33**	**8.62**
25% RCM + 75% Aggregate	**39.53**	**43.38**
50% RCM + 50% Aggregate	**302.76**	**185.26**
75% RCM + 25% Aggregate	**151.99**	**113.73**
100% RCM	**85.05**	**146.63**
5% Foundry Sand + 95% Aggregate	**1.26**	**0.46**
10% Foundry Sand + 90% Aggregate	**5.27**	**0.37**
15% Foundry Sand + 85% Aggregate	**3.34**	**0.11**

CONCLUSIONS

The leaching results show that addition of RAP, FA, and RCM to virgin aggregates will not lead to substantial leaching of various inorganic chemicals to the surrounding environment. Since the leaching experiments were done in batch (continuous shaking) and in small column studies (30.5 cm length), there is minimal risk that these chemicals will enter the ground water system because of the presence of additional soil below the base and subbase layers.

Except for FS mixtures, the hydraulic conductivity of FA, RAP and RCM mixtures with aggregates was higher than the corresponding hydraulic conductivities of virgin aggregates under both saturated and unsaturated conditions. This indicates that addition of these recycled materials will have little effect on drainage if used in base and subbase layers. Since hydraulic conductivity of FS mixtures was lower than that of aggregates, it is likely to have some impact on water flow and thus on drainage.

CHAPTER 6-OVERALL CONCLUSIONS

Water retention characteristics reflect the pore size distribution of a porous media which in turn affects the hydraulic conductivity, and stiffness and strength of the material. Comparisons of the water retention characteristic with 100% virgin aggregates showed that the shape of the pore size distribution curves of recycled mixtures used in this study are nearly similar to that of 100% aggregates. This suggests that for most part drainage, stiffness, and strength characteristics of recycled materials mixtures with virgin aggregates will also be somewhat similar to that of 100% virgin aggregates. The M_R and shear strength measurements in this study showed that FA, RAP, and RCM will be good substitutes for virgin aggregates as base and subbase materials in road construction. However, these materials should be further tested in-situ before full implementation of these findings. The leaching results showed that addition of RAP, FA, and RCM to virgin aggregates will not lead to substantial leaching of various inorganic chemicals to the surrounding environment. Since the leaching experiments were done in batch (continuous shaking) and in small column studies (15.2 cm length), there is minimal risk that these chemicals will enter the ground water system because of the presence of additional soil below the base and subbase layers. Except for FS mixtures, the hydraulic conductivity of FA, RAP and RCM mixtures with aggregates was higher than the corresponding hydraulic conductivities of virgin aggregates under both saturated and unsaturated conditions. This indicates that addition of these recycled materials will have little effect on drainage if used in base and subbase layers. Since hydraulic conductivity of FS mixtures was lower than that of aggregates, it is likely to have some impact on water flow and thus on drainage.

Based on the above water retention, hydraulic conductivity, resilient modulus, shear strength, and leaching tests, we conclude that FA, RAP, and RCM mixtures will be good substitutes for virgin aggregates as base and subbase materials in road construction. Comparatively, FS may not be suitable for use as base and subbase material because of lower hydraulic conductivities of FS-aggregate mixtures relative to 100% virgin aggregates. However, further in-situ testing of these materials should be undertaken before any implementation of our findings.

REFERENCES

Abrol, I. P., and Palta. J. P. 1968. "Bulk Density Determination of Soil Clods Using Rubber Solution as a Coating Material". *Soil Sci.* 106:465-468.

ACPA. 1993. *Concrete Paving Technology: Recycling Concrete Pavement*, American Concrete Pavement Association, Skokie, IL.

Apul, D. S., Gardner, K. H., and Eighmy, T. T., 2005. "A Review of Roadway Water Movement for Beneficial Use of Recycled Materials". *The Handbook of Environmental Chemistry*, Springer Berlin, 5:241-269.

Arya, L.R. and Paris. J.F., 1986. "A Physico-Empirical Model to Predict the Soil Moisture Characteristics from Particle Size Distribution and Bulk Density Data". *Soil Sci. Soc. Am. J.* 45: 1023-1030.

ASTM C 136-01, 2001. Standard *Test Method for Sieve Analysis of Fine and Coarse Aggregate*, Philadelphia, PA.

ASTM C 618-03, 2003. S*tandard Specification for Coal Fly Ash and Raw or Calcined Natural Pozzolan for Use as a Mineral Admixture in Concrete*, Philadelphia, PA.

ASTM D 698-00ae1, 2000. *Standard Test Method for Laboratory Compaction Characteristics Using Standard Effort*, Philadelphia, PA.

ASTM D 2850-95, 1999. *Standard Test Method for Unconsolidated-Undrained Triaxial Compression Test on Cohesive Soils*, Philadelphia, PA.

ASTM D 3387-83, 2003, *Standard Test Method for Compaction and Shear Properties of Bituminous Mixtures by Means of the U.S. Corps of Engineers Gyratory Testing Machine (GTM)*, Philadelphia, PA.

Barksdale, R. D., Itani, S. Y. and Swor, T. E., 1992. "Evaluation of Recycled Concrete, open Graded Aggregate, and Large Top-Size Aggregate Base". *Transportation Research Record* 1345, Transportation Research Board, 92-100.

Benson, C. H., Edil, T. B., Ebrahimi, A., Kootsra, A., Li, L., and Bloom. P. R., 2009. *Use of Fly ash for reconstruction of bituminous roads*. Final Report to Local Road Research Board, 847. Pp 24, St. Paul, MN.

Blake, G.R. 1965. *Methods of Soil Analysis*. Part 1. ASA, Madison, WI. 374-390.

Bloom, P. R., Halbach, T. R., and Grosenheider, K. E., 2006. *Chemical inventory and data base development for recycled material substitutes*, Minnesota Department of Transportation. Report No. Mn/DOT 2006-28, St. Paul, MN.

Brooks, R. H., and Corey, A. T. 1964. "Hydraulic Properties of Porous Media". Hydrol. Paper 3, Colorado State University, Fort Collins, CO.

Browne M. J. 2006. "Feasibility of Using a Gyratory Compactor to Determine Compaction Characteristics of Soil". M. S. Thesis. Montana State University, Bozeman, MT.

Buczko, U., Hopp, L., Berger, W., Durner, W., Peiffer S., and Scheithauer, M. 2004. "Simulation of chromium transport in the unsaturated zone for predicting contaminant entries into the groundwater". *J. Plant Nutr. Soil Sci*. 167: 284-292.

Campbell, G. S. 1974. "A simple Method for Determining Unsaturated Conductivity from Moisture Retention Data". *Soil Sci*. 117: 311-314.

Chadbourn, B., 2005. *Resilient Modulus Testing at Mn/DOT*. Minnesota Department of Transportation Internal Report, St. Paul, MN.

Chesner, W. H., Collins, R. J., and MacKay, M. H., 1997. *User Guidelines for Waste and By-Product Materials in Pavement Construction*. Report No. FHWA-RD-97-148, Federal Highway Administration, US Department of Transportation, Washington, DC.

Chini, A. R., Muszynski, L. C., Bergin, M., and Ellis, B. S., 2001. "Reuse of Wastewater Generated at Concrete Plants in Florida in the Production of Fresh Concrete". *Magazine of Concrete Research*, 53(5): 311-319.

Collins, R. J., and Ciesielski, S. K., 1994. *NCHRP Synthesis of Highway Practice 199: Recycling and Use of Waste Materials and By-products in Highway Construction*, Transportation Research Board, National Research Council, Washington, DC.

Cresswell, H. P., and Hamilton, G. J., 2002. "Soil Physical Measurement and Interpretation for Land Evaluation". *Aust. Soil and Land Surv. Handbk. Ser.* CSIRO, Melbourne, Australia, 5:35-38.

Davich, P., Labuz, J. F., Guzina, B., and Drescher, A., 2004. *Small Grain and Resilient Modulus Testing of Granular Soils*. Final Report 2004-39, Minnesota Department of Transportation, St. Paul, MN.

Fredlund, D. G. and Rahardjo, H., 1993. *Soil Mechanics for Unsaturated Soils*. John Wiley and Sons, New York, NY.

Fredlund, D.G. and Xing. A., 1994. "Equations for the Soil-Water Characteristics Curve". *Canadian Geotechnical Journal*, 31: 521-532.

Garg, N., and Thompson, M. R., 1996. "Lincoln Avenue Reclaimed Asphalt Pavement Base Project". *Transportation Research Record* 1547, National Research Council, Washington, DC.

Gupta, S. C., and Larson, W. E., 1979. "Estimating Soil Water Retention Characteristics from Particle Size Distribution, Organic Matter Content and Bulk Density". *Water Resource Research*, 15(6):1633-1635.

Gupta, S. C. and Wang, D., 2002. "Soil Water Retention". *Encyclopedia of Soil Science*. Marcel Dekker, Inc. 1393-1398.

Gupta, S. C., Singh, A., and Ranaivoson, A., 2004. *Moisture Retention Characteristics of Base and Sub-base Materials*. Report no. Mn/DOT 2005-06, Minnesota Department of Transportation, St. Paul, MN.

Gupta, S. C., and Ranaivoson, A., 2007. *Pavement Design Using Unsaturated Soil Technology*. Report no. Mn/DOT 2007-11, Minnesota Department of Transportation, St. Paul, MN.

Grosenheider, K. E., Bloom, P. R., Halbach, T. R., and Simcik, M., 2006. *Chemical inventory and database development for recycled material substitutes*. Report No. Mn/DOT 2006-28, Minnesota department of Transportation, St. Paul, MN.

Hanks, A. J. and Magni, E. R., 1989. *The Use of Recovered Bituminous and Concrete Materials in Granular Base and Earth*, Report MI-137, Ontario Ministry of Transportation, Downsview, Ontario.

Harrington, J., 2005. "Recycled Roadways: FHWA and the Agency's Partners are Engineering High-Quality Pavements Using Reclaimed Materials". *Public Roads*, 68(4): 9-17.

Hooper, F., and Marr, W. A., 2004. "Effects of Reclaimed Asphalt Shingles on Engineering Properties of Soils", in Recycled Materials in Geotechnics (GSP 127), Proceedings of Sessions of the ASCE Civil Engineering Conference and Exposition, October 19-21, 2004, Baltimore, MD.

Huang, C., Lu, C., and Tzeng, J., 1998. "Model of Leaching Behavior from Fly ash Landfills with Different Age Refuses". *J. of Environmental Engineering*. 124 (8): 767.

Kang, D.H., Gupta, S.C, Ranaivoson, A., Siekmeier, J, and Roberson, R. 2010. "Hydraulic and mechanical characteristics of recycled materials and aggregate mixtures used in road construction". *Transportation Research Board* (submitted).

Kanare, H. K., and West, P. B., 1993. "Leachability of Selected Chemical Elements from Concrete", Proceedings of the Symposium on Cement and Concrete in the Global Environment. SP114, Portland Cement Association, 366, Chicago, IL.

Kim, W. S, and Labuz, J. F., 2007. *Resilient Modulus and Strength of Base Course with Recycled Bituminus Material*, Report no. Mn/DOT 2007-05, Minnesota department of Transportation, St. Paul, MN.

Li, L., Tuncer, E. B., and Benson, C. H., 2009. "Properties of pavement geomaterials stabilized with fly ash". World of Coal Ash Conference, May 4-7 2009, Lexington, KY. http://www.worldofcoalash.org/2009/ashpdf/a030-wen2009.pdf (Date accessed September 2009).

McRae, J. L., and. McDaniel, A. R., 1962. *Gyratory Compaction Method for Determining Density Requirements for Subgrade and Base of Flexible Pavements*. U.S. Army Engineer Waterways Experiment Station, CE, Vicksburg, MS.

Maher, M. H., and Popp, W., Jr., 1997. "Recycled Asphalt Pavement as a Base and Subbase Material". ASTM STP 1275, ASTM, West Conshohoken, PA.

Minnesota Department of Transportation, Mn/DOT Specification. 2000. 3138.3, http://www.dot.state.mn.us/pre-letting/spec/2005/3101-3491.pdf (Date accessed-October 2009).

Mualem, Y., 1976. "A New Model for Predicting the Hydraulic Conductivity of Unsaturated Porous Media". *Water Resources Research* 12: 593-622.

Mulligan, S., 2002. *Recycled Concrete Materials Report*, Ohio Department of Transportation, Columbus, OH.

Munyankusi, E., 1992. "Effect of Long-Term Manure and Fertilizer Application on Earthworm Macropores and Water and Tracer Transport through a Typic Hapludalf". Master's Thesis, University of Minnesota. Saint Paul, MN.

National Cooperative Highway Research Program. 2002. *Recommended Standard Method for Routine Resilient Modulus Testing of Unbound Granular Base/Subbase Materials and Subgrade Soils*, Protocol 1-28A. National Cooperative Highway Research Program, Washington, DC.

National Cooperative Highway Research Program. 2004. "Laboratory determination of resilient modulus for flexible pavement design". *Research Results Digest*, 285. Transportation Research Board, Washington, DC. Pp 48.

Page, G. C., 1987. *Florida's Experience in Hot Mix Asphalt Recycling*, Florida Department of Transportation, Report No. FLP-13, Tallahassee, FL.

Papp, W. J. Jr., Maher, M. H., Bennert, T. A., and Gucumski, N., 1998. "Behavior of Construction and Demolition Debris in Base and Subbase Application". *Recycled Materials in Geotechnical Application*, 79:122-136.

Pezo, R. F., 1993. "A General Method of Reporting Resilient Modulus Tests of Soils-A Pavement Engineer's Point of View". Presented at 72nd Annual Meeting of the Transportation Research Board, Washington D.C.

Sayed, S. M., Pulsifer, J. M., and Schmitt, R. C., 1993. "Construction and Performance of Shoulders using UNRAP Base". *Journal of Materials in Civil Engineering*, 5(3), 321-338.

Sangha, C. M., Hillier, S. R., Plunkett, B. A., and Walden, P. J., 1999. "Long-Term Leaching of Toxic Trace Metals from Portland Cement Concrete", *Cement and Concrete Research* 29:515-521.

Taha, R., Ali, G., Basma, A., and Al-Turk, O., 1999. "Evaluation of Reclaimed Asphalt Pavement Aggregate in Road Bases and Subbases". *Transportation Research Record* 1652, 264-269.

Townsend, T. and Brantley, A., 1998. *Leaching Characteristics of Asphalt Road Waste*. Florida Center for Solid and Hazardous Waste Management, Gainesville, FL., Report No. 98-2.

Uzan, J., 1985. "Characterization of Granular Materials". In *Transportation Research Board*. 1022, 52-59.

van Genuchten, M. Th. 1980. "A Closed-Form Equation for Predicting the Hydraulic Conductivity of Unsaturated Soils". *Soil Sci. Soc. Am. J.* 44: 892-898.

White, D., Thompson, M., and Vennapusa, P., 2007. *Field Validation of Intelligent Compaction Monitoring Technology for Unbound Materials*. Report No. MN/RC 2007-10, Minnesota Department of Transportation, St. Paul, MN.

Witczak, M. W., and Uzan, J., 1988. *The Universal Airport Pavement Design System, I of IV: Granular Material Characterization*, University of Maryland, College of Engineering, College Park, MD.

Zapata, C . E., 1999. "Uncertainty in Soil-Water Characteristic Curve and Impacts on Unsaturated Shear Strength Predictions". Ph.D. Dissertation, Arizona State University, Tempe, AZ.

Zhang, X ., D. L. Gress, S. Karpinski, and T. T. Eighmy, 1999. "Utilization of Municipal Solid Waste Combustion Bottom Ash as a Paving Material", *Transport Research Record* 1652:257-263.

Appendix A
Supporting Data on Hydraulic, Mechanical, and Leaching Properties of Recycled Materials

Table A1. Particle size distribution of various recycled materials and its mixtures with aggregates.

	Sieve No.	Sieve Size (mm)	RAP			
			25%	50%	75%	100%
Coarse Grained Soil		19.05	100.00	100.00	100.00	100.00
		9.25	89.36	84.43	81.88	79.96
		5.66	76.49	68.89	64.38	56.69
Fine Grained Soil	10	2.00	55.04	43.66	38.18	23.19
	18	1.00	38.37	28.12	22.92	10.64
	20	0.85	32.88	23.70	19.16	8.58
	35	0.50	13.72	9.89	8.28	3.72
	40	0.43	10.30	7.31	6.15	2.80
	50	0.30	5.29	3.69	2.93	1.13
	60	0.25	3.88	2.63	2.01	0.67
	70	0.21	3.05	2.02	1.46	0.44
	140	0.11	0.97	0.57	0.33	0.07

	Sieve No.	Sieve Size (mm)	Fly Ash					
			1*	2*	3*	4*	5*	6*
Coarse Grained Soil		19.05	100.00	100.00	100.00	100.00	100.00	100.00
		9.25	82.85	87.95	88.74	88.52	84.66	83.20
		5.66	66.57	75.52	74.46	72.02	64.08	67.06
Fine Grained Soil	10	2.00	44.26	52.66	48.60	44.88	33.62	38.54
	18	1.00	29.62	36.94	31.88	29.85	19.27	22.82
	20	0.85	25.62	32.52	27.06	26.15	16.23	19.66
	35	0.50	11.84	17.35	12.63	14.69	7.87	11.07
	40	0.43	9.42	14.69	10.09	12.62	6.46	9.45
	50	0.30	5.84	10.56	5.95	9.01	3.75	6.04
	60	0.25	4.76	9.24	4.75	7.91	2.90	4.80
	70	0.21	4.07	8.40	3.99	7.16	2.37	4.16
	140	0.11	2.20	5.96	2.14	5.10	1.13	2.51

1*. 5% Fly Ash +25% RAP+70 %Aggregate
2*. 15% Fly Ash +25% RAP+60 %Aggregate
3*. 5% Fly Ash +50% RAP+45 %Aggregate
4*. 15% Fly Ash +50% RAP+35 %Aggregate
5*. 5% Fly Ash +75% RAP+20 %Aggregate
6* 15% Fly Ash +75% RAP+10 %Aggregate

‖	Sieve No.	Sieve Size (mm)	RCM			
			25%	50%	75%	100%
Coarse Grained Soil		19.05	100.00	100.00	100.00	100.00
		9.25	89.36	84.43	81.88	79.96
		5.66	76.49	68.89	64.38	56.69
Fine Grained Soil	10	2	55.04	43.66	38.18	23.19
	18	1	38.37	28.12	22.92	10.64
	20	0.85	32.88	23.70	19.16	8.58
	35	0.5	13.72	9.89	8.28	3.72
	40	0.425	10.30	7.31	6.15	2.80
	50	0.297	5.29	3.69	2.93	1.13
	60	0.25	3.88	2.63	2.01	0.67
	70	0.21	3.05	2.02	1.46	0.44
	140	0.106	0.97	0.57	0.33	0.07

	Sieve No.	Sieve Size (mm)	Foundry Sand			Aggregate
			5%	10%	15%	100%
Coarse Grained Soil		19.05	100.00	100.00	100.00	100
		9.25	86.63	84.99	87.30	87.938
		5.66	76.39	74.86	76.72	76.929
Fine Grained Soil	10	2	58.45	59.49	58.94	59.872
	18	1	42.94	45.78	43.56	40.192
	20	0.85	37.02	40.69	38.20	34.503
	35	0.5	17.29	22.45	23.20	13.793
	40	0.425	13.96	18.61	20.79	11.072
	50	0.297	5.29	3.69	2.93	1.13
	60	0.25	3.88	2.63	2.01	0.67
	70	0.21	3.05	2.02	1.46	0.44
	140	0.106	0.97	0.57	0.33	0.07

Table A2. Specific gravity, porosity, void ratio, particle distribution by textural groups, particle passing various sieve sizes, coefficient of curvature and coefficient of uniformity for recycled materials and its mixtures with aggregates.

	Gs	Porosity, n	Void Ratio, e	USDA soil classification			
				<0.002mm	0.002-0.05mm	0.05-2.0mm	>2.0mm
				% clay	% slit	% Sand	% Coarse
25% RAP+75%Agg	2.675	0.228	0.295	0	0	21.53	78.47
50% RAP+50%Agg	2.588	0.200	0.250	0	0	18.44	81.56
75% RAP+25%Agg	2.528	0.178	0.217	0	0	11.64	88.36
100% RAP	2.509	0.155	0.183	0	0	21.14	78.86
5% FA+25% RAP+70% Agg	2.785	0.264	0.359	0	0	26.54	73.46
15% FA+25% RAP+60% Agg	2.880	0.323	0.477	0	0	25.40	74.60
5% FA+50% RAP+45% Agg	2.686	0.233	0.304	0	0	23.81	76.19
15% FA+50% RAP+35% Agg	2.755	0.285	0.399	0	0	17.52	82.48
5% FA+75% RAP+20% Agg	2.572	0.199	0.248	0	0	19.05	80.95
15% FA+75% RAP+10% Agg	2.639	0.242	0.319	0	0	28.16	71.84
25% RCM+75% Agg	2.770	0.278	0.385	0	0	21.53	78.47
50% RCM+50% Agg	2.746	0.279	0.387	0	0	18.44	81.56
75% RCM+25% Agg	2.660	0.267	0.364	0	0	11.64	88.36
100 % RCM	2.608	0.256	0.344	0	0	27.94	72.06
5% FS + 95% Agg	2.879	0.281	0.391	0	0	27.48	72.52
10% FS + 90% Agg	2.863	0.277	0.383	0	0	28.35	71.65
15% FS + 85% Agg	2.859	0.276	0.381	0	0	29.11	70.89
100% Agg	2.786	0.257	0.346	0	0	21.53	78.47

	D_5	D_{10}	D_{16}	D_{20}	D_{25}	D_{30}	D_{50}	D_{60}	D_{75}	D_{84}	D_{95}	C_c	C_u	D_e
25% RAP+75%Agg	0.39	0.58	0.78	0.94	1.11	1.26	1.85	2.85	5.41	7.75	14.47	0.96	4.90	1.32
50% RAP+50%Agg	0.54	0.83	1.12	1.25	1.41	1.56	2.89	4.31	7.01	9.15	15.94	0.69	5.19	1.79
75% RAP+25%Agg	0.65	1.04	1.25	1.38	1.55	1.72	3.65	5.05	7.84	10.40	16.38	0.56	4.84	2.01
100% RAP	1.12	1.36	1.65	1.85	2.19	2.72	4.85	6.08	8.46	11.24	16.64	0.89	4.46	2.97
5% FA+25% RAP+70% Agg	0.48	0.77	1.09	1.22	1.38	1.54	2.94	4.58	7.52	9.91	16.23	0.67	5.93	1.73
15% FA+25% RAP+60% Agg	0.26	0.54	0.80	1.02	1.17	1.32	1.92	3.18	5.58	8.11	15.01	0.83	5.22	1.56
5% FA+50% RAP+45% Agg	0.43	0.69	1.02	1.14	1.29	1.44	2.20	3.61	5.80	8.06	14.73	0.83	5.22	1.56
15% FA+50% RAP+35% Agg	0.37	0.73	1.08	1.21	1.37	1.53	2.69	4.04	6.31	8.27	14.81	0.79	5.52	1.72
5% FA+75% RAP+20% Agg	0.79	1.13	1.35	1.50	1.68	1.87	3.97	5.17	7.56	9.13	15.89	0.60	4.58	2.24
15% FA+75% RAP+10% Agg	0.61	1.04	1.24	1.38	1.54	1.71	3.47	4.75	7.43	9.72	16.17	0.59	4.57	2.05
25% RCM+75% Agg	0.39	0.58	0.78	0.94	1.11	1.26	1.85	2.85	5.41	7.75	14.47	0.96	4.90	1.32
50% RCM+50% Agg	0.54	0.83	1.12	1.25	1.41	1.56	2.92	4.37	7.07	9.15	15.94	0.68	5.27	1.75
75% RCM+25% Agg	0.65	1.04	1.25	1.38	1.55	1.72	3.65	5.05	7.84	10.40	16.38	0.56	4.84	2.07
100 % RCM	1.12	1.36	1.65	1.85	2.20	2.74	4.93	6.17	8.48	11.24	16.64	0.90	4.53	2.99
5% FS + 95% Agg	0.31	0.50	0.68	0.80	1.00	1.15	1.75	2.32	5.38	8.33	15.42	1.15	4.67	1.15
10% FS + 90% Agg	0.27	0.40	0.59	0.71	0.89	1.09	1.71	2.12	5.71	8.90	15.82	1.40	5.35	1.04
15% FS + 85% Agg	0.26	0.37	0.59	0.75	0.97	1.13	1.73	2.22	5.31	8.13	15.22	1.54	5.93	1.02
100% Agg	0.35	0.55	0.72	0.83	1.03	1.17	1.72	2.03	5.25	7.97	15.02	1.22	3.69	1.22

(continue)

	Cc*	Cu**	De***	Percent Passing			
				2mm (No.10)	0.425mm (No.40)	0.075mm (No.200)	AASHTO Classification
25% RAP+75%Agg	0.96	4.90	1.32	55.04	10.3	0.35	A-1-a
50% RAP+50%Agg	0.69	5.19	1.79	43.66	7.31	0.13	A-1-a
75% RAP+25%Agg	0.56	4.84	2.01	38.18	6.15	0	A-1-a
100% RAP	0.89	4.46	2.97	23.19	2.8	0	A-1-a
5% FA+25% RAP+70% Agg	0.67	5.93	1.73	44.26	9.42	1.64	A-1-a
15% FA+25% RAP+60% Agg	0.83	5.22	1.56	52.66	14.69	5.23	A-1-a
5% FA+50% RAP+45% Agg	0.83	5.22	1.56	48.6	10.09	1.59	A-1-a
15% FA+50% RAP+35% Agg	0.79	5.52	1.72	44.88	12.62	4.49	A-1-a
5% FA+75% RAP+20% Agg	0.60	4.58	2.24	33.62	6.46	0.76	A-1-a
15% FA+75% RAP+10% Agg	0.59	4.57	2.05	38.54	9.45	2.01	A-1-a
25% RCM+75% Agg	0.96	4.90	1.32	53.53	12.08	0.63	A-1-a
50% RCM+50% Agg	0.68	5.27	1.75	53.66	16.74	1.15	A-1-a
75% RCM+25% Agg	0.56	4.84	2.07	52.9	20.61	1.45	A-1-a
100 % RCM	0.90	4.53	2.99	46.79	22.31	1.11	A-1-a
5% FS + 95% Agg	1.15	4.67	1.15	58.45	13.96	0	A-1-a
10% FS + 90% Agg	1.40	5.35	1.04	59.49	18.61	0	A-1-a
15% FS + 85% Agg	1.54	5.93	1.02	58.94	20.79	0	A-1-a
100% Agg	1.22	3.69	1.22	59.87	11.07	0.68	A-1-a

*Cc :Coefficient of Curvature
**Cu Coefficient of Uniformity
***De : Effective Grain Diameter, mm

A. Experiment Procedure of Water Retention Test for Small Specimen

Water retention of recyclable materials was also evaluated on small (38.1 mm diameter and 76.2 mm height) specimens. This was done to evaluate the effect of size and the method of packing on water retention. Small specimens were packed in a cylindrical split mold with a hydraulic jack. Before water retention measurements, small specimens of 18 recycled material mixtures were also evaluated for optimal water content and maximum dry density.

The procedure for water retention measurement of small specimens involved preparing the specimen in a split mold, enclosing the specimen with a rubber membrane. A small amount of fine clay soil was spread on the pressure plate where the specimens were placed. This helped to improve the contact between the plate and the specimens. The specimens were gently embedded into clay layer on the ceramic plate, and then saturated from bottom up under a small head of water. Several specimens of the same recyclable materials were placed on a given ceramic plate and then the specimens and the ceramic plate allowed to saturate for 2~3 days and until the top of the soil glistened. After saturation, the saturated ceramic plate with specimens were placed in a pressure chambers and then simultaneously desorbed at a given pressure. Two ceramic chambers (low pressure chamber for saturation, 300, 500, and 1000 cm suction and high pressure chamber for 5000cm suction) were used to simulate the complete range of pressure for water retention. Once the specimens reached equilibrium, they were taken out of the pressure chamber and weighed after shear strength test. The samples were oven dried at 105 ^{o}C and then weighed again. Desorbed water volume by applied suctions was calculated by subtracting from the specimen weight at saturated condition to the weight of specimen at equilibrium conditions after suction application procedure. Soil moisture content was calculated as the weight difference between wet and dry soil divided by weight of dry soil. Water retention curves of small specimens were drawn as the degree of saturation vs. applied suction (Figures A.1 to A4 by Fredlund and Xing Equation, and Figures A6, A8, A10, and A12 by van Genuchten Equation). Water retention curves of large specimens by van Genuchten Equation are also included (Figure A5, A7, A9, and A11).

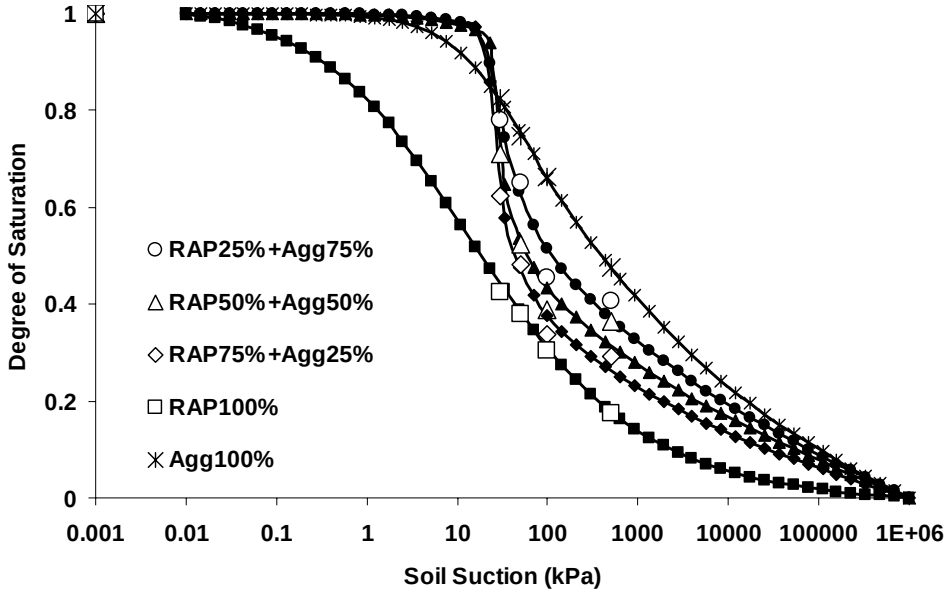

Figure A1. Water retention characteristic of RAP-Aggregate mixtures. Empty symbols are measured values obtained using small specimens (38.1 mm diameter and 76.2 mm height). Solid line is the best fit line representing the Fredlund and Xing equation.

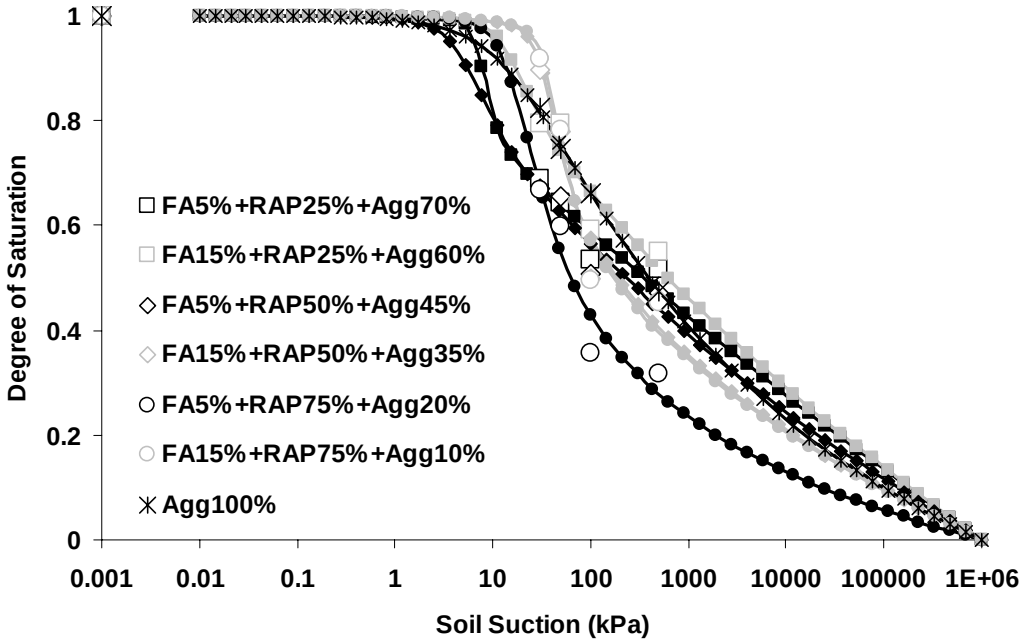

Figure A2. Water retention characteristic of Fly Ash-RAP-Aggregate mixtures. Empty symbols are measured values obtained using small specimens (38.1 mm diameter and 76.2 mm height). Solid line is the best fit line representing the Fredlund and Xing equation.

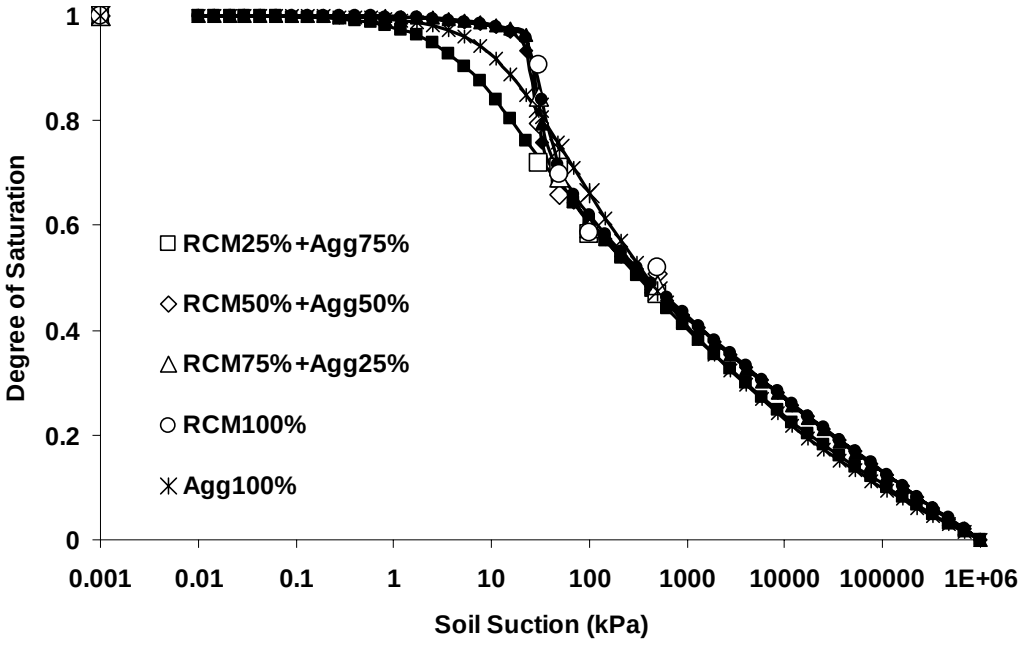

Figure A3. Water retention characteristic of RCM-Aggregate mixtures. Empty symbols are measured values obtained using small specimens (38.1 mm diameter and 76.2 mm height). Solid line is the best fit line representing the Fredlund and Xing equation.

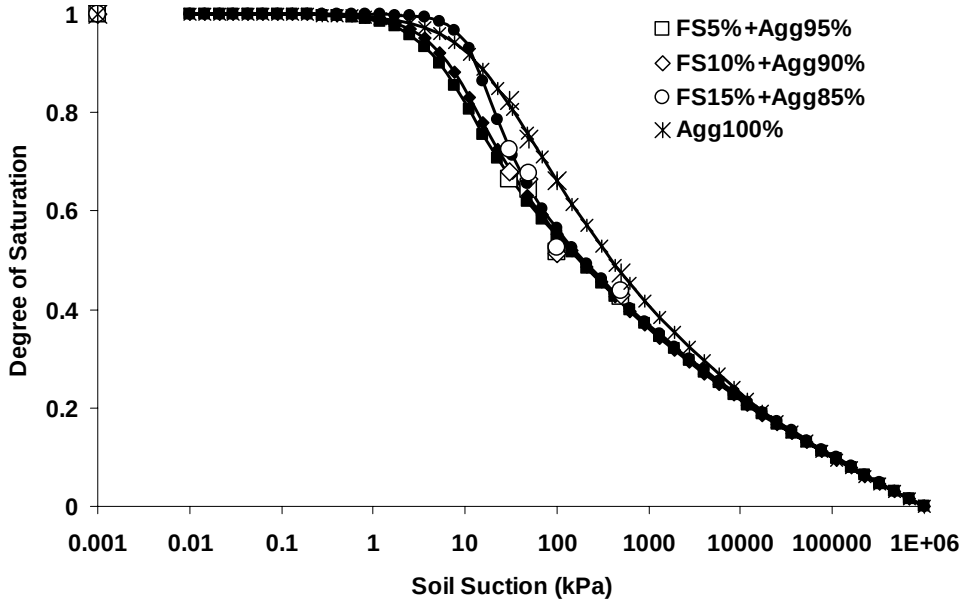

Figure A4. Water retention characteristic of Foundry Sand-Aggregate mixtures: Solid line is the best fit line representing the Fredlund and Xing equation. Empty symbols are measured values obtained using small specimens (38.1 mm diameter and 76.2 mm height).

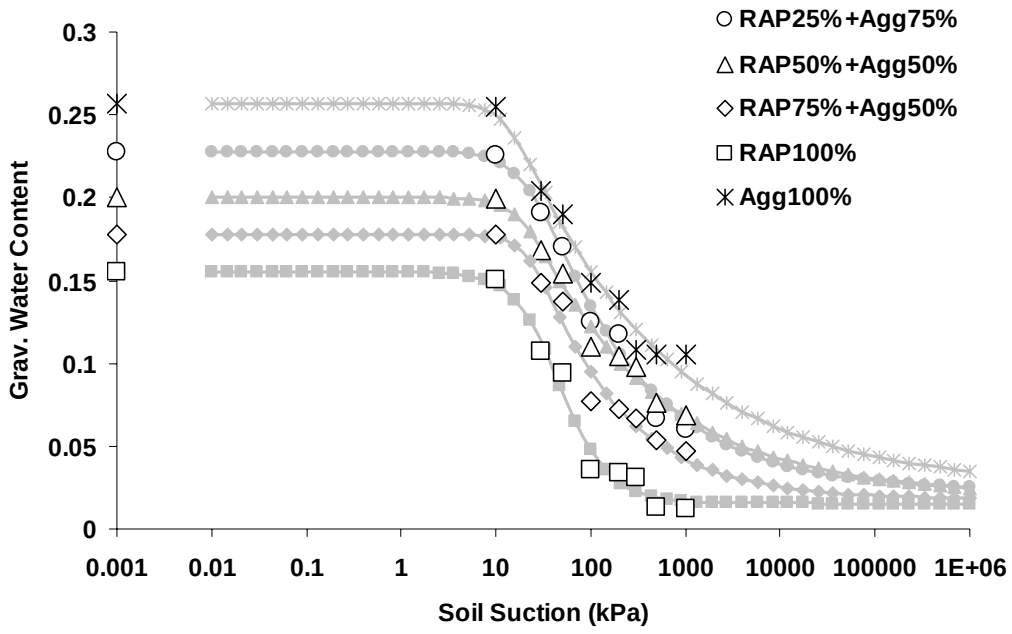

Figure A5. Water retention characteristic of RAP-Aggregate mixtures. Empty symbols are measured values obtained using large specimens (diameter: 152.4 mm and height: 76.2 mm). Solid line is the best fit line representing the van Genuchten equation.

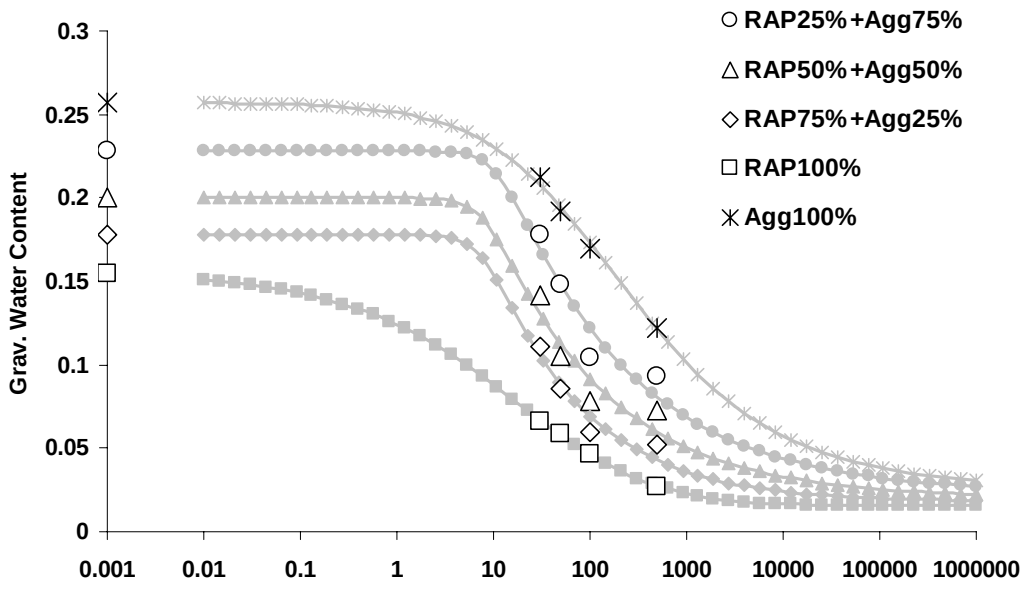

Figure A6. Water retention characteristic of RAP- Aggregate mixtures. Empty symbols are measured values obtained using small specimens (38.1 mm diameter and 76.2 mm height). Solid line is the best fit line representing the van Genuchten equation.

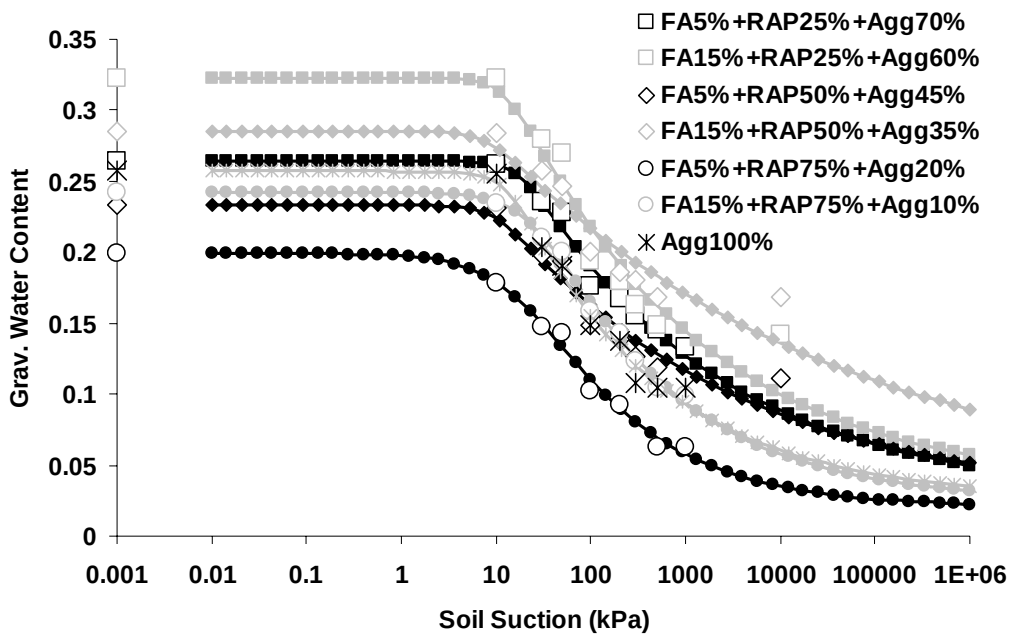

Figure A7. Water retention characteristic of Fly Ash-RAP-Aggregate mixtures. Empty symbols are measured values obtained using large specimens (diameter: 152.4 mm and height: 76.2 mm). Solid line is the best fit line representing the van Genuchten equation.

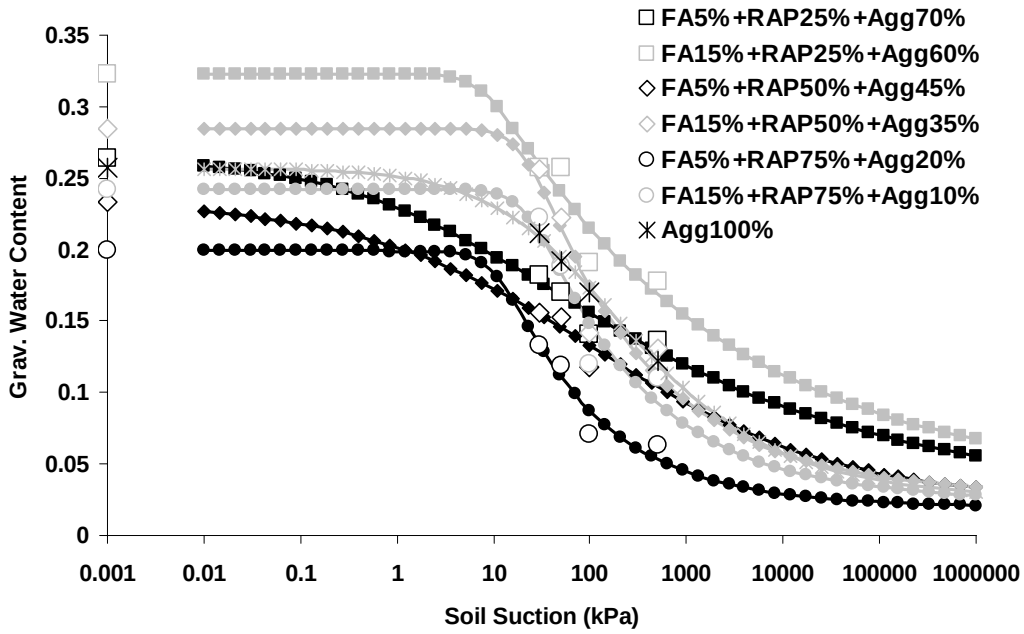

Figure A8. Water retention characteristic curves of Fly Ash-RAP-Aggregate mixtures. Empty symbols are measured values obtained using small specimens (38.1 mm diameter and 76.2 mm height). Solid line is the best fit line representing the van Genuchten equation.

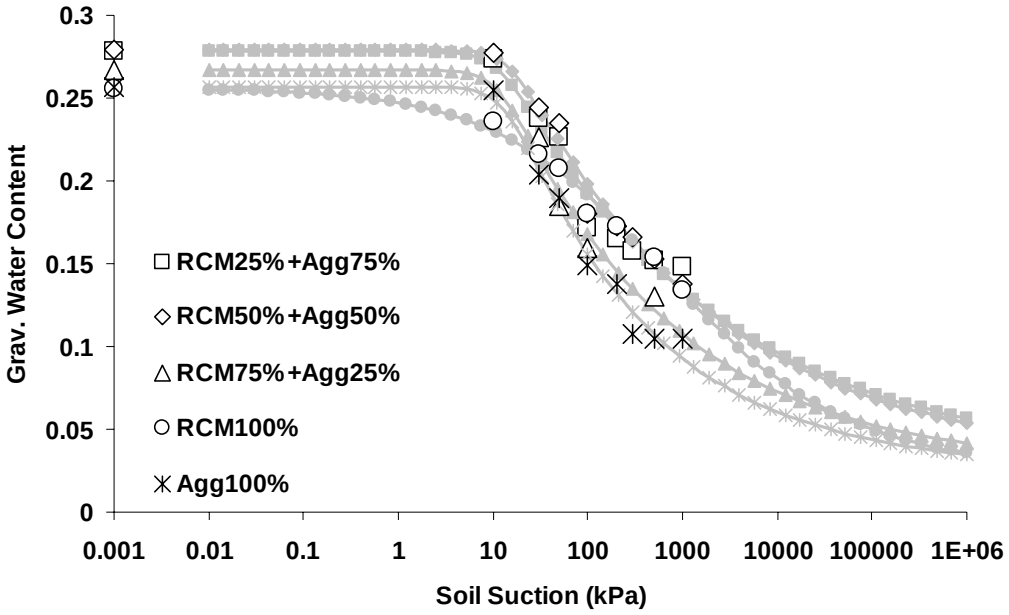

Figure A9. Water retention characteristic curves of RCM-Aggregate Mixtures. Empty symbols are measured values obtained using large specimens (diameter: 152.4 mm and height: 76.2 mm). Solid line is the best fit line representing the by van Genuchten equation.

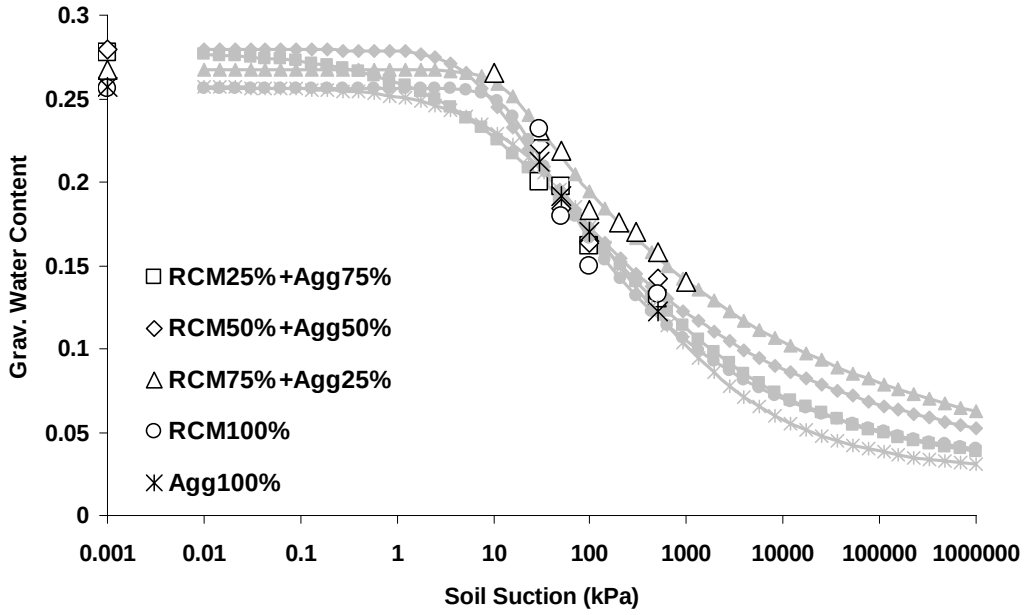

Figure A10. Water retention characteristic curves of RCM-Aggregate mixtures. Empty symbols are measured values obtained using small specimens (38.1 mm diameter and 76.2 mm height). Solid line is the best fit line representing the by van Genuchten equation.

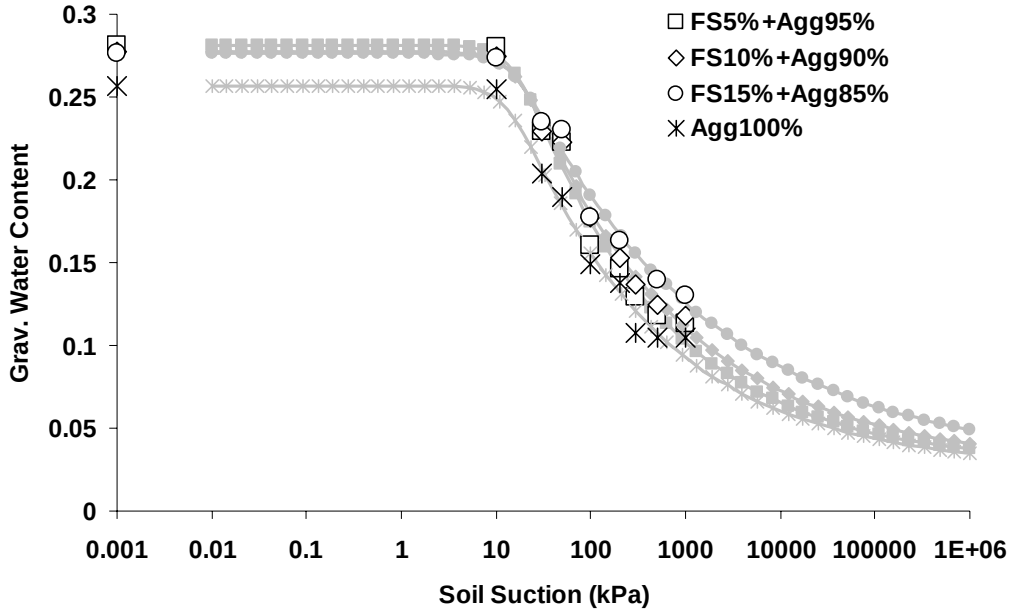

Figure A11. Water retention characteristic curves of Foundry Sand-Aggregate mixtures. Empty symbols are measured values obtained using large specimens (diameter: 152.4 mm and height: 76.2 mm). Solid line is the best fit line representing the by van Genuchten equation.

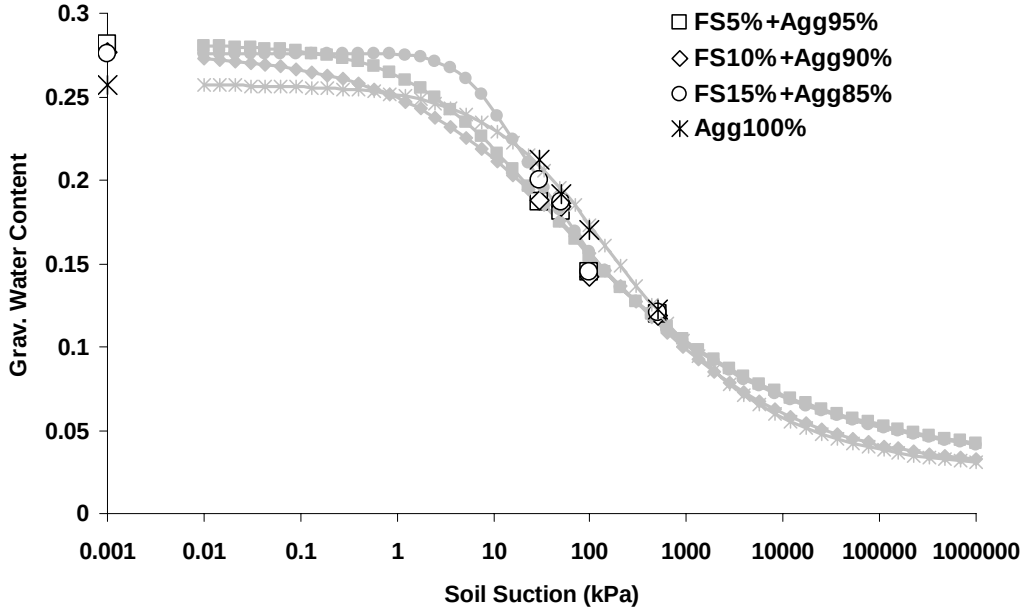

Figure A12. Water retention characteristic curves of Foundry Sand-Aggregate Mixtures. Empty symbols are measured values obtained using small specimens (38.1 mm diameter and 76.2 mm height). Solid line is the best fit line representing the by van Genuchten equation.

Table A3. Fredlund and Xing equation parameters for RAP - Aggregate mixtures.

	Specimen	θ_s	a_f	n_f	m_f	h_r	R^2
25 % RAP+75% Agg	Large		33.349	1.484	1.676	455.170	0.98
	Small		22.296	6.706	0.244	65.336	0.98
50 % RAP+50% Agg %	Large		25.062	2.582	0.357	172.306	0.99
	Small		24.669	20.000	0.209	37.468	0.98
75 % RAP+25% Agg	Large		31.446	3.196	0.461	142.289	0.98
	Small		22.023	14.991	0.275	49.917	0.99
100% RAP	Large		31.343	2.051	1.148	149.658	0.98
	Small		5.394	0.530	1.646	196.297	1.00

Table A4. Fredlund and Xing equation parameters for Fly Ash, RAP, and Aggregate mixtures.

	Specimen	θ_s	a_f	n_f	m_f	h_r	R^2
5% FA+25% RAP+70% Agg	Large		26.060	3.353	0.179	122.708	0.98
	Small		6.811	17.948	0.100	35.225	0.97
15% FA+25% RAP+60% Agg	Large		24.877	20.000	0.080	57.061	0.89
	Small		4.205	2.650	0.211	47.231	0.97
5% FA+50% RAP+45% Agg	Large		26.053	20.000	0.040	35.686	0.75
	Small		31.542	5.715	0.246	89.328	0.95
15% FA+50% RAP+35% Agg	Large		19.383	1.169	0.693	392.232	0.99
	Small		31.542	5.715	0.246	89.328	0.95
5% FA+75% RAP+20% Agg	Large		19.383	1.169	0.693	392.232	0.99
	Small		16.319	2.934	0.455	86.835	0.97
15% FA+75% RAP+10% Agg	Large		30.745	1.602	0.448	408.066	0.99
	Small		34.671	6.893	0.238	86.900	0.96

Table A5. Fredlund and Xing equation parameters for RCM - Aggregate mixtures.

	Specimen	θ_s	a_f	n_f	m_f	h_r	R^2
25% RCM+75% Agg	Large		21.441	6.007	0.129	71.519	0.97
	Small		6.723	1.012	0.438	315.757	0.99
50% RCM+50% Agg	Large		22.890	3.656	0.166	104.237	0.98
	Small		23.080	30.000	0.112	45.180	0.99
75% RCM+25% Agg	Large		18.966	5.477	0.101	67.838	0.99
	Small		26.235	19.980	0.119	59.092	1.00
100 % RCM	Large		1651.853	0.427	2.853	27844.400	0.99
	Small		28.889	20.000	0.111	44.714	0.98

Table A6. Fredlund and Xing equation parameters for Foundry Sand- Aggregate mixtures.

	Specimen	θ_s	a_f	n_f	m_f	h_r	R^2
5% FS+ 95% Agg	Large		22.823	2.546	0.326	156.062	0.98
	Small		4.905	1.549	0.341	109.732	0.99
10% FS+ 90 % Agg	Large		22.790	2.096	0.332	210.942	0.99
	Small		6.180	1.594	0.346	111.416	0.98
15% FS+ 85% Agg	Large		21.224	2.753	0.217	137.829	0.98
	Small		11.979	2.902	0.270	93.865	0.99
100 % Agg	Large		19.258	2.708	0.306	135.664	0.98
	Small		18.926	1.118	0.491	448.019	1.00

Table A7. van Genuchten equation parameters for RAP- Aggregate mixtures.

	Specimen	θ_s	θ_r	α	n	m	R^2
25 % RAP+75% Agg	Large	0.228	0.06	0.041	2.131	0.197	0.978
	Small	0.228	0.093	0.086	3.000	0.113	0.956
50 % RAP+50% Agg %	Large	0.200	0.069	0.055	3.000	0.110	0.987
	Small	0.200	0.073	0.121	3.000	0.123	0.952
75 % RAP+25% Agg	Large	0.178	0.047	0.043	3.000	0.168	0.978
	Small	0.178	0.052	0.123	3.000	0.151	0.981
100% RAP	Large	0.155	0.012	0.025	1.880	0.785	0.983
	Small	0.155	0.047	0.009	0.455	2.250	0.999

Table A8. van Genuchten equation parameters for Fly Ash, RAP, and Aggregate mixtures.

	Specimen	θ_s	θ_r	a	n	m	R^2
5% FA+25% RAP+70% Agg	Large	0.264	0.133	0.057	3.000	0.071	0.981
	Small	0.264	0.136	0.221	0.443	0.381	0.972
15% FA+25% RAP+60% Agg	Large	0.323	0.142	0.106	3.000	0.058	0.926
	Small	0.323	0.178	0.014	0.367	0.858	0.966
5% FA+50% RAP+45% Agg	Large	0.233	0.111	0.128	3.000	0.041	0.877
	Small	0.233	0.110	0.049	3.000	0.118	0.913
15% FA+50% RAP+35% Agg	Large	0.285	0.168	0.050	1.202	0.330	0.987
	Small	0.285	0.131	0.049	3.000	0.118	0.913
5% FA+75% RAP+20% Agg	Large	0.199	0.063	0.050	1.202	0.330	0.987
	Small	0.199	0.063	0.095	3.000	0.145	0.965
15% FA+75% RAP+10% Agg	Large	0.242	0.099	0.038	1.756	0.179	0.993
	Small	0.242	0.110	0.145	3.000	0.124	0.910

Table A9. van Genuchten equation parameters for RCM- Aggregate mixtures.

	Specimen	θ_s	θ_r	a	n	m	R^2
25% RCM+75% Agg	Large	0.274	0.148	0.089	3.000	0.064	0.963
	Small	0.274	0.093	0.026	0.533	0.578	0.988
50% RCM+50% Agg	Large	0.277	0.138	0.067	3.000	0.068	0.979
	Small	0.277	0.073	0.174	2.045	0.098	0.968
75% RCM+25% Agg	Large	0.265	0.14	0.085	3.000	0.056	0.989
	Small	0.265	0.052	0.089	3.000	0.081	0.972
100 % RCM	Large	0.236	0.134	0.003	0.506	0.769	0.981
	Small	0.236	0.047	0.073	3.000	0.083	0.915

Table A10. van Genuchten equation parameters for Foundry Sand- Aggregate mixtures.

	Specimen	θ_s	θ_r	a	n	m	R^2
5% FS+ 95% Agg	Large	0.281	0.113	0.063	3.000	0.099	0.982
	Small	0.281	0.12	0.145	0.713	0.339	0.989
10% FS+ 90 % Agg	Large	0.277	0.118	0.063	3.000	0.089	0.991
	Small	0.277	0.119	0.011	0.442	0.935	0.979
15% FS+ 85% Agg	Large	0.276	0.13	0.067	3.000	0.073	0.981
	Small	0.276	0.121	0.148	1.828	0.132	0.984
100 % Agg	Large	0.257	0.105	0.075	3.000	0.095	0.984
	Small	0.257	0.122	0.013	0.702	0.577	0.997

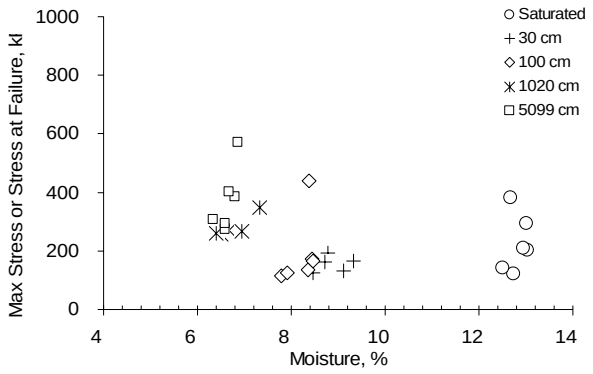

a) 5% Fly Ash + 25% RAP+ 70% Aggregate

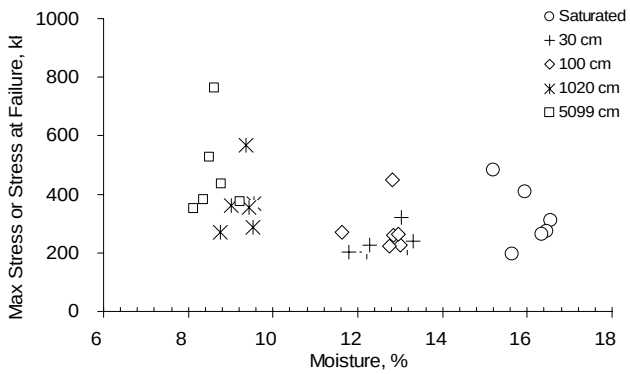

b) 15% Fly Ash + 25% RAP + 60% Aggregate

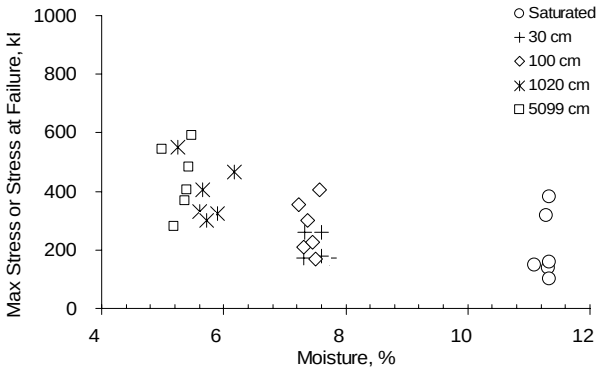

c) 5% Fly Ash + 50% RAP+ 45% Aggregate

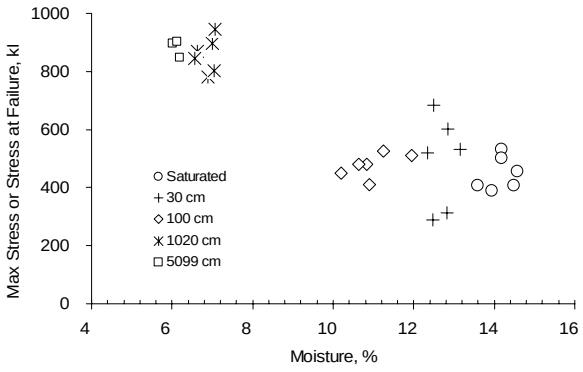

d) 15% Fly Ash + 50% RAP+ 35% Aggregate

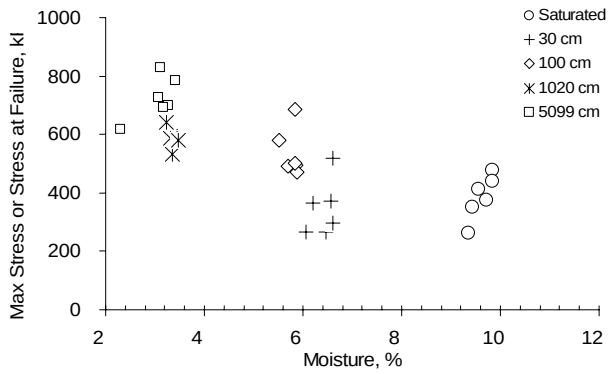

e) 5% Fly Ash + 75% RAP+ 20% Aggregate

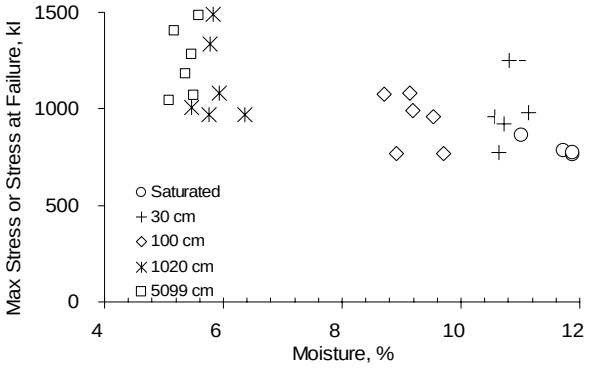

f) 15% Fly Ash + 75% RAP+ 10% Aggregate

Figure A13. Maximum stress or stress at failure (kPa) vs. moisture content (%) during shear strength measurements on small cores of Fly Ash, RAP, and Aggregate mixtures. Numbers in index refer to suctions at which these specimens were equilibrated at before testing.

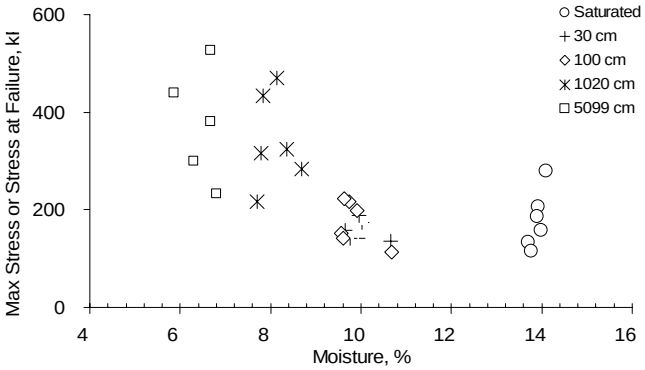

a) 25 % RCM + 75% Aggregate

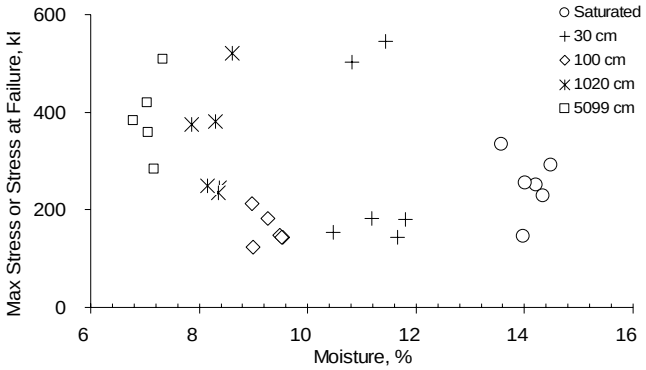

b) 50 % RCM + 50% Aggregate

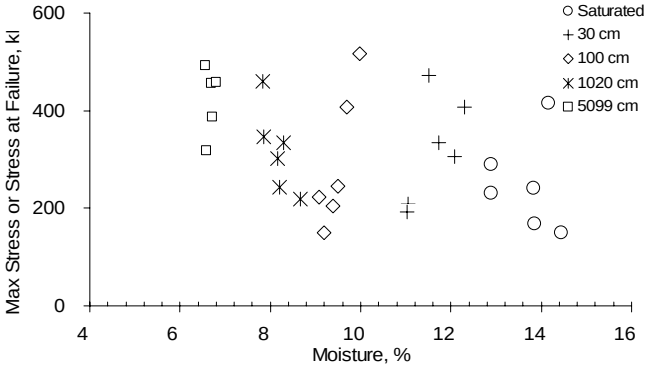

c) 75 % RCM + 25% Aggregate

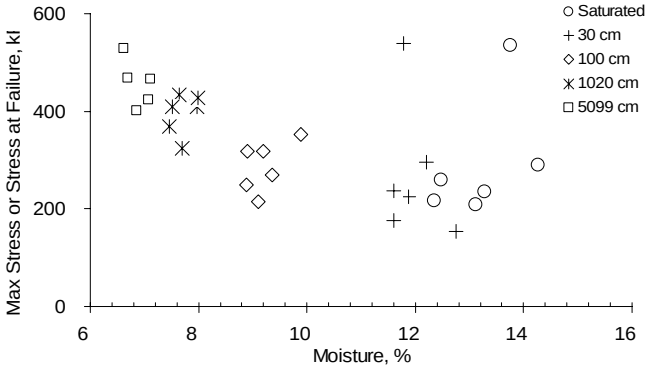

d) 100% RCM

Figure A14. Maximum stress or stress at failure (kPa) vs. moisture content (%) during shear strength measurements on small cores of RCM and Aggregate mixtures. Numbers in index refer to suctions at which these specimens were equilibrated at before testing.

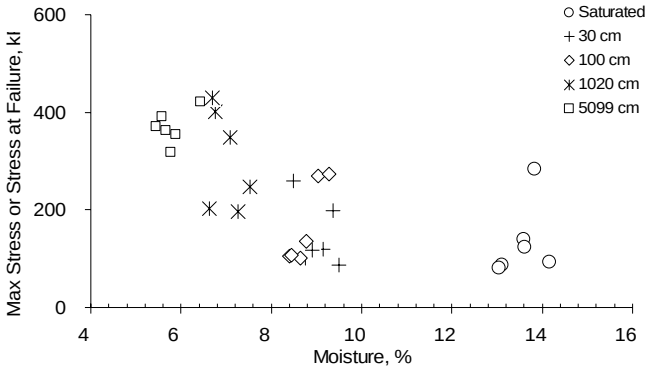

a) 5% Foundry Sand + 95% Aggregate

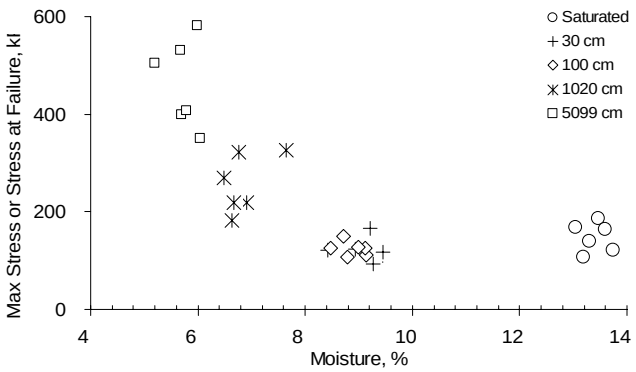

b) 10% Foundry Sand+90% Aggregate

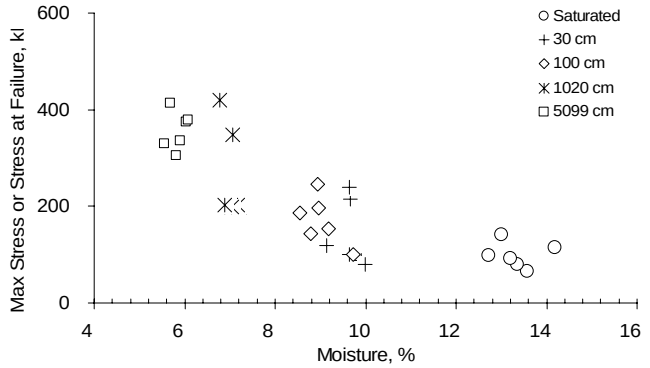

c) 15% Foundry Sand +85% Aggregate

Figure A15. Maximum stress or stress at failure (kPa) vs. moisture content (%) during shear strength measurements on small cores of Foundry Sand and Aggregate mixtures. Numbers in index refer to suctions at which these specimens were equilibrated at before testing.

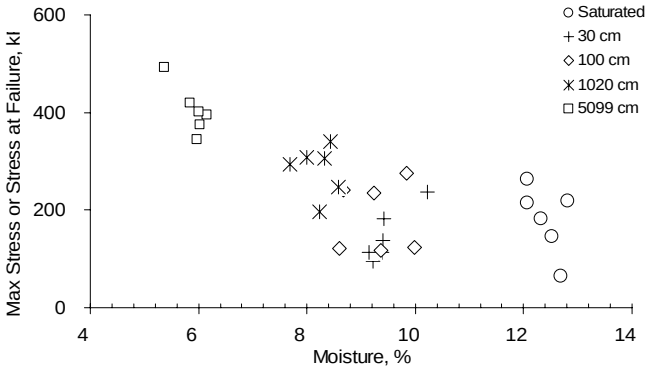

Figure A16. Maximum stress or stress at failure (kPa) vs. moisture content (%) during shear strength measurements on small cores of 100% Aggregates. Numbers in index refer to suctions at which these specimens were equilibrated at before testing.

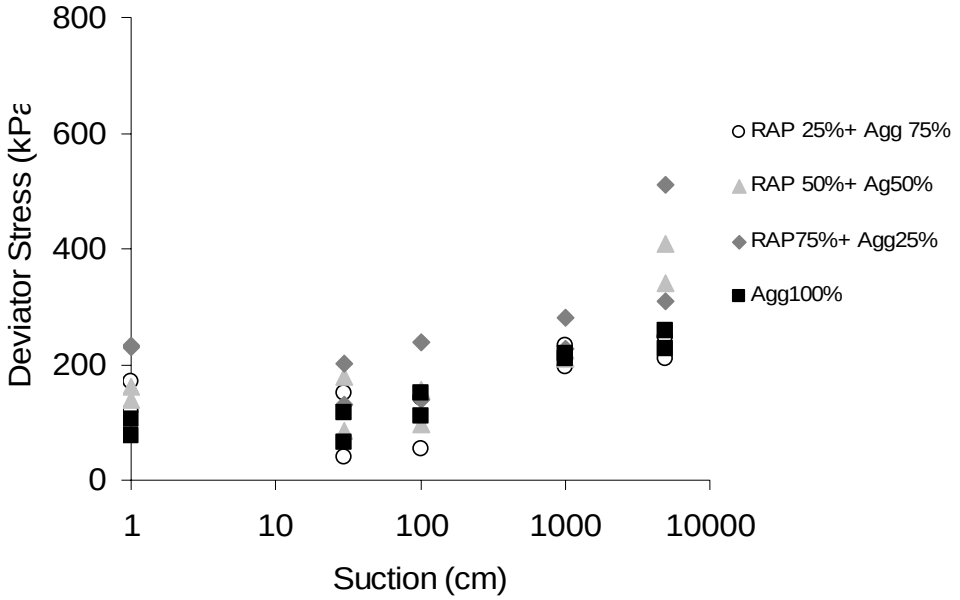

Figure A17. Variation in deviator stress at 5% strain as a function of soil suction for RAP and aggregate mixtures.

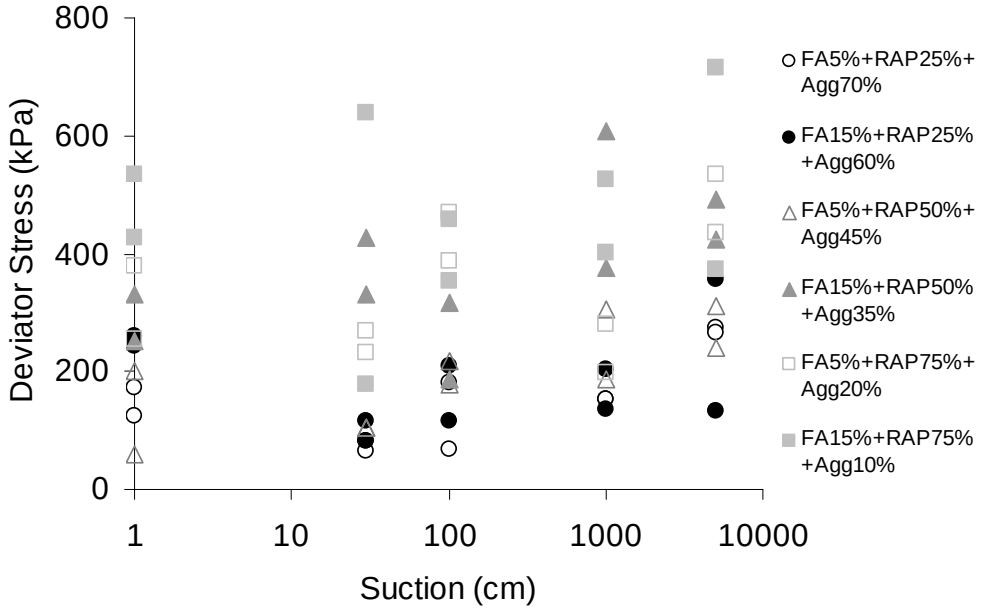

Figure A18. Variation in deviator stress at 5% Strain as a function of soil suction for Fly Ash, RAP and Aggregate mixtures.

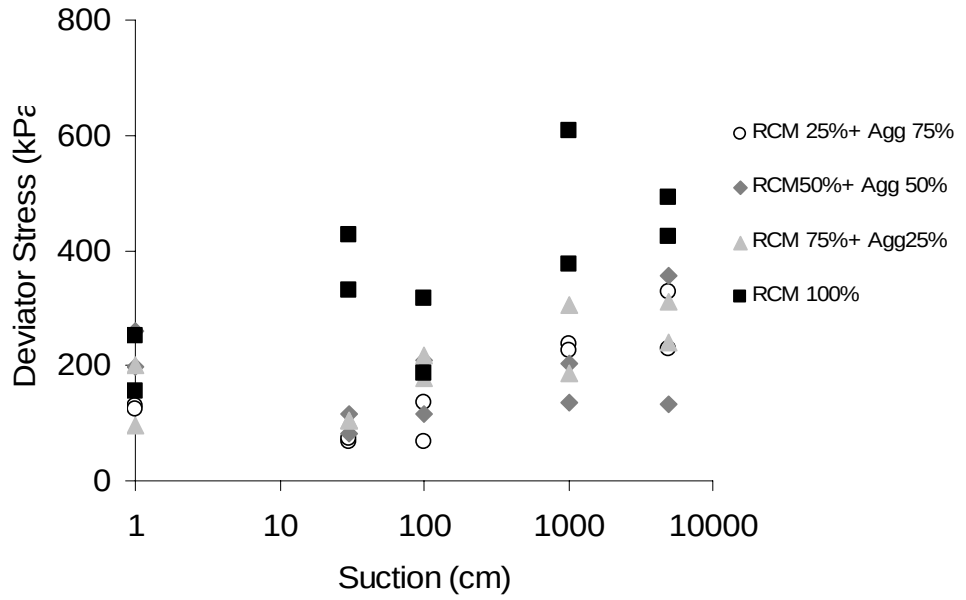

Figure A19. Variation in deviator stress at 5% Strain as a function of soil suction for RCM and Aggregate mixtures.

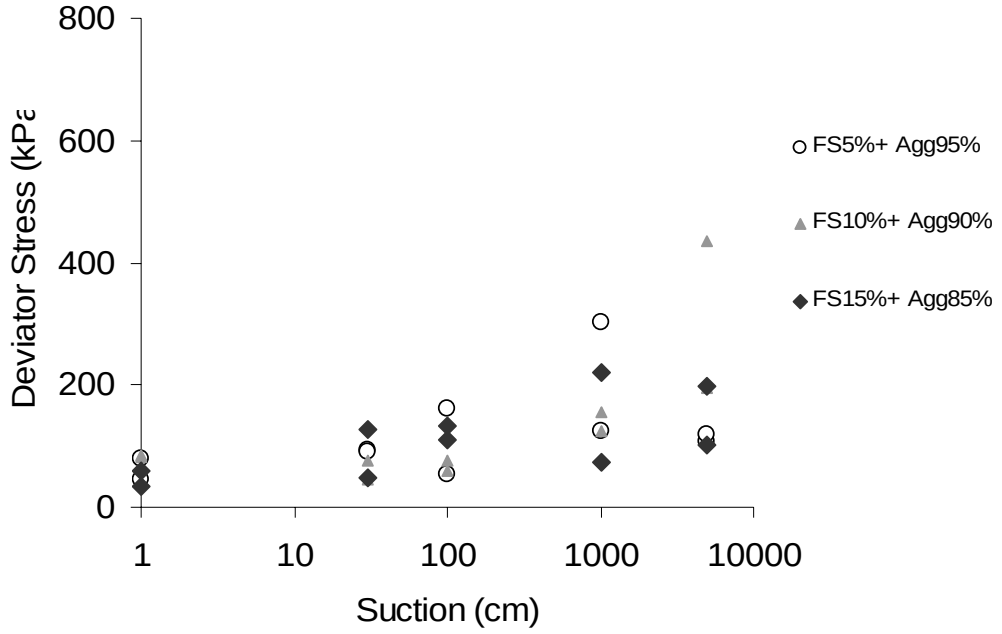

Figure A20. Variation in deviator stress at 5% Strain as a function of soil suction for Foundry Sand and Aggregate mixtures.

Table A11. Confining, deviator, and mean stresses, resilient modulus (M_R), rotation, and homogeneous deformation coefficient (HDC) during resilient modulus measurement of 25% RAP+ 75% Aggregate mixture at 6.4% moisture content and 2.069 g/cm^3 dry density.

Sq	Confining kPa	Deviator kPa	Mean Stress kPa	M_R MPa	Rotation θ(°)	HDC α
1	20.68	9.14	23.73	29.61	0.00838	0.307005
2	41.37	19.06	47.75	62.53	0.00599	0.222387
3	68.95	33.38	80.13	121.33	0.00323	0.132762
4	103.42	50.40	120.30	202.66	0.00249	0.113116
5	137.90	67.30	160.43	276.50	0.00230	0.106972
6	20.68	18.93	27.01	28.26	0.00951	0.160457
7	41.37	40.30	54.83	73.22	0.00456	0.09384
8	68.95	67.45	91.48	126.76	0.00405	0.086108
9	103.42	101.43	137.31	200.94	0.00311	0.069832
10	137.90	135.43	183.14	273.83	0.00256	0.05848
11	20.68	40.20	34.10	39.15	0.01273	0.140227
12	41.37	80.97	68.39	91.07	0.00421	0.053598
13	68.95	135.00	114.00	145.95	0.00233	0.028538
14	103.42	202.85	171.12	211.64	0.00204	0.024074
15	137.90	270.26	228.09	271.98	0.00146	0.016597
16	20.68	60.37	40.82	48.08	0.01567	0.141209
17	41.37	121.09	81.76	102.48	0.00724	0.069406
18	68.95	202.55	136.52	163.59	0.00461	0.04215
19	103.42	303.56	204.69	226.72	0.00453	0.038293
20	137.90	404.88	272.96	284.44	0.00561	0.044589
21	20.68	101.57	54.56	61.96	0.02733	0.188653
22	41.37	203.55	109.25	126.89	0.01307	0.092222
23	68.95	338.99	182.00	186.74	0.01156	0.072086

Table A12. Confining, deviator, and mean stresses, resilient modulus (M_R), rotation, and homogeneous deformation coefficient (HDC) during resilient modulus measurement of 25% RAP+ 75% Aggregate mixture at 5.3 % moisture content and 2.087 g/cm^3 dry density.

Sq	Confining kPa	Deviator kPa	Mean Stress kPa	M_R MPa	Rotation θ(°)	HDC α
1	20.68	10.22	24.09	159.89	0.00451	0.075855
2	41.37	19.59	47.93	276.56	0.00500	0.084885
3	68.95	33.75	80.25	418.02	0.00152	0.230576
4	103.42	50.53	120.34	528.33	0.00086	0.113833
5	137.90	67.41	160.47	630.00	0.00108	0.156737
6	20.68	20.34	27.48	207.36	0.00694	0.106409
7	41.37	40.65	54.95	308.87	0.00934	0.122089
8	68.95	67.71	91.57	414.53	0.00161	0.117502
9	103.42	101.60	137.37	504.14	0.00104	0.062781
10	137.90	135.88	183.29	599.19	0.00132	0.070915
11	20.68	40.65	34.25	215.07	0.01333	0.087046
12	41.37	81.17	68.46	307.13	0.00673	0.073743
13	68.95	135.32	114.11	391.66	0.00201	0.068483
14	103.42	202.89	171.13	483.98	0.00157	0.04725
15	137.90	274.26	229.42	565.21	0.00068	0.033759
16	20.68	60.71	40.94	202.23	0.02006	0.08095
17	41.37	121.64	81.95	290.59	0.00251	0.034163
18	68.95	203.26	136.75	383.06	0.00134	0.033618
19	103.42	307.89	206.13	489.70	0.00144	0.030361
20	137.90	477.92	297.31	499.87	0.00637	0.092362
21	20.68	101.99	54.70	192.31	0.00148	0.039153
22	41.37	203.92	109.37	264.22	0.00213	0.033554
23	68.95	341.12	182.71	372.12	0.00302	0.039395
24	103.42	511.20	273.90	471.95	0.00488	0.05543
25	137.90	680.99	365.00	521.66	0.00586	0.056715
26	20.68	141.26	67.79	179.37	0.00580	0.086579
27	41.37	283.36	135.85	273.55	0.00500	0.058884
28	68.95	474.21	227.07	388.42	0.00761	0.074658
29	103.42	706.89	339.13	469.85	0.01420	0.112372
30	137.90	936.54	450.18	511.66	0.02410	0.153829

Table A13. Confining, deviator, and mean stresses, resilient modulus (M_R), rotation, and homogeneous deformation coefficient (HDC) during resilient modulus measurement of 50% RAP + 50% Aggregate mixture at 6.2 % moisture content and 2.083 g/cm^3 dry density.

Sq	Confining kPa	Deviator kPa	Mean Stress kPa	M_R MPa	Rotation θ(°)	HDC α
1	20.68	9.75	23.94	52.46	0.01287	1.418182
2	41.37	19.05	47.75	106.67	0.00104	0.080209
3	68.95	33.59	80.20	182.51	0.00503	0.327471
4	103.42	50.21	120.24	305.34	0.00322	0.230733
5	137.90	67.14	160.38	411.92	0.00288	0.243936
6	20.68	19.65	27.25	64.80	0.00270	0.125058
7	41.37	39.97	54.72	90.06	0.01499	0.398004
8	68.95	67.01	91.34	178.01	0.00826	0.264417
9	103.42	100.71	137.07	302.82	0.00518	0.217581
10	137.90	134.63	182.88	402.06	0.00482	0.197897
11	20.68	39.55	33.88	58.89	0.02488	0.43866
12	41.37	80.15	68.12	110.12	0.01929	0.317278
13	68.95	134.39	113.80	192.46	0.01243	0.22296
14	103.42	201.85	170.78	300.65	0.00944	0.179711
15	137.90	269.80	227.93	386.93	0.00829	0.165769
16	20.68	60.04	40.71	68.01	0.02563	0.350989
17	41.37	120.30	81.50	124.72	0.01847	0.238336
18	68.95	201.20	136.07	207.87	0.01007	0.139528
19	103.42	302.43	204.31	312.06	0.00745	0.115773
20	137.90	403.31	272.44	394.81	0.00766	0.112637
21	20.68	100.24	54.11	83.04	0.01505	0.163466
22	41.37	200.98	108.39	151.47	0.00474	0.05862
23	68.95	334.18	180.39	231.08	0.01487	0.125688
24	103.42	501.00	270.50	320.76	0.02662	0.208586
25	137.90	664.60	359.53	395.37	0.03266	0.239009
26	20.68	140.13	67.41	89.45	0.03598	0.290139
27	41.37	280.34	134.85	165.67	0.03540	0.264063
28	68.95	465.74	224.25	289.22	0.04538	0.440637
29	103.42	705.90	338.80	329.62	0.01027	0.066244
30	137.90	937.27	450.42	407.05	0.01792	0.10727

Table A14. Confining, deviator, and mean stresses, resilient modulus (M_R), rotation, and homogeneous deformation coefficient (HDC) during resilient modulus measurement of 50% RAP + 50% Aggregate mixture at 4.2 % moisture content and 2.110 g/cm^3 dry density.

Sq	Confining kPa	Deviator kPa	Mean Stress kPa	M_R MPa	Rotation θ(°)	HDC α
1	20.68	10.26	24.10	147.36	0.00358	0.375513
2	41.37	19.33	47.84	245.15	0.00428	0.513229
3	68.95	33.55	80.18	412.81	0.00256	0.381069
4	103.42	50.65	120.38	545.59	0.00205	0.262268
5	137.90	67.75	160.58	653.86	0.00205	0.242079
6	20.68	20.27	27.46	154.39	0.01272	0.669275
7	41.37	40.31	54.84	269.55	0.00873	0.679657
8	68.95	67.34	91.45	395.05	0.00496	0.340825
9	103.42	101.24	137.25	513.93	0.00366	0.216259
10	137.90	136.04	183.35	632.54	0.00502	0.27264
11	20.68	40.36	34.15	164.42	0.02143	1.01676
12	41.37	81.07	68.42	273.23	0.01332	0.523451
13	68.95	135.57	114.19	401.95	0.00708	0.245146
14	103.42	204.41	171.64	532.93	0.00706	0.21574
15	137.90	271.87	228.62	590.90	0.00814	0.207891
16	20.68	60.79	40.96	162.07	0.02927	0.908624
17	41.37	121.68	81.96	266.39	0.01705	0.435177
18	68.95	203.37	136.79	401.32	0.00787	0.181312
19	103.42	306.02	205.51	507.97	0.00841	0.164429
20	137.90	408.14	274.05	563.34	0.00962	0.155892
21	20.68	101.09	54.40	169.07	0.03232	0.629749
22	41.37	202.21	108.80	274.36	0.02243	0.354947
23	68.95	338.15	181.72	411.89	0.01369	0.194753
24	103.42	504.22	271.57	504.61	0.01276	0.149023
25	137.90	672.22	362.07	582.13	0.01029	0.105193
26	20.68	141.49	67.86	187.44	0.02693	0.415748
27	41.37	282.90	135.70	284.74	0.01980	0.058884
28	68.95	471.57	226.19	422.21	0.01267	0.133593
29	103.42	705.83	338.78	528.69	0.00717	0.06378
30	137.90	936.25	450.08	591.63	0.01108	0.083335

Table A15. Confining, deviator, and mean stresses, resilient modulus (M_R), rotation, and homogeneous deformation coefficient (HDC) during resilient modulus measurement of 75% RAP + 25% Aggregate mixture at 5.6 % moisture content and 2.084 g/cm^3 dry density.

Sq	Confining kPa	Deviator kPa	Mean Stress kPa	M_R MPa	Rotation θ(°)	HDC α
1	20.68	9.59	23.88	62.24	0.00278	0.231441
2	41.37	18.89	47.70	105.99	0.00247	0.154743
3	68.95	33.12	80.04	195.51	0.00168	0.10754
4	103.42	49.68	120.06	333.28	0.00130	0.100031
5	137.90	66.65	160.22	473.39	0.00149	0.122135
6	20.68	19.61	27.24	62.07	0.00551	0.211235
7	41.37	39.56	54.59	120.58	0.00426	0.156488
8	68.95	66.35	91.12	191.79	0.00417	0.137427
9	103.42	99.48	136.66	328.13	0.00267	0.116518
10	137.90	133.03	182.34	440.84	0.00164	0.065347
11	20.68	39.34	33.81	70.41	0.00939	0.198369
12	41.37	79.44	67.88	145.52	0.00631	0.140297
13	68.95	132.60	113.20	214.88	0.00445	0.095562
14	103.42	199.23	169.91	327.84	0.00281	0.05772
15	137.90	266.22	226.74	420.23	0.00179	0.035341
16	20.68	59.31	40.47	75.66	0.01149	0.180785
17	41.37	119.71	81.30	159.85	0.00659	0.108475
18	68.95	199.43	135.48	230.66	0.00405	0.057471
19	103.42	299.42	203.31	331.34	0.00388	0.050266
20	137.90	403.55	272.52	425.00	0.00588	0.072005
21	20.68	100.20	54.10	90.75	0.01421	0.154616
22	41.37	201.67	108.62	184.30	0.00992	0.105942
23	68.95	334.83	180.61	252.30	0.01371	0.119688
24	103.42	502.51	271.00	343.80	0.01771	0.137777
25	137.90	667.77	360.59	424.41	0.02190	0.16239
26	20.68	140.65	67.58	96.14	0.01869	0.143204
27	41.37	282.47	135.56	194.28	0.01546	0.122691
28	68.95	470.66	225.89	282.29	0.02133	0.150931
29	103.42	703.57	338.02	365.10	0.02607	0.158602
30	137.90	932.09	448.70	423.77	0.03454	0.186355

Table A16. Confining, deviator, and mean stresses, resilient modulus (M_R), rotation, and homogeneous deformation coefficient (HDC) during resilient modulus measurement of 75% RAP + 25% Aggregate mixture at 3.2 % moisture content and 2.109 g/cm^3 dry density.

Sq	Confining kPa	Deviator kPa	Mean Stress kPa	M_R MPa	Rotation θ(°)	HDC α
1	20.68	9.99	24.02	100.70	0.01045	1.081357
2	41.37	19.19	47.80	284.18	0.00364	0.632235
3	68.95	33.38	80.13	420.26	0.00234	0.345782
4	103.42	49.99	120.16	574.77	0.00188	0.260871
5	137.90	66.99	160.33	706.56	0.00168	0.214569
6	20.68	19.90	27.33	131.32	0.01712	1.314558
7	41.37	40.23	54.81	262.05	0.00690	0.52416
8	68.95	66.93	91.31	390.88	0.00533	0.363982
9	103.42	100.62	137.04	528.53	0.00352	0.224381
10	137.90	134.52	182.84	662.48	0.00288	0.16825
11	20.68	39.94	34.01	151.00	0.02125	0.935565
12	41.37	80.31	68.17	255.32	0.01205	0.446868
13	68.95	134.17	113.72	394.86	0.00810	0.277822
14	103.42	201.01	170.50	537.39	0.00597	0.186083
15	137.90	268.91	227.64	629.61	0.00669	0.183143
16	20.68	60.43	40.84	167.51	0.02257	0.728768
17	41.37	120.93	81.71	260.05	0.01614	0.404864
18	68.95	201.11	136.04	406.12	0.01003	0.237166
19	103.42	301.71	204.07	524.28	0.00881	0.179789
20	137.90	401.96	271.99	613.86	0.00928	0.16635
21	20.68	100.72	54.27	194.93	0.02179	0.492367
22	41.37	201.39	108.53	288.10	0.01788	0.298877
23	68.95	335.43	180.81	425.72	0.01280	0.190393
24	103.42	503.52	271.34	529.71	0.01197	0.148093
25	137.90	669.94	361.31	617.30	0.01030	0.112721
26	20.68	140.62	67.57	225.19	0.00726	0.139285
27	41.37	281.95	135.38	313.80	0.01434	0.187592
28	68.95	470.06	225.69	448.73	0.00991	0.112708
29	103.42	703.58	338.03	538.50	0.00641	0.060218
30	137.90	934.72	449.57	606.80	0.00315	0.031261

Table A17. Confining, deviator, and mean stresses, resilient modulus (M_R), rotation, and homogeneous deformation coefficient (HDC) during resilient modulus measurement of 100% RAP at 4.5 % moisture content and 2.126 g/cm^3 dry density.

Sq	Confining kPa	Deviator kPa	Mean Stress kPa	M_R MPa	Rotation θ(°)	HDC α
1	20.68	9.82	23.96	76.41	0.00739	0.665854
2	41.37	19.81	48.00	191.61	0.00263	0.287188
3	68.95	34.00	80.33	332.33	0.00113	0.13668
4	103.42	51.39	120.63	512.45	0.00156	0.190043
5	137.90	69.13	161.04	652.33	0.00187	0.183254
6	20.68	20.03	27.38	86.13	0.00974	0.482468
7	41.37	40.50	54.90	181.62	0.00482	0.25264
8	68.95	67.81	91.60	348.99	0.00295	0.172538
9	103.42	101.93	137.48	504.13	0.00280	0.158623
10	137.90	137.13	183.71	592.87	0.00116	0.056553
11	20.68	40.51	34.20	102.45	0.01481	0.431881
12	41.37	81.20	68.47	206.54	0.00733	0.214243
13	68.95	135.98	114.33	352.32	0.00405	0.122304
14	103.42	200.77	170.42	487.36	0.00622	0.174996
15	137.90	275.03	229.68	564.88	0.00224	0.052027
16	20.68	60.65	40.92	116.71	0.01367	0.303297
17	41.37	122.19	82.13	222.15	0.00783	0.163725
18	68.95	204.41	137.14	348.11	0.00496	0.096056
19	103.42	304.96	205.15	471.48	0.00381	0.067662
20	137.90	427.27	280.42	554.97	0.00284	0.05393
21	20.68	101.32	54.47	139.22	0.01134	0.172029
22	41.37	203.05	109.08	250.48	0.00597	0.082198
23	68.95	338.85	181.95	364.16	0.00343	0.039494
24	103.42	506.95	272.48	473.86	0.00302	0.031786
25	137.90	672.54	362.18	558.17	0.00254	0.02301
26	20.68	141.84	67.98	149.87	0.01177	0.133479
27	41.37	283.76	135.99	276.68	0.00625	0.064076
28	68.95	471.56	226.19	378.72	0.00709	0.061129
29	103.42	705.73	338.74	474.69	0.01002	0.076551
30	137.90	936.13	450.04	745.60	0.04119	0.382527

Table A18. Confining, deviator, and mean stresses, resilient modulus (M_R), rotation, and homogeneous deformation coefficient (HDC) during resilient modulus measurement of 100% RAP at 3.2 % moisture content and 2.119 g/cm^3 dry density.

Sq	Confining kPa	Deviator kPa	Mean Stress kPa	M_R MPa	Rotation θ(°)	HDC α
1	20.68	9.83	23.96	76.57	0.00708	0.643976
2	41.37	19.24	47.81	160.48	0.00452	0.44436
3	68.95	33.82	80.27	330.95	0.00224	0.274525
4	103.42	50.42	120.31	500.21	0.00189	0.218596
5	137.90	67.20	160.40	651.33	0.00124	0.154485
6	20.68	19.92	27.34	80.89	0.01335	0.631527
7	41.37	40.15	54.78	162.23	0.00890	0.41861
8	68.95	67.66	91.55	329.44	0.00470	0.268989
9	103.42	101.10	137.20	486.28	0.00335	0.189251
10	137.90	135.04	183.01	612.67	0.00304	0.161714
11	20.68	40.50	34.20	98.56	0.01809	0.5135
12	41.37	81.21	68.47	193.25	0.01206	0.335216
13	68.95	135.35	114.12	340.89	0.00647	0.194069
14	103.42	203.08	171.19	481.95	0.00500	0.140097
15	137.90	270.23	228.08	582.47	0.00453	0.118401
16	20.68	60.79	40.96	115.71	0.01731	0.384361
17	41.37	121.26	81.82	206.03	0.01326	0.264543
18	68.95	202.52	136.51	352.25	0.00686	0.140851
19	103.42	303.82	204.77	479.49	0.00543	0.102376
20	137.90	404.40	272.80	573.85	0.00517	0.088048
21	20.68	101.72	54.61	142.06	0.01613	0.267049
22	41.37	202.30	108.83	248.00	0.01099	0.161215
23	68.95	337.57	181.52	376.15	0.00445	0.062145
24	103.42	505.53	272.01	488.91	0.00265	0.035531
25	137.90	672.75	362.25	579.61	0.00126	0.019577
26	20.68	141.85	67.98	166.30	0.00968	0.177147
27	41.37	282.32	135.51	282.69	0.00431	0.069425
28	68.95	470.36	225.79	401.08	0.00255	0.032604
29	103.42	706.78	339.09	500.11	0.00693	0.059448
30	137.90	937.24	450.41	572.79	0.01027	0.075384

Table A19. Confining, deviator, and mean stresses, resilient modulus (M_R), rotation, and homogeneous deformation coefficient (HDC) during resilient modulus measurement of 5% Fly Ash +25% RAP + 70% Aggregate mixture at 8.6 % moisture content and 2.032 g/cm^3 dry density.

Sq	Confining kPa	Deviator kPa	Mean Stress kPa	M_R MPa	Rotation θ(°)	HDC α
1	20.68	9.41	23.82	32.31	0.02044	0.023362
2	41.37	19.19	47.80	73.24	0.01838	0.024113
3	68.95	33.76	80.25	151.46	0.00048	0.041101
4	103.42	50.62	120.37	250.50	0.00064	0.040456
5	137.90	67.83	160.61	345.98	0.00110	0.066856
6	20.68	18.92	27.01	32.66	0.04062	0.011037
7	41.37	39.90	54.70	71.10	0.00914	0.191097
8	68.95	67.43	91.48	142.99	0.00108	0.030232
9	103.42	101.27	137.26	241.94	0.00134	0.037707
10	137.90	135.29	183.10	336.54	0.00169	0.048057
11	20.68	39.36	33.82	42.69	0.02493	0.315603
12	41.37	80.45	68.22	76.60	0.00357	0.039475
13	68.95	135.20	114.07	150.67	0.00253	0.032516
14	103.42	202.57	171.02	242.50	0.00339	0.045187
15	137.90	270.29	228.10	323.87	0.00398	0.052556
16	20.68	59.92	40.67	43.61	0.00536	0.055164
17	41.37	121.35	81.85	86.62	0.00498	0.042553
18	68.95	202.65	136.55	158.35	0.00437	0.038713
19	103.42	304.15	204.88	245.85	0.00532	0.049408
20	137.90	405.43	273.14	320.97	0.00654	0.058208
21	20.68	100.43	54.18	53.52	0.00789	0.054204
22	41.37	202.18	108.79	107.85	0.00591	0.039496
23	68.95	337.59	181.53	181.82	0.00721	0.045403
24	103.42	506.10	272.20	256.01	0.00934	0.054755
25	137.90	674.01	362.67	323.70	0.01431	0.079535
26	20.68	140.79	67.63	62.67	0.01785	0.096323
27	41.37	282.86	135.69	131.24	0.01469	0.082621
28	68.95	470.24	225.75	202.97	0.01976	0.101491
29	103.42	703.49	338.00	264.31	0.02449	0.10869
30	137.90	922.71	445.57	301.96	0.20549	0.050253

Table A20. Confining, deviator, and mean stresses, resilient modulus (M_R), rotation, and homogeneous deformation coefficient (HDC) during resilient modulus measurement of 5% Fly Ash +25% RAP + 70% Aggregate mixture at 5.6 % moisture content and 2.037 g/cm^3 dry density.

Sq	Confining	Deviator	Mean Stress	M_R	Rotation	HDC
	kPa	kPa	kPa	MPa	θ(°)	α
1	20.68	10.18	24.08	209.62	0.00545	1.021379
2	41.37	19.63	47.94	263.04	0.00608	0.479882
3	68.95	33.44	80.15	362.32	0.00653	0.108102
4	103.42	50.50	120.33	488.10	0.00734	0.125021
5	137.90	66.93	160.31	622.47	0.00772	0.179857
6	20.68	20.07	27.39	213.21	0.00907	0.770416
7	41.37	40.82	55.01	262.10	0.01146	0.259598
8	68.95	67.49	91.50	329.86	0.01439	0.061368
9	103.42	101.38	137.29	456.10	0.01581	0.137482
10	137.90	135.05	183.02	583.14	0.01661	0.176876
11	20.68	40.95	34.35	221.26	0.01481	0.448084
12	41.37	81.01	68.40	258.44	0.02213	0.094699
13	68.95	135.22	114.07	327.20	0.02908	0.066052
14	103.42	202.82	171.11	481.13	0.02998	0.139125
15	137.90	269.83	227.94	565.14	0.01102	0.143395
16	20.68	60.94	41.01	217.12	0.02080	0.279243
17	41.37	121.56	81.92	261.24	0.03277	0.074336
18	68.95	203.05	136.68	327.47	0.02363	0.064306
19	103.42	304.02	204.84	405.21	0.01506	0.233794
20	137.90	405.02	273.01	477.96	0.01755	0.241393
21	20.68	101.42	54.51	172.16	0.02221	0.439441
22	41.37	202.72	108.97	239.13	0.01778	0.244702
23	68.95	337.65	181.55	316.74	0.01706	0.18675
24	103.42	506.96	272.49	386.09	0.02943	0.261206
25	137.90	675.20	363.07	454.41	0.03300	0.258763
26	20.68	141.84	67.98	173.70	0.02158	0.307809
27	41.37	284.10	136.10	243.50	0.02020	0.201794
28	68.95	473.23	226.74	327.83	0.02548	0.205965
29	103.42	708.09	339.53	384.46	0.04336	0.274362
30	137.90	940.93	451.64	439.71	0.04475	0.243764

Table A21. Confining, deviator, and mean stresses, resilient modulus (M_R), rotation, and homogeneous deformation coefficient (HDC) during resilient modulus measurement of 15% Fly Ash +25% RAP + 60% Aggregate mixture at 10.3 % moisture content and 1.867 g/cm^3 dry density.

Sq	Confining kPa	Deviator kPa	Mean Stress kPa	M_R MPa	Rotation θ(°)	HDC α
1	20.68	9.93	24.00	46.33	0.01540	0.17763
2	41.37	19.18	47.79	93.21	0.01448	0.073292
3	68.95	33.48	80.16	161.58	0.01455	0.045841
4	103.42	49.87	120.12	235.77	0.00152	0.084372
5	137.90	66.59	160.20	314.90	0.00214	0.123113
6	20.68	19.64	27.25	39.74	0.03493	0.10456
7	41.37	39.77	54.66	82.98	0.03365	0.034869
8	68.95	66.56	91.19	141.96	0.00922	0.025727
9	103.42	99.88	136.79	214.74	0.00350	0.08672
10	137.90	133.49	182.50	300.39	0.00381	0.096678
11	20.68	39.52	33.87	41.17	0.06754	0.063537
12	41.37	80.00	68.07	83.76	0.03001	0.026657
13	68.95	133.56	113.52	149.03	0.00455	0.058474
14	103.42	200.37	170.29	233.99	0.00526	0.072094
15	137.90	267.74	227.25	301.66	0.00570	0.074612
16	20.68	59.65	40.58	44.91	0.04972	0.032473
17	41.37	120.05	81.42	88.83	0.00362	0.031901
18	68.95	200.69	135.90	156.40	0.00539	0.049821
19	103.42	300.10	203.53	229.69	0.00573	0.051446
20	137.90	400.22	271.41	293.46	0.00619	0.053528
21	20.68	99.94	54.01	54.36	0.00145	0.012294
22	41.37	201.00	108.40	102.71	0.00460	0.028986
23	68.95	334.29	180.43	172.55	0.00511	0.031622
24	103.42	500.87	270.46	244.07	0.00496	0.028621
25	137.90	666.67	360.22	306.13	0.00530	0.027959
26	20.68	140.23	67.44	63.23	0.00518	0.025339
27	41.37	281.15	135.12	118.53	0.00711	0.033526
28	68.95	468.06	225.02	193.52	0.00908	0.042579
29	103.42	699.91	336.80	261.48	0.01789	0.076205
30	137.90	927.22	447.07	309.31	0.03916	0.149341

Table A22. Confining, deviator, and mean stresses, resilient modulus (M_R), rotation, and homogeneous deformation coefficient (HDC) during resilient modulus measurement of 15% Fly Ash +25% RAP + 60% Aggregate mixture at 8.7 % moisture content and 1.86 g/cm^3 dry density.

Sq	Confining kPa	Deviator kPa	Mean Stress kPa	M_R MPa	Rotation θ(°)	HDC α
1	20.68	10.08	24.04	79.33	0.01717	1.343343
2	41.37	19.57	47.92	185.98	0.00902	0.574475
3	68.95	33.70	80.23	242.12	0.00434	0.369239
4	103.42	50.53	120.34	342.26	0.00429	0.339203
5	137.90	67.32	160.44	434.81	0.00408	0.308813
6	20.68	20.17	27.42	51.71	0.02722	0.022609
7	41.37	40.56	54.92	164.25	0.01750	0.491638
8	68.95	67.51	91.50	213.58	0.01039	0.383189
9	103.42	101.48	137.33	308.37	0.00928	0.328624
10	137.90	135.88	183.29	418.65	0.00766	0.275072
11	20.68	40.89	34.33	111.51	0.03544	0.892428
12	41.37	81.37	68.52	155.70	0.01798	0.394852
13	68.95	135.25	114.08	219.85	0.01717	0.324966
14	103.42	202.96	171.15	333.15	0.01337	0.255728
15	137.90	271.21	228.40	415.31	0.01295	0.230931
16	20.68	61.03	41.04	115.65	0.03089	0.679486
17	41.37	121.71	81.97	160.80	0.03085	0.337519
18	68.95	203.10	136.70	226.11	0.02294	0.297422
19	103.42	304.61	205.04	320.27	0.01698	0.208098
20	137.90	405.94	273.31	379.78	0.01694	0.184679
21	20.68	101.48	54.53	98.06	0.05618	0.63212
22	41.37	203.44	109.21	151.19	0.04106	0.355407
23	68.95	339.00	182.00	239.53	0.02559	0.210704
24	103.42	507.93	272.81	309.77	0.02488	0.176848
25	137.90	677.21	363.74	376.37	0.02425	0.157147
26	20.68	142.34	68.15	106.90	0.04227	0.369779
27	41.37	284.66	136.29	157.92	0.03060	0.197855
28	68.95	475.11	227.37	237.25	0.02679	0.155956
29	103.42	711.92	340.81	323.24	0.02350	0.124487
30	137.90	945.79	453.26	387.33	0.01972	0.094403

Table A23. Confining, deviator, and mean stresses, resilient modulus (M_R), rotation, and homogeneous deformation coefficient (HDC) during resilient modulus measurement of 5% Fly Ash +50% RAP + 45% Aggregate mixture at 7.8 % moisture content and 2.042 g/cm^3 dry density.

Sq	Confining kPa	Deviator kPa	Mean Stress kPa	M_R MPa	Rotation θ(°)	HDC α
1	20.68	9.81	23.96	63.20	0.00133	0.104289
2	41.37	19.18	47.79	142.46	0.00155	0.140547
3	68.95	33.39	80.13	243.29	0.00189	0.16106
4	103.42	50.15	120.22	366.66	0.00164	0.13581
5	137.90	67.24	160.41	489.06	0.00194	0.165558
6	20.68	19.81	27.30	54.14	0.00278	0.093468
7	41.37	40.15	54.78	130.24	0.00314	0.123204
8	68.95	66.88	91.29	235.73	0.00294	0.124687
9	103.42	100.24	136.91	357.60	0.00331	0.136158
10	137.90	134.06	182.69	468.21	0.00251	0.10156
11	20.68	39.96	34.02	59.16	0.00520	0.091423
12	41.37	80.06	68.09	131.72	0.00536	0.102357
13	68.95	133.74	113.58	249.37	0.00481	0.104445
14	103.42	200.97	170.49	365.59	0.00515	0.109315
15	137.90	267.61	227.20	456.03	0.00507	0.098761
16	20.68	60.13	40.74	65.15	0.00443	0.057928
17	41.37	120.30	81.50	144.96	0.00412	0.058862
18	68.95	201.16	136.05	253.55	0.00428	0.061708
19	103.42	301.50	204.00	358.95	0.00462	0.063255
20	137.90	401.08	271.69	441.54	0.00492	0.062186
21	20.68	99.98	54.03	78.77	0.00290	0.031559
22	41.37	200.95	108.38	165.41	0.00419	0.038558
23	68.95	335.04	180.68	265.64	0.00643	0.058181
24	103.42	501.97	270.82	367.02	0.00998	0.08329
25	137.90	667.90	360.63	451.11	0.01445	0.112939
26	20.68	140.42	67.51	90.72	0.00731	0.050654
27	41.37	281.68	135.29	187.38	0.01117	0.083612
28	68.95	468.38	225.13	291.30	0.01734	0.122203
29	103.42	699.08	336.53	375.91	0.02872	0.177377
30	137.90	925.50	446.50	443.18	0.04124	0.228895

Table A24. Confining, deviator, and mean stresses, resilient modulus (M_R), rotation, and homogeneous deformation coefficient (HDC) during resilient modulus measurement of 5% Fly Ash +50% RAP + 45% Aggregate mixture at 5.2 % moisture content and 2.012 g/cm^3 dry density.

Sq	Confining kPa	Deviator kPa	Mean Stress kPa	M_R MPa	Rotation θ(°)	HDC α
1	20.68	10.43	24.16	1342.13	0.00033	
2	41.37	19.69	47.96	379.75	0.00366	0.044296
3	68.95	33.78	80.26	564.06	0.00421	0.03071
4	103.42	50.86	120.45	701.35	0.00510	0.062714
5	137.90	67.45	160.48	805.08	0.00589	0.030177
6	20.68	20.32	27.47	291.42	0.00491	0.07636
7	41.37	40.59	54.93	334.81	0.00851	0.013389
8	68.95	67.47	91.49	484.95	0.00976	0.002572
9	103.42	101.75	137.42	618.70	0.01155	0.033174
10	137.90	136.03	183.34	741.01	0.01288	0.012738
11	20.68	40.63	34.24	281.68	0.01012	0.00839
12	41.37	81.16	68.45	328.01	0.01736	0.008815
13	68.95	136.01	114.34	463.67	0.02058	0.014185
14	103.42	204.77	171.76	602.85	0.02160	0.007572
15	137.90	271.16	228.39	675.54	0.02787	0.012704
16	20.68	61.24	41.11	247.19	0.01738	0.008782
17	41.37	121.63	81.94	295.86	0.02781	0.004882
18	68.95	203.33	136.78	414.27	0.03196	0.008634
19	103.42	304.73	205.08	555.29	0.02602	0.022396
20	137.90	406.16	273.39	586.37	0.01263	0.21276
21	20.68	101.39	54.50	238.46	0.02982	0.009096
22	41.37	203.06	109.09	307.51	0.00602	0.035826
23	68.95	338.00	181.67	380.47	0.01729	0.227262
24	103.42	507.34	272.61	486.67	0.02016	0.225959
25	137.90	675.37	363.12	563.30	0.02509	0.244064
26	20.68	141.60	67.90	206.83	0.01822	0.309951
27	41.37	283.89	136.03	277.03	0.02449	0.278515
28	68.95	473.87	226.96	383.41	0.02814	0.265486
29	103.42	709.15	339.88	481.26	0.03449	0.272795
30	137.90	941.97	451.99	545.02	0.04542	0.306327

Table A25. Confining, deviator, and mean stresses, resilient modulus (M_R), rotation, and homogeneous deformation coefficient (HDC) during resilient modulus measurement of 15% Fly Ash +50% RAP + 35% Aggregate mixture at 8.2 % moisture content and 1.89 g/cm^3 dry density.

Sq	Confining kPa	Deviator kPa	Mean Stress kPa	M_R MPa	Rotation θ(°)	HDC α
1	20.68	9.89	23.98	54.06	0.00420	0.264868
2	41.37	19.47	47.89	101.66	0.00466	0.280394
3	68.95	33.80	80.27	172.54	0.00403	0.218502
4	103.42	51.00	120.50	265.78	0.00315	0.180661
5	137.90	67.98	160.66	361.76	0.00447	0.272235
6	20.68	20.05	27.38	49.64	0.00992	0.285833
7	41.37	40.53	54.91	78.18	0.00908	0.206234
8	68.95	67.98	91.66	151.48	0.00806	0.19785
9	103.42	102.23	137.58	247.07	0.00733	0.201133
10	137.90	135.90	183.30	336.86	0.00885	0.253615
11	20.68	40.27	34.12	50.83	0.01467	0.213144
12	41.37	81.26	68.49	81.74	0.01386	0.162396
13	68.95	135.91	114.30	158.16	0.01289	0.173279
14	103.42	203.66	171.39	257.06	0.01183	0.167968
15	137.90	271.50	228.50	339.70	0.01043	0.151626
16	20.68	61.01	41.04	56.54	0.01357	0.144621
17	41.37	121.90	82.03	91.63	0.01360	0.117198
18	68.95	203.36	136.79	166.46	0.01143	0.105275
19	103.42	305.05	205.18	261.25	0.01111	0.111461
20	137.90	405.81	273.27	332.44	0.01179	0.109384
21	20.68	101.25	54.45	66.04	0.01228	0.090977
22	41.37	202.76	108.99	114.21	0.01564	0.099712
23	68.95	338.56	181.85	191.50	0.01375	0.089262
24	103.42	507.31	272.60	275.98	0.01358	0.084472
25	137.90	674.48	362.83	342.94	0.01246	0.073736
26	20.68	141.95	68.02	77.50	0.01075	0.065125
27	41.37	282.27	135.49	138.65	0.02863	0.162314
28	68.95	473.70	226.90	215.52	0.01354	0.070923
29	103.42	707.84	339.45	294.62	0.01624	0.079538
30	137.90	940.55	451.52	347.86	0.02407	0.104745

Table A26. Confining, deviator, and mean stresses, resilient modulus (M_R), rotation, and homogeneous deformation coefficient (HDC) during resilient modulus measurement of 15% Fly Ash +50% RAP + 35% Aggregate mixture at 6.9 % moisture content and 1.836 g/cm^3 dry density.

Sq	Confining kPa	Deviator kPa	Mean Stress kPa	M_R MPa	Rotation θ(°)	HDC α
1	20.68	10.16	24.07	93.82	0.00123	0.134808
2	41.37	19.58	47.93	126.60	0.00200	0.153017
3	68.95	33.71	80.24	236.00	0.00197	0.163264
4	103.42	50.44	120.31	343.81	0.00182	0.145982
5	137.90	67.40	160.47	454.61	0.00239	0.192444
6	20.68	20.08	27.39	87.29	0.00256	0.130468
7	41.37	40.23	54.81	110.55	0.00512	0.163819
8	68.95	67.28	91.43	206.50	0.00402	0.145265
9	103.42	101.37	137.29	315.50	0.00410	0.152644
10	137.90	135.60	183.20	422.63	0.00434	0.158067
11	20.68	40.81	34.30	87.92	0.00546	0.137284
12	41.37	81.44	68.55	121.82	0.00971	0.169787
13	68.95	135.48	114.16	211.24	0.00882	0.160257
14	103.42	203.08	171.19	328.04	0.00823	0.155216
15	137.90	270.99	228.33	413.17	0.00957	0.169981
16	20.68	60.82	40.97	90.66	0.00803	0.139852
17	41.37	121.44	81.88	132.67	0.01233	0.15696
18	68.95	202.84	136.61	213.64	0.01265	0.155388
19	103.42	304.56	205.02	313.13	0.01356	0.162606
20	137.90	405.77	273.26	381.92	0.01639	0.179914
21	20.68	101.12	54.41	98.36	0.01194	0.135249
22	41.37	202.93	109.04	150.87	0.01830	0.158742
23	68.95	338.06	181.69	227.08	0.02044	0.160418
24	103.42	507.06	272.52	305.72	0.02763	0.194192
25	137.90	675.81	363.27	369.71	0.03778	0.240902
26	20.68	141.35	67.82	100.75	0.02080	0.173235
27	41.37	283.69	135.96	156.89	0.03170	0.20448
28	68.95	473.52	226.84	235.61	0.03985	0.231158
29	103.42	709.06	339.85	310.03	0.05474	0.278864
30	137.90	942.65	452.22	357.12	0.07596	0.335275

Table A27. Confining, deviator, and mean stresses, resilient modulus (M_R), rotation, and homogeneous deformation coefficient (HDC) during resilient modulus measurement of 5% Fly Ash +75% RAP + 20% Aggregate mixture at 6.4 % moisture content and 2.05 g/cm^3 dry density.

Sq	Confining kPa	Deviator kPa	Mean Stress kPa	M_R MPa	Rotation θ(°)	HDC α
1	20.68	9.79	23.95	68.48	0.01053	0.275866
2	41.37	19.17	47.79	126.20	0.00763	0.587778
3	68.95	33.25	80.08	260.68	0.00262	0.241786
4	103.42	50.07	120.19	401.99	0.00201	0.21054
5	137.90	66.68	160.23	524.67	0.00186	0.184832
6	20.68	19.63	27.24	47.26	0.03170	0.881613
7	41.37	40.19	54.80	118.70	0.01738	0.590669
8	68.95	67.01	91.34	252.71	0.00859	0.377462
9	103.42	101.22	137.24	401.14	0.00474	0.219143
10	137.90	135.11	183.04	506.97	0.00489	0.223505
11	20.68	39.90	34.00	56.86	0.04595	0.756713
12	41.37	80.58	68.26	137.35	0.02407	0.473626
13	68.95	134.56	113.85	269.20	0.01124	0.259001
14	103.42	203.27	171.26	395.62	0.00810	0.183955
15	137.90	270.59	228.20	496.47	0.00624	0.128758
16	20.68	60.50	40.87	68.41	0.04076	0.533457
17	41.37	121.29	81.83	154.10	0.01859	0.27324
18	68.95	202.57	136.52	274.80	0.01029	0.159604
19	103.42	303.71	204.74	395.84	0.00791	0.117678
20	137.90	405.07	273.02	487.50	0.00637	0.089202
21	20.68	100.64	54.25	87.12	0.03021	0.302728
22	41.37	201.90	108.70	180.19	0.01503	0.154182
23	68.95	338.09	181.70	293.43	0.00801	0.080662
24	103.42	504.97	271.82	398.32	0.00544	0.05446
25	137.90	672.86	362.29	484.33	0.00842	0.07593
26	20.68	141.29	67.80	100.30	0.01704	0.145003
27	41.37	282.75	135.65	205.12	0.01040	0.092389
28	68.95	471.85	226.28	309.24	0.01312	0.107693
29	103.42	705.50	338.67	390.97	0.02333	0.153917
30	137.90	936.00	450.00	462.55	0.03175	0.187723

Table A28. Confining, deviator, and mean stresses, resilient modulus (M_R), rotation, and homogeneous deformation coefficient (HDC) during resilient modulus measurement of 5% Fly Ash +75% RAP + 20% Aggregate mixture at 3.8 % moisture content and 1.978 g/cm^3 dry density.

Sq	Confining kPa	Deviator kPa	Mean Stress kPa	M_R MPa	Rotation θ(°)	HDC α
1	20.68	10.12	24.06	128.59	0.00787	1.163814
2	41.37	19.21	47.80	171.06	0.00652	0.071015
3	68.95	33.19	80.06	411.87	0.00239	0.346585
4	103.42	50.08	120.19	608.98	0.00210	0.304139
5	137.90	66.93	160.31	763.07	0.00197	0.263789
6	20.68	20.21	27.44	117.42	0.01153	0.045331
7	41.37	40.08	54.76	249.16	0.00914	0.662373
8	68.95	66.88	91.29	399.43	0.00531	0.371711
9	103.42	101.15	137.22	595.58	0.00431	0.295882
10	137.90	134.33	182.78	746.89	0.00418	0.270663
11	20.68	40.45	34.18	198.26	0.01718	0.980575
12	41.37	81.01	68.40	275.58	0.01391	0.551037
13	68.95	134.67	113.89	399.60	0.00972	0.336694
14	103.42	202.27	170.92	597.01	0.00759	0.264198
15	137.90	269.89	227.96	726.03	0.00767	0.240725
16	20.68	60.88	40.99	208.20	0.02038	0.811989
17	41.37	121.25	81.82	292.37	0.01660	0.467501
18	68.95	201.94	136.31	416.75	0.01334	0.321571
19	103.42	302.93	204.48	597.88	0.01003	0.230632
20	137.90	403.64	272.55	720.87	0.00919	0.191456
21	20.68	101.47	54.52	230.07	0.02280	0.601886
22	41.37	202.11	108.77	330.34	0.02086	0.397548
23	68.95	337.12	181.37	449.88	0.01550	0.242571
24	103.42	505.55	272.02	614.73	0.01193	0.170028
25	137.90	671.31	361.77	726.23	0.01089	0.138062
26	20.68	141.56	67.89	250.79	0.02012	0.415667
27	41.37	282.49	135.56	351.95	0.01853	0.269511
28	68.95	470.72	225.91	486.69	0.01450	0.17591
29	103.42	705.53	338.68	645.72	0.00723	0.080261
30	137.90	937.42	450.47	741.02	0.00515	0.052237

Table A29. Confining, deviator, and mean stresses, resilient modulus (M_R), rotation, and homogeneous deformation coefficient (HDC) during resilient modulus measurement of 15% Fly Ash +75% RAP + 10% Aggregate mixture at 7.4 % moisture content and 1.892 g/cm^3 dry density.

Sq	Confining kPa	Deviator kPa	Mean Stress kPa	M_R MPa	Rotation θ(°)	HDC α
1	20.68	10.19	24.08	105.04	0.00107	0.126238
2	41.37	19.41	47.87	171.15	0.00137	0.14347
3	68.95	33.37	80.12	276.92	0.00147	0.156124
4	103.42	49.87	120.12	394.61	0.00149	0.134928
5	137.90	66.81	160.27	512.57	0.00203	0.184314
6	20.68	20.10	27.40	78.77	0.00214	0.099832
7	41.37	39.90	54.70	148.37	0.00299	0.133416
8	68.95	66.67	91.22	255.95	0.00257	0.117987
9	103.42	100.35	136.95	373.28	0.00294	0.134814
10	137.90	133.22	182.41	482.96	0.00303	0.118852
11	20.68	39.67	33.92	71.36	0.00524	0.103642
12	41.37	79.87	68.02	152.73	0.00556	0.116327
13	68.95	134.23	113.74	265.67	0.00405	0.092627
14	103.42	200.43	170.31	386.36	0.00402	0.092412
15	137.90	267.56	227.19	464.07	0.00462	0.089806
16	20.68	59.99	40.70	73.11	0.00772	0.109234
17	41.37	120.02	81.41	157.11	0.00550	0.077865
18	68.95	200.85	135.95	268.72	0.00458	0.067934
19	103.42	300.48	203.66	369.61	0.00547	0.075411
20	137.90	400.53	271.51	439.46	0.00558	0.070053
21	20.68	100.05	54.05	85.17	0.00891	0.084887
22	41.37	200.52	108.24	172.59	0.00607	0.057754
23	68.95	333.71	180.24	279.17	0.00552	0.050537
24	103.42	499.90	270.13	363.54	0.00562	0.044899
25	137.90	663.91	359.30	430.43	0.00440	0.032266
26	20.68	139.94	67.35	96.44	0.00990	0.07494
27	41.37	280.47	134.89	180.85	0.00555	0.041235
28	68.95	466.47	224.49	290.31	0.00406	0.028244
29	103.42	695.79	335.43	380.01	0.00261	0.017406
30	137.90	923.50	445.83	447.32	0.00652	0.039549

Table A30. Confining, deviator, and mean stresses, resilient modulus (M_R), rotation, and homogeneous deformation coefficient (HDC) during resilient modulus measurement of 15% Fly Ash +75% RAP + 10% Aggregate mixture at 7.1 % moisture content and 1.883 g/cm^3 dry density.

Sq	Confining kPa	Deviator kPa	Mean Stress kPa	M_R MPa	Rotation θ(°)	HDC α
1	20.68	9.41	23.82	46.33	0.01139	0.652904
2	41.37	18.92	47.71	89.27	0.00786	0.431727
3	68.95	33.10	80.03	198.88	0.00484	0.338419
4	103.42	49.70	120.07	311.93	0.00222	0.166233
5	137.90	66.57	160.19	448.70	0.00083	0.066476
6	20.68	19.36	27.15	45.41	0.01760	0.481103
7	41.37	39.60	54.60	75.16	0.01802	0.398596
8	68.95	66.51	91.17	176.51	0.00912	0.282282
9	103.42	99.57	136.69	305.75	0.00550	0.199059
10	137.90	133.24	182.41	435.06	0.00429	0.164318
11	20.68	39.70	33.93	53.47	0.02563	0.402493
12	41.37	79.82	68.01	92.19	0.02646	0.355961
13	68.95	133.40	113.47	197.48	0.01779	0.306835
14	103.42	200.47	170.32	323.57	0.01280	0.241268
15	137.90	266.81	226.94	412.11	0.01203	0.216691
16	20.68	59.87	40.66	60.93	0.03391	0.402035
17	41.37	120.03	81.41	106.60	0.03618	0.374459
18	68.95	200.81	135.94	200.63	0.02924	0.340492
19	103.42	300.49	203.66	308.54	0.02426	0.29096
20	137.90	400.61	271.54	385.27	0.02291	0.257142
21	20.68	100.11	54.07	73.24	0.04799	0.409067
22	41.37	200.72	108.31	130.82	0.04962	0.376792
23	68.95	334.83	180.61	216.24	0.04820	0.362859
24	103.42	501.37	270.62	297.93	0.05305	0.367303
25	137.90	666.37	360.12	366.61	0.05472	0.350782
26	20.68	140.09	67.40	82.07	0.05857	0.399788
27	41.37	280.71	134.97	147.07	0.05766	0.352477
28	68.95	468.39	225.13	233.27	0.06484	0.376439
29	103.42	700.94	337.15	295.22	0.09494	0.465839
30	137.90	928.05	447.35	338.30	0.11094	0.471195

Table A31. Confining, deviator, and mean stresses, resilient modulus (M_R), rotation, and homogeneous deformation coefficient (HDC) during resilient modulus measurement of 25% RCM + 75% Aggregate mixture at 9.2 % moisture content and 1.996 g/cm^3 dry density.

Sq	Confining kPa	Deviator kPa	Mean Stress kPa	M_R MPa	Rotation θ(°)	HDC α
1	20.68	10.10	24.05	136.47	0.00693	0.720771
2	41.37	19.47	47.89	156.55	0.00974	0.403337
3	68.95	33.62	80.21	213.45	0.01143	0.217396
4	103.42	50.65	120.38	315.17	0.01167	0.216445
5	137.90	67.63	160.54	414.89	0.01167	0.164402
6	20.68	20.28	27.46	132.93	0.01336	0.609993
7	41.37	40.74	54.98	157.03	0.01958	0.32565
8	68.95	68.19	91.73	189.12	0.02644	0.25028
9	103.42	101.61	137.37	286.69	0.02555	0.193907
10	137.90	135.68	183.23	373.24	0.02600	0.163764
11	20.68	41.14	34.41	135.23	0.02530	0.520805
12	41.37	82.04	68.75	163.99	0.03753	0.31009
13	68.95	136.10	114.37	244.02	0.03911	0.010107
14	103.42	203.91	171.47	299.14	0.04846	0.135593
15	137.90	271.24	228.41	364.61	0.01729	0.119657
16	20.68	61.62	41.24	135.51	0.03527	0.385678
17	41.37	122.23	82.14	165.97	0.05349	0.219762
18	68.95	202.84	136.61	215.38	0.04849	0.144757
19	103.42	304.02	204.84	282.36	0.00848	0.092386
20	137.90	405.48	273.16	351.67	0.00858	0.086876
21	20.68	101.79	54.63	140.34	0.01632	0.246543
22	41.37	203.67	109.29	170.47	0.02164	0.211119
23	68.95	339.30	182.10	236.84	0.01204	0.098218
24	103.42	507.75	272.75	308.01	0.00650	0.046148
25	137.90	675.62	363.21	380.61	0.01305	0.085742
26	20.68	142.59	68.23	143.09	0.00811	0.094948
27	41.37	285.12	136.44	195.58	0.00694	0.05586
28	68.95	474.83	227.28	265.08	0.00790	0.051781
29	103.42	710.75	340.42	313.05	0.04662	0.239229
30	137.90	935.71	449.90	382.60	0.02600	0.12436

Table A32. Confining, deviator, and mean stresses, resilient modulus (M_R), rotation, and homogeneous deformation coefficient (HDC) during resilient modulus measurement of 25% RCM + 75% Aggregate mixture at 7.8 % moisture content and 2.014 g/cm^3 dry density.

Sq	Confining kPa	Deviator kPa	Mean Stress kPa	M_R MPa	Rotation θ(°)	HDC α
1	20.68	10.10	24.05	136.47	0.00693	0.720771
2	41.37	19.47	47.89	156.55	0.00974	0.403337
3	68.95	33.62	80.21	213.45	0.01143	0.217396
4	103.42	50.65	120.38	315.17	0.01167	0.216445
5	137.90	67.63	160.54	414.89	0.01167	0.164402
6	20.68	20.28	27.46	132.93	0.01336	0.609993
7	41.37	40.74	54.98	157.03	0.01958	0.32565
8	68.95	68.19	91.73	189.12	0.02644	0.25028
9	103.42	101.61	137.37	286.69	0.02555	0.193907
10	137.90	135.68	183.23	373.24	0.02600	0.163764
11	20.68	41.14	34.41	135.23	0.02530	0.520805
12	41.37	82.04	68.75	163.99	0.03753	0.31009
13	68.95	136.10	114.37	244.02	0.03911	0.010107
14	103.42	203.91	171.47	299.14	0.04846	0.135593
15	137.90	271.24	228.41	364.61	0.01729	0.119657
16	20.68	61.62	41.24	135.51	0.03527	0.385678
17	41.37	122.23	82.14	165.97	0.05349	0.219762
18	68.95	202.84	136.61	215.38	0.04849	0.144757
19	103.42	304.02	204.84	282.36	0.00848	0.092386
20	137.90	405.48	273.16	351.67	0.00858	0.086876
21	20.68	101.79	54.63	140.34	0.01632	0.246543
22	41.37	203.67	109.29	170.47	0.02164	0.211119
23	68.95	339.30	182.10	236.84	0.01204	0.098218
24	103.42	507.75	272.75	308.01	0.00650	0.046148
25	137.90	675.62	363.21	380.61	0.01305	0.085742
26	20.68	142.59	68.23	143.09	0.00811	0.094948
27	41.37	285.12	136.44	195.58	0.00694	0.05586
28	68.95	474.83	227.28	265.08	0.00790	0.051781
29	103.42	710.75	340.42	313.05	0.04662	0.239229
30	137.90	935.71	449.90	382.60	0.02600	0.12436

Table A33. Confining, deviator, and mean stresses, resilient modulus (M_R), rotation, and homogeneous deformation coefficient (HDC) during resilient modulus measurement of 50% RCM + 50% Aggregate mixture at 9.7 % moisture content and 1.951 g/cm^3 dry density.

Sq	Confining kPa	Deviator kPa	Mean Stress kPa	M_R MPa	Rotation θ(°)	HDC α
1	20.68	9.97	24.01	84.80	0.00848	0.091556
2	41.37	19.46	47.89	135.45	0.01029	0.031529
3	68.95	33.45	80.15	246.77	0.00239	0.201203
4	103.42	50.56	120.35	345.15	0.00026	0.020299
5	137.90	67.21	160.40	441.89	0.00182	0.136322
6	20.68	19.71	27.27	62.22	0.02334	0.200683
7	41.37	40.24	54.81	130.44	0.00953	0.119951
8	68.95	67.22	91.41	202.89	0.00709	0.244161
9	103.42	101.39	137.30	304.51	0.00673	0.230792
10	137.90	135.36	183.12	398.05	0.00745	0.250059
11	20.68	40.73	34.28	59.70	0.02701	0.357448
12	41.37	81.44	68.55	110.49	0.01444	0.223606
13	68.95	135.38	114.13	201.18	0.01166	0.197896
14	103.42	203.43	171.31	301.47	0.01050	0.177854
15	137.90	271.10	228.37	389.85	0.01031	0.169259
16	20.68	60.76	40.95	60.95	0.02107	0.24117
17	41.37	121.87	82.02	116.52	0.01370	0.149528
18	68.95	203.39	136.80	202.77	0.01150	0.130828
19	103.42	305.18	205.23	300.11	0.01218	0.136699
20	137.90	406.23	273.41	383.50	0.01210	0.130338
21	20.68	102.06	54.72	95.60	0.01358	0.1452
22	41.37	203.38	109.19	176.69	0.01449	0.14366
23	68.95	338.24	181.75	277.50	0.01208	0.113139
24	103.42	508.19	272.90	364.84	0.01172	0.09605
25	137.90	677.07	363.69	438.75	0.01373	0.101536
26	20.68	142.12	68.07	100.24	0.01245	0.100249
27	41.37	284.62	136.27	187.15	0.01026	0.076984
28	68.95	474.04	227.01	276.92	0.01032	0.068829
29	103.42	709.54	340.01	331.41	0.01196	0.063768
30	137.90	939.94	451.31	399.54	0.00943	0.046619

Table A34. Confining, deviator, and mean stresses, resilient modulus (M_R), rotation, and homogeneous deformation coefficient (HDC) during resilient modulus measurement of 50% RCM + 50% Aggregate mixture at 7.8 % moisture content and 1.903 g/cm^3 dry density.

Sq	Confining kPa	Deviator kPa	Mean Stress kPa	M_R MPa	Rotation θ(°)	HDC α
1	20.68	10.33	24.13	131.50	0.00270	0.399587
2	41.37	19.65	47.95	210.45	0.00147	0.193078
3	68.95	34.19	80.40	285.90	0.00845	0.103577
4	103.42	50.93	120.48	414.67	0.00238	0.226988
5	137.90	67.84	160.61	538.94	0.00238	0.221546
6	20.68	20.47	27.52	117.30	0.00510	0.342101
7	41.37	40.90	55.03	180.57	0.00507	0.260726
8	68.95	68.19	91.73	280.28	0.00537	0.257423
9	103.42	101.98	137.49	396.11	0.00538	0.244216
10	137.90	136.28	183.43	509.03	0.00539	0.235256
11	20.68	40.93	34.34	115.88	0.00977	0.3221
12	41.37	81.71	68.64	182.45	0.01084	0.28186
13	68.95	135.91	114.30	292.55	0.01066	0.267232
14	103.42	204.12	171.54	422.35	0.01009	0.243397
15	137.90	272.09	228.70	507.41	0.01120	0.243335
16	20.68	61.45	41.18	122.47	0.01268	0.294493
17	41.37	122.40	82.20	188.13	0.01522	0.272702
18	68.95	204.57	137.19	301.82	0.01493	0.256799
19	103.42	305.60	205.37	408.34	0.01569	0.244182
20	137.90	407.02	273.67	497.06	0.01709	0.243101
21	20.68	102.01	54.70	138.14	0.01686	0.265949
22	41.37	203.79	109.33	210.55	0.02225	0.267774
23	68.95	339.67	182.22	291.75	0.08367	0.1832
24	103.42	509.38	273.29	409.75	0.02510	0.235182
25	137.90	676.60	363.53	496.74	0.02530	0.216341
26	20.68	142.60	68.23	151.18	0.02037	0.251649
27	41.37	285.51	136.57	235.33	0.02592	0.248889
28	68.95	475.89	227.63	323.50	0.02696	0.213558
29	103.42	710.56	340.35	394.34	0.02826	0.182667
30	137.90	944.41	452.80	452.67	0.02153	0.120372

Table A35. Confining, deviator, and mean stresses, resilient modulus (M_R), rotation, and homogeneous deformation coefficient (HDC) during resilient modulus measurement of 75% RCM + 25% Aggregate mixture at 9.3 % moisture content and 1.925 g/cm^3 dry density.

Sq	Confining kPa	Deviator kPa	Mean Stress kPa	M_R MPa	Rotation θ(°)	HDC α
1	20.68	9.91	23.99	51.36	0.00751	0.451987
2	41.37	19.34	47.85	72.80	0.00723	0.315658
3	68.95	33.78	80.26	141.79	0.00566	0.27609
4	103.42	50.50	120.33	265.35	0.00449	0.280926
5	137.90	67.78	160.59	392.12	0.00355	0.249866
6	20.68	19.80	27.30	50.18	0.01200	0.354321
7	41.37	40.48	54.89	83.61	0.01169	0.281585
8	68.95	67.45	91.48	139.44	0.00934	0.223107
9	103.42	101.38	137.29	249.42	0.00753	0.2153
10	137.90	135.27	183.09	369.32	0.00634	0.200302
11	20.68	40.38	34.16	60.69	0.01830	0.31908
12	41.37	81.19	68.46	110.62	0.01542	0.243873
13	68.95	135.07	114.02	171.80	0.01450	0.214694
14	103.42	203.45	171.32	272.98	0.01146	0.179126
15	137.90	270.46	228.15	368.88	0.01102	0.174735
16	20.68	60.80	40.97	68.40	0.01661	0.218001
17	41.37	121.19	81.80	156.68	0.01105	0.165514
18	68.95	201.83	136.28	275.00	0.01015	0.162357
19	103.42	303.05	204.52	398.55	0.01029	0.160237
20	137.90	403.07	272.36	487.61	0.01194	0.165145
21	20.68	101.10	54.40	89.40	0.02156	0.222718
22	41.37	201.94	108.71	170.44	0.01737	0.171645
23	68.95	335.98	180.99	271.59	0.01362	0.12735
24	103.42	503.45	271.32	378.64	0.01437	0.126817
25	137.90	669.24	361.08	470.45	0.01613	0.130859
26	20.68	141.33	67.81	100.33	0.02010	0.165672
27	41.37	282.96	135.72	188.18	0.01460	0.113181
28	68.95	469.47	225.49	278.79	0.01531	0.105335
29	103.42	701.94	337.48	359.10	0.01909	0.112573
30	137.90	931.60	448.53	436.92	0.01933	0.105481

Table A36. Confining, deviator, and mean stresses, resilient modulus (M_R), rotation, and homogeneous deformation coefficient (HDC) during resilient modulus measurement of 75% RCM + 25% Aggregate mixture at 8.2 % moisture content and 1.906 g/cm^3 dry density.

Sq	Confining kPa	Deviator kPa	Mean Stress kPa	M_R MPa	Rotation θ(°)	HDC α
1	20.68	10.20	24.08	175.23	0.00270	0.543508
2	41.37	19.37	47.86	282.54	0.00101	0.183189
3	68.95	33.64	80.21	400.26	0.00130	0.184732
4	103.42	50.49	120.33	525.68	0.00100	0.142741
5	137.90	66.94	160.31	686.78	0.00088	0.115915
6	20.68	20.29	27.46	125.39	0.00334	0.453891
7	41.37	40.52	54.91	251.32	0.00061	0.056097
8	68.95	67.20	91.40	361.52	0.00076	0.056465
9	103.42	100.90	137.13	498.57	0.00124	0.075186
10	137.90	134.66	182.89	655.04	0.00080	0.049816
11	20.68	40.44	34.18	148.90	0.00413	0.178124
12	41.37	80.74	68.31	238.27	0.00275	0.094933
13	68.95	134.72	113.91	368.84	0.00303	0.096839
14	103.42	201.84	170.78	517.01	0.00213	0.0655
15	137.90	269.21	227.74	612.12	0.00253	0.067287
16	20.68	60.91	41.00	151.27	0.00525	0.152771
17	41.37	121.24	81.81	241.58	0.00461	0.107034
18	68.95	202.51	136.50	362.54	0.03924	0.048906
19	103.42	301.99	204.16	493.29	0.00411	0.078326
20	137.90	406.27	273.42	583.13	0.00490	0.083546
21	20.68	101.92	54.67	162.42	0.00859	0.160391
22	41.37	203.80	109.33	259.25	0.00926	0.137323
23	68.95	338.78	181.93	386.69	0.00820	0.109322
24	103.42	508.29	272.93	501.78	0.00810	0.093111
25	137.90	676.56	363.52	600.04	0.00889	0.096358
26	20.68	142.73	68.28	174.44	0.00875	0.124738
27	41.37	285.20	136.47	277.32	0.01123	0.127311
28	68.95	475.31	227.44	412.07	0.01018	0.102967
29	103.42	708.95	339.82	530.01	0.01026	0.089369
30	137.90	942.88	452.29	618.36	0.01246	0.095258

Table A37. Confining, deviator, and mean stresses, resilient modulus (M_R), rotation, and homogeneous deformation coefficient (HDC) during resilient modulus measurement of 100% RCM at 9.4 % moisture content and 1.907 g/cm^3 dry density.

Sq	Confining kPa	Deviator kPa	Mean Stress kPa	M_R MPa	Rotation θ(°)	HDC α
1	20.68	10.01	24.02	72.64	0.00997	0.202129
2	41.37	19.52	47.91	128.04	0.01070	0.038531
3	68.95	33.85	80.28	236.96	0.00285	0.254448
4	103.42	51.07	120.52	371.71	0.00228	0.202361
5	137.90	67.86	160.62	512.07	0.00211	0.204547
6	20.68	20.32	27.47	63.25	0.00979	0.355327
7	41.37	40.79	55.00	116.56	0.00827	0.27283
8	68.95	67.77	91.59	223.25	0.00486	0.176775
9	103.42	101.89	137.46	359.75	0.00351	0.131317
10	137.90	135.60	183.20	494.84	0.00317	0.136414
11	20.68	40.92	34.34	74.33	0.01599	0.336481
12	41.37	81.27	68.49	133.61	0.01228	0.232452
13	68.95	135.86	114.29	244.69	0.00848	0.180141
14	103.42	203.67	171.39	381.28	0.00558	0.11439
15	137.90	271.22	228.41	488.82	0.00512	0.107602
16	20.68	61.02	41.04	84.89	0.01706	0.265754
17	41.37	121.86	82.02	154.77	0.01273	0.189181
18	68.95	203.40	136.80	262.35	0.00832	0.124357
19	103.42	305.24	205.25	385.06	0.00603	0.088961
20	137.90	406.80	273.60	493.44	0.00534	0.072455
21	20.68	101.92	54.67	107.10	0.01625	0.194421
22	41.37	203.11	109.10	197.30	0.01198	0.135588
23	68.95	339.50	182.17	302.10	0.00488	0.050518
24	103.42	507.94	272.81	419.61	0.00656	0.064181
25	137.90	675.21	363.07	525.17	0.00935	0.084737
26	20.68	142.00	68.03	122.05	0.01002	0.099667
27	41.37	284.36	136.19	231.26	0.00723	0.068403
28	68.95	473.37	226.79	334.91	0.01882	0.156022
29	103.42	708.31	339.60	429.41	0.03532	0.249695
30	137.90	939.19	451.06	519.94	0.04234	0.274896

Table A38. Confining, deviator, and mean stresses, resilient modulus (M_R), rotation, and homogeneous deformation coefficient (HDC) during resilient modulus measurement of 100% RCM at 8.5 % moisture content and 1.900 g/cm^3 dry density.

Sq	Confining kPa	Deviator kPa	Mean Stress kPa	M_R MPa	Rotation θ(°)	HDC α
1	20.68	10.33	24.13	38.23	0.01820	0.007605
2	41.37	19.50	47.90	151.66	0.00066	0.069334
3	68.95	33.47	80.16	239.75	0.00129	0.116781
4	103.42	50.44	120.31	370.03	0.00072	0.065938
5	137.90	67.19	160.40	522.77	0.00028	0.025991
6	20.68	20.20	27.43	43.45	0.03124	22.3062
7	41.37	40.42	54.87	141.69	0.00750	0.306306
8	68.95	67.48	91.49	249.19	0.00425	0.183955
9	103.42	101.19	137.23	376.12	0.00356	0.155265
10	137.90	135.33	183.11	518.74	0.00310	0.140778
11	20.68	40.65	34.25	115.75	0.03767	1.249051
12	41.37	81.59	68.60	161.09	0.01792	0.412042
13	68.95	136.10	114.37	285.03	0.01149	0.280969
14	103.42	203.02	171.17	417.70	0.00906	0.217194
15	137.90	270.37	228.12	521.66	0.00921	0.207232
16	20.68	61.23	41.11	122.22	0.04102	0.953289
17	41.37	122.09	82.10	177.86	0.02519	0.427403
18	68.95	203.27	136.76	293.48	0.01769	0.297445
19	103.42	304.42	204.97	414.79	0.01484	0.235636
20	137.90	404.96	272.99	510.52	0.01364	0.200351
21	20.68	101.62	54.57	138.44	0.04173	0.66194
22	41.37	202.87	109.02	214.38	0.02822	0.347266
23	68.95	337.89	181.63	329.13	0.02445	0.277409
24	103.42	506.69	272.40	445.78	0.02125	0.217721
25	137.90	673.17	362.39	547.85	0.01842	0.175595
26	20.68	142.24	68.11	152.13	0.03613	0.450005
27	41.37	284.69	136.30	247.32	0.02779	0.281199
28	68.95	473.12	226.71	378.90	0.02223	0.20745
29	103.42	707.60	339.37	495.76	0.01609	0.131408
30	137.90	940.30	451.43	601.64	0.01086	0.081043

Table A39. Confining, deviator, and mean stresses, resilient modulus (M_R), rotation, and homogeneous deformation coefficient (HDC) during resilient modulus measurement of 5% Foundry Sand + 95% Aggregate mixture at 9.2 % moisture content and 2.007 g/cm^3 dry density.

Sq	Confining kPa	Deviator kPa	Mean Stress kPa	M_R MPa	Rotation θ(°)	HDC α
1	20.68	9.69	23.92	37.80	0.01115	0.50939
2	41.37	19.37	47.86	70.72	0.00773	0.329912
3	68.95	33.99	80.33	128.25	0.00546	0.241771
4	103.42	50.79	120.43	208.87	0.00478	0.229383
5	137.90	68.31	160.77	295.73	0.00439	0.223175
6	20.68	19.72	27.27	36.82	0.01759	0.382635
7	41.37	40.54	54.91	69.95	0.01320	0.265773
8	68.95	67.99	91.66	128.65	0.00964	0.212577
9	103.42	101.84	137.45	206.54	0.00776	0.184008
10	137.90	136.38	183.46	293.30	0.00642	0.160959
11	20.68	40.05	34.05	43.74	0.02531	0.32255
12	41.37	81.34	68.51	84.64	0.01949	0.236195
13	68.95	135.80	114.27	147.90	0.01474	0.18745
14	103.42	204.02	171.51	225.83	0.01162	0.14985
15	137.90	271.72	228.57	292.29	0.01085	0.136494
16	20.68	60.62	40.91	49.96	0.02950	0.283678
17	41.37	122.30	82.17	97.82	0.02198	0.204883
18	68.95	203.59	136.86	160.36	0.01813	0.166533
19	103.42	305.28	205.26	230.24	0.01561	0.137086
20	137.90	406.74	273.58	291.28	0.01430	0.119695
21	20.68	101.11	54.40	61.04	0.03472	0.244962
22	41.37	203.49	109.23	120.91	0.02279	0.158313
23	68.95	339.28	182.09	188.19	0.01972	0.127495
24	103.42	507.97	272.82	250.49	0.02157	0.123955
25	137.90	676.10	363.37	310.72	0.03201	0.171364
26	20.68	140.25	67.45	73.12	0.07678	0.476559
27	41.37	280.55	134.92	146.14	0.05595	0.346826
28	68.95	467.28	224.76	217.15	0.06417	0.354867
29	103.42	697.54	336.01	287.69	0.09823	0.482107
30	137.90	922.31	445.44	365.81	0.16590	0.800752

Table A40. Confining, deviator, and mean stresses, resilient modulus (M_R), rotation, and homogeneous deformation coefficient (HDC) during resilient modulus measurement of 5% Foundry Sand + 95% Aggregate mixture at 7.2 % moisture content and 2.093 g/cm^3 dry density.

Sq	Confining kPa	Deviator kPa	Mean Stress kPa	M_R MPa	Rotation θ(°)	HDC α
1	20.68	10.21	24.09	133.48	0.00151	0.240352
2	41.37	19.56	47.92	159.81	0.00149	0.149214
3	68.95	33.78	80.26	210.51	0.00036	0.039205
4	103.42	50.95	120.48	273.35	0.00047	0.03487
5	137.90	67.74	160.58	345.64	0.00055	0.034472
6	20.68	20.16	27.42	131.90	0.00245	0.189691
7	41.37	40.47	54.89	144.20	0.00157	0.067144
8	68.95	67.82	91.61	186.25	0.00079	0.031661
9	103.42	101.89	137.46	247.73	0.00158	0.045215
10	137.90	136.40	183.47	323.03	0.00135	0.039632
11	20.68	40.59	34.23	124.72	0.00208	0.077521
12	41.37	81.78	68.66	146.79	0.00224	0.051118
13	68.95	136.12	114.37	193.06	0.00202	0.033905
14	103.42	203.98	171.49	271.71	0.00284	0.046095
15	137.90	271.69	228.56	312.29	0.00326	0.04433
16	20.68	61.23	41.11	124.69	0.00250	0.059571
17	41.37	122.58	82.26	149.60	0.00460	0.065804
18	68.95	203.68	136.89	196.87	0.00568	0.064224
19	103.42	305.08	205.19	249.92	0.00669	0.063947
20	137.90	408.07	274.02	305.14	0.00788	0.069005
21	20.68	101.84	54.65	119.83	0.00867	0.119077
22	41.37	204.02	109.41	159.47	0.01039	0.094896
23	68.95	340.28	182.43	207.52	0.01762	0.125353
24	103.42	509.30	273.27	264.66	0.02320	0.140622
25	137.90	670.19	361.40	312.17	0.01921	0.106959
26	20.68	141.31	67.80	106.74	0.01465	0.132152
27	41.37	283.26	135.82	162.56	0.01670	0.114684
28	68.95	471.61	226.20	222.07	0.02187	0.123032

Table A41. Confining, deviator, and mean stresses, resilient modulus (M_R), rotation, and homogeneous deformation coefficient (HDC) during resilient modulus measurement of 10% Foundry Sand + 90% Aggregate mixture at 9.3 % moisture content and 2.067 g/cm^3 dry density.

Sq	Confining kPa	Deviator kPa	Mean Stress kPa	M_R MPa	Rotation θ(°)	HDC α
1	20.68	9.52	23.86	36.63	0.01338	0.035083
2	41.37	18.76	47.65	52.24	0.00161	0.054651
3	68.95	33.16	80.05	87.14	0.00122	0.045929
4	103.42	49.91	120.14	145.78	0.00198	0.069025
5	137.90	67.17	160.39	222.48	0.00254	0.099594
6	20.68	19.17	27.09	35.17	0.00308	0.068572
7	41.37	39.63	54.61	56.61	0.00346	0.059718
8	68.95	66.91	91.30	89.29	0.00362	0.058509
9	103.42	100.16	136.89	146.54	0.00430	0.073925
10	137.90	133.75	182.58	214.47	0.00454	0.085296
11	20.68	39.63	33.91	39.17	0.00470	0.057042
12	41.37	80.04	68.08	72.17	0.00562	0.060967
13	68.95	134.07	113.69	111.19	0.00514	0.050864
14	103.42	201.15	170.55	165.90	0.00668	0.06443
15	137.90	268.10	227.37	219.63	0.00700	0.067176
16	20.68	59.81	40.64	43.06	0.00657	0.059434
17	41.37	120.17	81.46	80.80	0.00710	0.057064
18	68.95	200.96	135.99	122.48	0.01198	0.085388
19	103.42	301.06	203.85	179.95	0.01363	0.095368
20	137.90	401.58	271.86	235.10	0.01542	0.10541
21	20.68	100.36	54.15	53.20	0.02214	0.138467
22	41.37	201.13	108.44	93.87	0.02484	0.136294
23	68.95	334.30	180.43	145.27	0.03080	0.159733
24	103.42	505.91	272.14	194.28	0.03085	0.141352
25	137.90	662.98	358.99	258.17	0.17366	1.005072
26	20.68	139.65	67.25	57.04	0.16558	1.009281
27	41.37	279.71	134.64	119.21	0.11010	0.313351

Table A42. Confining, deviator, and mean stresses, resilient modulus (M_R), rotation, and homogeneous deformation coefficient (HDC) during resilient modulus measurement of 10% Foundry Sand + 90% Aggregate mixture at 7.3 % moisture content and 2.083 g/cm^3 dry density.

Sq	Confining kPa	Deviator kPa	Mean Stress kPa	M_R MPa	Rotation θ(°)	HDC α
1	20.68	10.21	24.09	140.13	0.00445	0.074694
2	41.37	19.56	47.92	179.48	0.00768	0.084124
3	68.95	33.85	80.28	218.48	0.01088	0.054176
4	103.42	50.72	120.41	294.62	0.01213	0.077102
5	137.90	67.73	160.58	371.24	0.01283	0.055976
6	20.68	20.25	27.45	163.17	0.00903	0.221703
7	41.37	40.46	54.89	158.85	0.01787	0.025844
8	68.95	67.65	91.55	191.99	0.02474	0.040212
9	103.42	101.66	137.39	266.01	0.02683	0.037773
10	137.90	135.43	183.14	350.49	0.02712	0.031187
11	20.68	40.68	34.26	142.87	0.02010	0.097938
12	41.37	81.34	68.51	156.64	0.03643	0.023332
13	68.95	135.11	114.04	197.53	0.04798	0.022081
14	103.42	203.10	171.20	279.90	0.02481	0.021012
15	137.90	270.80	228.27	323.16	0.00352	0.049861
16	20.68	60.81	40.97	132.85	0.03210	0.01606
17	41.37	121.65	81.95	156.47	0.01505	0.036572
18	68.95	203.20	136.73	195.67	0.00841	0.095164
19	103.42	304.32	204.94	255.81	0.00593	0.059119
20	137.90	406.70	273.57	313.75	0.00608	0.054952
21	20.68	101.47	54.52	116.77	0.01337	0.179584
22	41.37	202.83	109.01	158.38	0.01183	0.108441
23	68.95	338.29	181.76	214.15	0.00749	0.056075
24	103.42	507.01	272.50	274.10	0.00782	0.050033
25	137.90	674.30	362.77	335.84	0.01187	0.069932
26	20.68	141.49	67.86	124.58	0.00722	0.075189
27	41.37	284.01	136.07	175.30	0.00687	0.050224
28	68.95	472.40	226.47	240.85	0.01178	0.07029
29	103.42	707.82	339.44	259.54	0.02670	0.117134

Table A43. Confining, deviator, and mean stresses, resilient modulus (M_R), rotation, and homogeneous deformation coefficient (HDC) during resilient modulus measurement of 15%Foundry Sand + 85% Aggregate mixture at 9.4 % moisture content and 2.075 g/cm^3 dry density.

Sq	Confining kPa	Deviator kPa	Mean Stress kPa	Mr MPa	Rotation θ(°)	HDC α
1	20.68	9.22	23.76	33.04	0.00615	0.261709
2	41.37	18.51	47.57	52.70	0.00466	0.157631
3	68.95	32.82	79.94	95.17	0.00346	0.119588
4	103.42	49.93	120.14	165.13	0.00261	0.104268
5	137.90	66.32	160.11	237.75	0.00246	0.106483
6	20.68	18.02	26.71	26.45	0.01030	0.180652
7	41.37	39.34	54.51	57.29	0.00648	0.11437
8	68.95	66.24	91.08	103.16	0.00539	0.09965
9	103.42	100.13	136.88	168.59	0.00456	0.092581
10	137.90	133.12	182.37	237.43	0.00389	0.082398
11	20.68	38.89	33.66	33.25	0.01565	0.158938
12	41.37	79.77	67.99	73.96	0.00871	0.096361
13	68.95	133.04	113.35	129.73	0.00727	0.083994
14	103.42	200.21	170.24	188.94	0.00673	0.075231
15	137.90	266.30	226.77	240.64	0.00697	0.075204
16	20.68	59.17	40.42	38.88	0.02055	0.160658
17	41.37	119.65	81.28	86.84	0.01251	0.107517
18	68.95	199.71	135.57	143.40	0.01269	0.114663
19	103.42	299.07	203.19	196.14	0.01898	0.14717
20	137.90	398.66	270.89	245.56	0.02273	0.165529
21	20.68	99.56	53.89	52.77	0.03609	0.226666
22	41.37	199.98	108.06	111.91	0.03045	0.201761
23	68.95	331.14	179.38	163.92	0.05288	0.309471
24	103.42	501.42	270.64	209.45	0.11813	0.261009
25	137.90	665.13	359.71	270.66	0.05122	0.251725
26	20.68	140.91	67.67	65.74	0.07649	0.43122
27	41.37	281.98	135.39	130.39	0.05185	0.289668

Table A44. Confining, deviator, and mean stresses, resilient modulus (M_R), rotation, and homogeneous deformation coefficient (HDC) during resilient modulus measurement of 15%Foundry Sand + 85% Aggregate mixture at 7.2 % moisture content and 2.079 g/cm^3 dry density.

Sq	Confining kPa	Deviator kPa	Mean Stress kPa	M_R MPa	Rotation θ(°)	HDC α
1	20.68	10.24	24.10	110.45	0.00642	0.809935
2	41.37	19.57	47.92	125.63	0.00586	0.438259
3	68.95	33.74	80.25	168.64	0.00221	0.128719
4	103.42	50.82	120.44	238.03	0.00213	0.118705
5	137.90	67.61	160.54	310.73	0.00213	0.114882
6	20.68	20.37	27.49	105.38	0.01013	0.611635
7	41.37	40.47	54.89	121.56	0.00755	0.264467
8	68.95	67.40	91.47	151.91	0.00339	0.091172
9	103.42	101.56	137.35	218.41	0.00380	0.095115
10	137.90	135.68	183.23	291.09	0.00331	0.083377
11	20.68	40.60	34.23	101.67	0.01271	0.372071
12	41.37	81.04	68.41	124.63	0.00763	0.138155
13	68.95	135.48	114.16	167.33	0.00593	0.085388
14	103.42	203.83	171.44	238.92	0.00642	0.087928
15	137.90	271.26	228.42	278.00	0.00662	0.079353
16	20.68	60.89	41.00	102.44	0.01128	0.221272
17	41.37	121.84	82.01	129.32	0.00812	0.100697
18	68.95	203.02	136.67	177.78	0.00802	0.082183
19	103.42	304.45	204.98	224.86	0.01002	0.086584
20	137.90	406.22	273.41	279.89	0.01249	0.100357
21	20.68	101.12	54.41	105.76	0.00605	0.074159
22	41.37	203.24	109.15	146.65	0.01073	0.090744
23	68.95	339.24	182.08	200.69	0.01870	0.129382
24	103.42	499.42	269.97	260.60	0.04441	0.274143
25	137.90	664.43	359.48	347.64	0.06902	0.427057
26	20.68	140.52	67.54	108.36	0.01930	0.1762
27	41.37	468.40	197.53	235.81	0.04708	0.280799
28	68.95	468.31	225.10	241.99	0.05695	0.347675

Table A45. Confining, deviator, and mean stresses, resilient modulus (M_R), rotation, and homogeneous deformation coefficient (HDC) during resilient modulus measurement of 100% aggregates at 8.8 % moisture content and 2.065 g/cm^3 dry density.

Sq	Confining kPa	Deviator kPa	Mean Stress kPa	M_R MPa	Rotation θ(°)	HDC α
1	20.68	9.48	23.84	32.45	0.02006	0
2	41.37	19.29	47.83	83.80	0.01615	0.007291
3	68.95	33.36	80.12	129.25	0.01832	0.126035
4	103.42	50.22	120.24	259.73	0.01010	0.608488
5	137.90	67.41	160.47	292.76	0.00206	0.105585
6	20.68	19.59	27.23	41.97	0.00662	0.165727
7	41.37	40.32	54.84	65.83	0.00820	0.156234
8	68.95	67.59	91.53	123.62	0.00798	0.170221
9	103.42	101.66	137.39	204.50	0.00684	0.160376
10	137.90	135.46	183.15	291.18	0.00648	0.162951
11	20.68	39.80	33.97	42.54	0.01450	0.180684
12	41.37	80.75	68.32	75.28	0.01786	0.194695
13	68.95	135.39	114.13	140.18	0.01512	0.182515
14	103.42	203.71	171.40	214.11	0.01406	0.172448
15	137.90	271.28	228.43	287.91	0.01339	0.165492
16	20.68	60.32	40.81	48.20	0.02034	0.189643
17	41.37	121.62	81.94	86.52	0.02065	0.171593
18	68.95	202.97	136.66	147.79	0.01901	0.161394
19	103.42	305.70	205.40	224.92	0.01930	0.165535
20	137.90	406.99	273.66	289.55	0.02008	0.166368
21	20.68	101.07	54.39	58.91	0.02661	0.181585
22	41.37	203.11	109.10	107.31	0.02610	0.160919
23	68.95	338.57	181.86	170.13	0.02612	0.153065
24	103.42	507.13	272.54	235.37	0.02792	0.150914
25	137.90	672.38	362.13	311.68	0.03338	0.182842
26	20.68	141.50	67.87	72.06	0.03848	0.87539
27	41.37	283.32	135.84	142.23	0.02826	0.167662
28	68.95	471.53	226.18	206.09	0.02716	0.140306
29	103.42	704.36	338.29	251.54	0.03594	0.15177

Table A46. Confining, deviator, and mean stresses, resilient modulus (M_R), rotation, and homogeneous deformation coefficient (HDC) during resilient modulus measurement of 100% aggregates at 7.2 % moisture content and 2.087 g/cm^3 dry density.

Sq	Confining kPa	Deviator kPa	Mean Stress kPa	M_R MPa	Rotation θ(°)	HDC α
2	41.37	19.43	47.88	129.19	0.00527	0.200167
3	68.95	33.56	80.19	168.97	0.00266	0.156865
4	103.42	50.16	120.22	250.94	0.00636	0.371685
5	137.90	67.28	160.43	319.10	0.00568	0.313844
6	20.68	20.18	27.43	107.64	0.01228	0.731703
7	41.37	40.47	54.89	123.42	0.00797	0.284565
8	68.95	67.38	91.46	150.55	0.01101	0.286524
9	103.42	101.50	137.33	224.58	0.01303	0.335805
10	137.90	135.43	183.14	303.01	0.01052	0.274219
11	20.68	40.35	34.15	105.34	0.01694	0.515133
12	41.37	81.54	68.58	129.98	0.01859	0.345183
13	68.95	135.86	114.29	170.21	0.02304	0.336085
14	103.42	203.10	171.20	244.98	0.01803	0.253508
15	137.90	270.61	228.20	299.24	0.01554	0.200349
16	20.68	61.11	41.07	104.31	0.02558	0.508492
17	41.37	121.52	81.91	135.33	0.02544	0.329902
18	68.95	203.06	136.69	183.45	0.02675	0.28149
19	103.42	304.05	204.85	234.12	0.02165	0.194115
20	137.90	405.35	273.12	286.45	0.02096	0.172915
21	20.68	61.11	41.07	104.31	0.02558	0.508492
22	41.37	121.52	81.91	135.42	0.02547	0.330577
23	68.95	337.58	181.53	193.76	0.03790	0.253516
24	103.42	505.36	271.95	241.27	0.04758	0.264658
25	137.90	671.95	361.98	303.22	0.04538	0.238704
26	20.68	141.40	67.83	92.23	0.08695	0.660447
27	41.37	283.71	135.97	147.90	0.07176	0.435759
28	68.95	472.49	226.50	191.57	0.07865	0.270436

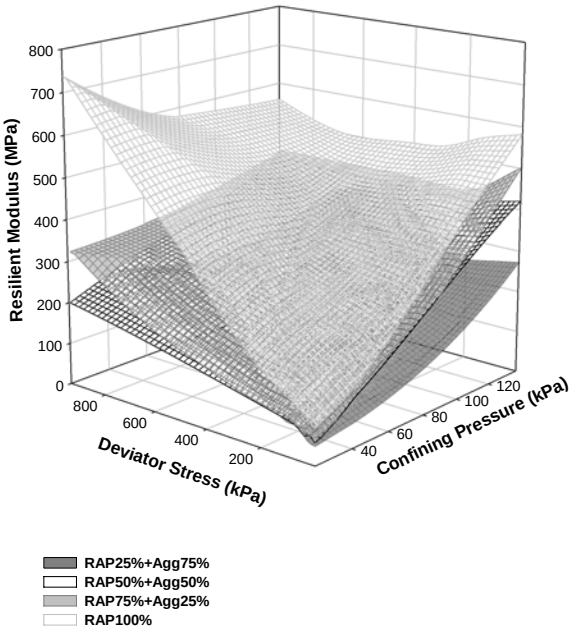

Figure A21. Variation in resilient modulus of RAP-aggregate mixtures as a function of deviator and confining stresses at optimum moisture content (<300 kPa suction).

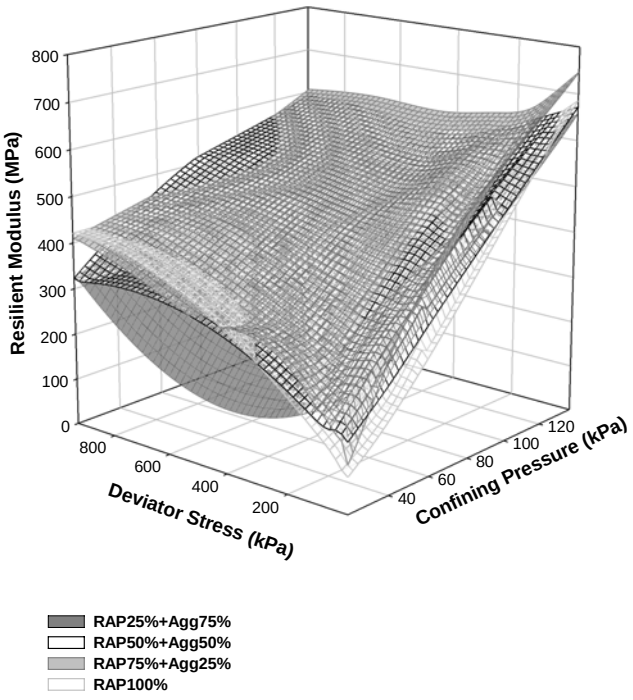

Figure A22. Variation in resilient modulus of RAP-aggregate mixtures as a function of deviator and confining stresses at moisture content corresponding to 300 kPa suction.

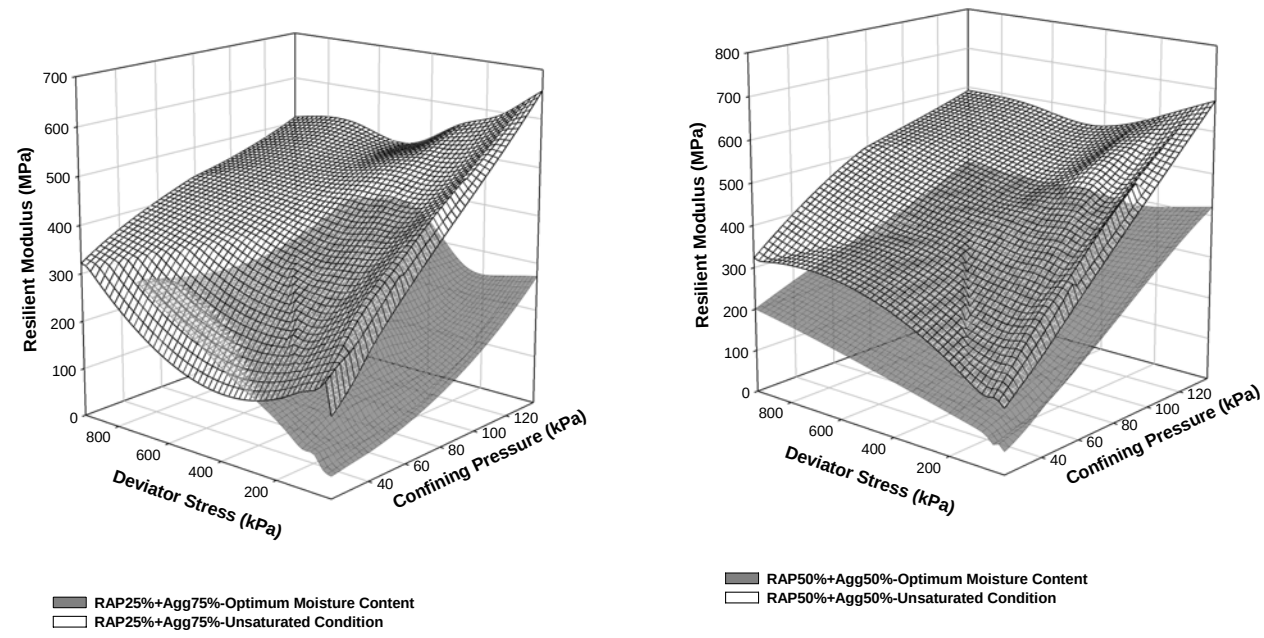

RAP25%+Agg 75%

RAP50%+Agg 50%

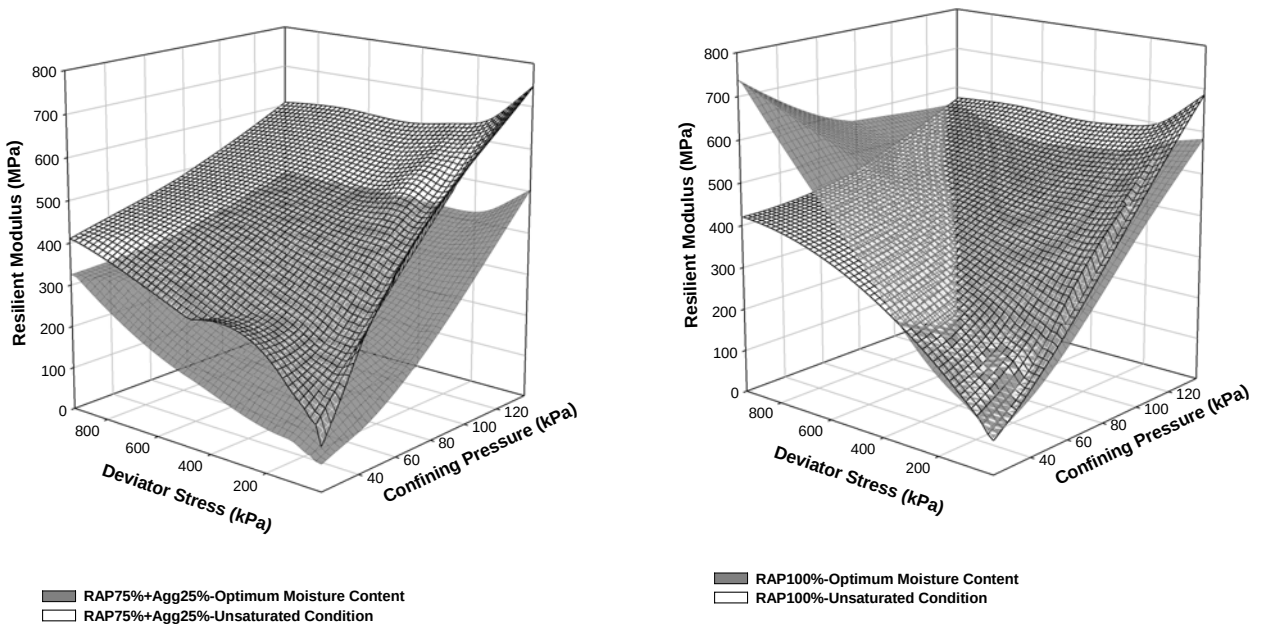

RAP75%+Agg 25%

RAP100%

Figure A23. Effect of water content on resilient modulus of RAP-aggregate mixtures as a function of deviator and confining stresses.

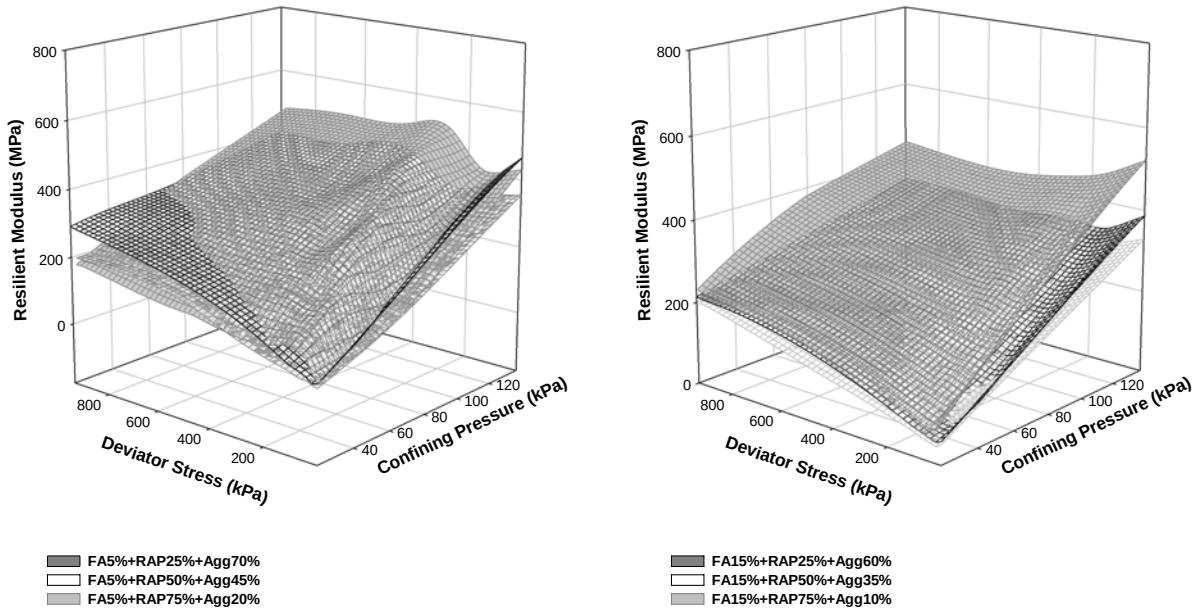

Figure A24. Variation in resilient modulus of fly ash, RAP, and aggregate mixtures as a function of deviator and confining stresses at optimum moisture content (<300 kPa suction).

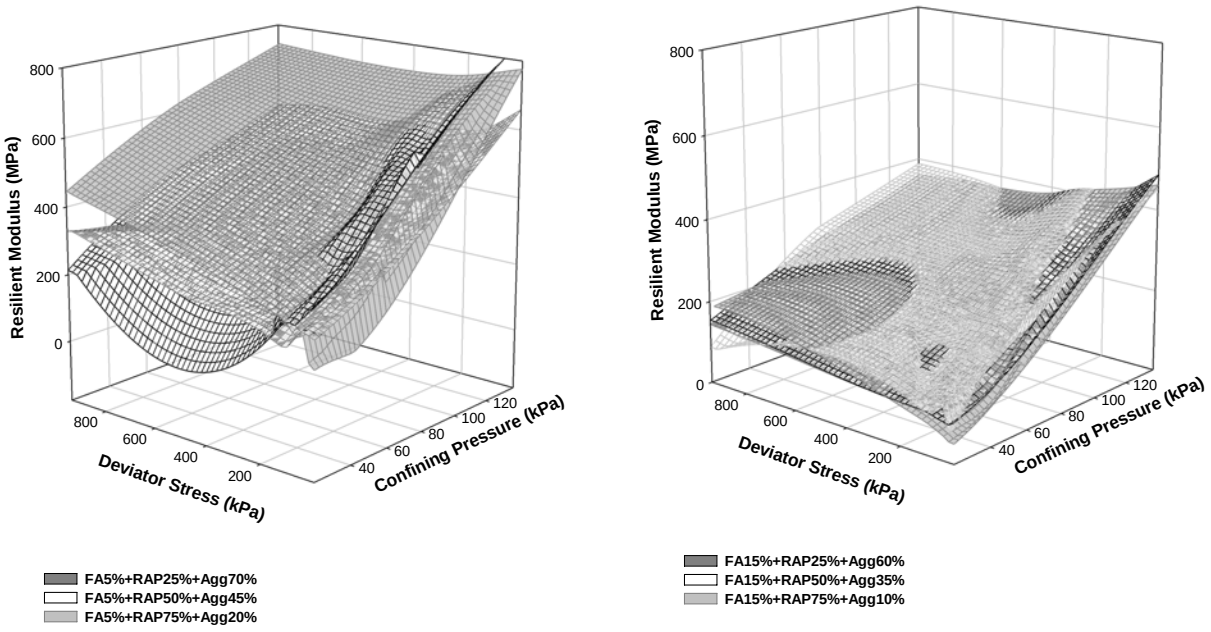

Figure A25. Variation in resilient modulus of fly ash, RAP, and aggregate mixtures as a function of deviator and confining stresses at water content corresponding to 300 kPa suction.

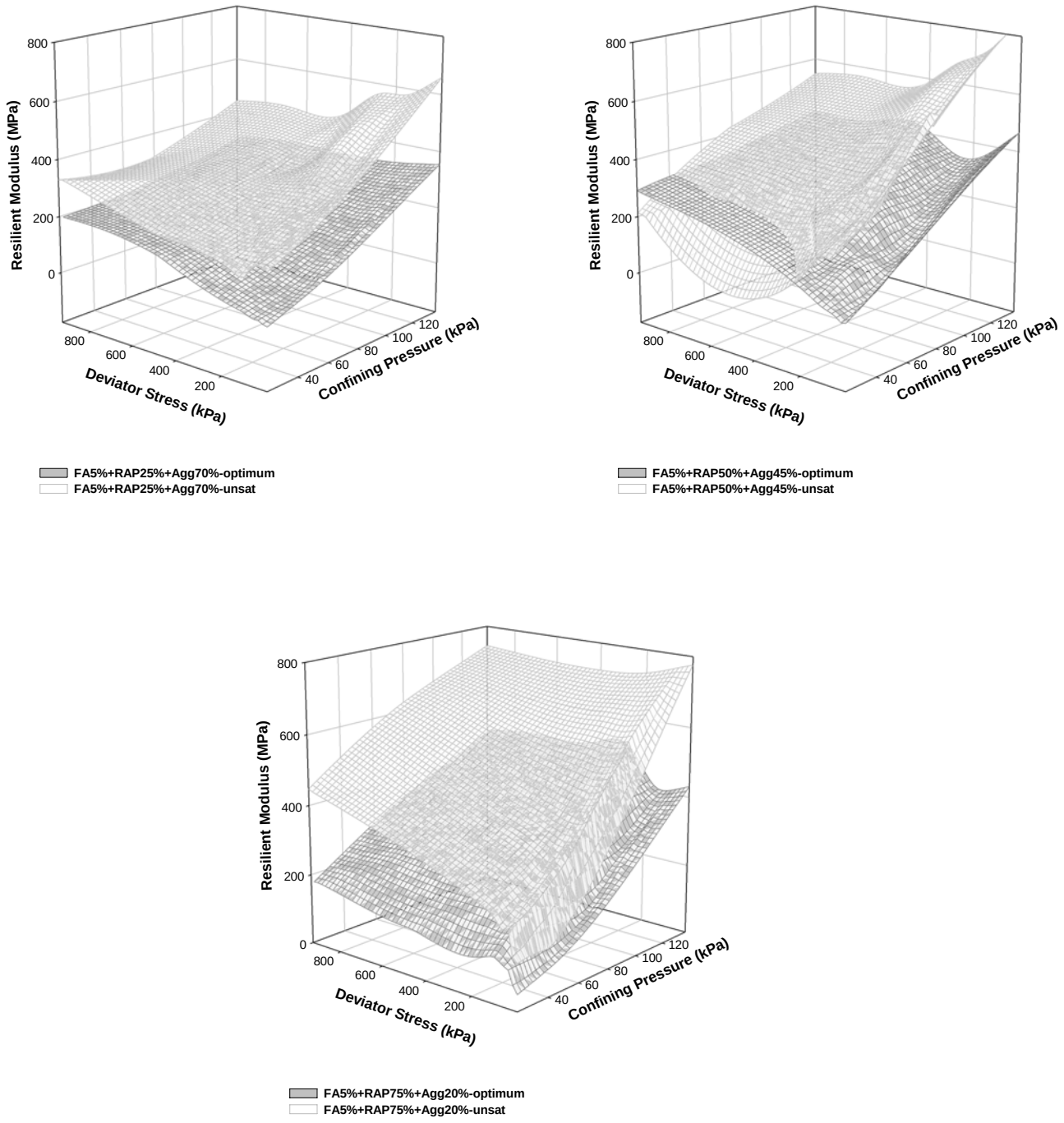

Figure A26. Effect of water content on resilient modulus of 5% fly ash, RAP and aggregate mixtures as a function of deviator and confining stresses.

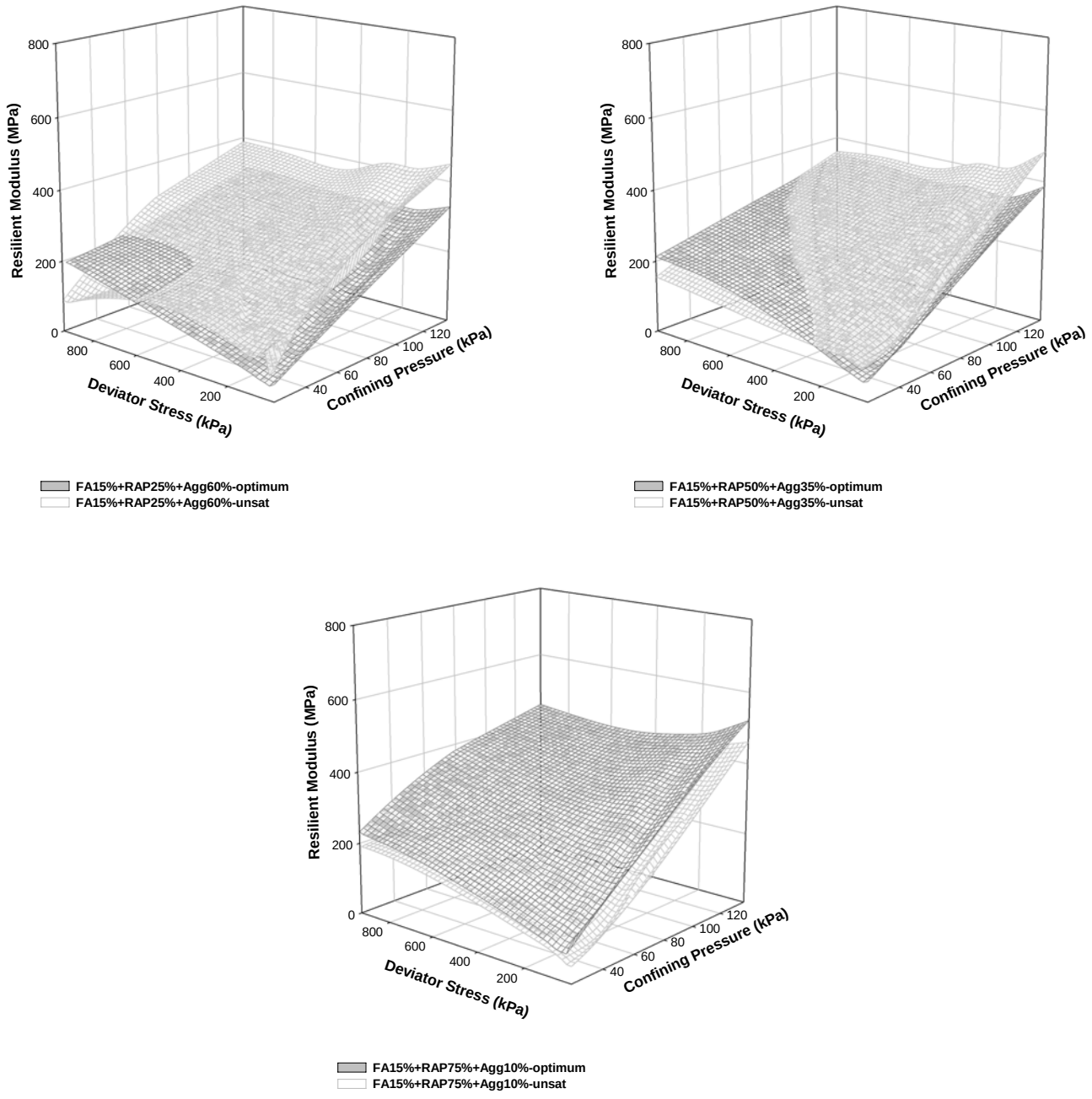

Figure A27. Effect of water content on resilient modulus of 15% fly ash, RAP and aggregate mixtures as a function of deviator and confining stresses.

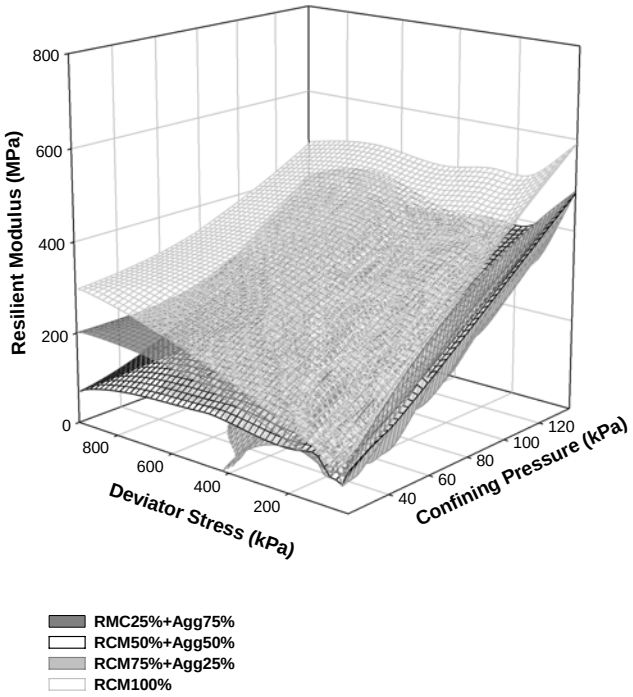

Figure A28. Variation in resilient modulus of RCM- aggregate mixtures as a function of deviator and confining stresses at optimum water content (<300 kPa suction).

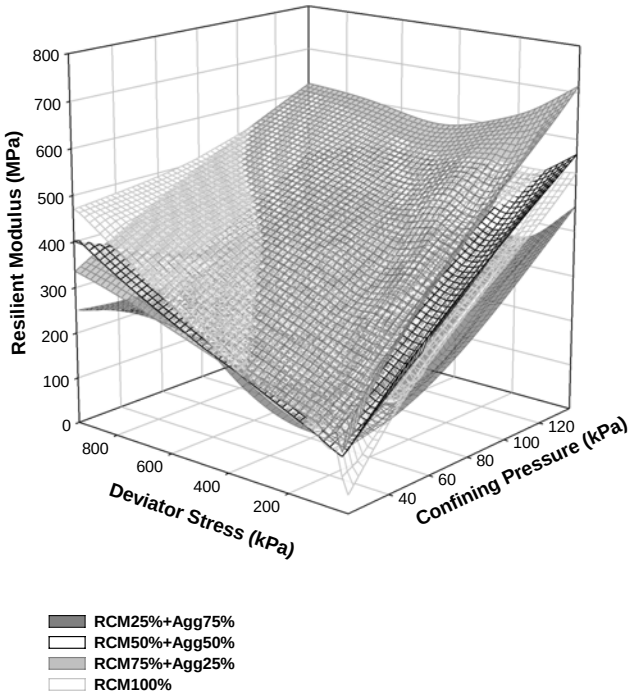

Figure A29. Variation in resilient modulus of RCM- aggregate mixtures as a function of deviator and confining stresses at water content corresponding to 300 kPa suction).

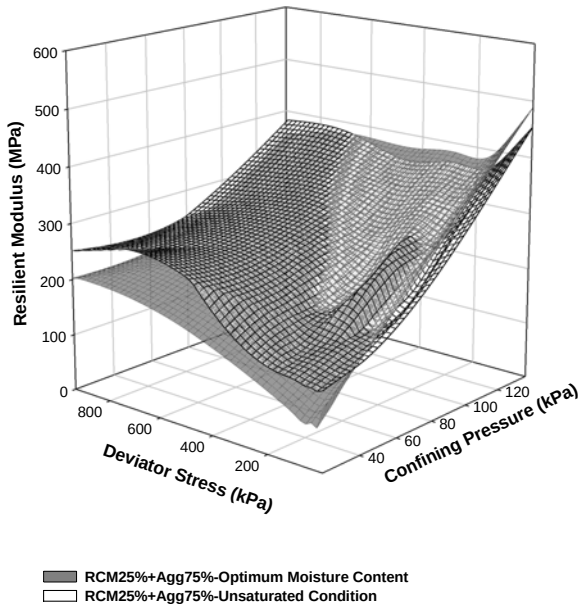

RCM25%+Agg75%

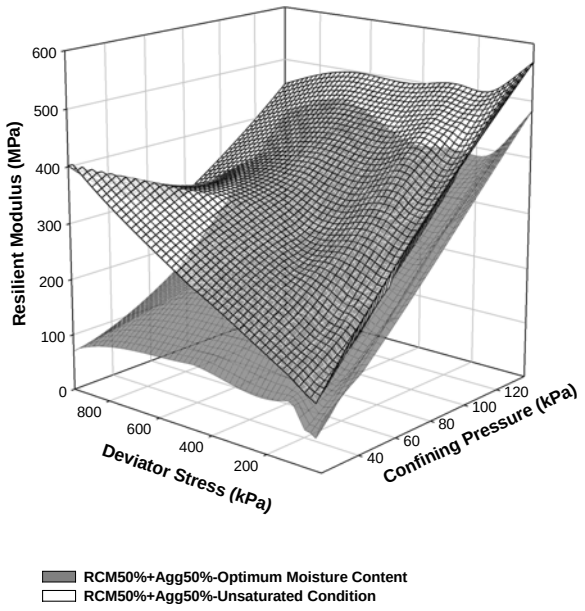

RCM50%+Agg50%

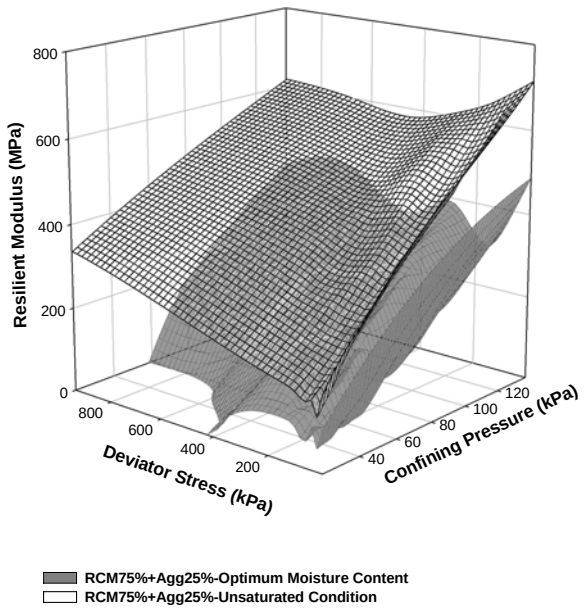

RCM75%+Agg25%

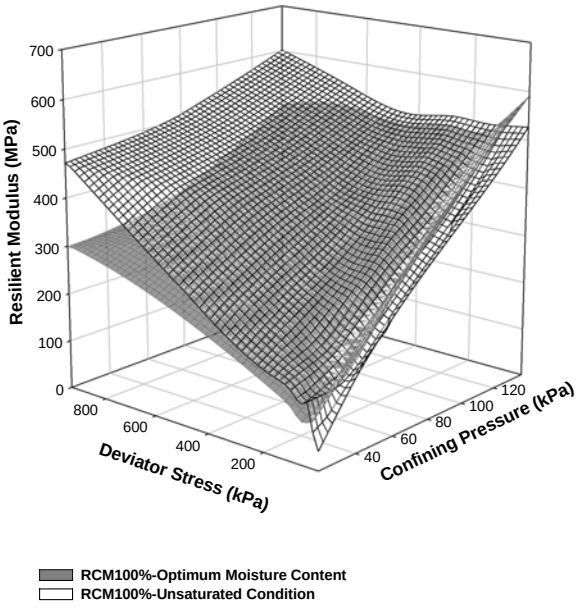

RCM100%

Figure A30. Effect of water content on resilient modulus of RCM-aggregate mixtures as a function of deviator and confining stresses.

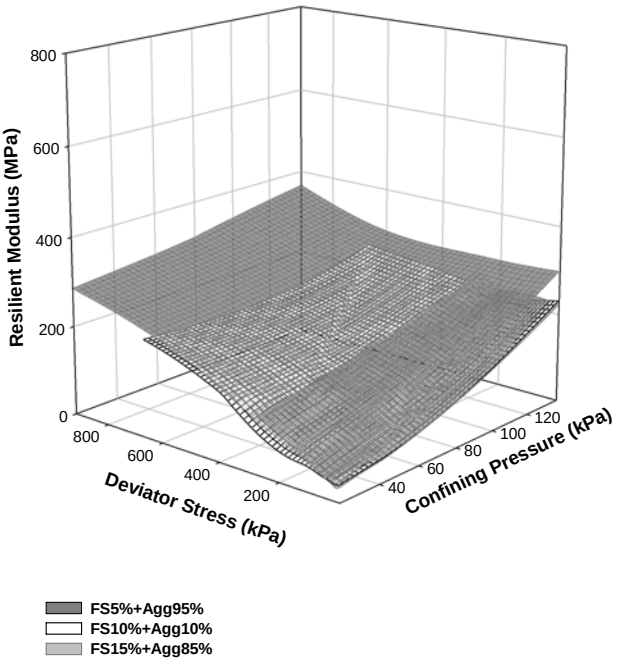

Figure A31. Variation in resilient modulus of foundry sand-aggregate mixtures as a function of deviator and confining stresses at optimum water content (<300 kPa suction).

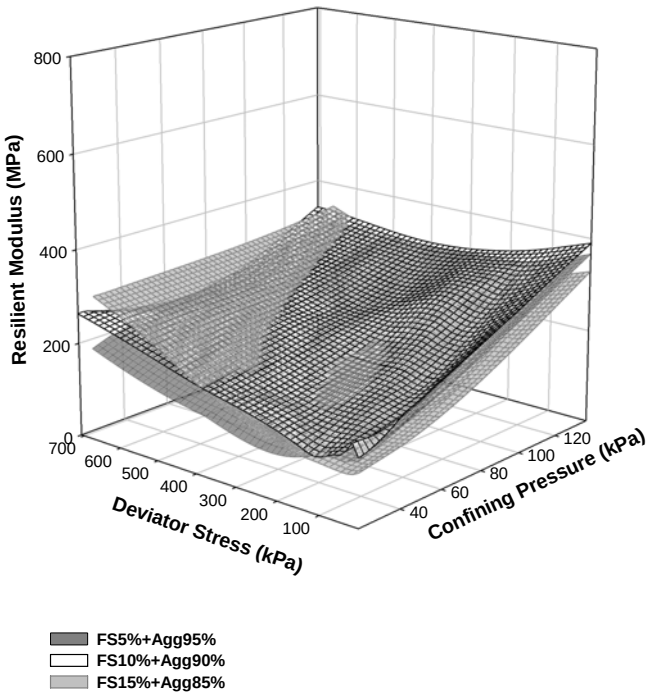

Figure A32. Variation in resilient modulus of foundry sand-aggregate mixtures as a function of deviator and confining stresses at water content corresponding to 300 kPa suction.

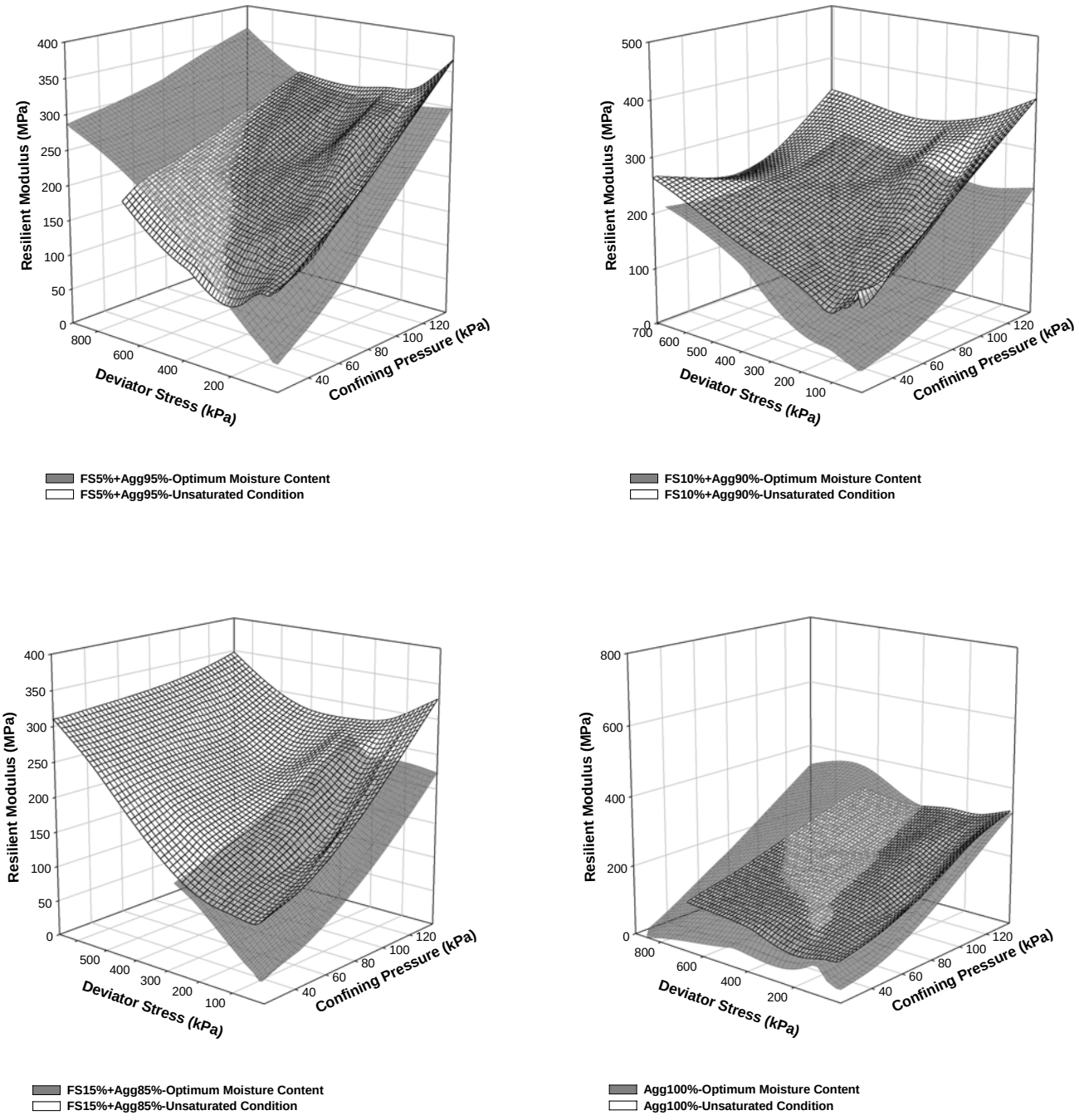

Figure A33. Effect of water content on resilient modulus of foundry sand-aggregate mixtures as a function of deviator and confining stresses.

Figure A34. Pictures of 25% RAP +75% Aggregate mixture failed specimen during resilient modulus and shear strength testing for Fig. A34 a) and A34b) correspond to optimum moisture contents (<300 kPa suction), and Fig. A34c) correspond to water content at 300 kPa suction. Confining pressures were 1 psi for A34a and A34c specimens and 5psi for A 34b specimen.

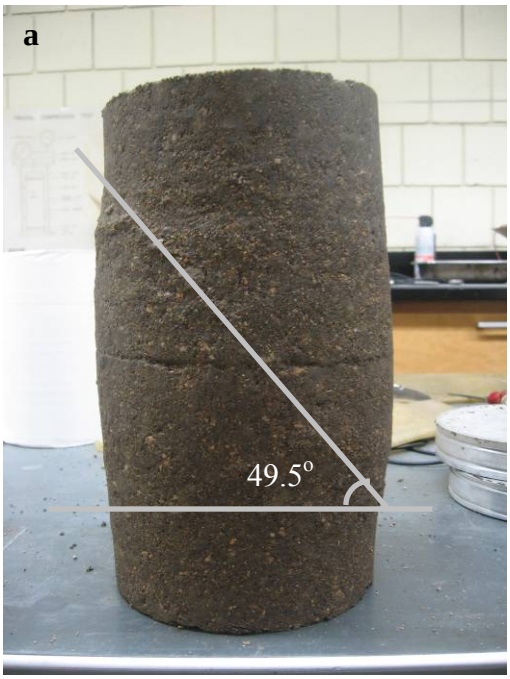

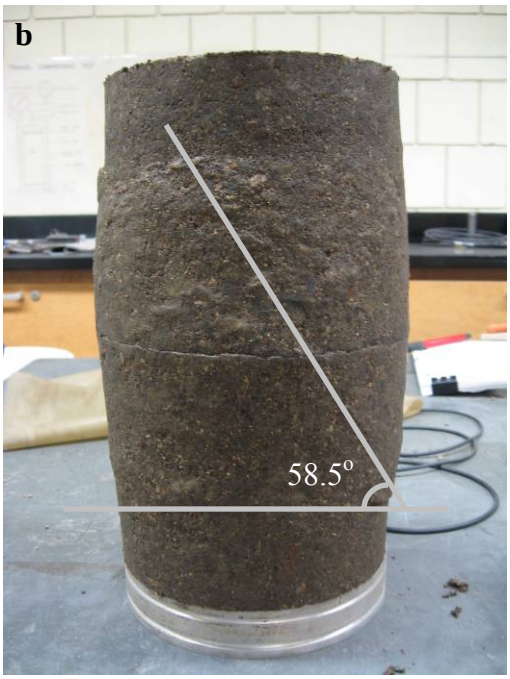

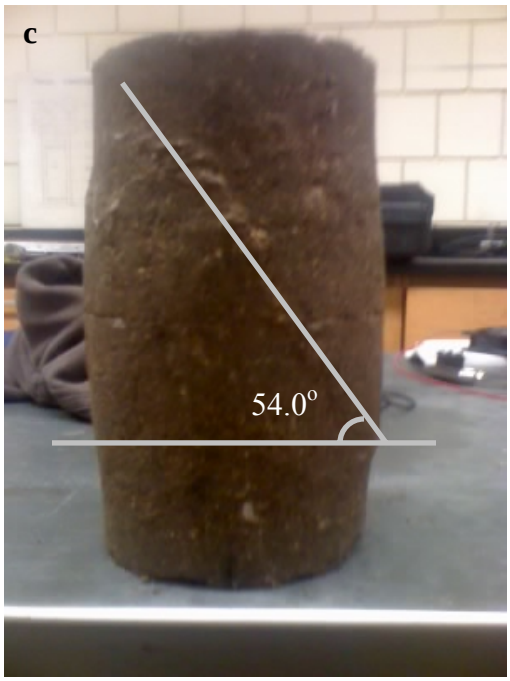

Figure A35. Pictures of 50%RAP + 50%Aggregate mixture failed specimen during resilient modulus and shear strength testing for Fig. A35 a) and A35b) correspond to optimum moisture contents (<300 kPa suction), and Fig. A35c) correspond to water content at 300 kPa suction. Confining pressures were 1 psi for A35a and A35c specimens and 5psi for A 35b specimen.

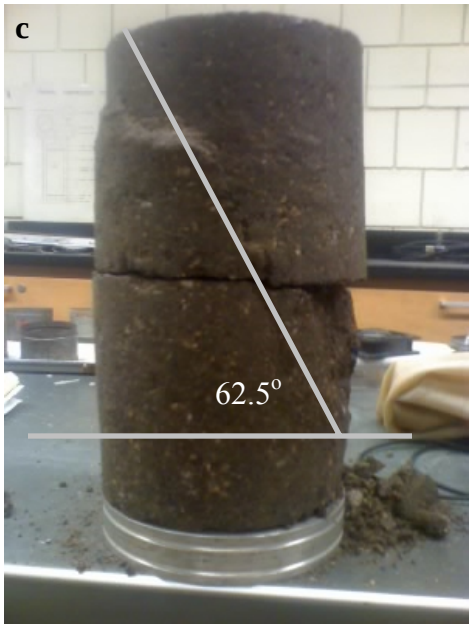

Figure A36. Pictures of 75 %RAP + 25 %Aggregate mixture failed specimen during resilient modulus and shear strength testing for Fig. A36 a) and A36b) correspond to optimum moisture contents (<300 kPa suction), and Fig. A36c) correspond to water content at 300 kPa suction. Confining pressures were 1 psi for A36a and A36c specimens and 5psi for A36b specimen.

Figure A37. Pictures of 100% RAP mixture failed specimen during resilient modulus and shear strength testing for Fig. A37 a) and A36b) correspond to optimum moisture contents (<300 kPa suction), and Fig. A37c) correspond to water content at 300 kPa suction. Confining pressures were 1 psi for A37a and A37c specimens and 5psi for A37b specimen.

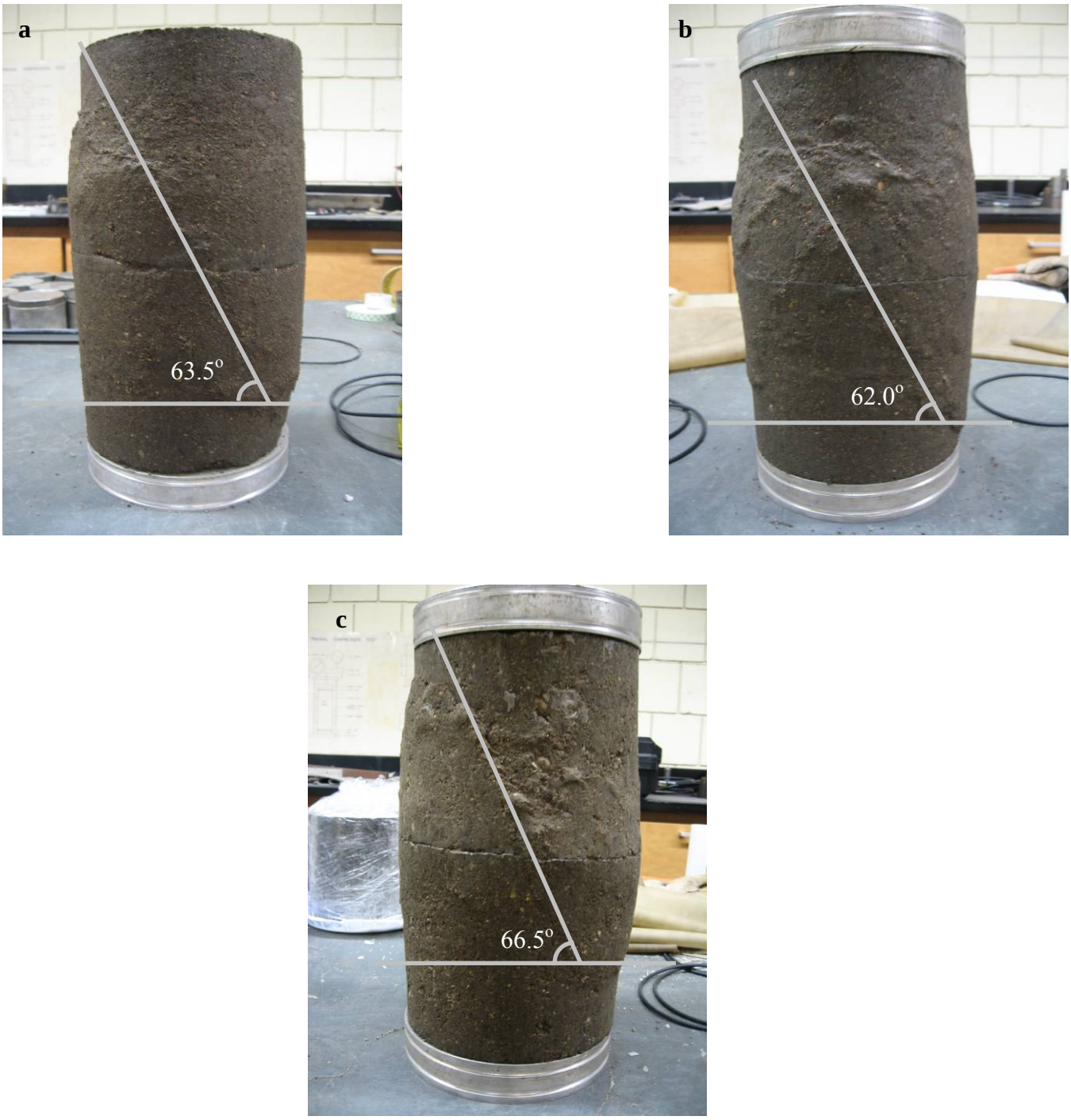

Figure A38. Pictures of 5% Fly Ash+25% RAP+70% Aggregate mixture failed specimen during resilient modulus and shear strength testing for Fig. A38 a) and A36b) correspond to optimum moisture contents (<300 kPa suction), and Fig. A38c) correspond to water content at 300 kPa suction. Confining pressures were 1 psi for A38a and A38c specimens and 5psi for A38b specimen.

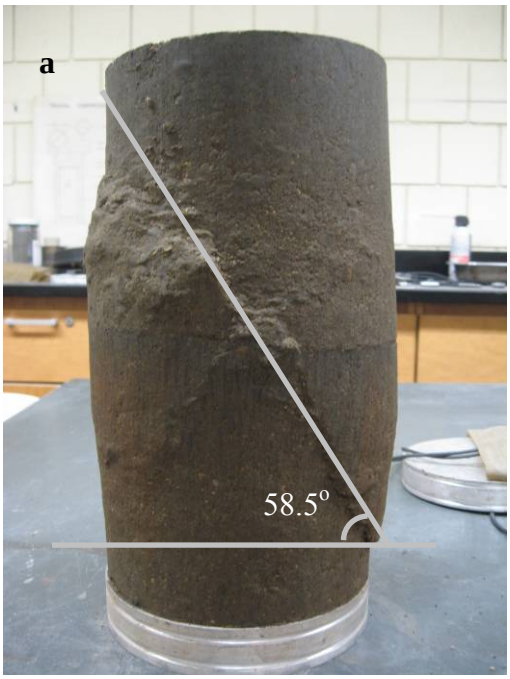

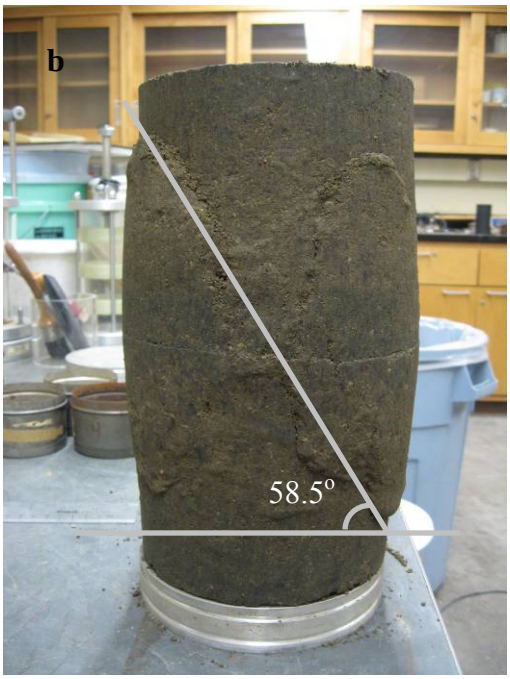

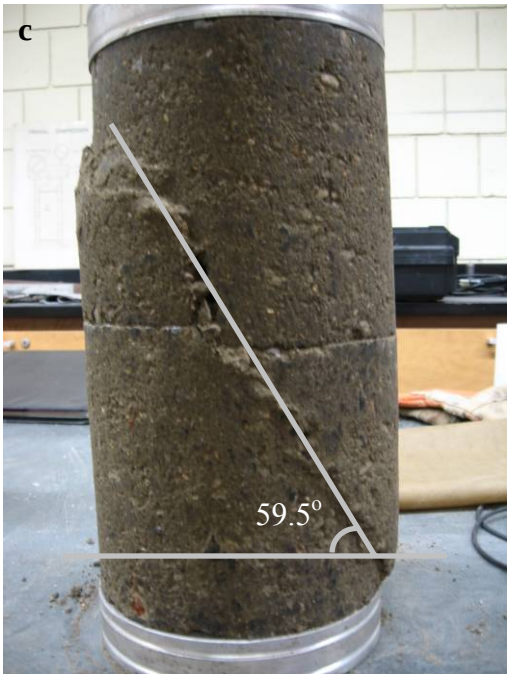

Figure A39. Pictures of 15% Fly Ash+25% RAP+60% Aggregate mixture failed specimen during resilient modulus and shear strength testing for Fig. A39 a) and A36b) correspond to optimum moisture contents (<300 kPa suction), and Fig. A39c) correspond to water content at 300 kPa suction. Confining pressures were 1 psi for A39a and A39c specimens and 5psi for A39b specimen.

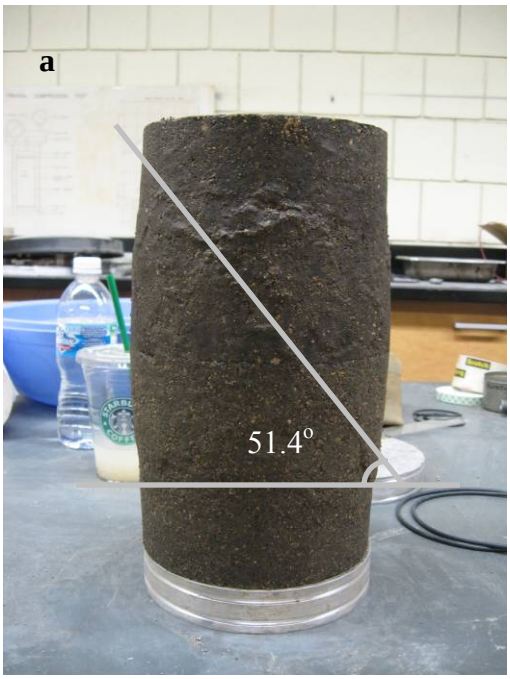

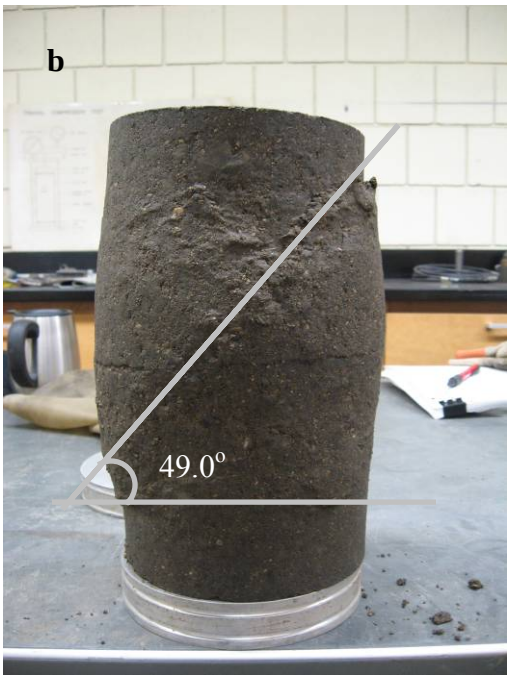

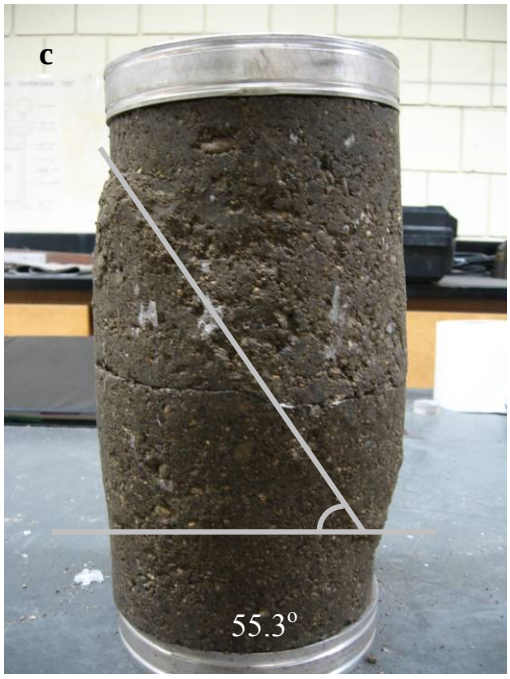

Figure A40. Pictures of 5% Fly Ash+50% RAP+45% Aggregate mixture failed specimen during resilient modulus and shear strength testing for Fig. A40 a) and A40b) correspond to optimum moisture contents (<300 kPa suction), and Fig. A40c) correspond to water content at 300 kPa suction. Confining pressures were 1 psi for A40a and A40c specimens and 5psi for A40b specimen.

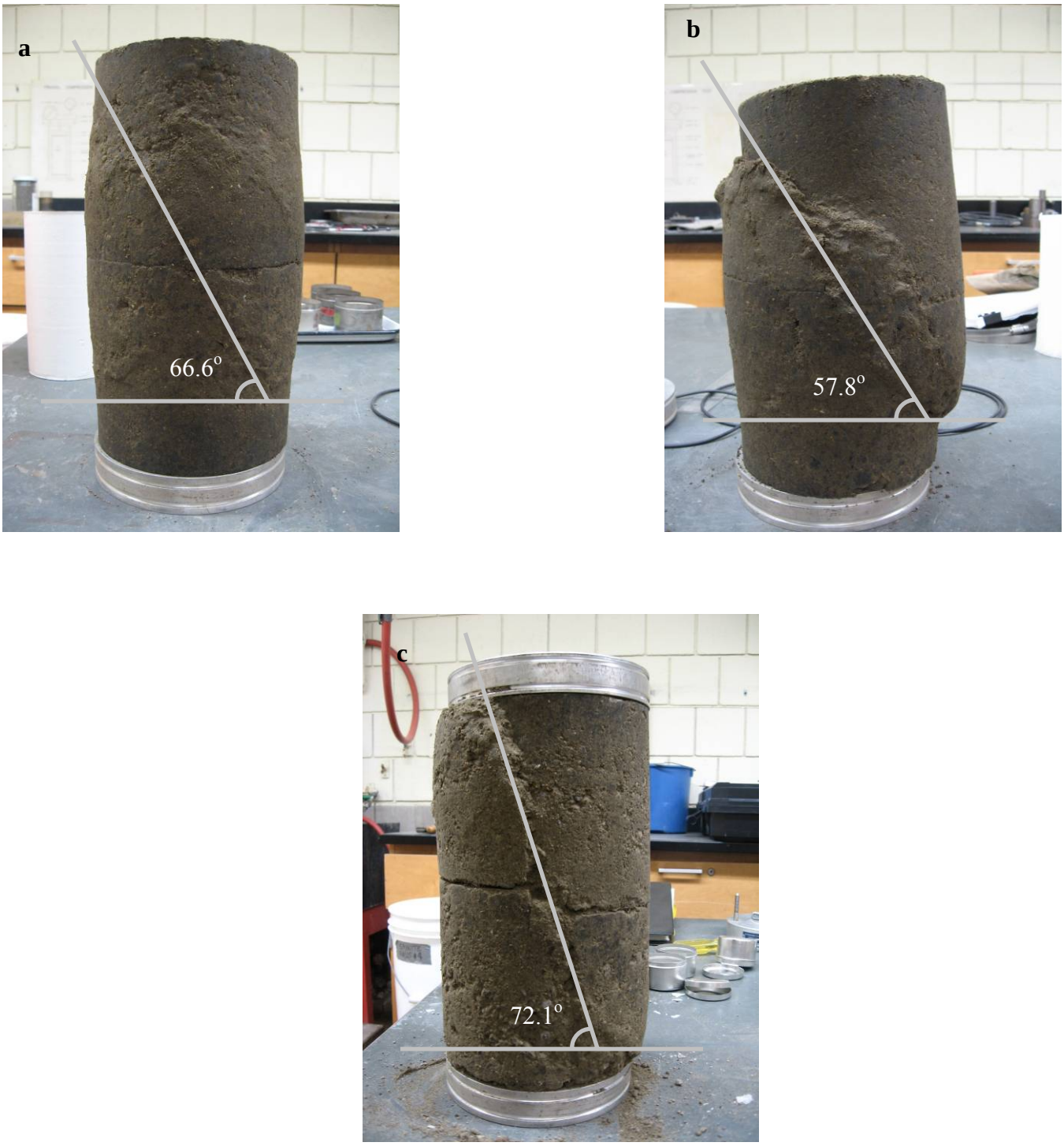

Figure A41. Pictures of 15% Fly Ash+50% RAP+35% Aggregate mixture failed specimen during resilient modulus and shear strength testing for Fig. A41 a) and A41b) correspond to optimum moisture contents (<300 kPa suction), and Fig. A41c) correspond to water content at 300 kPa suction. Confining pressures were 1 psi for A41a and A41c specimens and 5psi for A41b specimen.

Figure A42. Pictures of 5% Fly Ash+ 75% RAP+20% Aggregate mixture failed specimen during resilient modulus and shear strength testing for Fig. A42 a) and A42b) correspond to optimum moisture contents (<300 kPa suction), and Fig. A42c) correspond to water content at 300 kPa suction. Confining pressures were 1 psi for A42a and A42c specimens and 5psi for A42b specimen.

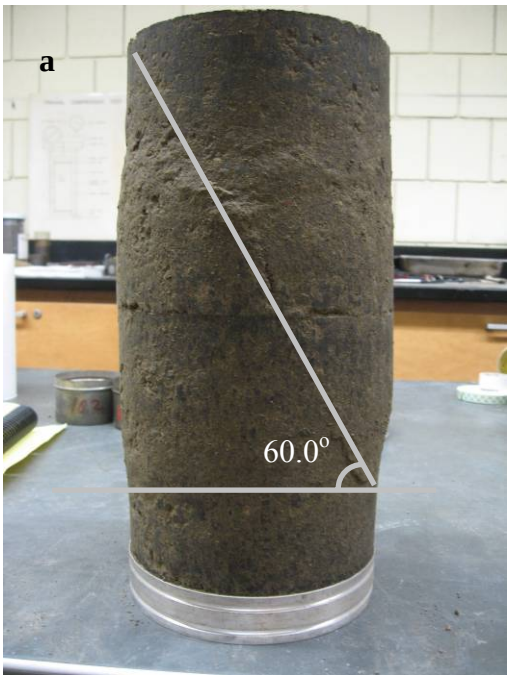

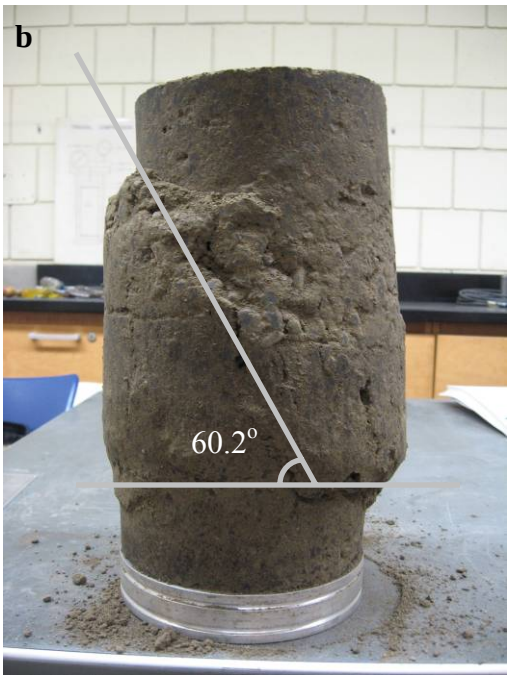

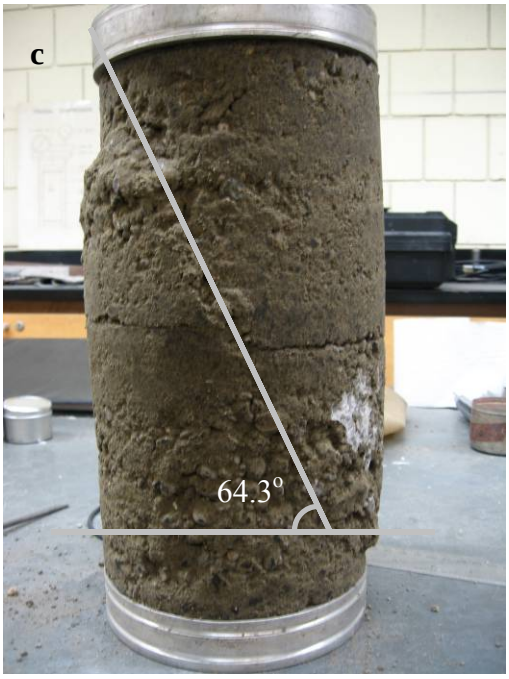

Figure A43. Pictures of 15% Fly Ash+75% RAP+10% Aggregate mixture failed specimen during resilient modulus and shear strength testing for Fig. A43 a) and A43b) correspond to optimum moisture contents (<300 kPa suction), and Fig. A43c) correspond to water content at 300 kPa suction. Confining pressures were 1 psi for A43a and A43c specimens and 5psi for A43b specimen.

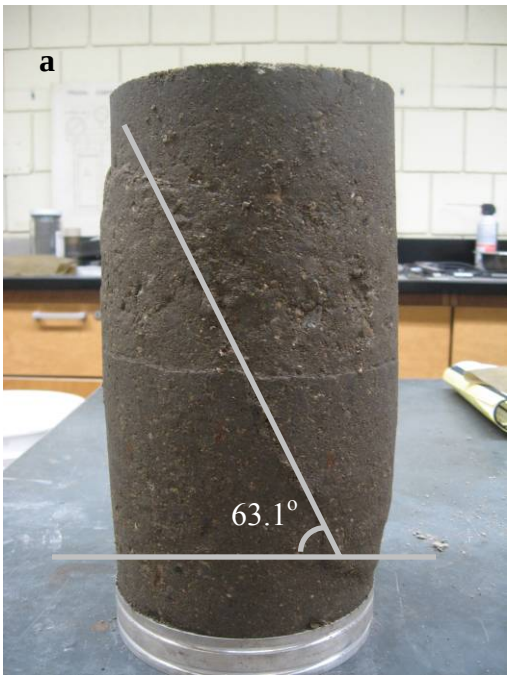

\

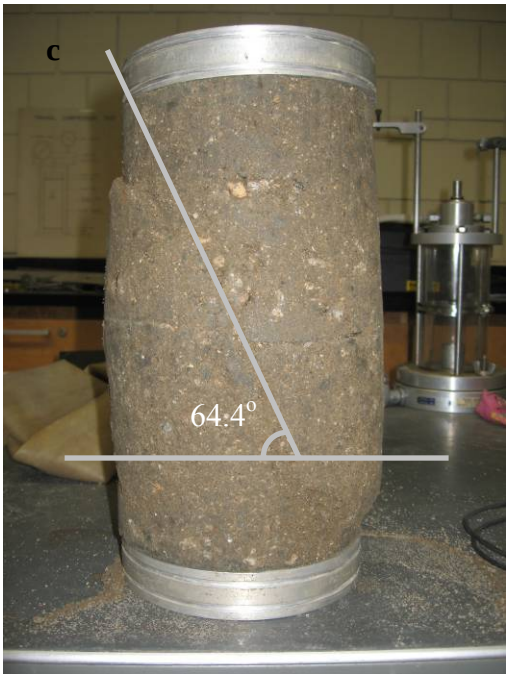

Figure A44. Pictures of 25% RCM + 75% Aggregate mixture failed specimen during resilient modulus and shear strength testing for Fig. A44 a) and A44b) correspond to optimum moisture contents (<300 kPa suction), and Fig. A44c) correspond to water content at 300 kPa suction. Confining pressures were 1 psi for A44a and A44c specimens and 5psi for A44b specimen.

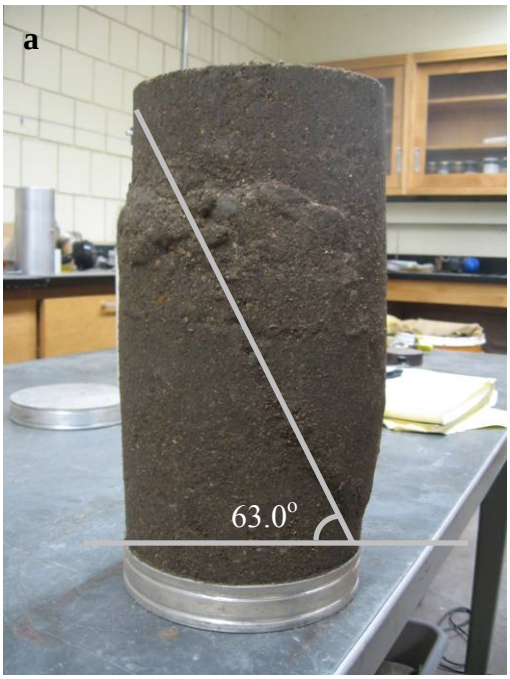

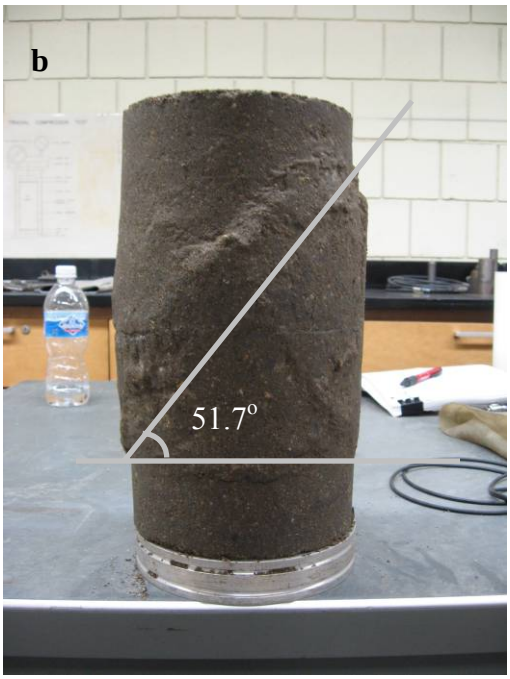

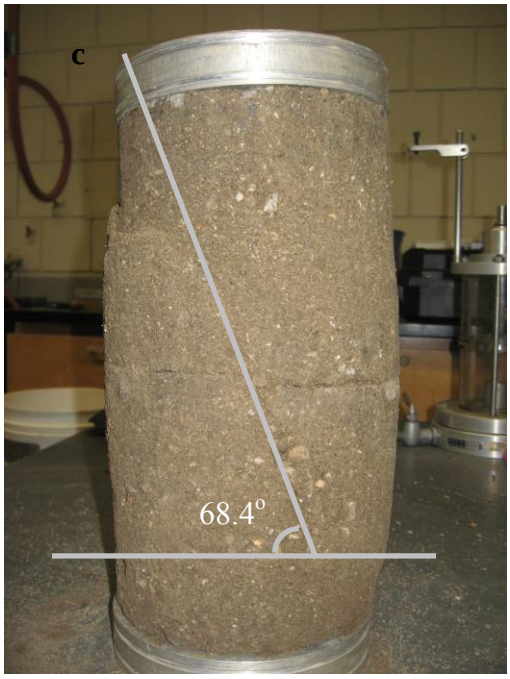

Figure A45. Pictures of 50% RCM + 50% Aggregate mixture failed specimen during resilient modulus and shear strength testing for Fig. A45 a) and A45b) correspond to optimum moisture contents (<300 kPa suction), and Fig. A45c) correspond to water content at 300 kPa suction. Confining pressures were 1 psi for A45a and A45c specimens and 5psi for A45b specimen.

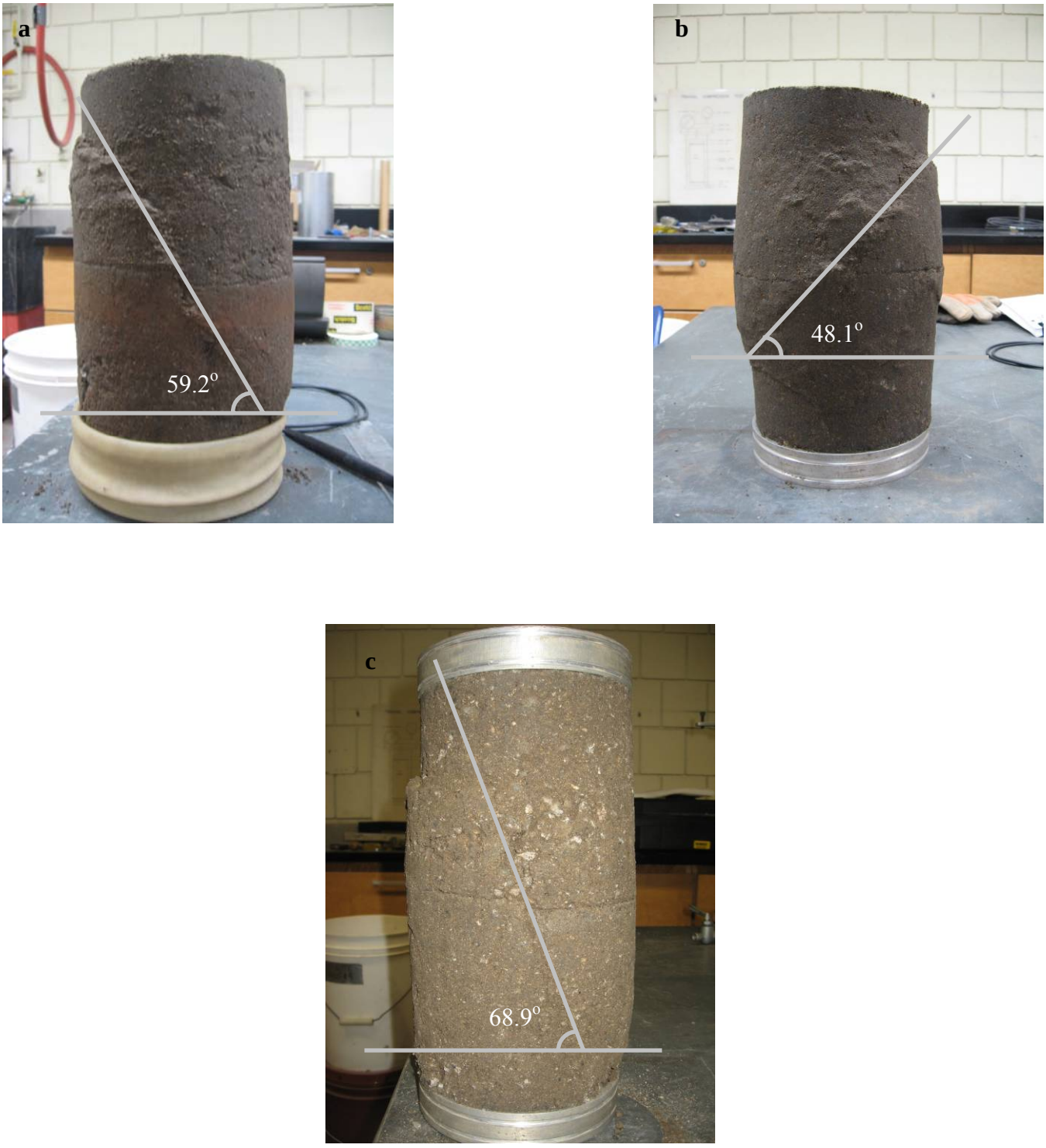

Figure A46. Pictures of 75% RCM + 25% Aggregate mixture failed specimen during resilient modulus and shear strength testing for Fig. A46 a) and A45b) correspond to optimum moisture contents (<300 kPa suction), and Fig. A46c) correspond to water content at 300 kPa suction. Confining pressures were 1 psi for A46a and A46c specimens and 5psi for A46b specimen.

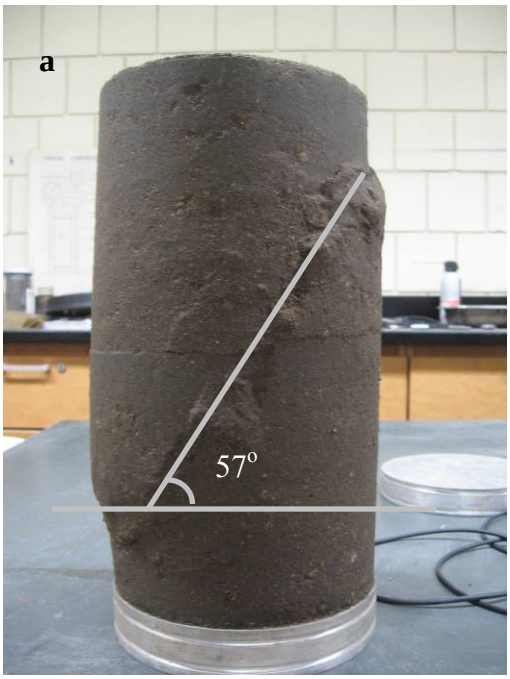

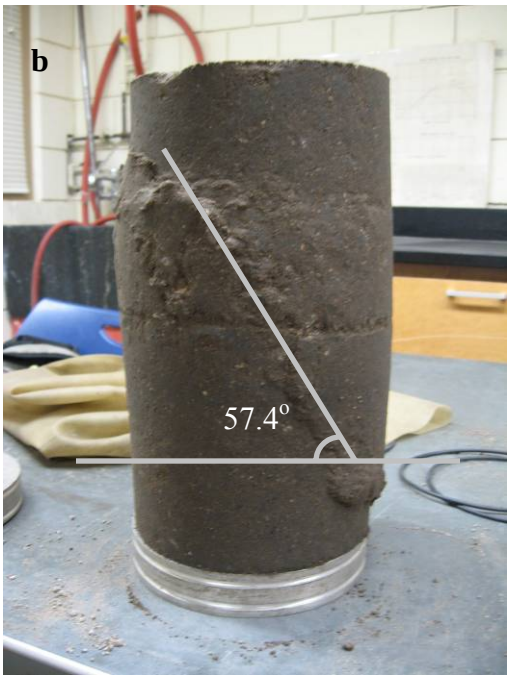

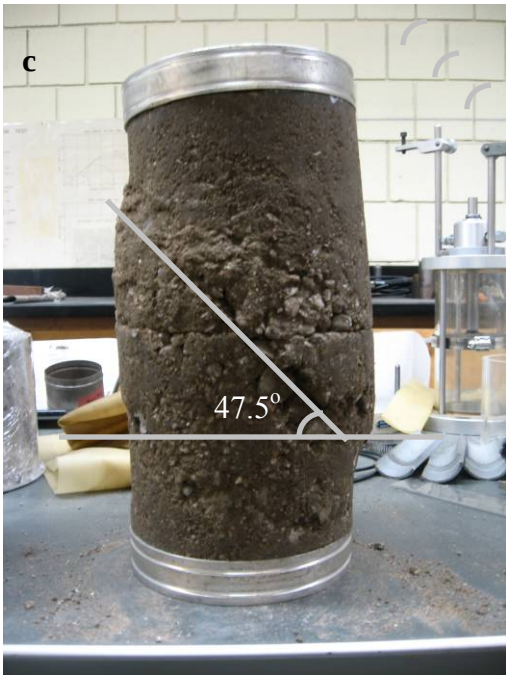

Figure A47. Pictures of 100% RCM mixture failed specimen during resilient modulus and shear strength testing for Fig. A47a and A45b correspond to optimum moisture contents (<300 kPa suction), and Fig. A47c correspond to water content at 300 kPa suction. Confining pressures were 1 psi for A47a and A47c specimens and 5psi for A47b specimen.

Figure A48. Pictures of 5%Foundry Sand + 95%Aggregate mixture failed specimen during resilient modulus and shear strength testing. Fig. A48a correspond to optimum moisture contents (<300 kPa suction), and Fig. A48b correspond to water content at 300 kPa suction.

Figure A49. Pictures of 10% Foundry Sand + 90% Aggregate mixture failed specimen during resilient modulus and shear strength testing. Fig. A49a correspond to optimum moisture contents (<300 kPa suction), and Fig. A49b correspond to water content at 300 kPa suction.

Figure A50. Pictures of 15% Foundry Sand + 85%Aggregate mixture failed specimen during resilient modulus and shear strength testing. Fig. A50a correspond to optimum moisture contents (<300 kPa suction), and Fig. A50b correspond to water content at 300 kPa suction.

Figure A51. Pictures of 100%Aggregate failed specimen during resilient modulus and shear strength testing. Fig. A51a correspond to optimum moisture contents (<300 kPa suction), and Fig. A51b correspond to water content at 300 kPa suction.

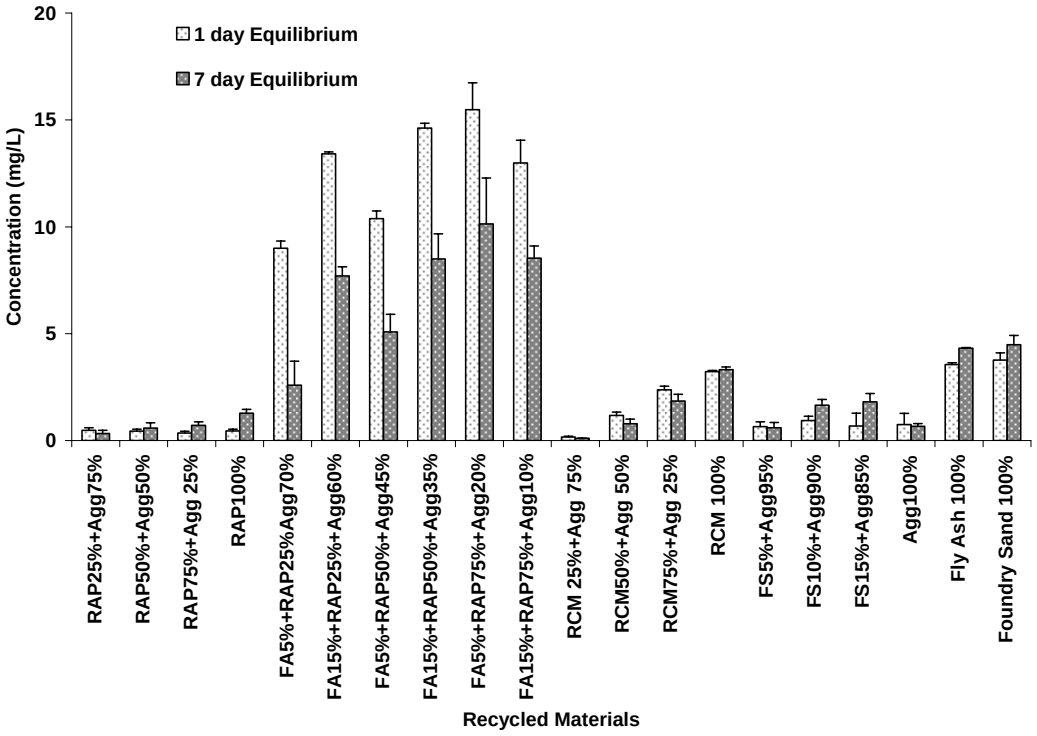

Figure A52. Aluminum concentration in the filtrate from the batch test after 18 hrs (1 day) and 7 day equilibrium time.

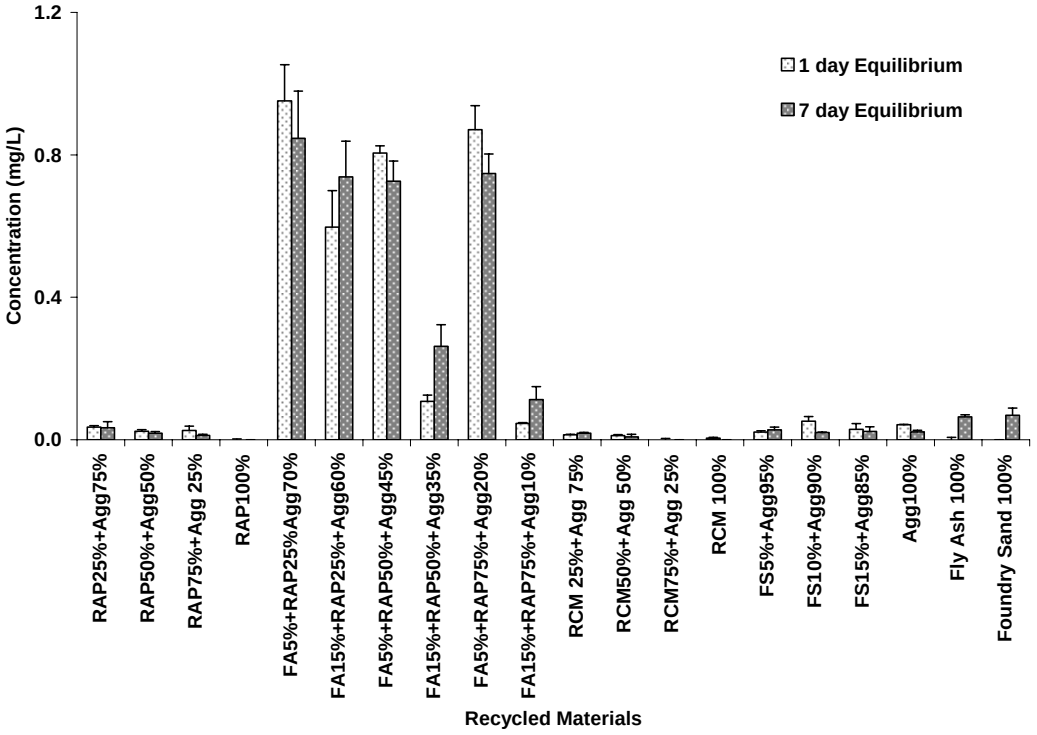

Figure A53. Boron concentration in the filtrate from the batch test after 18 hrs (1 day) and 7 day equilibrium time.

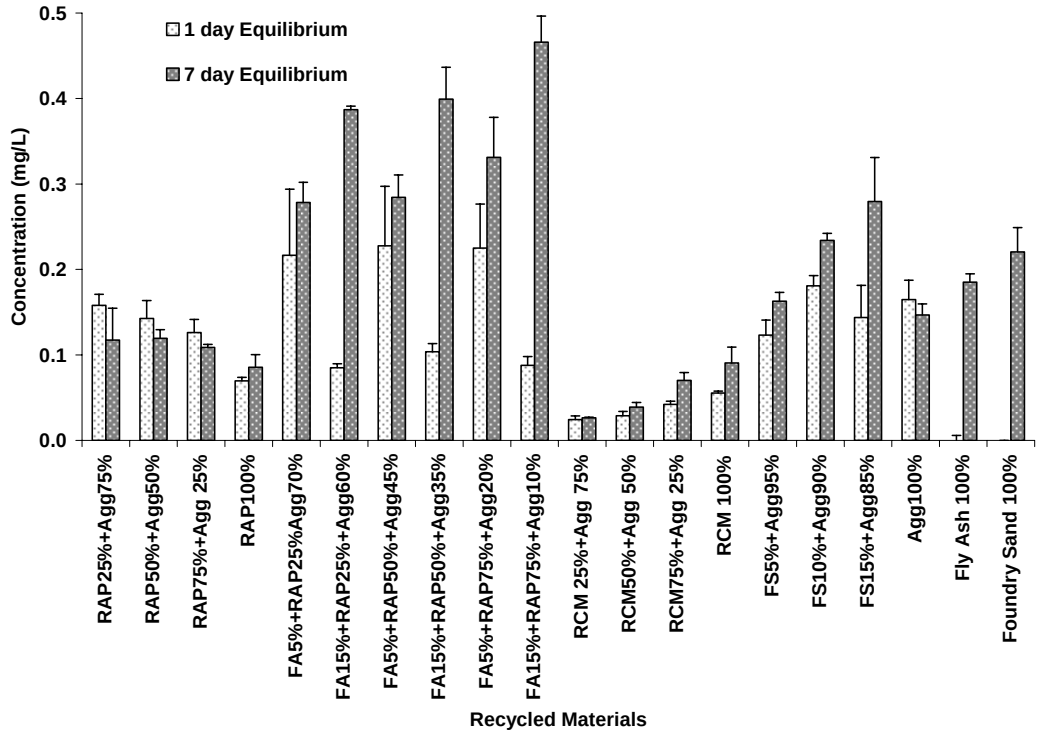

Figure A54. Barium concentration in the filtrate from the batch test after 18 hrs (1 day) and 7 day equilibrium time.

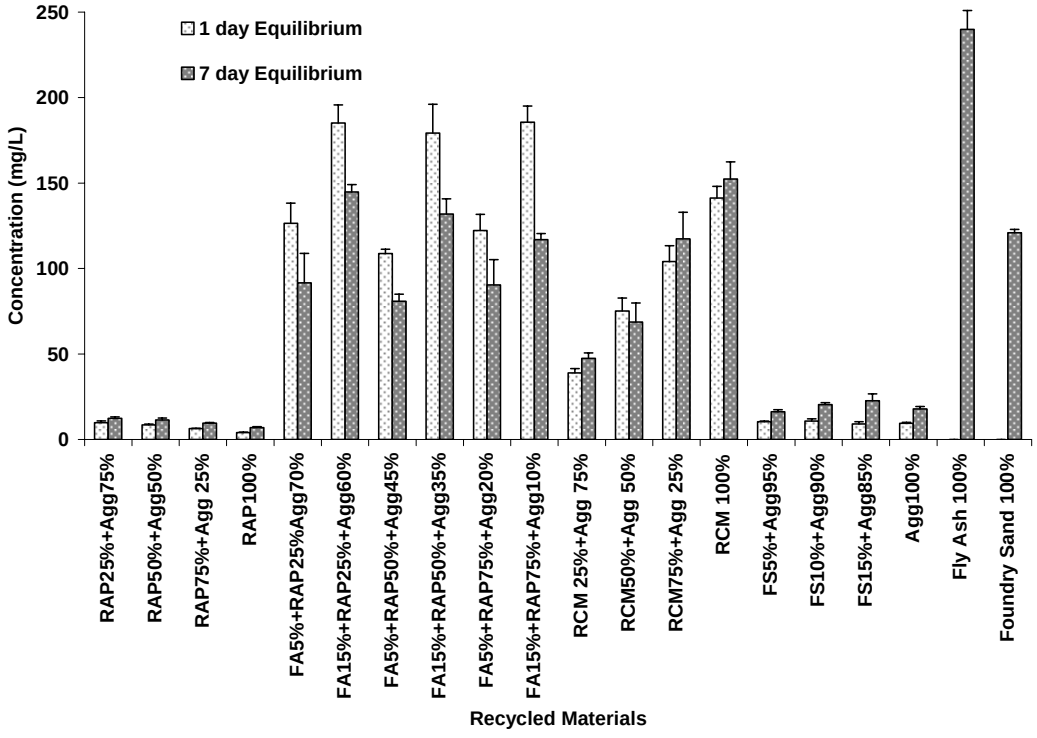

Figure A55. Calcium concentration in the filtrate from the batch test after 18 hrs (1 day) and 7 day equilibrium time.

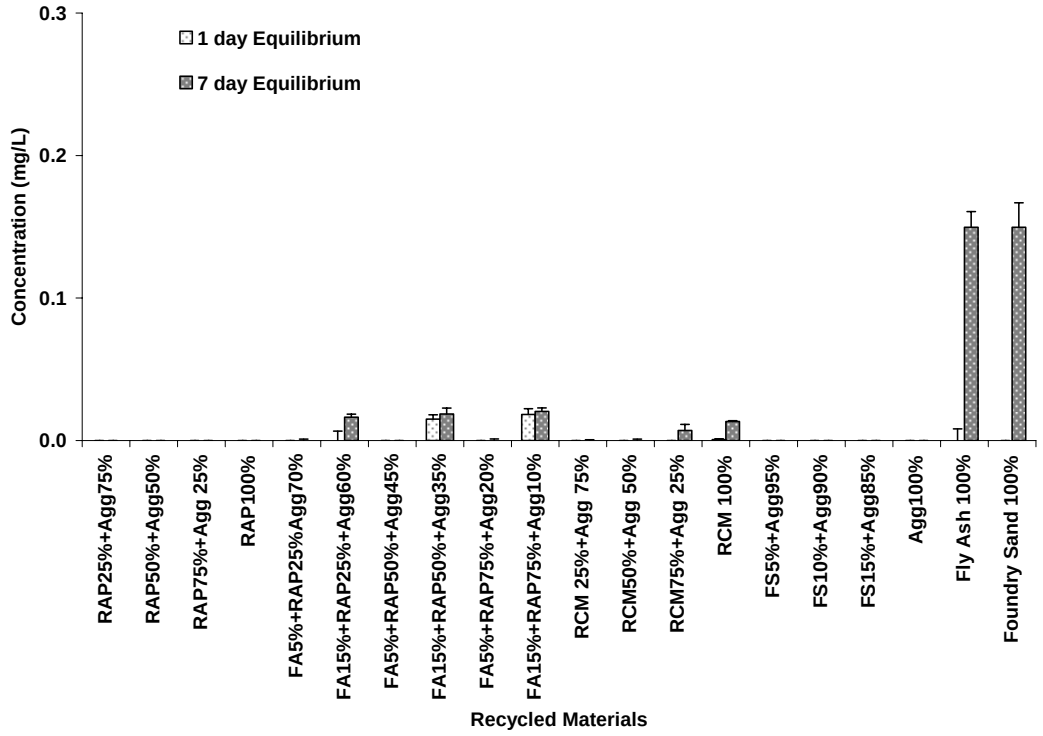

Figure A56. Chromium concentration in the filtrate from the batch test after 18 hrs (1 day) and 7 day equilibrium time.

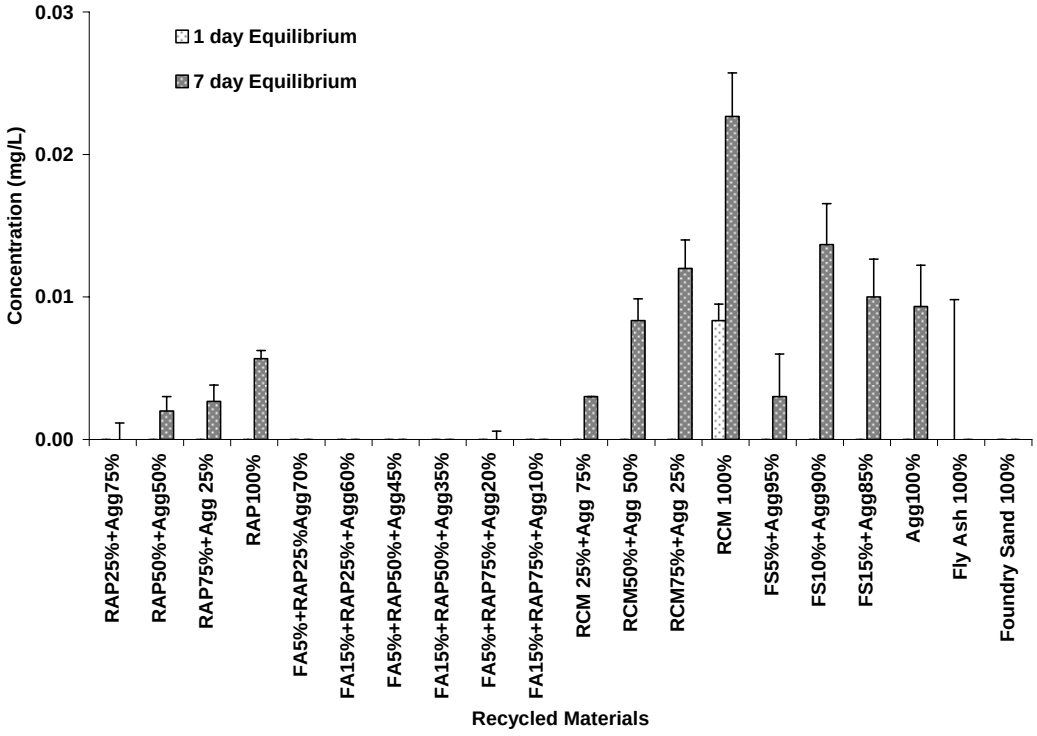

Figure A57. Copper concentration in the filtrate from the batch test after 18 hrs (1 day) and 7 day equilibrium time.

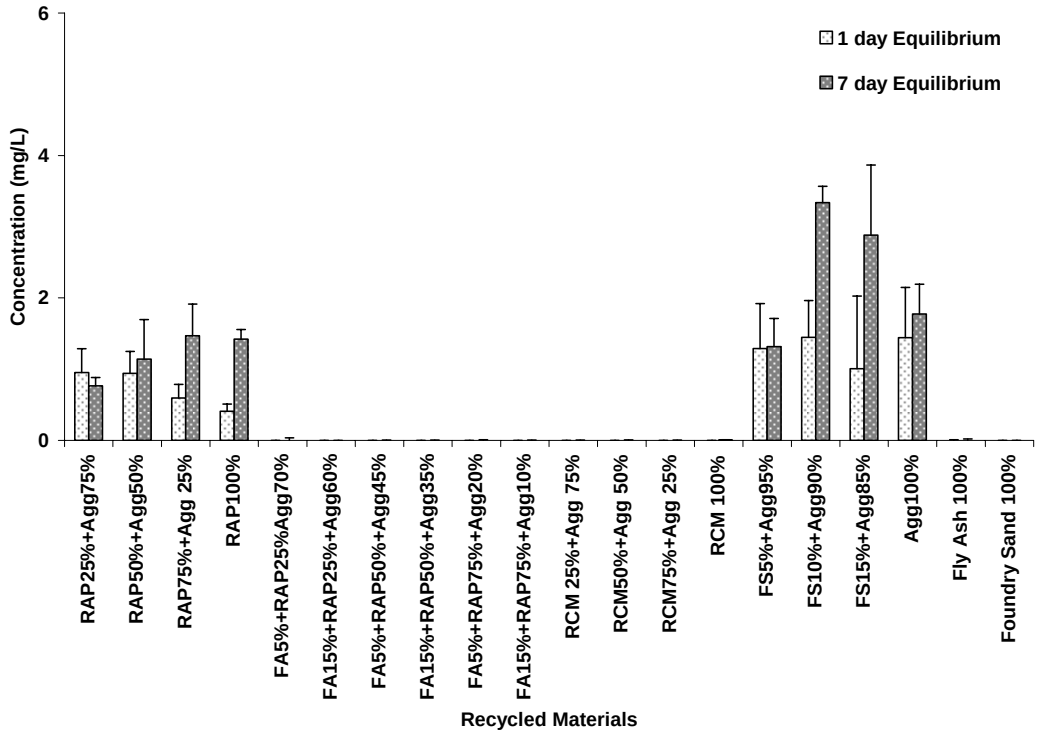

Figure A58. Iron concentration in the filtrate from the batch test after 18 hrs (1 day) and 7 day equilibrium time.

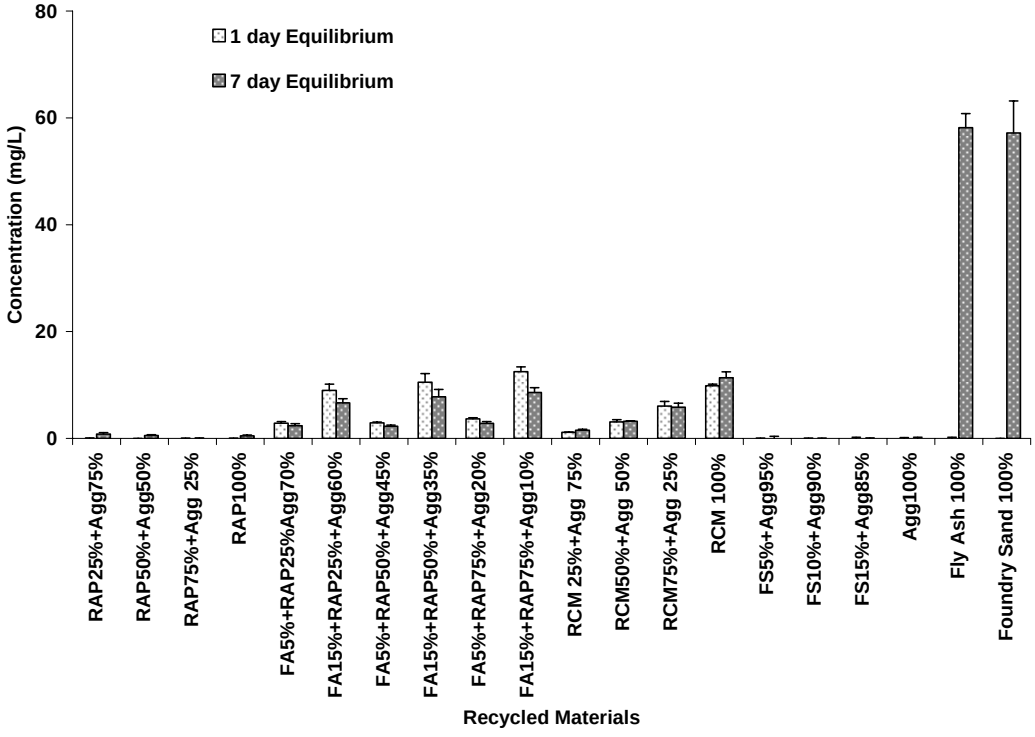

Figure A59. Potassium concentration in the filtrate from the batch test after 18 hrs (1 day) and 7 day equilibrium time.

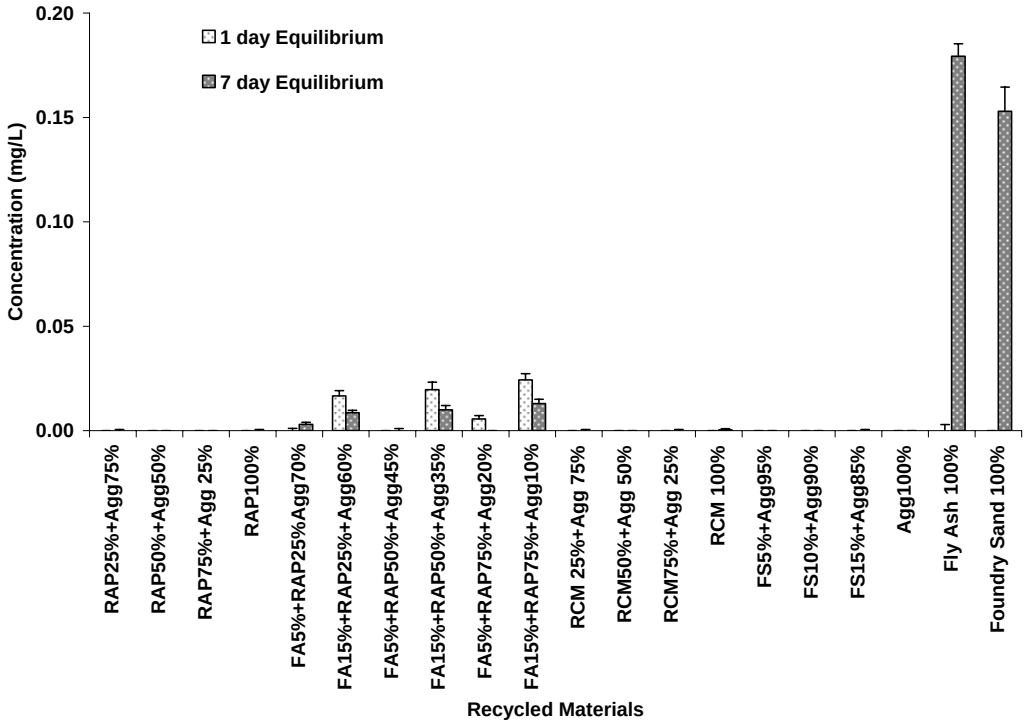

Figure A60. Lithium concentration in the filtrate from the batch test after 18 hrs (1 day) and 7 day equilibrium time.

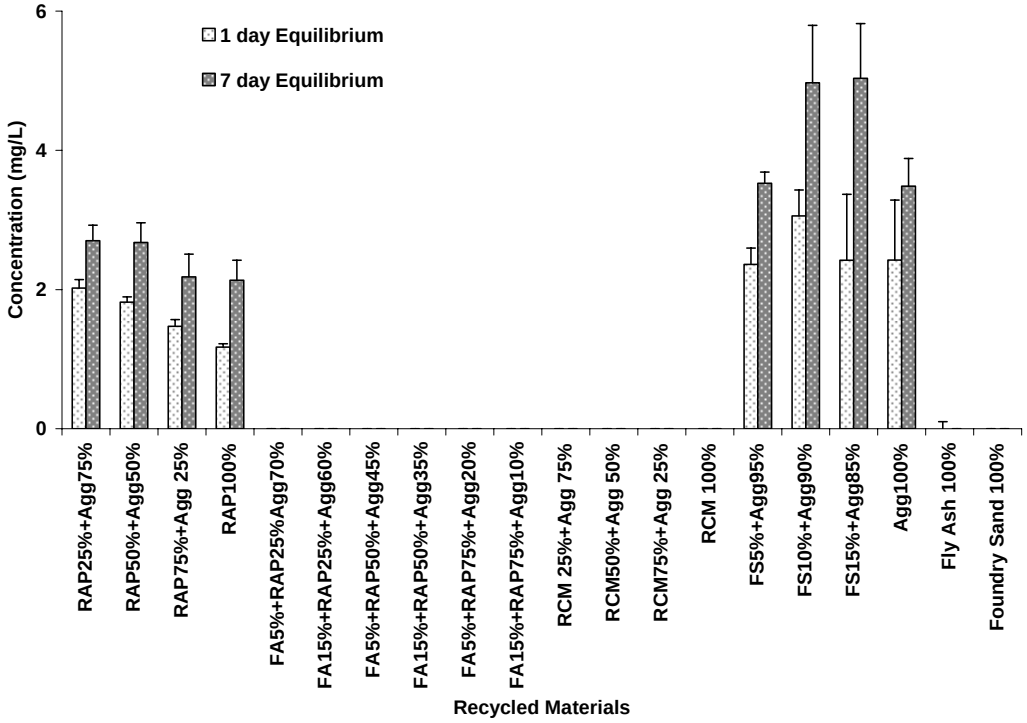

Figure A61. Magnesium concentration in the filtrate from the batch test after 18 hrs (1 day) and 7 day equilibrium time.

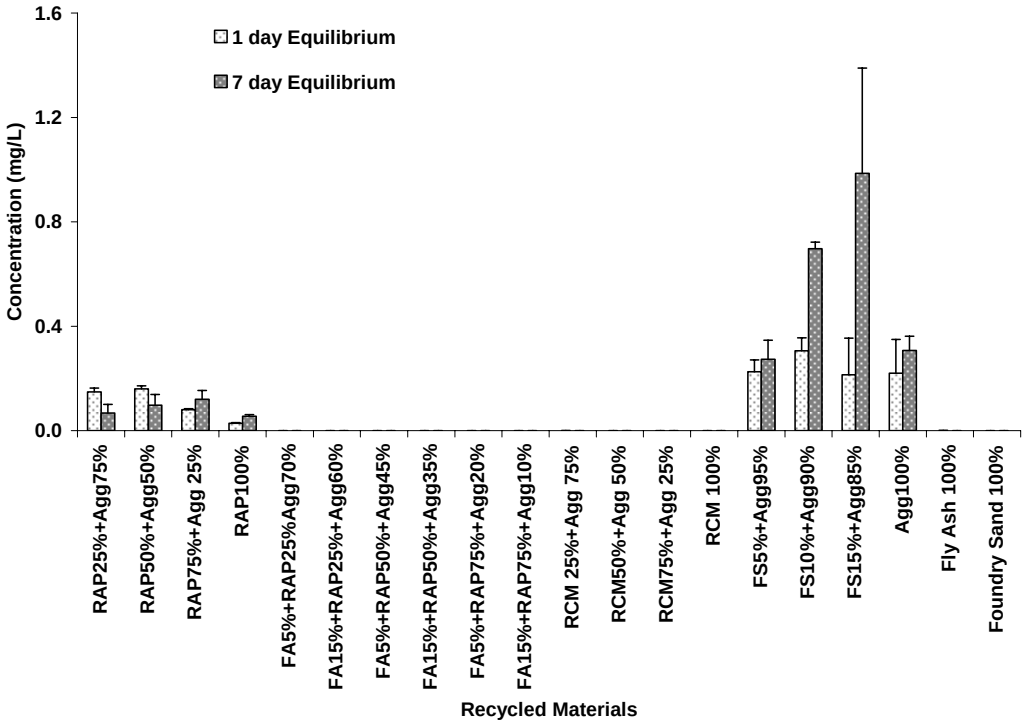

Figure A62. Manganese concentration in the filtrate from the batch test after 18 hrs (1 day) and 7 day equilibrium time.

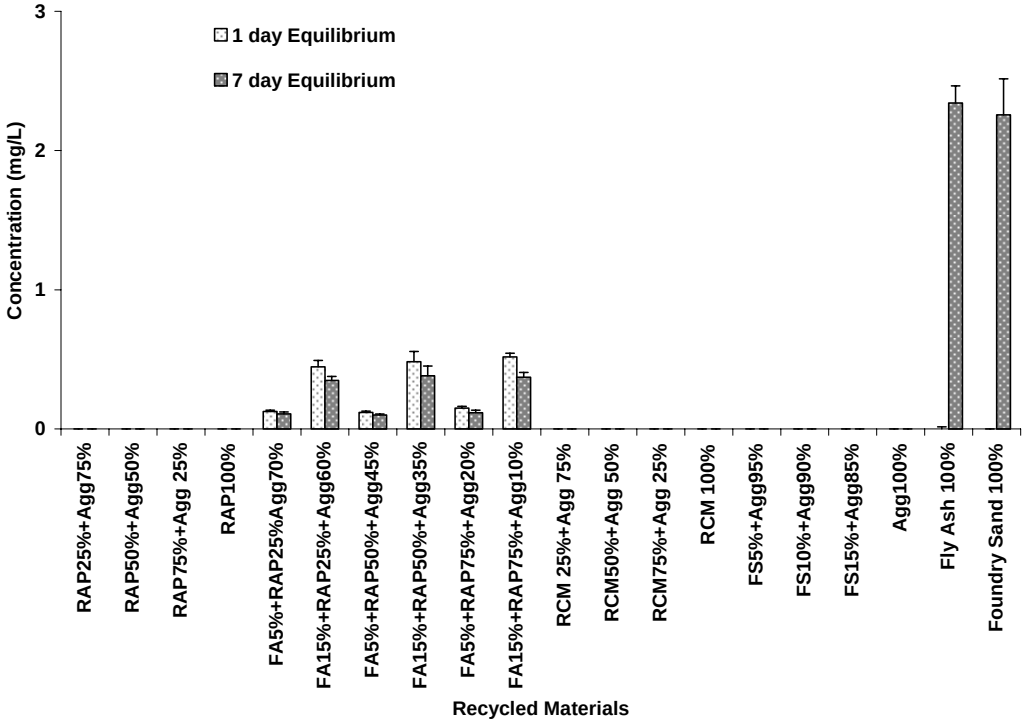

Figure A63. Molybdenum concentration in the filtrate from the batch test after 18 hrs (1 day) and 7 day equilibrium time.

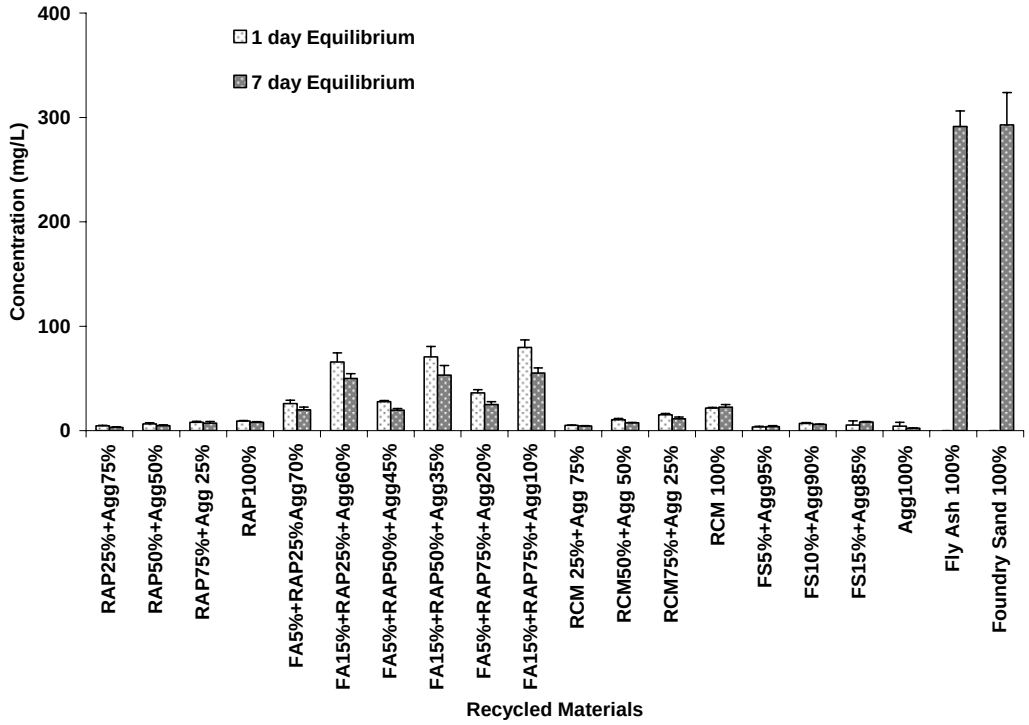

Figure A64. Sodium concentration in the filtrate from the batch test after 18 hrs (1 day) and 7 day equilibrium time.

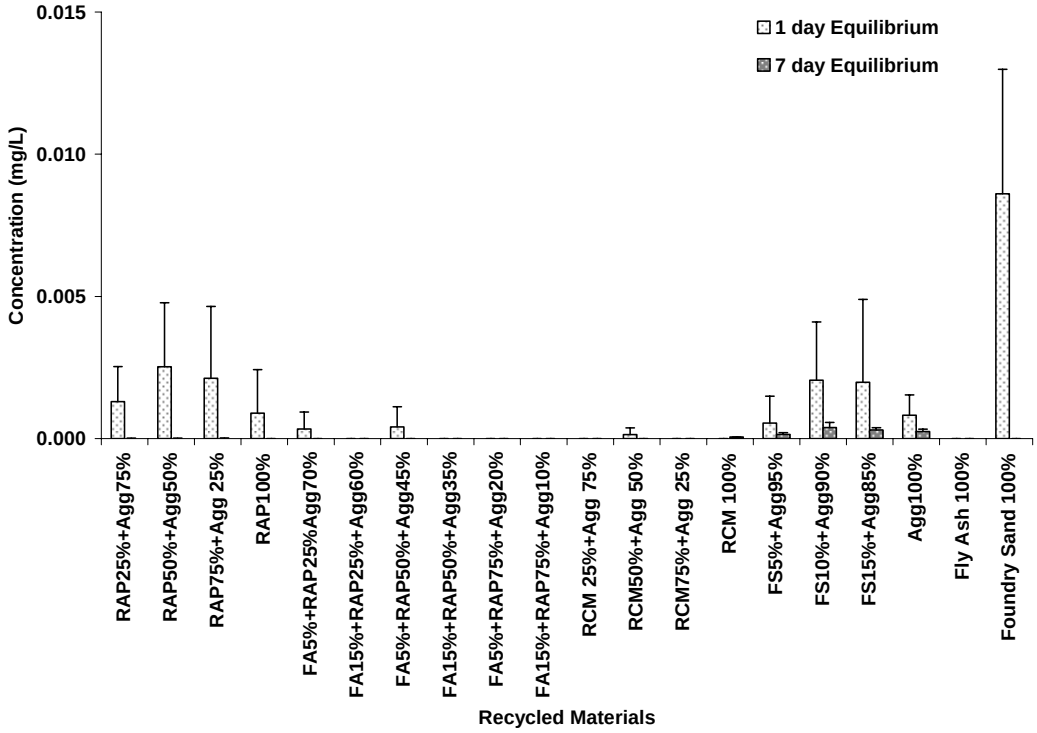

Figure A65. Lead concentration in the filtrate from the batch test after 18 hrs (1 day) and 7 day equilibrium time.

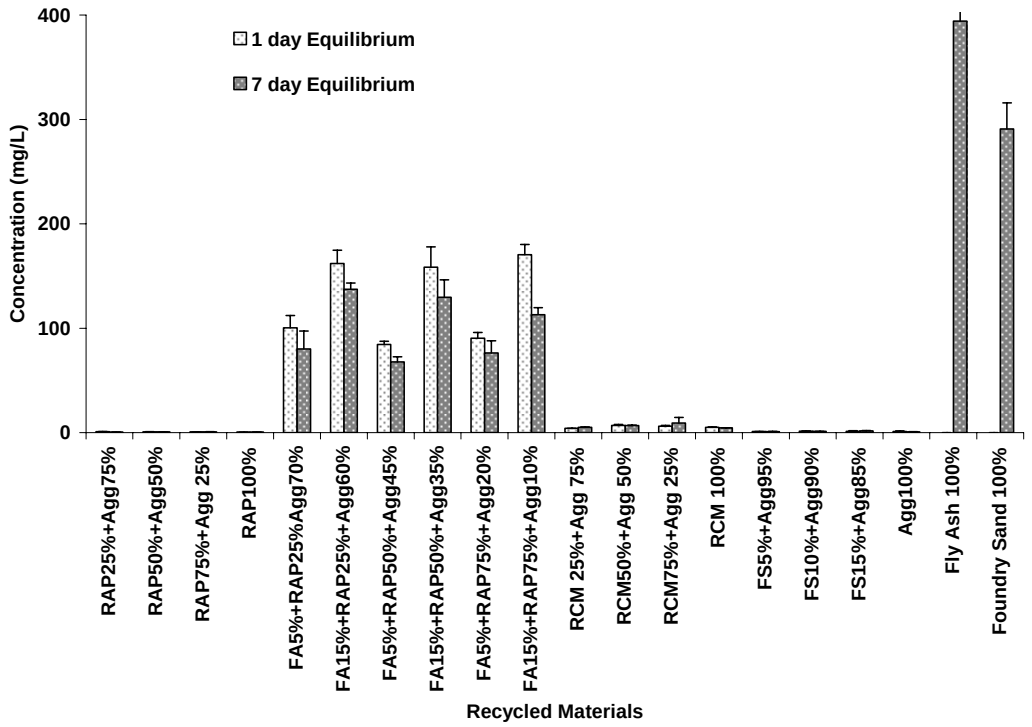

Figure A66. Sulfur concentration in the filtrate from the batch test after 18 hrs (1 day) and 7 day equilibrium time.

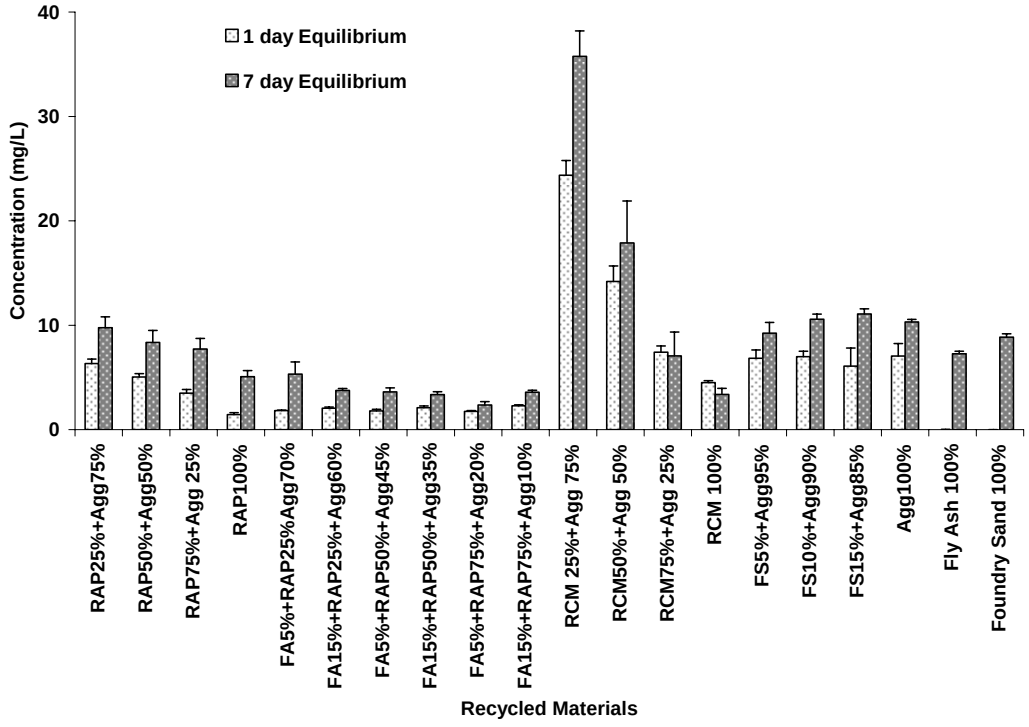

Figure A67. Silicon concentration in the filtrate from the batch test after 18 hrs (1 day) and 7 day equilibrium time.

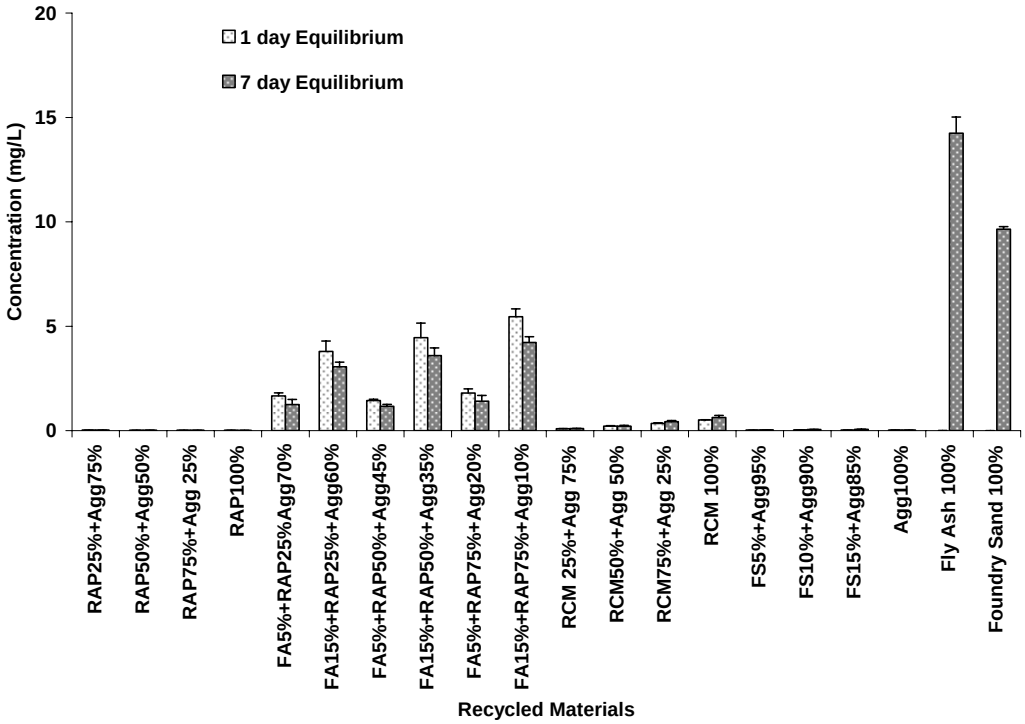

Figure A68. Strontium concentration in the filtrate from the batch test after 18 hrs (1 day) and 7 day equilibrium time.

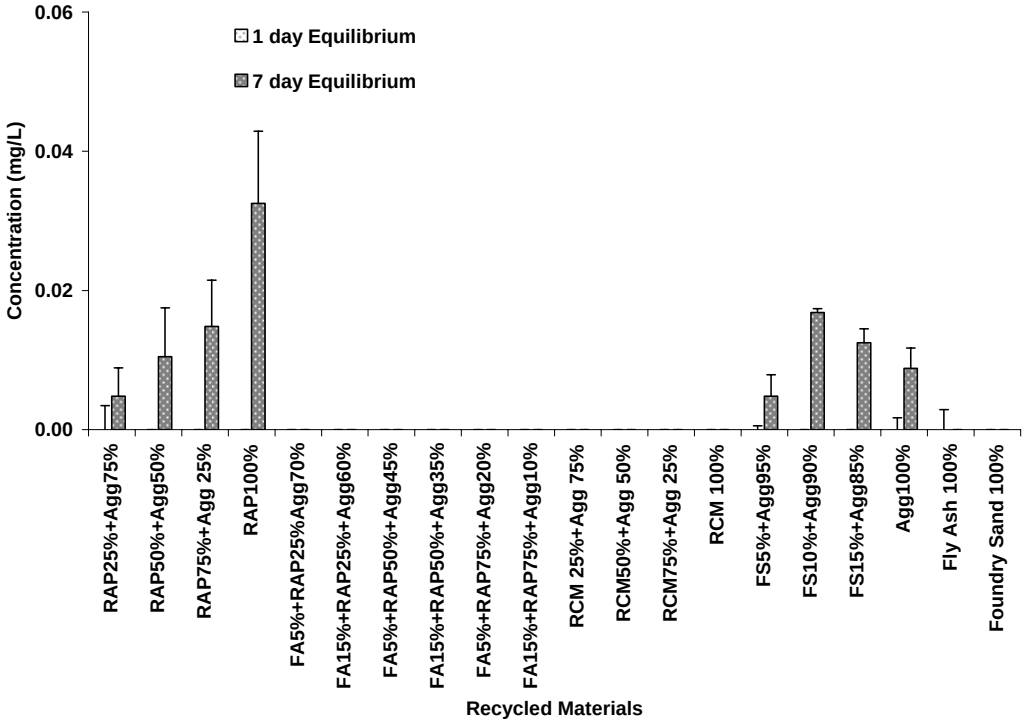

Figure A69. Titanium concentration in the filtrate from the batch test after 18 hrs (1 day) and 7 day equilibrium time.

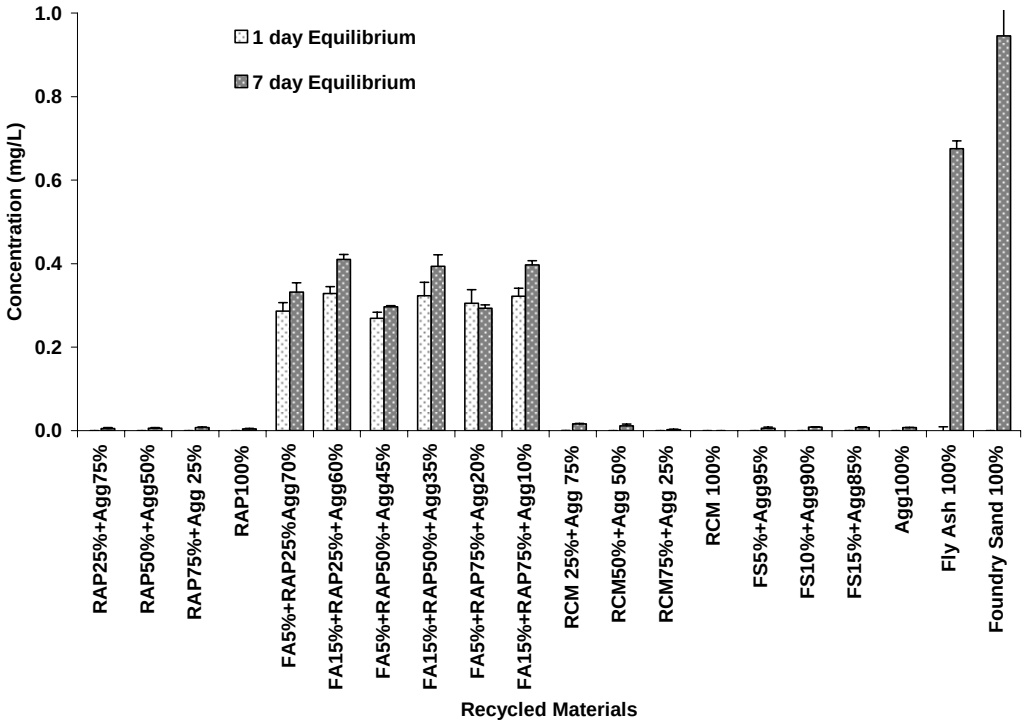

Figure A70. Vanadium concentration in the filtrate from the batch test after 18 hrs (1 day) and 7 day equilibrium time.

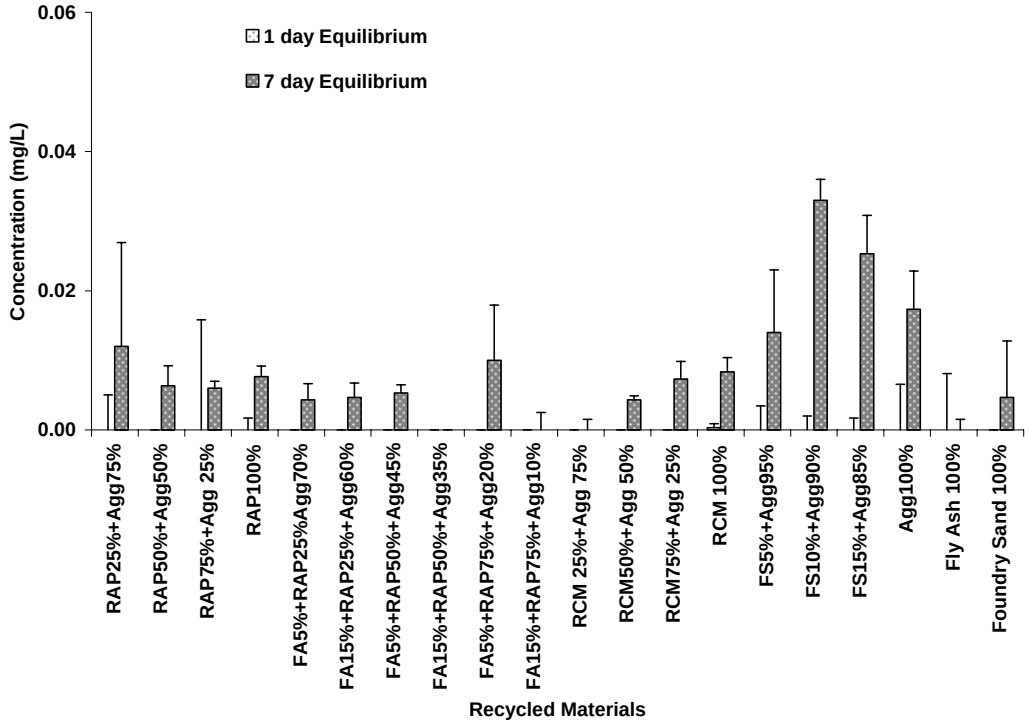

Figure A71. Zinc concentration in the filtrate from the batch test after 18 hrs (1 day) and 7 day equilibrium time.

Table A47. Inorganic chemical concentrations (mg/L) in the filtrate after 18 hrs (1 day) and 7 day batch tests.

Chemical	Al		As		B		Ba		Be		Ca		Cd		Co	
Material/Equilibrium Time	1 Day	7 Day	1 Day	7 Day	1 Day	7 Day	1 Day	7 Day	1 Day	7 Day	1 Day	7 Day	1 Day	7 Day	1 Day	7 Day
EPA Drinking Water STD (mg/L)	0.05~0.2		0.01		-		2		0.004		-		0.005		-	
25% RAP+75%Agg	0.397	0.324	0.143	0.243	0.035	0.034	0.158	0.117	<	<	9.800	12.290	<	<	<	<
50% RAP+50%Agg	0.356	0.566	0.105	<	0.024	0.018	0.143	0.119	<	<	8.463	11.345	<	<	<	<
75% RAP+25%Agg	0.264	0.694	0.269	<	0.026	0.012	0.126	0.109	<	<	6.299	9.513	<	<	<	<
100% RAP	0.372	1.267	0.179	0.017	<	<	0.070	0.085	<	<	4.063	6.934	<	<	<	<
5% FA+25% RAP+70% Agg	8.908	2.582	0.046	<	0.952	0.847	0.217	0.278	<	<	126.493	91.646	<	<	<	<
15% FA+25% RAP+60% Agg	13.331	7.692	<	<	0.597	0.738	0.085	0.387	<	<	185.173	144.760	<	<	<	<
5% FA+50% RAP+45% Agg	10.295	5.074	0.113	<	0.805	0.726	0.228	0.284	<	<	108.773	80.805	<	<	<	<
15% FA+50% RAP+35% Agg	14.536	8.488	<	<	0.107	0.262	0.104	0.399	<	<	179.313	131.872	<	<	<	<
5% FA+75% RAP+20% Agg	15.397	10.119	<	<	0.871	0.748	0.225	0.331	<	<	122.139	90.372	<	<	<	<
15% FA+75% RAP+10% Agg	12.909	8.528	<	<	0.046	0.113	0.088	0.466	<	<	185.609	116.909	<	<	<	<
25% RCM+75% Agg	0.083	0.093	<	<	0.014	0.018	0.024	0.026	<	<	38.979	47.400	<	<	<	<
50% RCM+50% Agg	1.097	0.768	0.021	<	0.012	0.008	0.029	0.039	<	<	75.049	68.729	<	<	<	<
75% RCM+25% Agg	2.288	1.841	0.097	<	<	<	0.042	0.070	<	<	104.023	117.314	<	<	<	<
100 % RCM	3.139	3.306	0.217	<	0.004	<	0.055	0.090	<	<	141.239	152.398	<	<	<	<
5% FS + 95% Agg	0.572	0.584	0.003	<	0.021	0.028	0.123	0.163	<	<	10.384	16.186	<	<	<	<
10% FS + 90% Agg	0.857	1.640	0.067	<	0.052	0.020	0.181	0.234	<	<	10.700	20.373	<	<	<	<
15% FS + 85% Agg	0.596	1.802	0.044	<	0.029	0.023	0.144	0.279	<	<	9.029	22.577	<	<	<	<
100% Agg	0.662	0.647	0.048	0.108	0.042	0.022	0.165	0.147	<	<	9.390	17.760	<	<	<	<
100% Fly Ash	<	3.541	<	0.010	<	0.064	0.000	0.185	<	<	<	239.877	<	<	<	<
100% Foundry Sand	<	4.307	0.620	<	<	0.069	0.000	0.220	<	<	<	120.915	<	<	<	<

(Continue)

Chemical	Cr		Cu		Fe		K		Li		Mg		Mn		Mo	
Material/Equilibrium Time	1 Day	7 Day	1 Day	7 Day	1 Day	7 Day	1 Day	7 Day	1 Day	7 Day	1 Day	7 Day	1 Day	7 Day	1 Day	7 Day
EPA Drinking Water STD (mg/L)	0.1		1.3		0.3		-		-		-		-		-	
25% RAP+75%Agg	<	<	<	<	7.10	0.77	<	0.80	<	<	2.02	2.70	0.23	0.07	<	<
50% RAP+50%Agg	<	<	<	0.002	6.58	1.14	<	0.52	<	<	1.82	2.68	0.31	0.10	<	<
75% RAP+25%Agg	<	<	<	0.003	3.65	1.47	<	<	<	<	1.47	2.18	0.12	0.12	<	<
100% RAP	<	<	<	0.006	2.04	1.42	<	0.49	<	<	1.17	2.13	0.00	0.06	<	<
5% FA+25% RAP+70% Agg	<	<	<	<	<	<	2.83	2.33	<	0.00	<	<	<	<	0.13	0.11
15% FA+25% RAP+60% Agg	<	0.016	<	<	<	<	8.98	6.65	0.02	0.01	<	<	<	<	0.45	0.35
5% FA+50% RAP+45% Agg	<	<	<	<	<	<	2.89	2.27	<	<	<	<	<	<	0.12	0.10
15% FA+50% RAP+35% Agg	0.015	0.019	<	<	<	<	10.50	7.79	0.02	0.01	<	<	<	<	0.48	0.38
5% FA+75% RAP+20% Agg	<	<	<	<	<	<	3.62	2.79	0.01	<	<	<	<	<	0.15	0.12
15% FA+75% RAP+10% Agg	0.018	0.020	<	<	<	<	12.49	8.61	0.02	0.01	<	<	<	<	0.52	0.37
25% RCM+75% Agg	<	<	<	0.003	<	<	1.16	1.51	<	<	<	<	<	<	<	<
50% RCM+50% Agg	<	<	<	0.008	<	<	3.09	3.21	<	<	<	<	<	<	<	<
75% RCM+25% Agg	<	0.007	<	0.012	<	<	6.01	5.85	<	<	<	<	<	<	<	<
100 % RCM	0.001	0.013	0.008333	0.023	<	0.00	9.85	11.35	<	0.00	<	<	<	<	<	<
5% FS + 95% Agg	<	<	<	0.003	10.79	1.32	<	<	<	<	2.36	3.53	0.75	0.27	<	<
10% FS + 90% Agg	<	<	<	0.014	8.34	3.34	<	<	<	<	3.06	4.97	0.77	0.70	<	<
15% FS + 85% Agg	<	<	<	0.010	17.77	2.88	<	<	<	<	2.42	5.03	2.51	0.99	<	<
100% Agg	<	<	<	0.009	19.06	1.77	<	<	<	<	2.43	3.49	3.42	0.31	<	<
100% Fly Ash	<	0.150	<	<	<	<	<	58.16	<	0.18	<	<	<	<	<	2.34
100% Foundry Sand	<	0.150	<	<	<	<	<	57.17	<	0.15	<	<	<	<	<	2.26

(Continue)

Chemical	Na		Ni		Pb		P		Rb		S		Si		Sr	
Material/Equilibrium Time	1 Day	7 Day	1 Day	7 Day	1 Day	7 Day	1 Day	7 Day	1 Day	7 Day	1 Day	7 Day	1 Day	7 Day	1 Day	7 Day
EPA Drinking Water STD (mg/L)					0.015											
25% RAP+75%Agg	4.675	3.107	<	<	0.888	<	<	<	<	<	0.890	0.640	6.276	9.782	<	0.026
50% RAP+50%Agg	6.537	4.961	<	<	2.322	<	<	<	<	<	0.720	0.691	4.984	8.372	<	0.022
75% RAP+25%Agg	8.138	7.418	<	<	2.117	<	<	<	<	<	0.586	0.808	3.440	7.723	<	0.019
100% RAP	9.267	8.103	<	<	<	2.800	<	<	<	<	0.402	0.612	1.388	5.082	<	0.013
5% FA+25% RAP+70% Agg	25.865	19.892	<	<	<	<	<	<	<	<	100.216	80.263	1.757	5.316	1.637	1.250
15% FA+25% RAP+60% Agg	65.800	49.962	<	<	<	<	<	<	<	<	161.884	137.368	1.997	3.762	3.775	3.061
5% FA+50% RAP+45% Agg	27.803	19.760	<	<	<	<	<	<	<	<	84.444	67.784	1.744	3.627	1.425	1.170
15% FA+50% RAP+35% Agg	70.709	53.166	<	<	<	<	<	<	<	<	158.434	129.645	2.042	3.360	4.431	3.597
5% FA+75% RAP+20% Agg	36.189	24.933	<	<	<	<	<	<	<	<	90.348	76.282	1.686	2.376	1.784	1.408
15% FA+75% RAP+10% Agg	79.617	55.270	<	<	<	<	<	<	<	<	170.437	112.912	2.235	3.599	5.434	4.229
25% RCM+75% Agg	5.064	4.542	<	<	<	<	<	<	<	<	4.000	5.105	24.320	35.746	0.071	0.107
50% RCM+50% Agg	10.507	7.534	<	<	<	<	<	<	<	<	6.797	6.795	14.131	17.900	0.195	0.216
75% RCM+25% Agg	15.141	11.546	<	<	<	<	<	<	<	<	6.101	9.227	7.360	7.070	0.325	0.435
100 % RCM	21.542	22.640	<	<	<	<	<	<	<	<	4.907	4.629	4.439	3.379	0.492	0.629
5% FS + 95% Agg	3.609	4.018	<	<	<	3.961	<	0.093	<	<	0.934	1.025	6.771	9.248	<	0.036
10% FS + 90% Agg	7.007	6.057	<	<	1.912	5.463	<	0.335	<	<	1.465	1.261	6.932	10.588	<	0.055
15% FS + 85% Agg	5.500	8.352	<	<	1.980	4.166	<	0.249	<	<	1.127	1.771	6.035	11.086	<	0.066
100% Agg	4.239	2.422	<	<	<	7.444	<	0.191	<	<	1.098	0.826	6.977	10.315	<	0.030
100% Fly Ash	<	291.392	<	<	<	<	<	<	<	<	<	394.170	<	7.268	<	14.250
100% Foundry Sand	<	292.825	<	<	8.605	14.614	<	<	<	<	<	291.024	<	8.877	<	9.654

(Continue)

Chemical	Ti		V		Zn	
Material/Equilibrium Time	1 Day	7 Day	1 Day	7 Day	1 Day	7 Day
EPA Drinking Water STD (mg/L)	-		-		5	
25% RAP+75%Agg	<	0.005	<	0.005	<	0.012
50% RAP+50%Agg	<	0.011	<	0.006	<	0.006
75% RAP+25%Agg	<	0.015	<	0.007	<	0.006
100% RAP	<	0.033	<	0.004	<	0.008
5% FA+25% RAP+70% Agg	<	<	0.286	0.332	<	0.004
15% FA+25% RAP+60% Agg	<	<	0.328	0.410	<	0.005
5% FA+50% RAP+45% Agg	<	<	0.269	0.296	<	0.005
15% FA+50% RAP+35% Agg	<	<	0.323	0.394	<	<
5% FA+75% RAP+20% Agg	<	<	0.305	0.293	<	0.010
15% FA+75% RAP+10% Agg	<	<	0.322	0.397	<	<
25% RCM+75% Agg	<	<	<	0.017	<	<
50% RCM+50% Agg	<	<	<	0.012	<	0.004
75% RCM+25% Agg	<	<	<	0.002	<	0.007
100 % RCM	<	<	<	<	0.000	0.008
5% FS + 95% Agg	<	0.005	<	0.006	<	0.014
10% FS + 90% Agg	<	0.017	<	0.009	<	0.033
15% FS + 85% Agg	<	0.013	<	0.008	<	0.025
100% Agg	<	0.009	<	0.007	<	0.017
100% Fly Ash	<	<	<	0.675	<	<
100% Foundry Sand	<	<	<	0.946	<	0.005

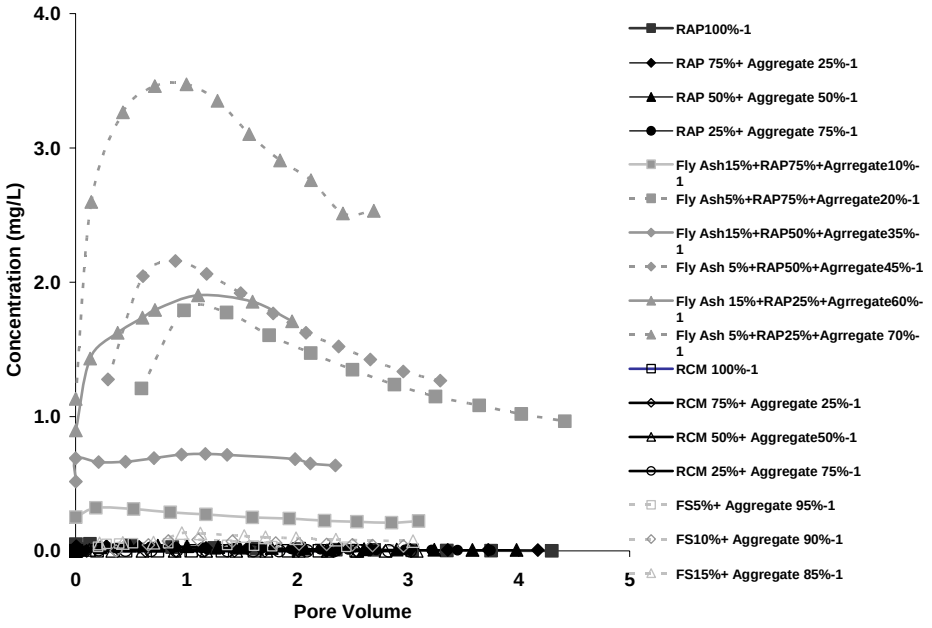

Figure A72. Variation in the concentration of boron as a function of pore volume during leaching under saturated conditions. Leachate from the fly ash mixtures had higher boron concentration than the leachate from other recycled material mixtures. Highest boron concentration was detected in the leachate from 5% Fly Ash + 25% RAP+ 70% Aggregate mixture.

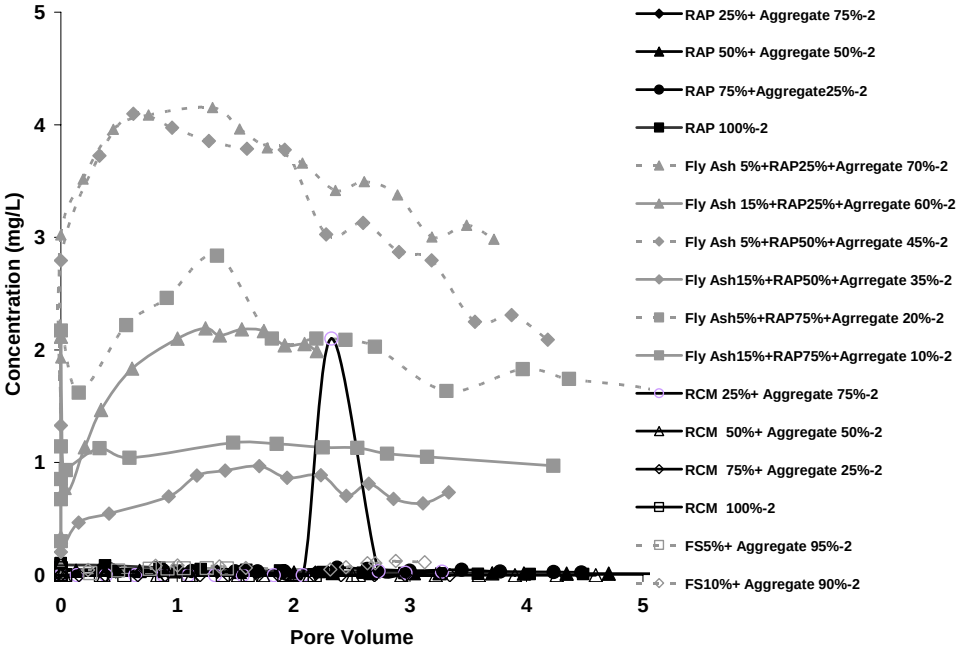

Figure A73. Variation in the concentration of boron as a function of pore volume during leaching under unsaturated conditions (2 kPa suction). Leachate from the fly ash mixtures had higher boron concentration than the leachate from other recycled material mixtures. Highest boron concentration was detected in the leachate from 5% Fly Ash + 25% RAP+ 70% Aggregate mixture.

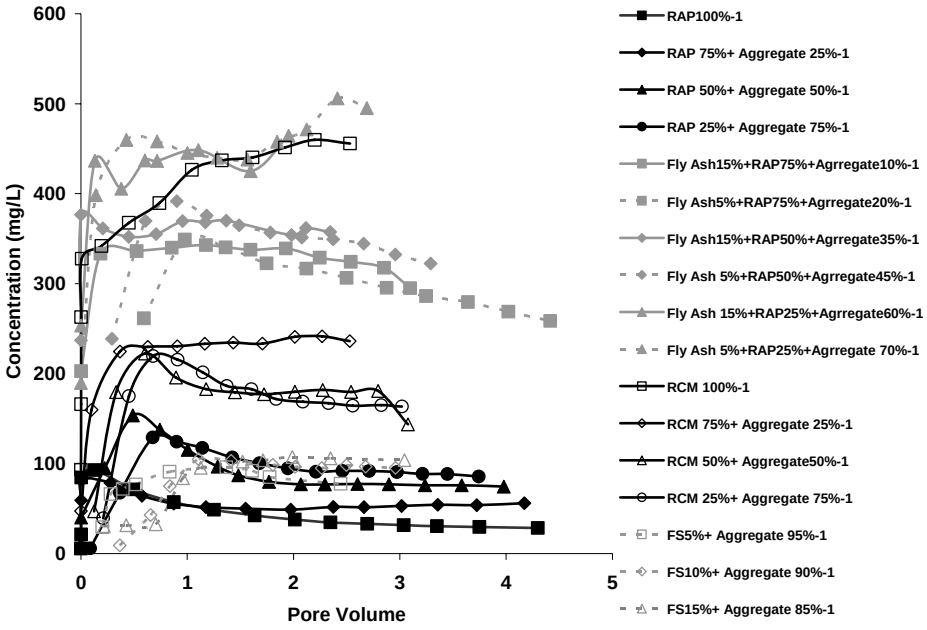

Figure A74. Variation in the concentration of calcium as a function of pore volume during leaching under saturated conditions. Highest calcium concentration was detected in the leachate from the fly ash mixtures and the fly ash and RCM mixtures.

.

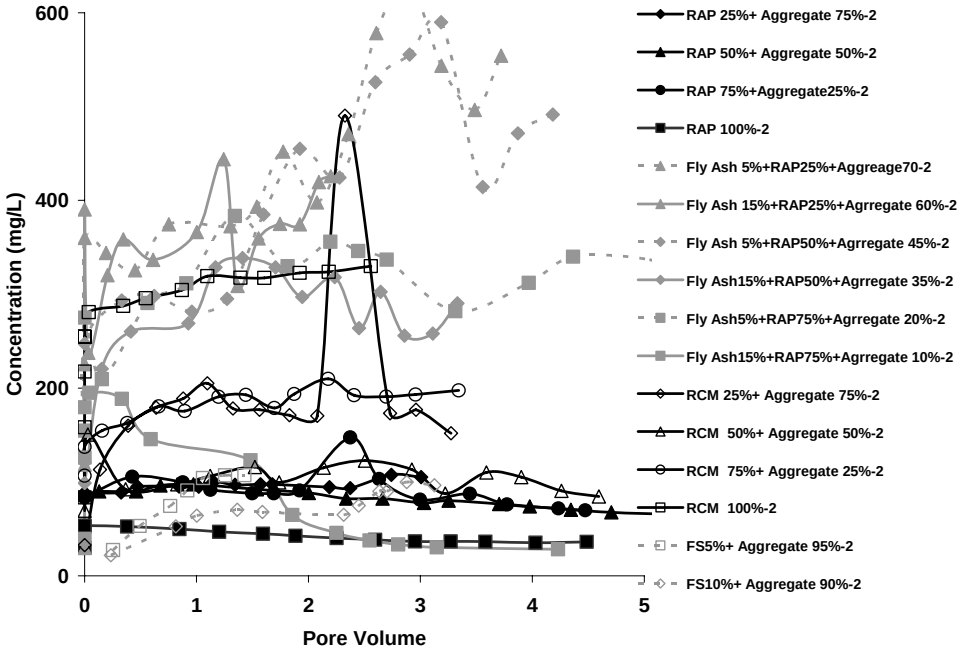

Figure A75. Variation in the concentration of calcium as a function of pore volume during leaching under unsaturated conditions (2 kPa suction). Highest calcium concentration was detected in the leachate from the fly ash mixtures and the fly ash and RCM mixtures.

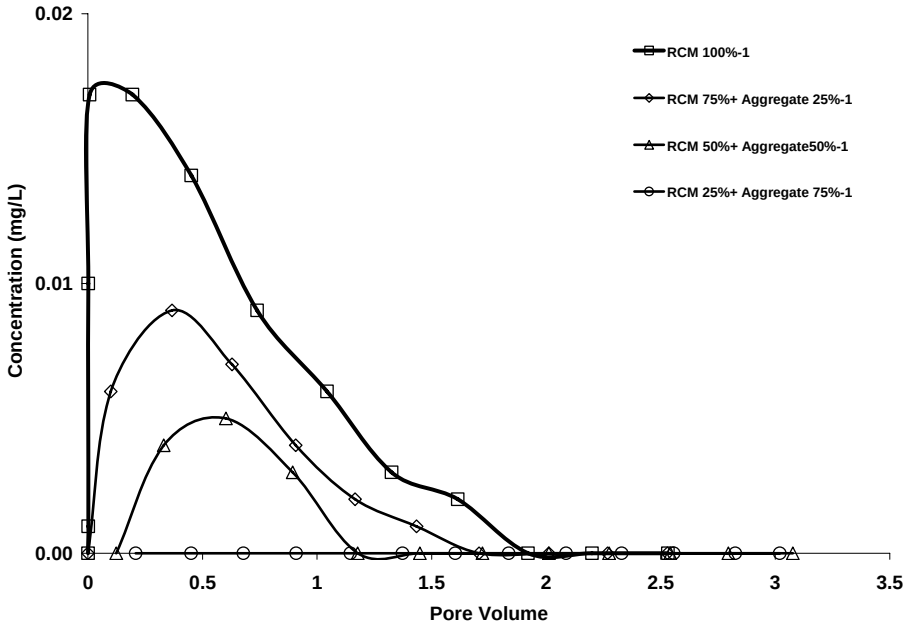

Figure A76. Variation in the concentration of cobalt as a function of pore volume during leaching under saturated conditions. Cobalt was detected in the leachate from mixtures of RCM only. Highest Cobalt concentration in the leachate was detected for 100% RCM.

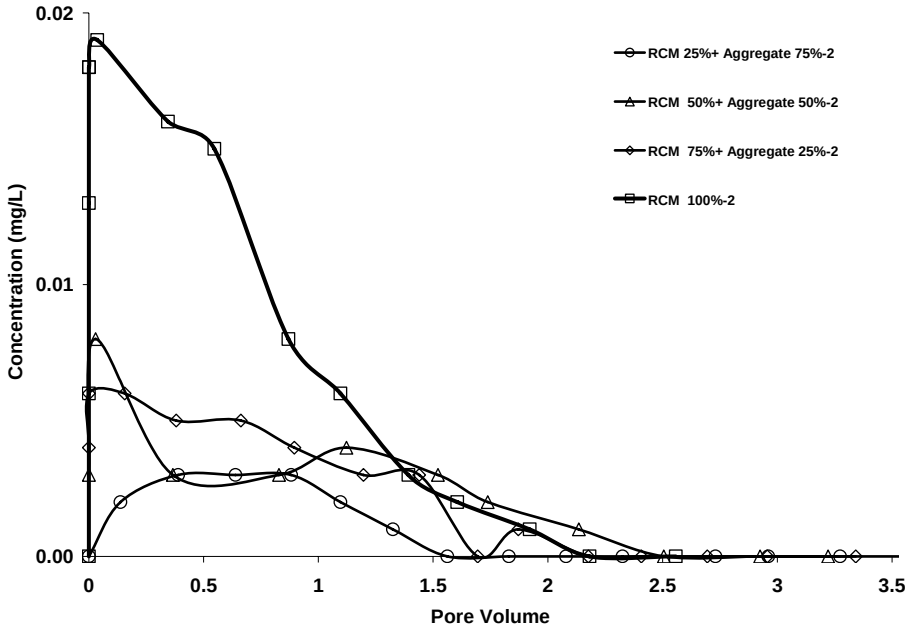

Figure A77. Variation in the concentration of cobalt as a function of pore volume during leaching under unsaturated conditions (2 kPa suction). Cobalt was detected in the leachate from mixtures of RCM only. Highest Cobalt concentration in the leachate was detected for 100% RCM.

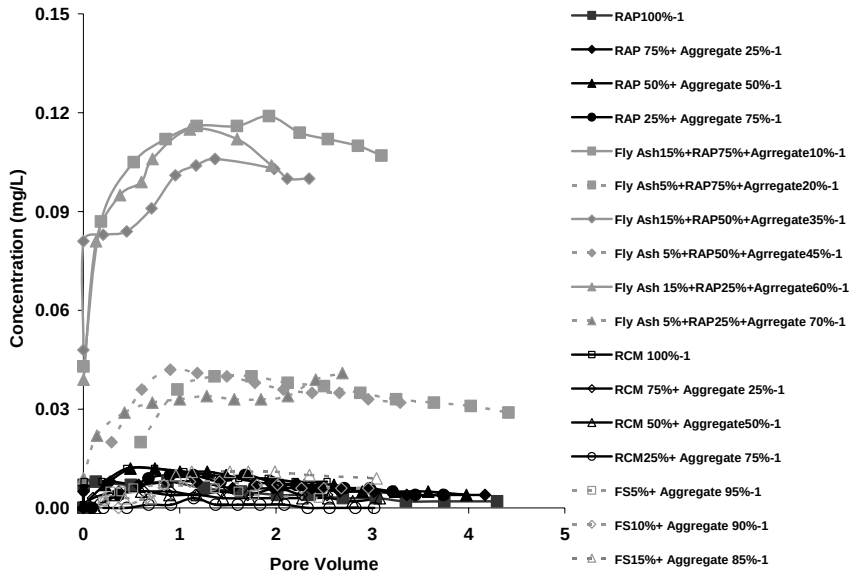

Figure A78. Variation in the concentration of lithium as a function of pore volume during leaching under saturated conditions. Leachate from the fly ash mixtures had higher lithium concentration than any other mixtures. Highest Li concentrations were in the leachate from mixtures containing 15% fly ash.

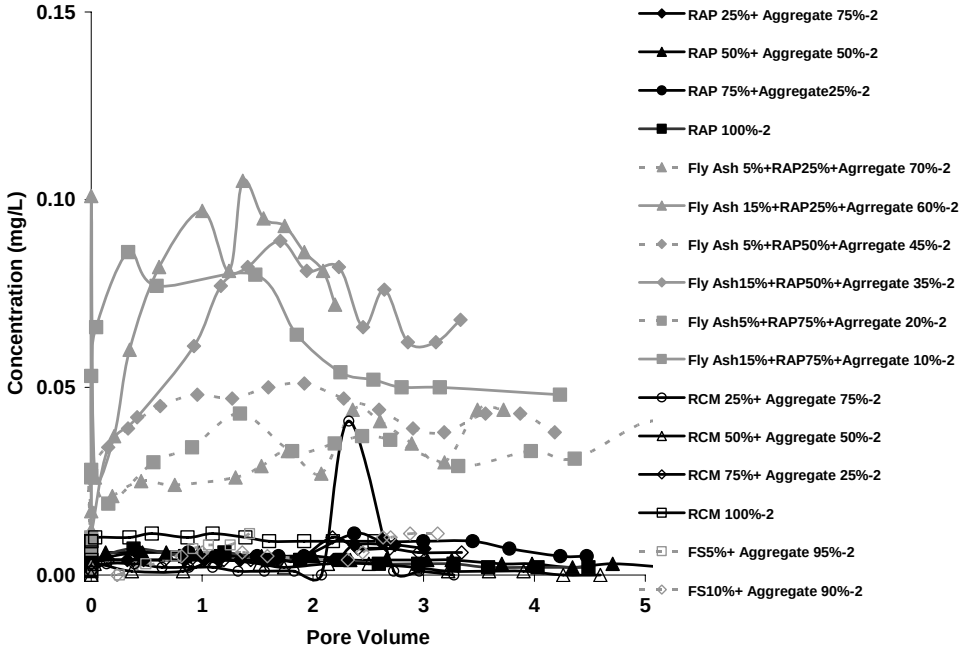

Figure A79. Variation in the concentration of lithium as a function of pore volume during leaching under unsaturated conditions (2 kPa suction). Leachate from the fly ash mixtures had higher Li concentration than any other mixtures. Highest Li concentrations were in the leachate from mixtures containing 15% fly ash.

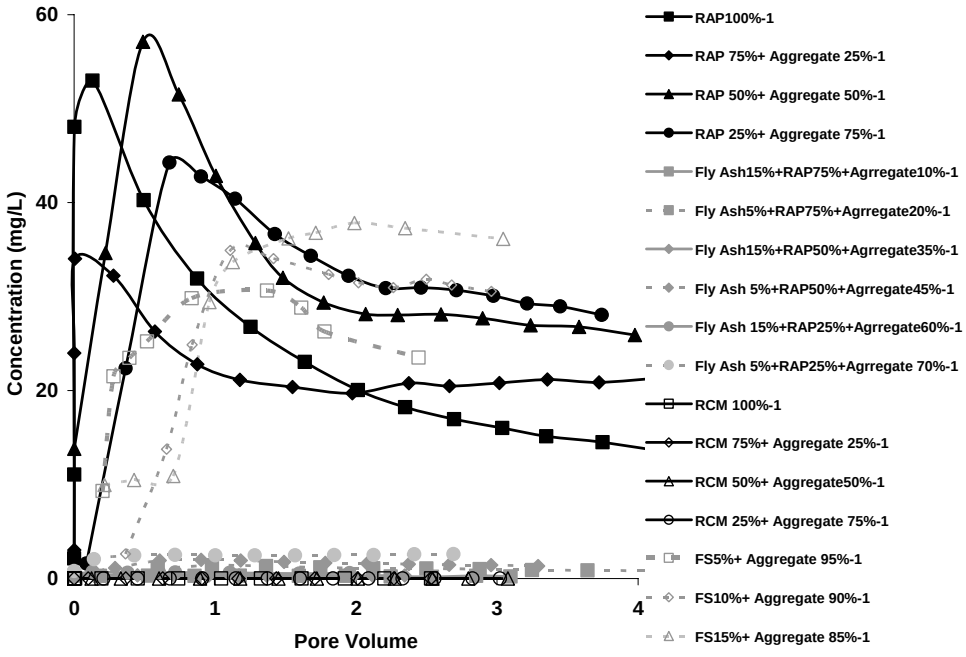

Figure A80. Variation in the concentration of magnesium as a function of pore volume during leaching under saturated conditions. Higher magnesium concentrations were detected in the leachate from RAP and Aggregate and FS and Aggregate mixtures.

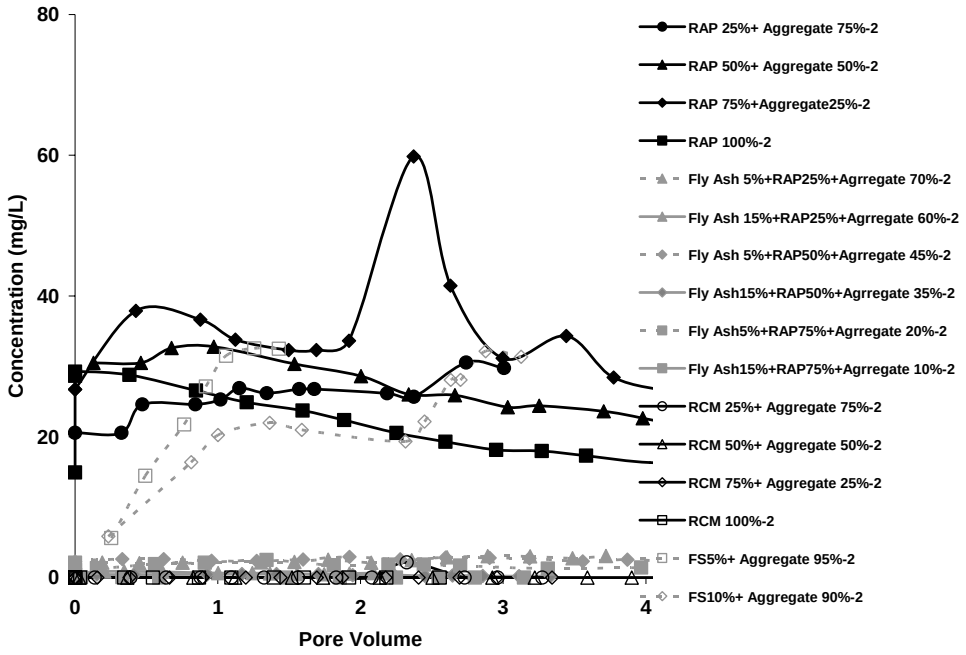

Figure A81. Variation in the concentration of magnesium as a function of pore volume during leaching under unsaturated conditions (2 kPa suction). Higher magnesium concentrations were detected in the leachate from RAP and Aggregate and FS and Aggregate mixtures.

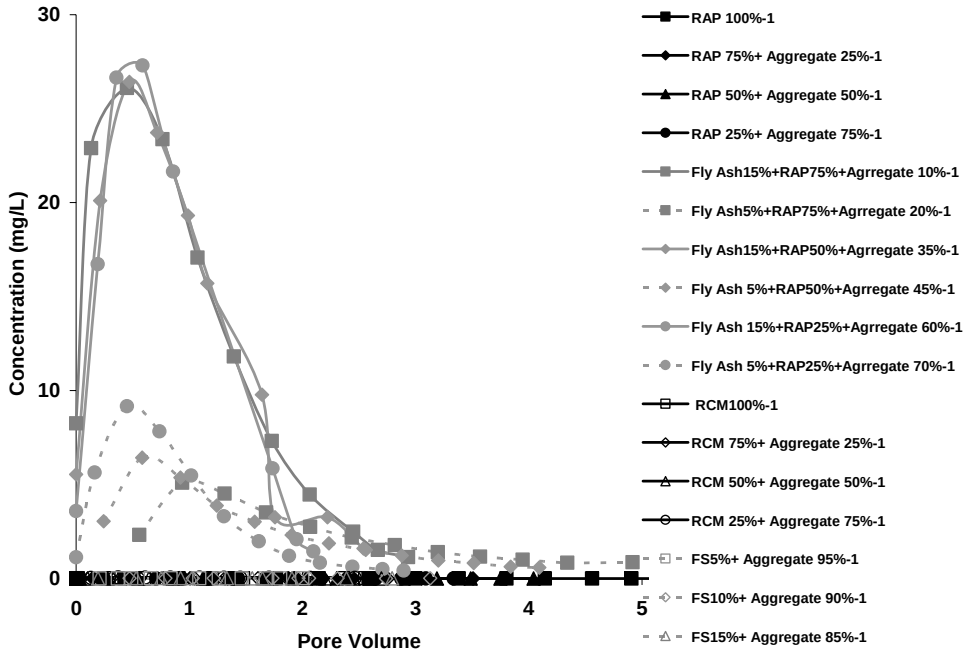

Figure A82. Variation in the concentration of molybdenum as a function of pore volume during leaching under saturated conditions. Higher molybdenum concentrations were detected in the leachate from mixtures of FA or RAP with aggregates. Molybdenum concentrations were also higher in leachate from mixtures containing 15% fly ash than mixtures containing 5% FA.

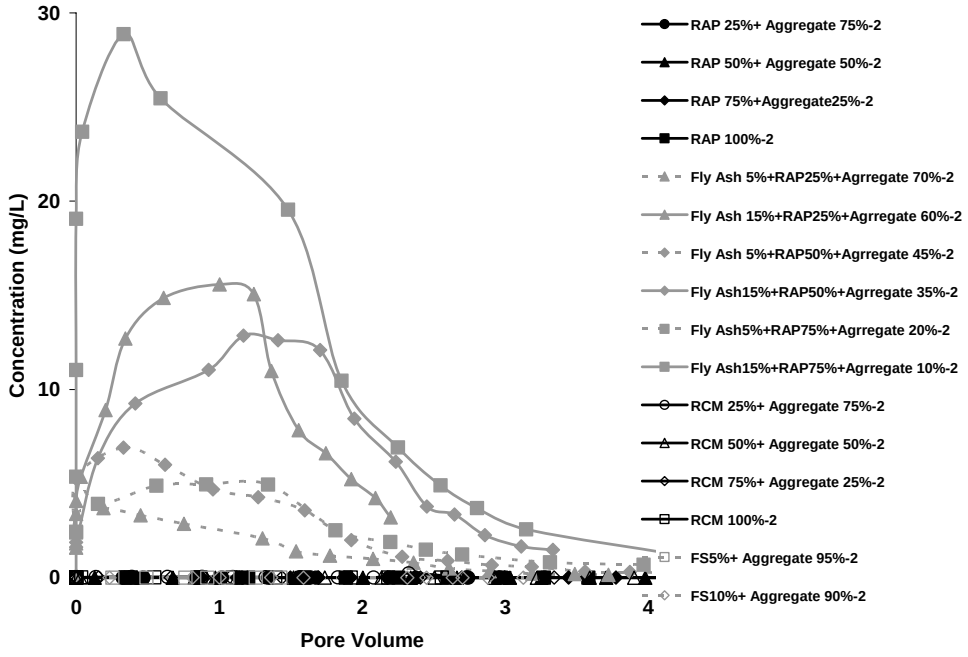

Figure A83. Variation in the concentration of molybdenum as a function of pore volume during leaching under unsaturated conditions (2 kPa suction). Higher molybdenum concentrations were detected in the leachate from mixtures of FA or RAP with aggregates. Molybdenum concentrations were also higher in leachate from mixtures containing 15% fly ash than mixtures containing 5% FA.

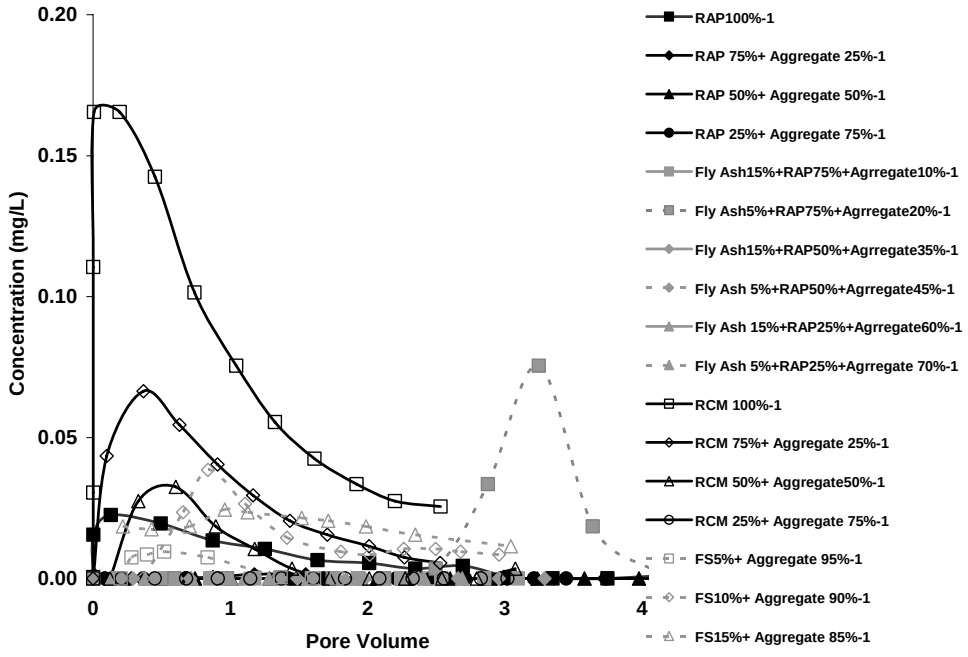

Figure A84. Variation in the concentration of nickel as a function of pore volume during leaching under saturated conditions. Higher nickel concentrations were detected in the leachate from mixtures of RCM and FS with aggregates.

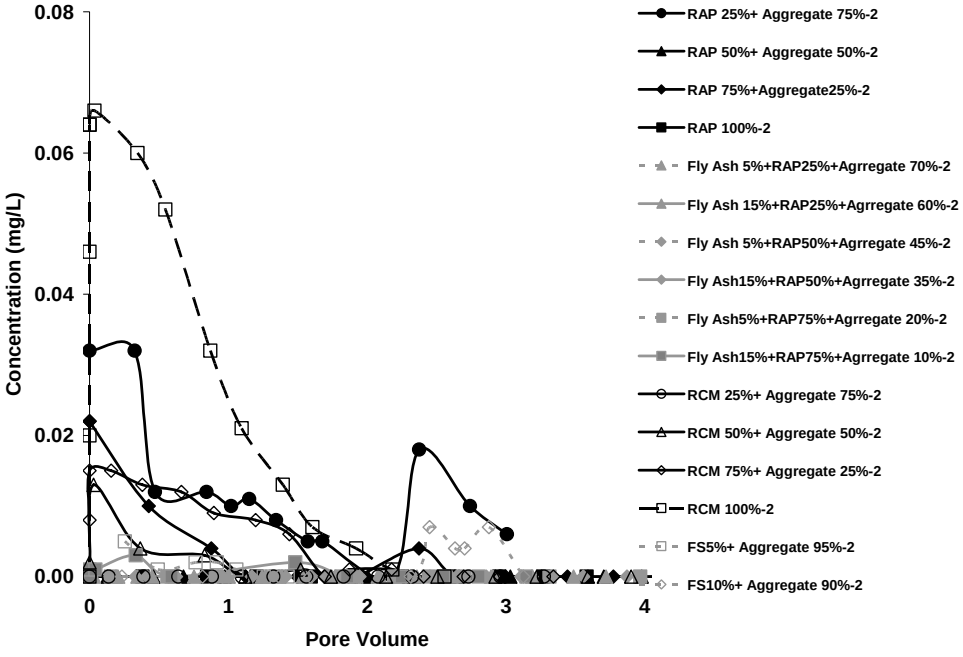

Figure A85. Variation in the concentration of nickel as a function of pore volume during leaching under unsaturated conditions (2 kPa suction). Higher nickel concentrations were detected in the leachate from mixtures of RCM and FS with aggregates.

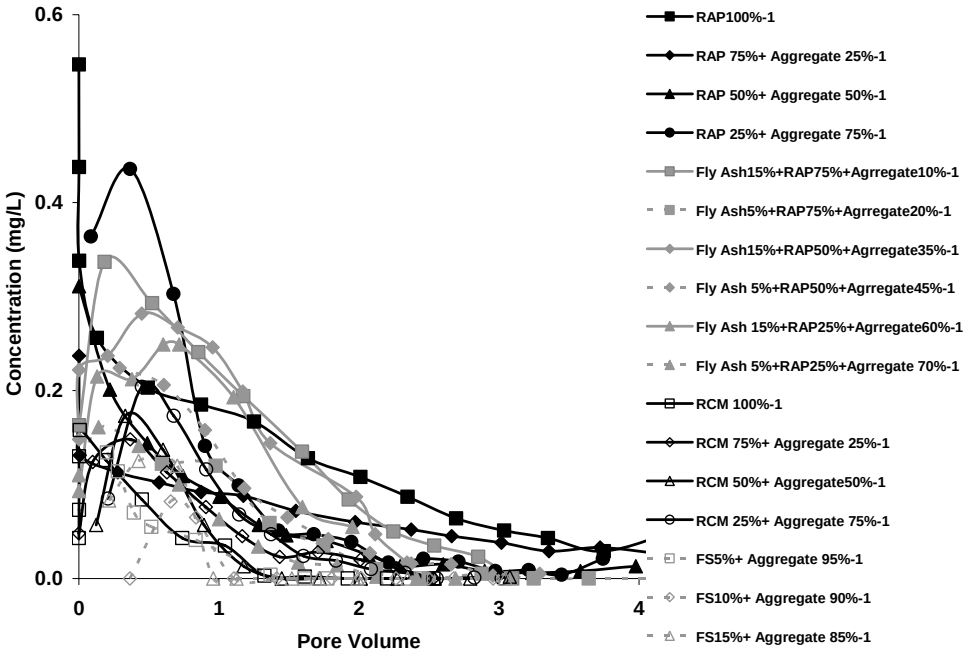

Figure A86. Variation in the concentration of phosphorus as a function of pore volume during leaching under saturated conditions.

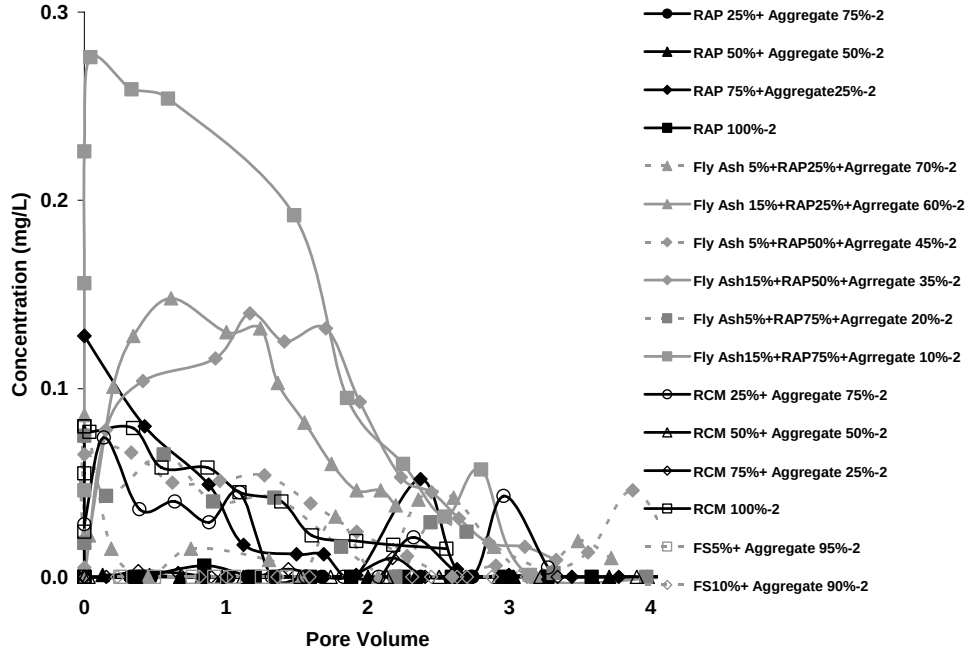

Figure A87. Variation in the concentration of nickel as a function of pore volume during leaching under unsaturated conditions (2 kPa suction).

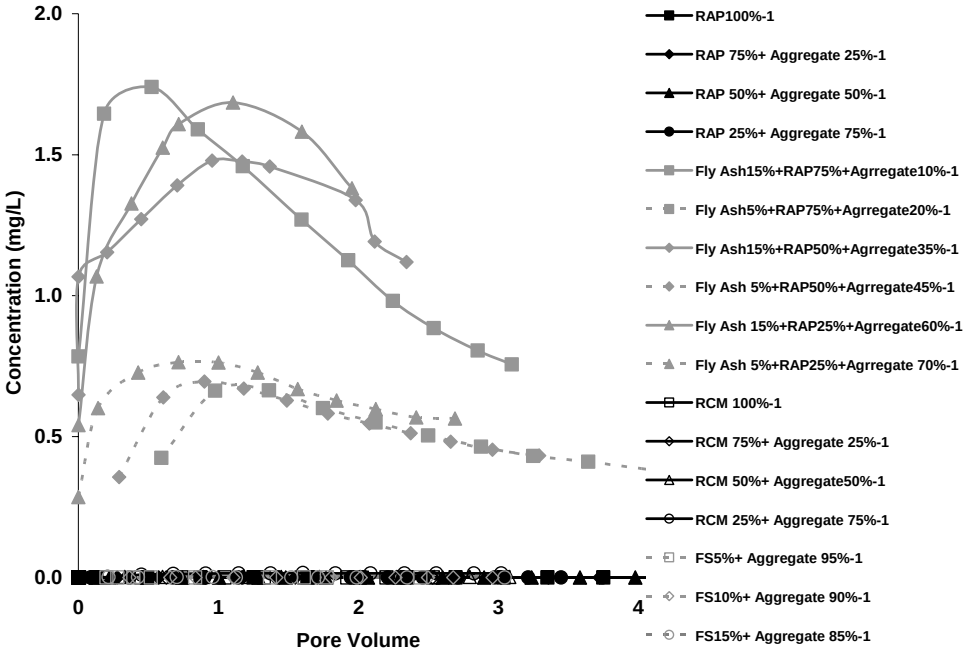

Figure A88. Variation in the concentration of vanadium as a function of pore volume during leaching under saturated conditions. Higher vanadium concentration was detected in the leachate from mixtures of FA and RAP with Aggregates. Vanadium concentrations were higher in the leachate from mixtures containing 15% fly ash than mixtures containing 5% FA.

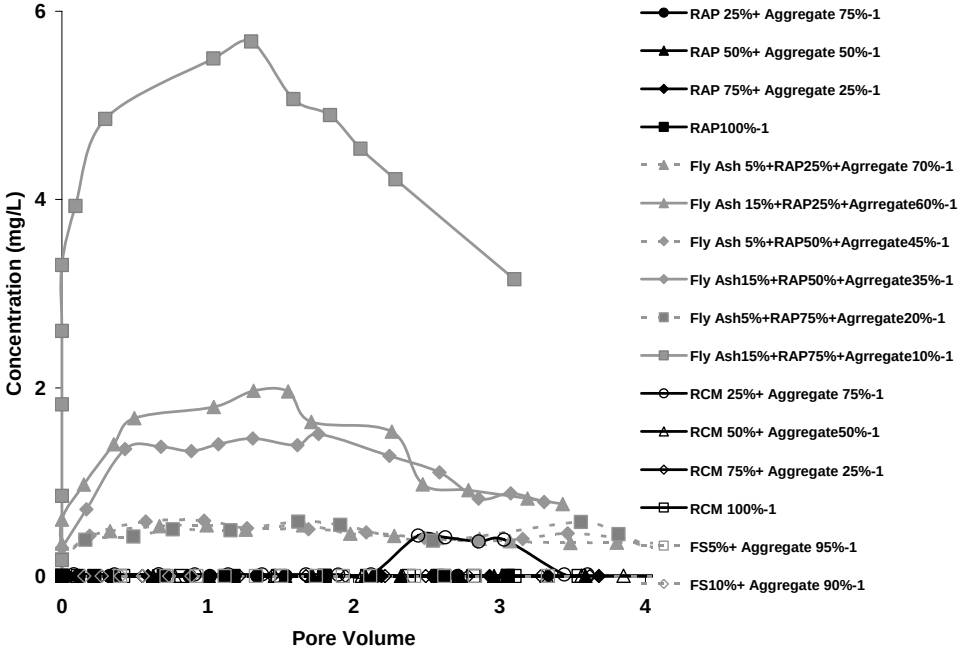

Figure A89. Variation in the concentration of vanadium as a function of pore volume during leaching under unsaturated conditions (2 kPa). Higher vanadium concentration was detected in the leachate from mixtures of FA and RAP with Aggregates. Vanadium concentrations were also higher in the leachate from mixtures containing 15% fly ash than mixtures containing 5% FA.

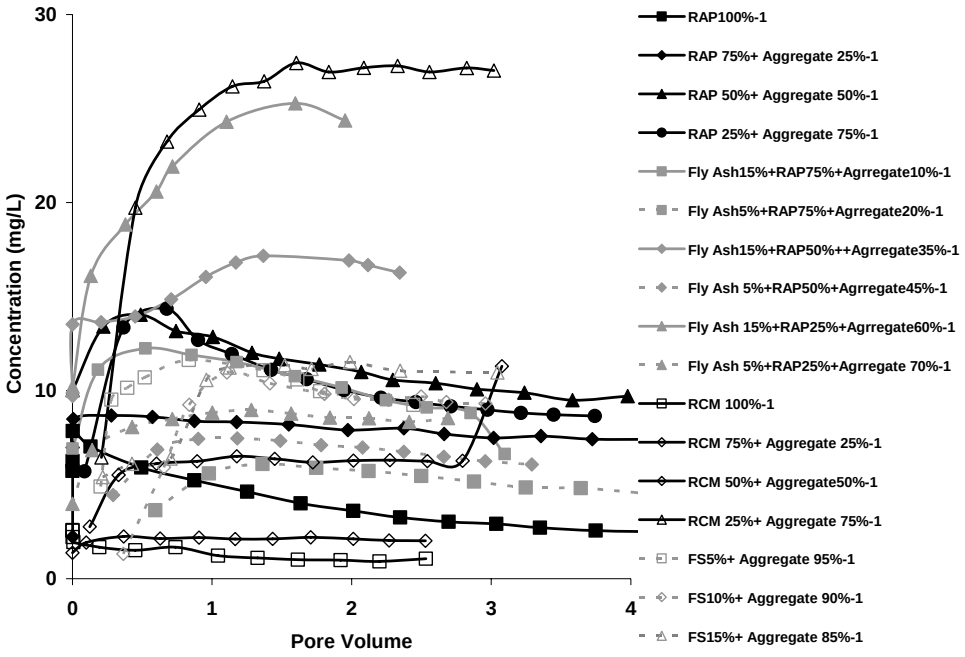

Figure A90. Variation in the concentration of silicon as a function of pore volume during leaching under saturated conditions.

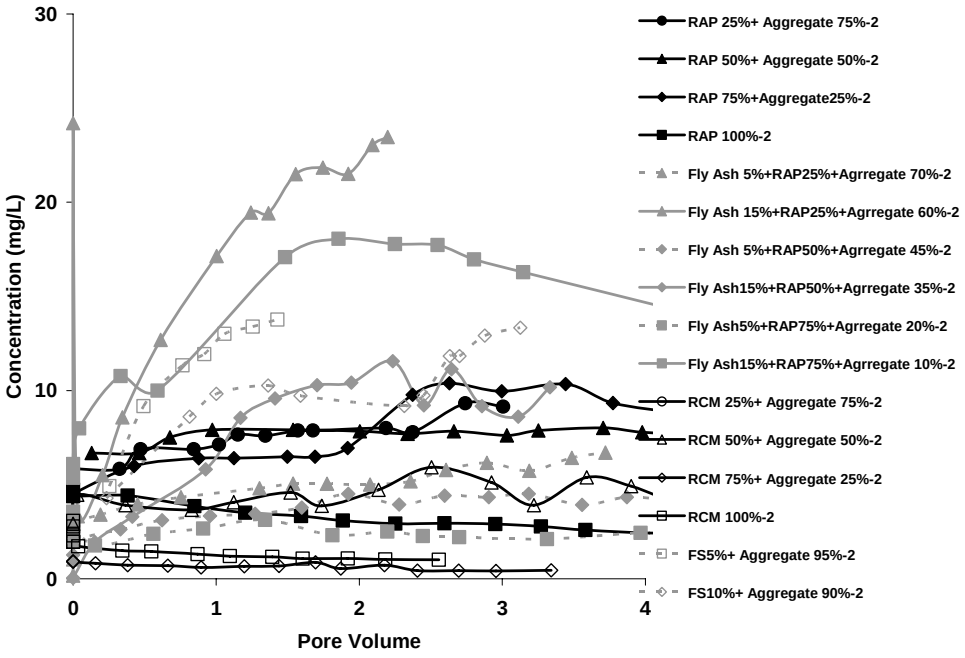

Figure A91. Variation in the concentration of silicon as a function of pore volume during leaching under unsaturated conditions (2 kPa).

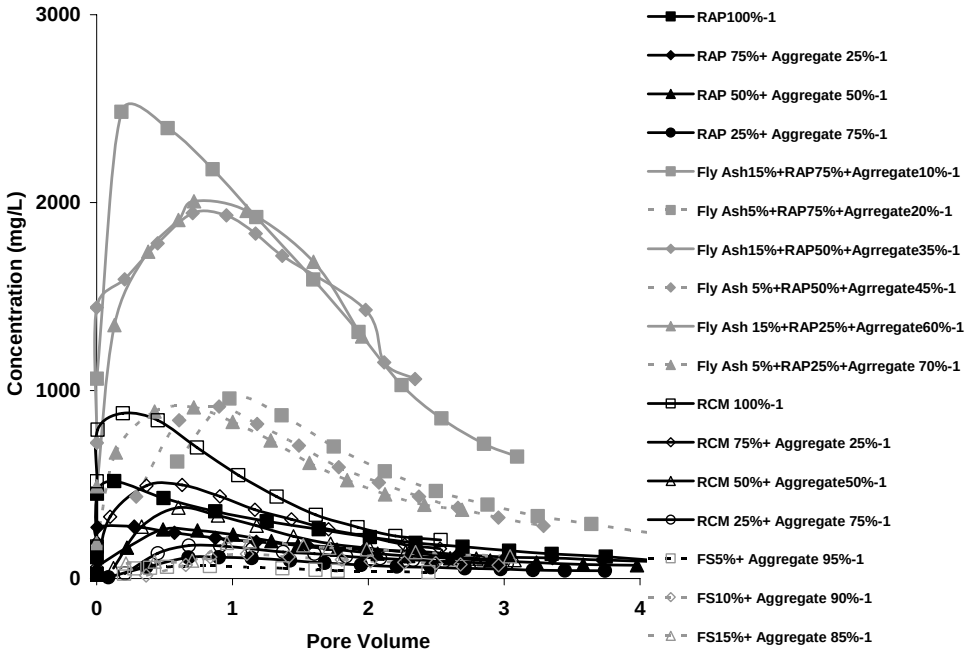

Figure A92. Variation in the concentration of sodium as a function of pore volume during leaching under saturated conditions. Sodium concentration in the leachate was higher from mixtures of FA and RAP with aggregates.

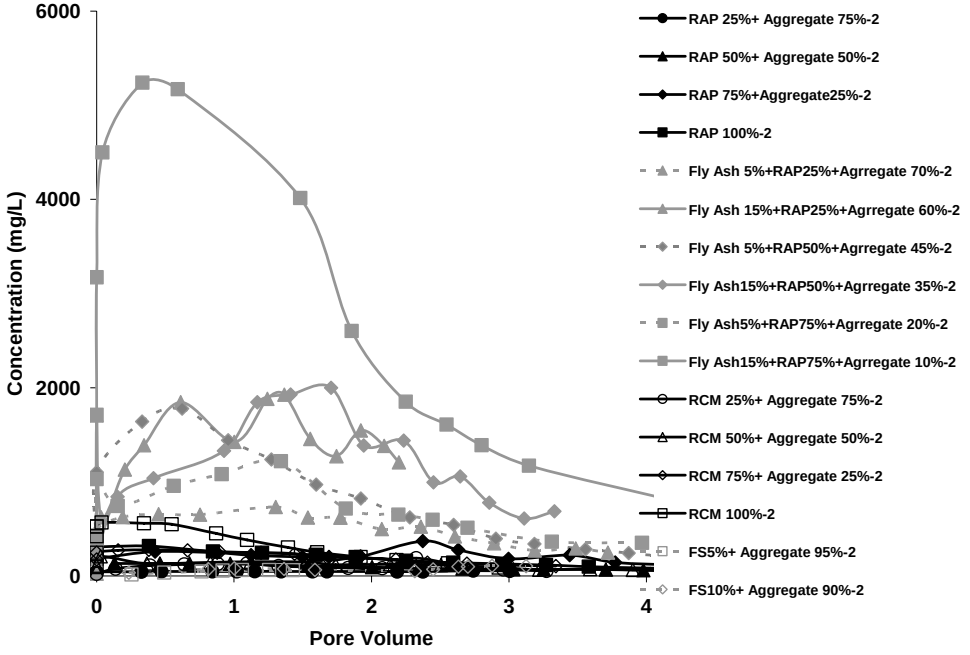

Figure A93. Variation in the concentration of sodium as a function of pore volume during leaching under unsaturated conditions (2 kPa suction). Sodium concentration in the leachate was higher from mixtures of FA and RAP with aggregates.

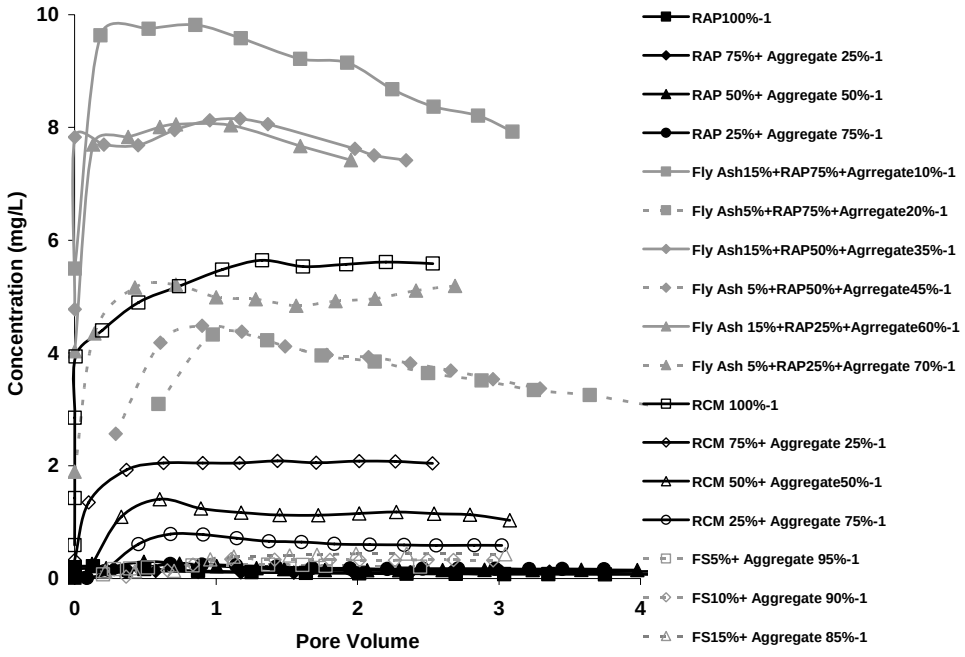

Figure A94. Variation in the concentration of strontium as a function of pore volume during leaching under saturated conditions. Strontium concentration in the leachate was higher from mixtures of FA and RAP with aggregates. Mixtures containing 15% FA leached more strontium that mixtures containing 5% FA. Increased proportion of RCM in the mixture also increased strontium concentration in the leachate from the mixtures.

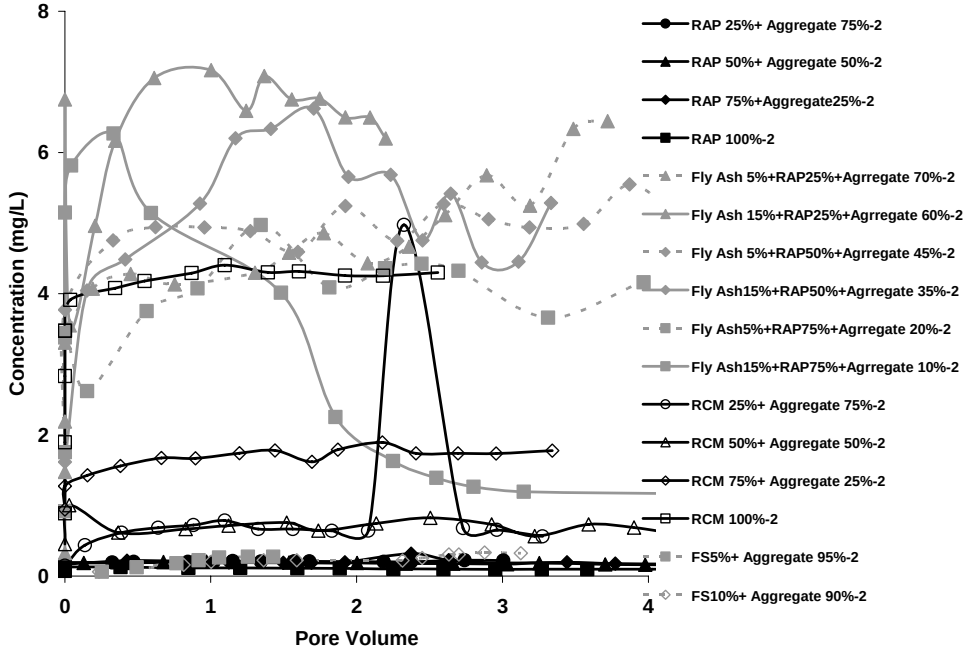

Figure A95. Variation in the concentration of strontium as a function of pore volume during leaching under unsaturated conditions (2 kPa suction). Strontium concentration in the leachate was higher from mixtures of FA and RAP with aggregates. Mixtures containing 15% FA leached more strontium that mixtures containing 5% FA. Increased proportion of RCM in the mixture also increased strontium concentration in the leachate from the mixtures.

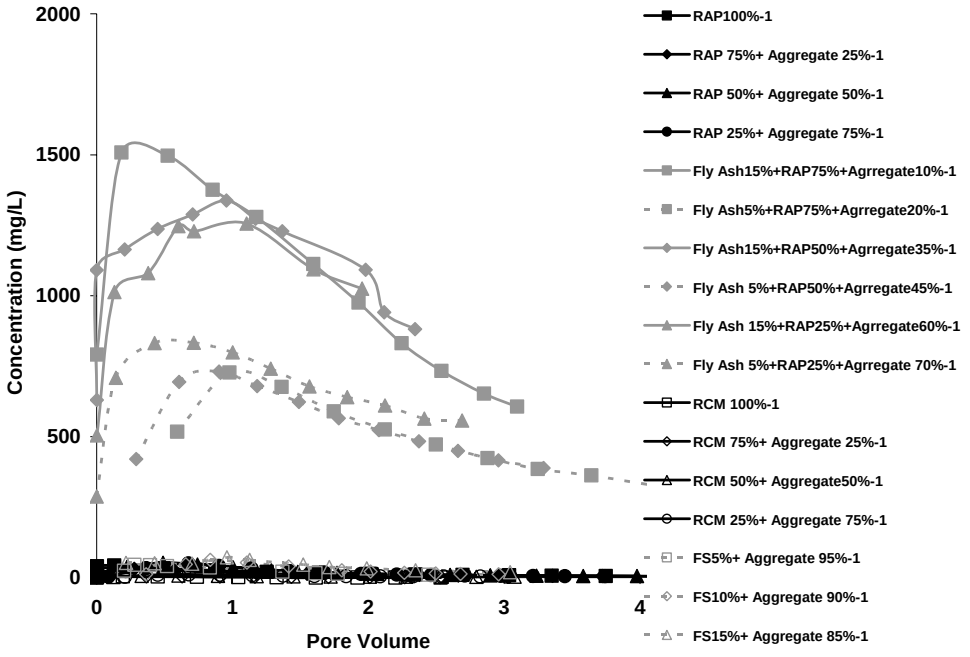

Figure A96. Variation in the concentration of sulfur as a function of pore volume during leaching under saturated conditions. Sulfur concentration in the leachate was higher from mixtures of FA and RAP with aggregates.

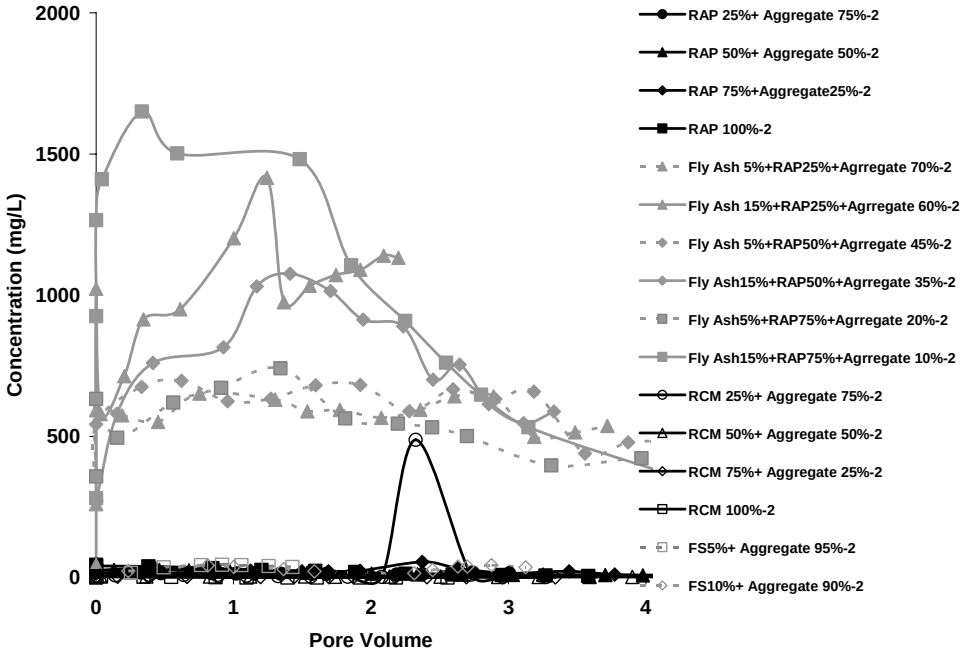

Figure A97. Variation in the concentration of sulfur as a function of pore volume during leaching under unsaturated conditions (2 kPa suction). Sulfur concentration in the leachate was higher from mixtures of FA and RAP with aggregates.

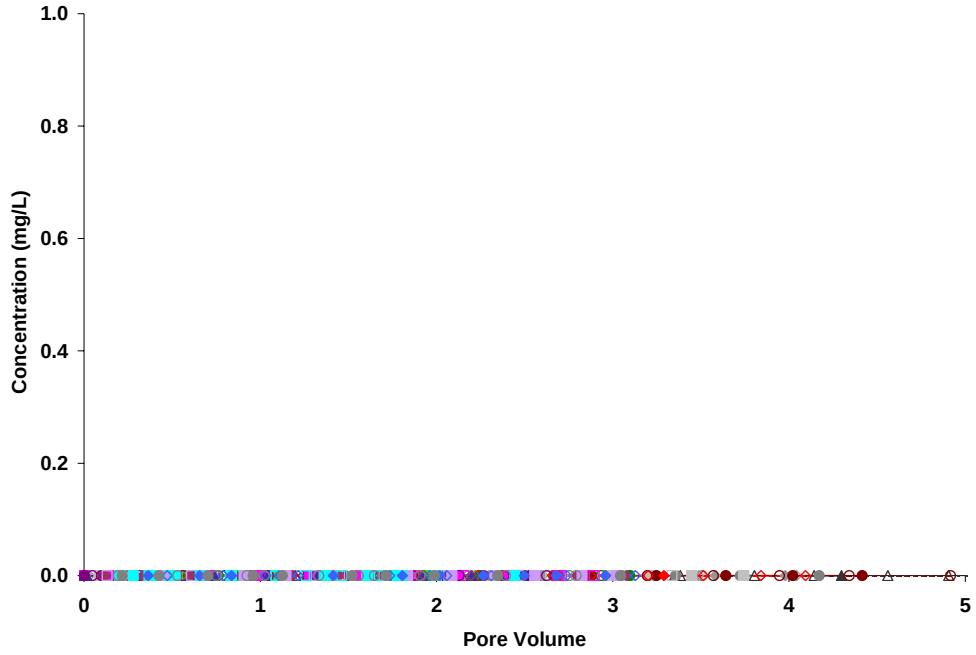

Figure A98. Variation in the concentration of potassium as a function of pore volume during leaching under saturated and unsaturated (2 kPa suction) conditions. Detected potassium concentration in the leachate was lower than the concentration in the DI water (control). Rubidium and titanium were also not detected in these leachate samples.